



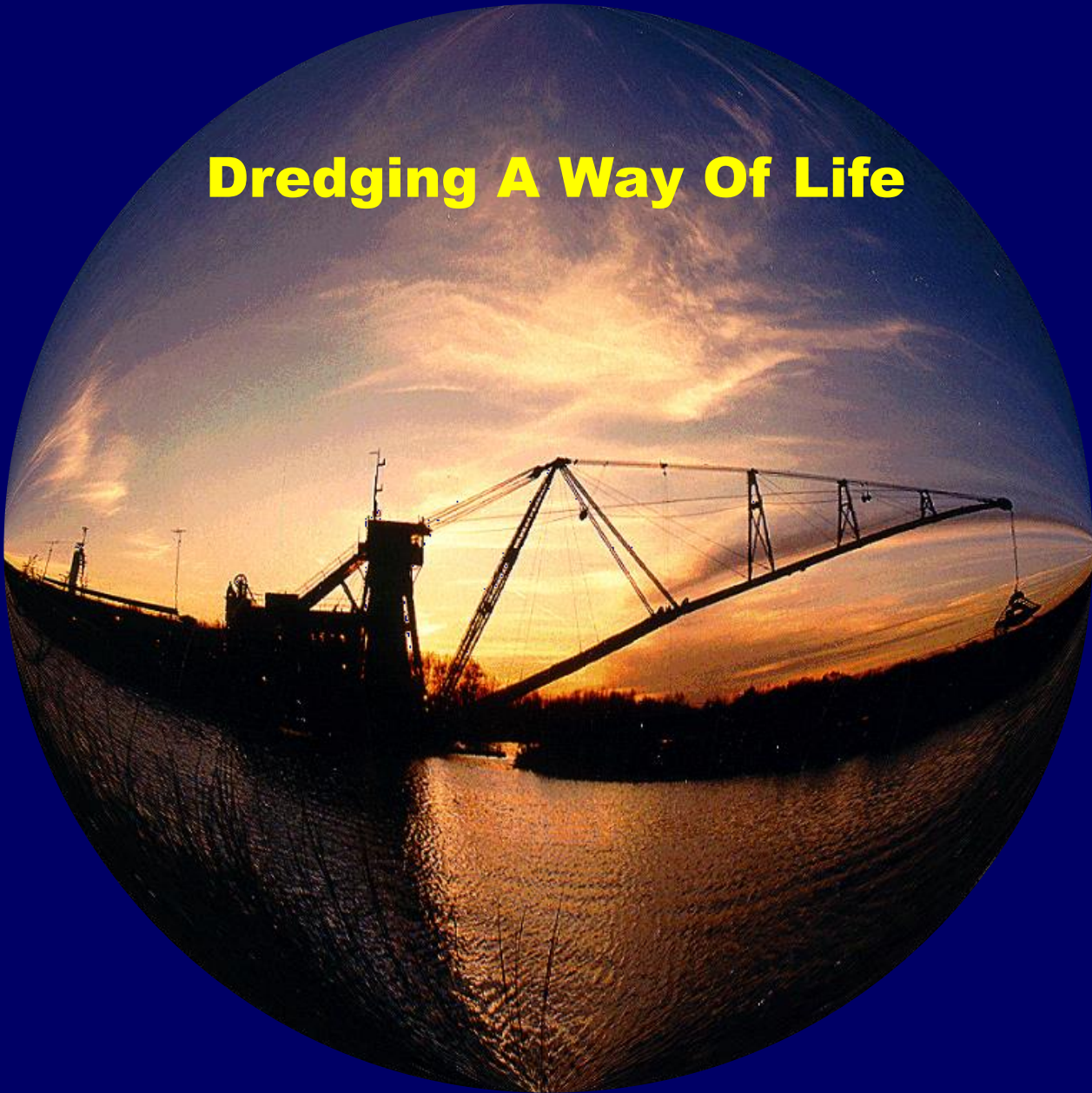
DHLLDV Framework Short Course on Slurry Transport

Dr.ir. Sape A. Miedema
Head of Studies
MSc Offshore & Dredging Engineering
& Marine Technology
&
Associate Professor of
Dredging Engineering

Sunday, November 15, 2020

Delft University of Technology



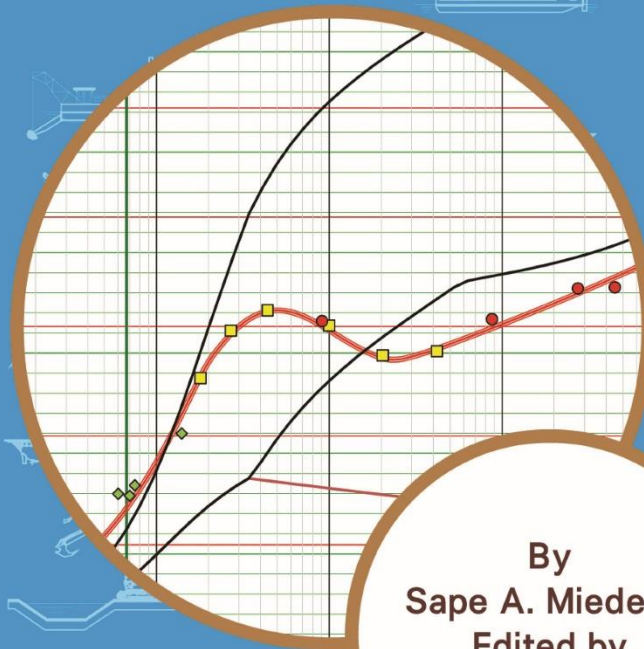


Dredging A Way Of Life



SLURRY TRANSPORT

Fundamentals, A Historical Overview
& The Delft Head Loss & Limit
Deposit Velocity Framework



By
Sape A. Miedema
Edited by
Robert C. Ramsdell



Contents of the Course

- Goals & Targets
- Basics
- The Solids Effect
- Darcy Weisbach
- Equivalent Liquid Model
- Relative Viscosity
- Settling Velocity
- Velocity Distribution
- Existing Models
- Flow Regimes History
- Flow Regime Identification
- Stationary Bed Regime
- Sliding Bed Regime
- Heterogeneous Flow Regime
- Homogeneous Flow Regime
- Sliding Flow Regime
- Limit Deposit Velocity
- Slip Velocity or Holdup Function
- Concentration Distribution
- Transition Heterogeneous-Homogeneous
- Comparison Transition Heterogeneous-Homogeneous
- Bed Height
- Graded Sands & Gravels
- Flow Regime Diagrams
- Inclined Pipes
- Using the DHLLDV Framework
- Main Conclusion



Goals & Targets

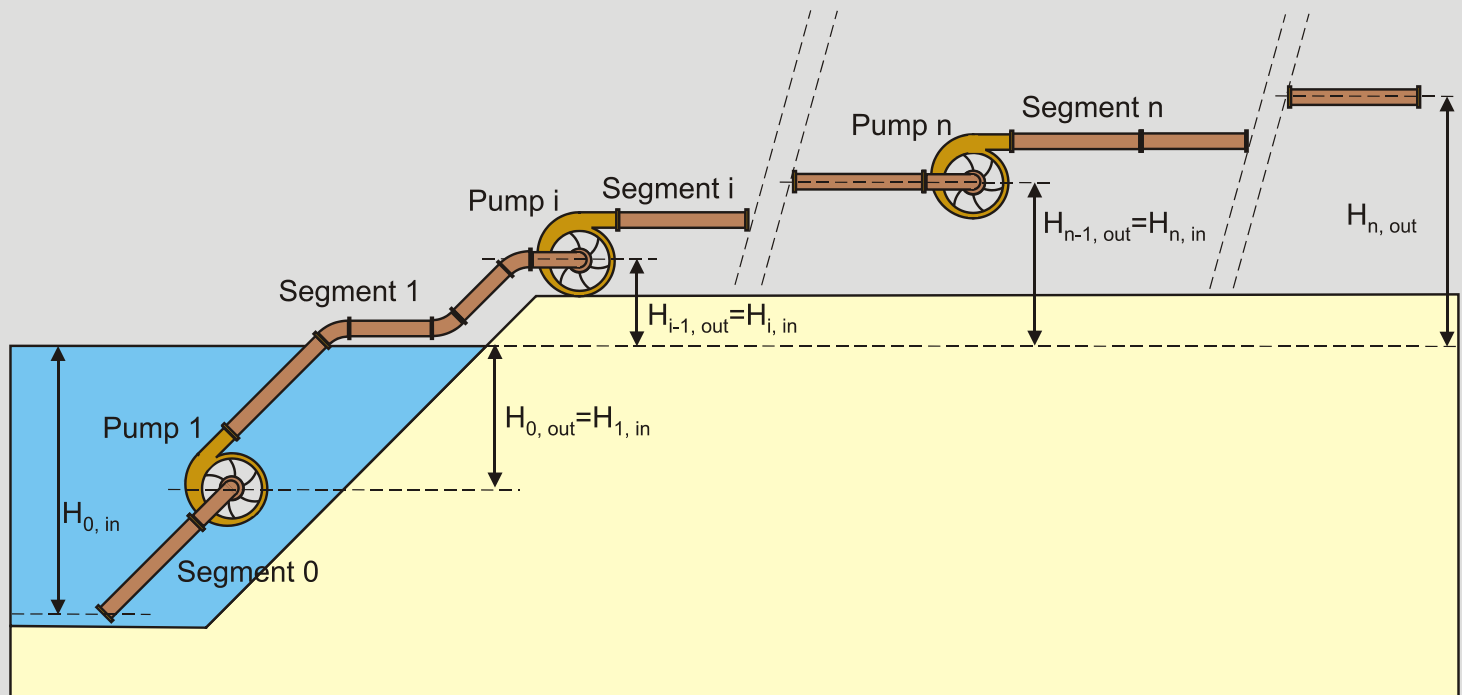


Goals & Targets

**Determining Slurry Transport
Behavior
Based On Known Parameters
Like:
Liquid Properties,
Pipe Diameter,
Particle Diameter,
Volumetric Concentration
As A Function Of The Flow Or
Line Speed**



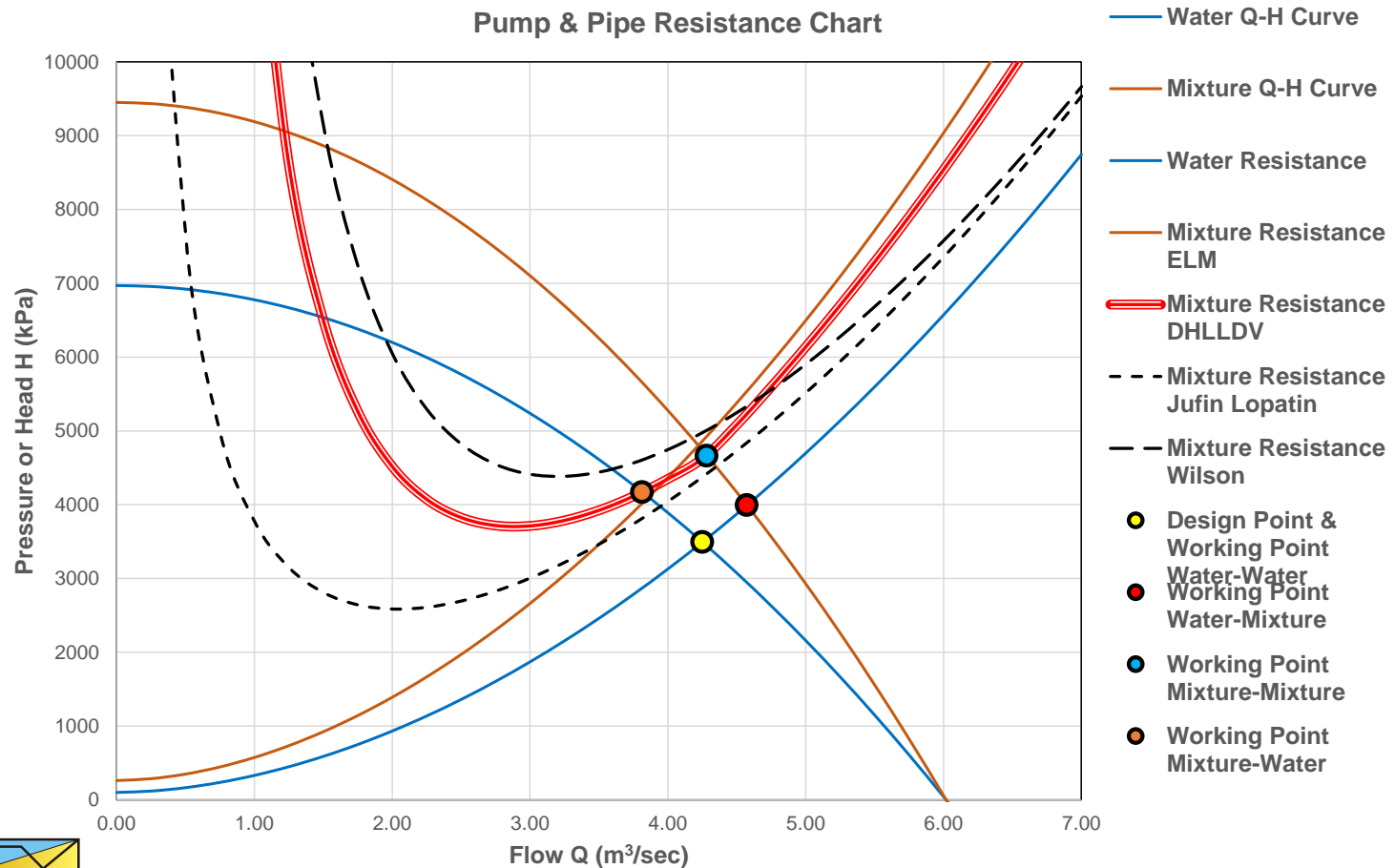
Pump/Pipeline System



- Total pressure/power required
- Limit Deposit Velocity
- Cavitation limit of each pump
- Deposition/plugging the pipeline



Pressure/Flow Graph (Q-H Graph)



- Working points/working area in a stationary situation





Basics



Equations in Graphs

Hydraulic Gradient i

$$i_l = \frac{\Delta p_l}{\rho_l \cdot g \cdot L} \quad \text{or} \quad i_m = \frac{\Delta p_m}{\rho_l \cdot g \cdot L}$$

for water as carrier fluid:

$$\frac{\lambda_1 \cdot \frac{\Delta L}{D_p} \cdot \frac{1}{2} \cdot \rho_l \cdot v_{ls}^2}{\rho_l \cdot g \cdot \Delta L} = \frac{\lambda_1 \cdot v_{ls}^2}{2 \cdot g \cdot D_p}$$

Relative Submerged Density R_{sd}

$$R_{sd} = \frac{\rho_s - \rho_l}{\rho_l}$$

Relative Excess Hydraulic Gradient E_{rhg}

$$E_{rhg} = \frac{i_m - i_l}{R_{sd} \cdot C_{vs}} \quad \text{or} \quad E_{rhg} = \frac{i_m - i_l}{R_{sd} \cdot C_{vt}}$$



Spatial versus Transport Concentration & the Slip Velocity

**Spatial Volumetric Concentration is volume based.
Transport Volumetric Concentration is volume flow based.**

$$C_{vt} = \left(1 - \frac{v_{sl}}{v_{ls}}\right) \cdot C_{vs} \quad \Rightarrow \quad C_{vt} < C_{vs} \quad C_{vs} = \left(\frac{v_{ls}}{v_{ls} - v_{sl}}\right) \cdot C_{vt}$$

**Relative Excess Hydraulic Gradient E_{rhg} ,
 $C_{vt} = \text{constant}$.**

$$E_{rhg} = \frac{i_m - i_l}{R_{sd} \cdot \left(1 - \frac{v_{sl}}{v_{ls}}\right) \cdot C_{vs}} = \left(\frac{v_{ls}}{v_{ls} - v_{sl}}\right) \cdot \frac{i_m - i_l}{R_{sd} \cdot C_{vs}}$$

The slip velocity here is the velocity difference between the line speed and the particle velocity.

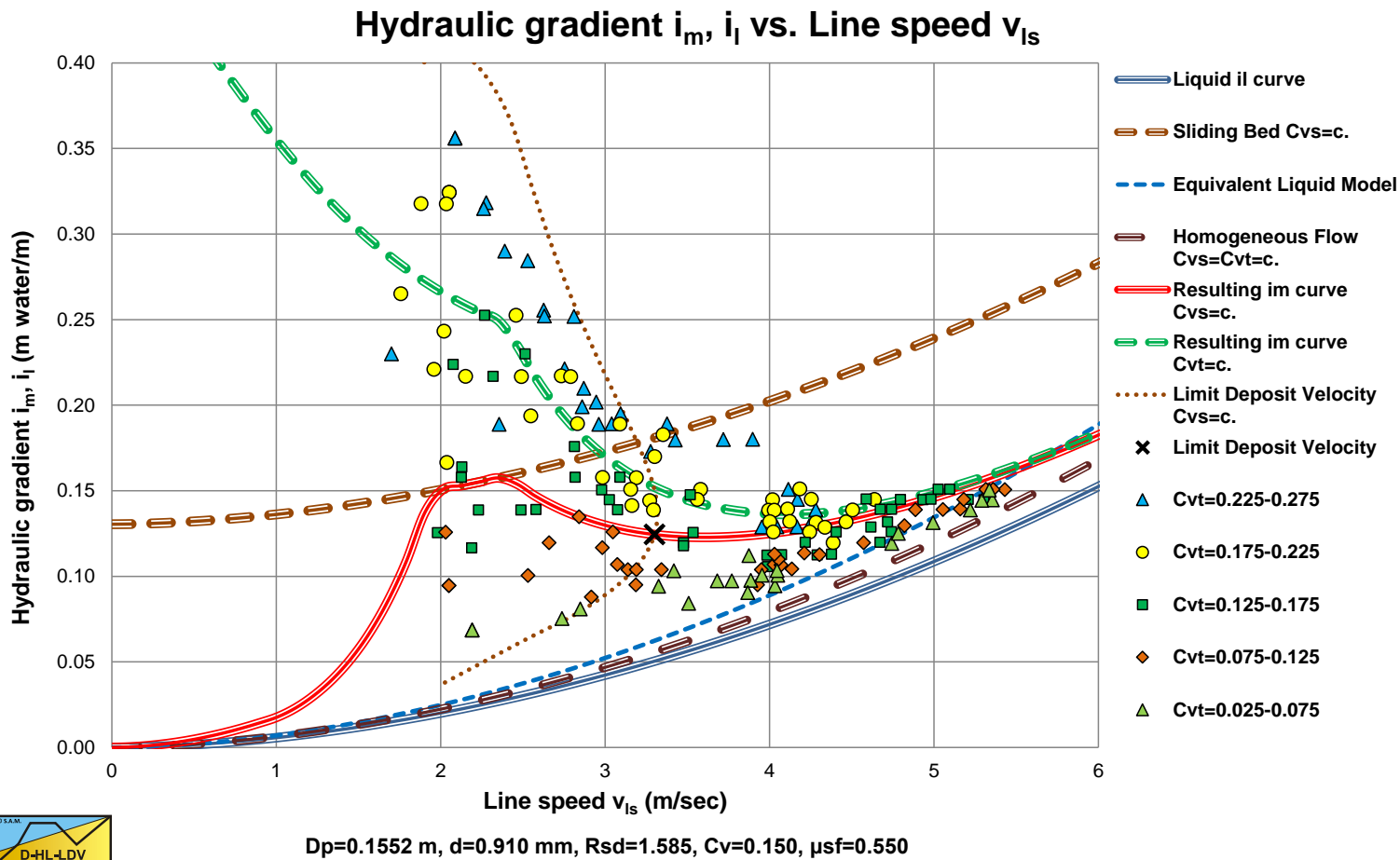




The Solids Effect



Data from Yagi et al., $i_m - v_{ls}$

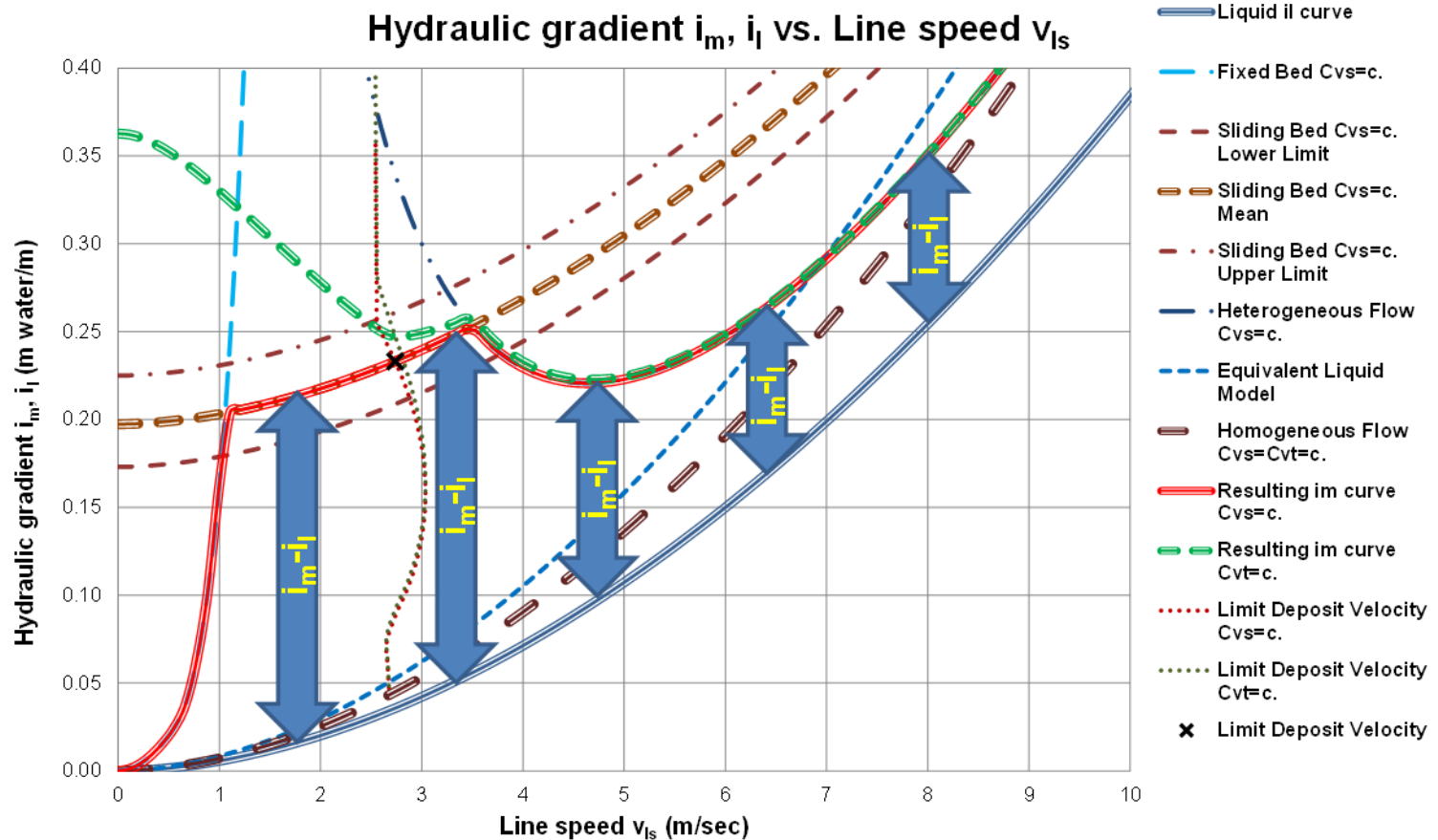


Data looks unorganized depending on the volumetric concentration of the solids.

Delft University of Technology – Offshore & Dredging Engineering



Solids Effect Spatial Concentration



$D_p=0.1524$ m, $d=1.500$ mm, $R_{sd}=1.585$, $C_v=0.300$, $\mu=0.420$

$$i_l = \frac{\Delta p_l}{\rho_l \cdot g \cdot \Delta L} = \frac{\lambda_1 \cdot v_{ls}^2}{2 \cdot g \cdot D_p}$$

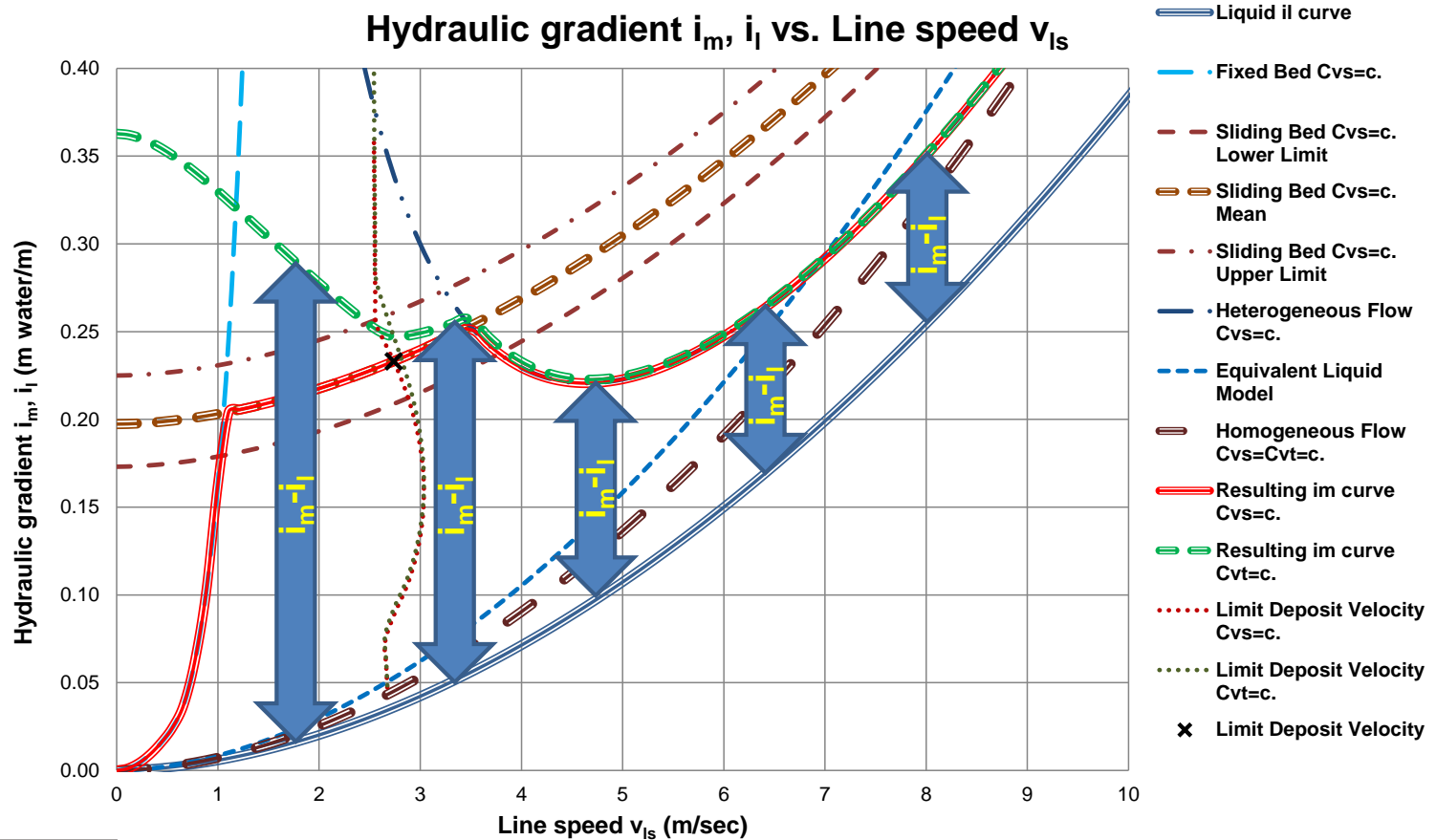
Hydraulic Gradient
Relative Excess H.G.

$$E_{rhg} = \frac{i_m - i_l}{R_{sd} \cdot C_v}$$

Delft University of Technology – Offshore & Dredging Engineering



Solids Effect Transport Concentration



$D_p=0.1524$ m, $d=1.500$ mm, $R_{sd}=1.585$, $C_v=0.300$, $\mu=0.420$

$$i_l = \frac{\Delta p_l}{\rho_l \cdot g \cdot \Delta L} = \frac{\lambda_1 \cdot v_{ls}^2}{2 \cdot g \cdot D_p}$$

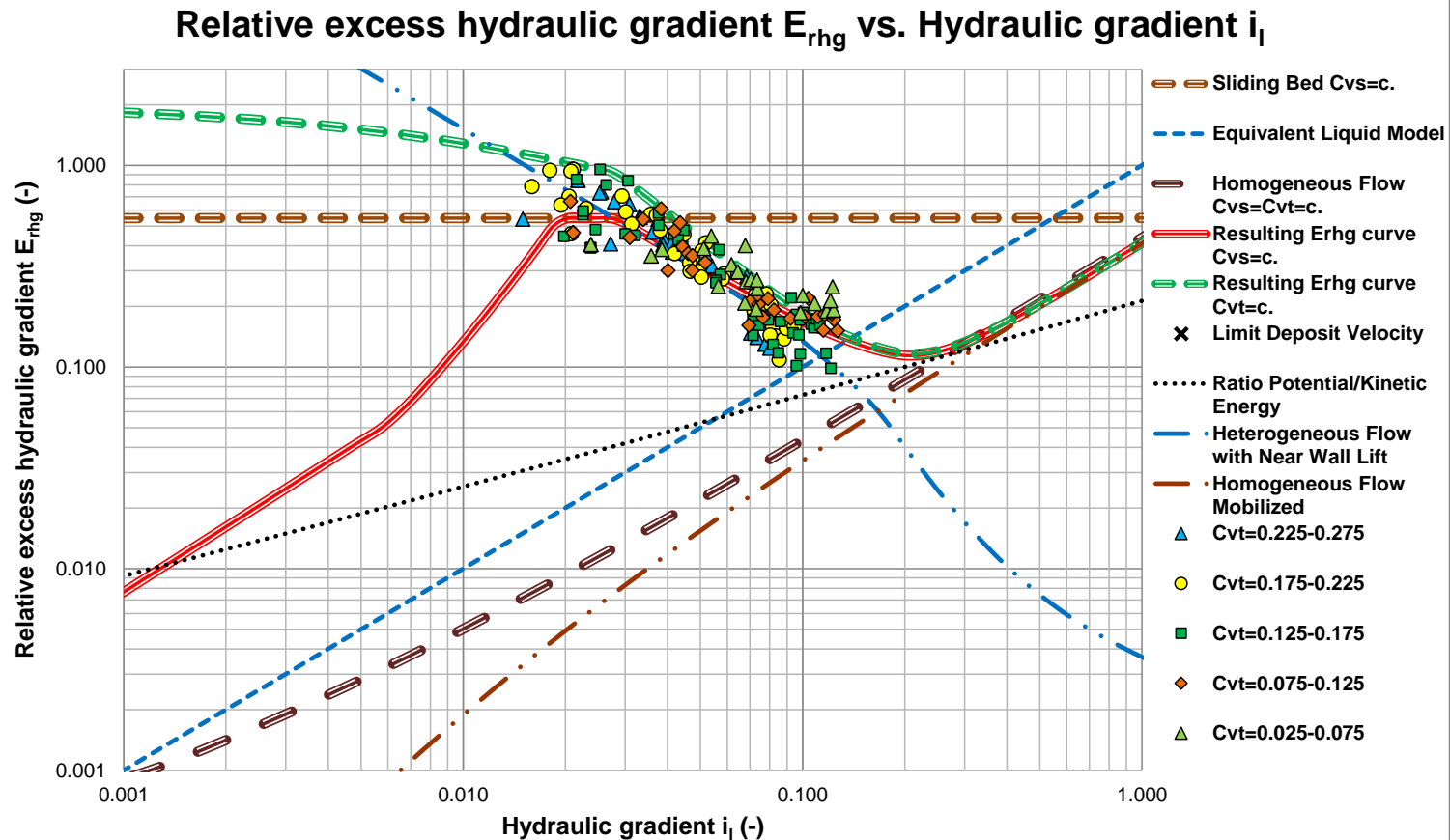
Hydraulic Gradient
Relative Excess H.G.

$$E_{rhg} = \frac{i_m - i_l}{R_{sd} \cdot C_v}$$

Delft University of Technology – Offshore & Dredging Engineering



Data from Yagi et al., $E_{rhg}-i_1$



$D_p=0.1552$ m, $d=0.910$ mm, $Rsd=1.585$, $Cv=0.150$, $\mu_{sf}=0.550$

Data looks more organized not depending on the volumetric concentration of the solids.

Delft University of Technology – Offshore & Dredging Engineering



Darcy Weisbach

Chapter 3



Darcy Weisbach

$$\Delta p_1 = \lambda_1 \cdot \frac{\Delta L}{D_p} \cdot \frac{1}{2} \cdot \rho_1 \cdot v_{ls}^2$$

$$i_1 = i_w = \frac{\Delta p_1}{\rho_1 \cdot g \cdot \Delta L} = \frac{\lambda_1 \cdot v_{ls}^2}{2 \cdot g \cdot D_p}$$

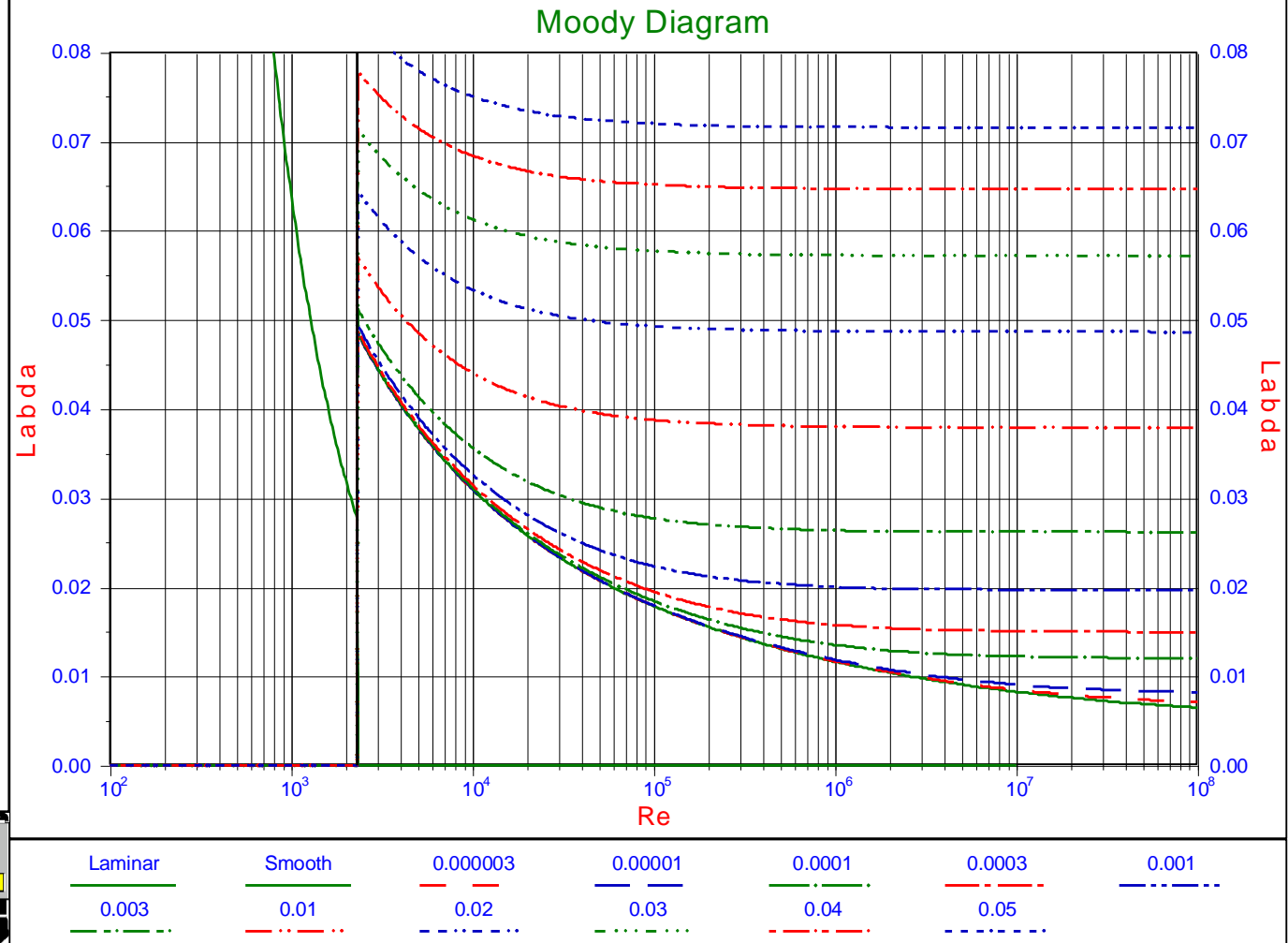
$$\lambda_1 = \frac{1.325}{\left(\ln \left(\frac{\varepsilon}{3.7 \cdot D_p} + \frac{5.75}{Re^{0.9}} \right) \right)^2} = \frac{0.25}{\left(\log_{10} \left(\frac{\varepsilon}{3.7 \cdot D_p} + \frac{5.75}{Re^{0.9}} \right) \right)^2}$$



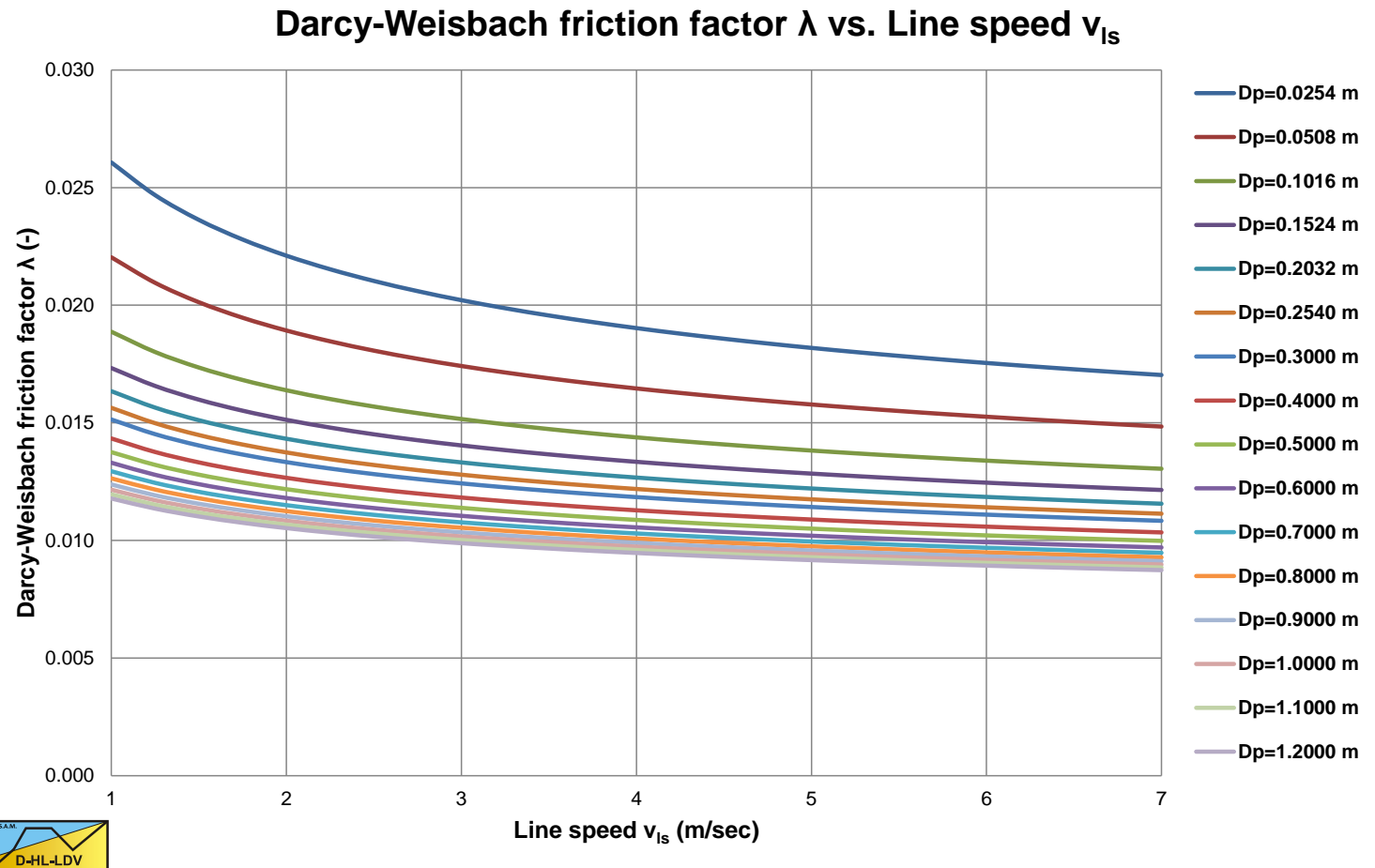
Moody Diagram



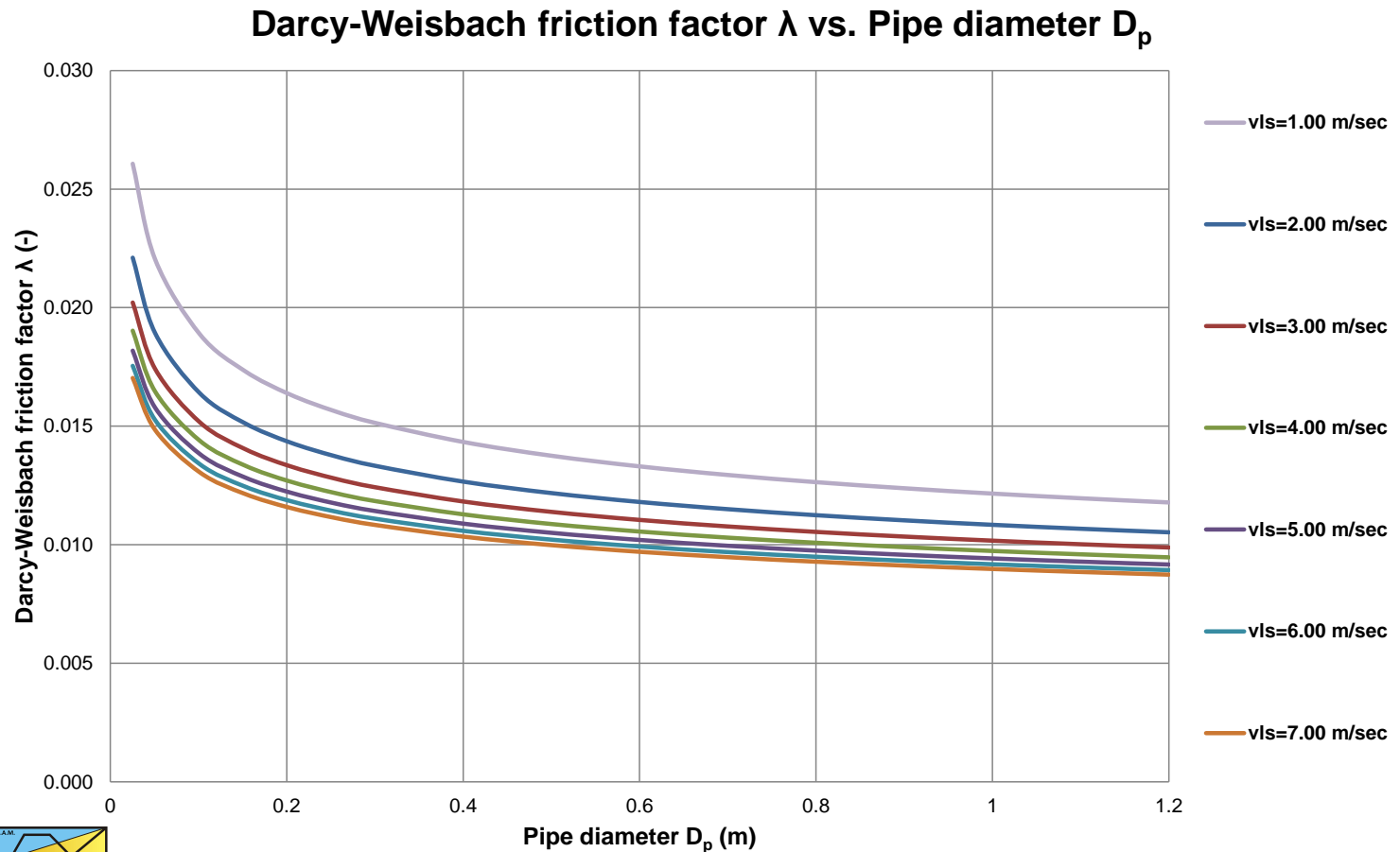
Moody diagram for the determination of the Darcy Weisbach friction coefficient. The legend shows the relative roughness.



Moody Friction Factor vs. Line Speed



Moody Friction Factor vs. Pipe Diameter



Moody Friction Factor Approximation

$$\lambda_1 = \alpha \cdot (v_{ls})^{\alpha_1} \cdot (D_p)^{\alpha_2}$$

$$\alpha = 0.01216$$

$$\alpha_1 = -0.1537 \cdot (D_p)^{-0.089} \quad \text{range: 0.170-0.202}$$

$$\alpha_2 = -0.2013 \cdot (v_{ls})^{-0.088} \quad \text{range: 0.152-0.216}$$





Equivalent Liquid Model

Chapter 3



Equivalent Liquid Model

$$\Delta p_m = \lambda_1 \cdot \frac{\Delta L}{D_p} \cdot \frac{1}{2} \cdot \rho_m \cdot v_{ls}^2$$

$$i_m = \frac{\Delta p_m}{\rho_l \cdot g \cdot \Delta L} = \frac{\rho_m}{\rho_l} \cdot \frac{\lambda_1 \cdot v_{ls}^2}{2 \cdot g \cdot D_p}$$

$$\lambda_1 = \frac{1.325}{\left(\ln \left(\frac{\varepsilon}{3.7 \cdot D_p} + \frac{5.75}{Re^{0.9}} \right) \right)^2} = \frac{0.25}{\left(\log_{10} \left(\frac{\varepsilon}{3.7 \cdot D_p} + \frac{5.75}{Re^{0.9}} \right) \right)^2}$$



Relative Excess Hydraulic Gradient (E_{rhg})

$$i_m = (1 + R_{sd} \cdot C_{vs}) \cdot \frac{\lambda_1 \cdot v_{ls}^2}{2 \cdot g \cdot D_p}$$

$$= i_1 \cdot (1 + R_{sd} \cdot C_{vs})$$

$$E_{rhg} = \frac{i_m - i_1}{R_{sd} \cdot C_{vs}} = i_1$$





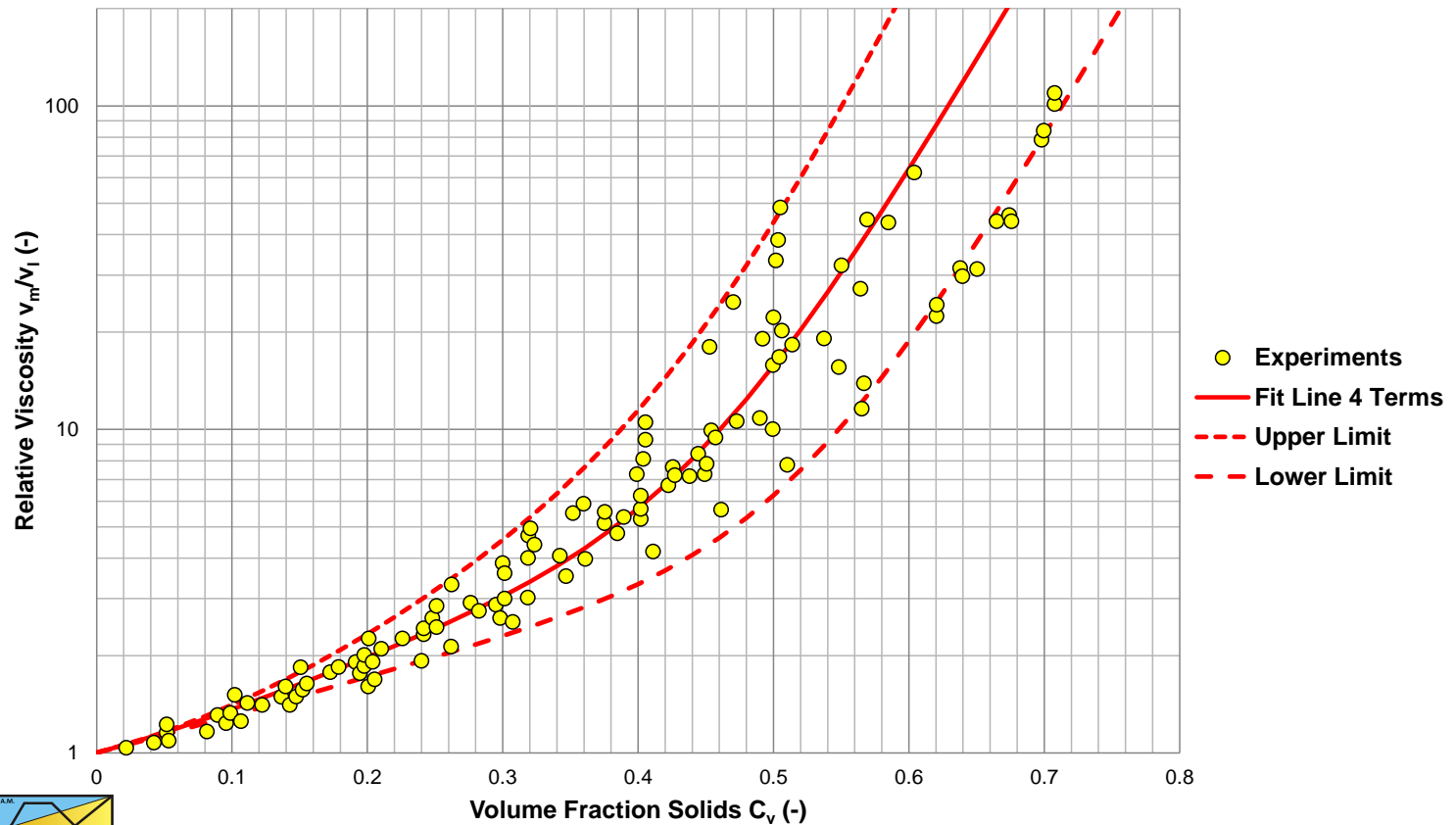
Relative Viscosity

Chapter 3



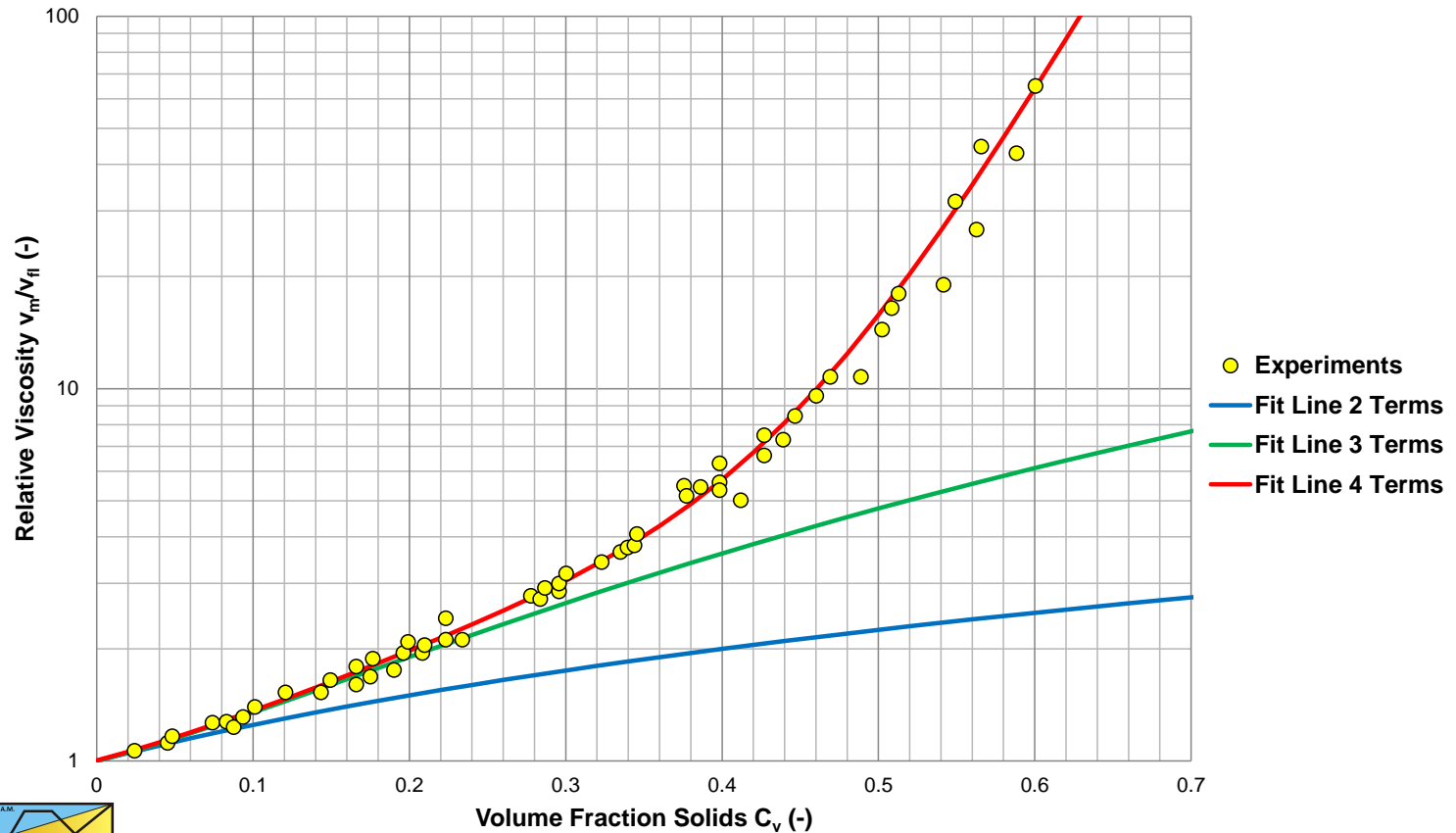
Relative Viscosity

Collected Relative Viscosity Data, From 16 Sources



Relative Viscosity, Selected

Collected Relative Viscosity Data, Reduced



Relative Viscosity, Approximation

$$\mu_r = \frac{\mu_m}{\mu_l} = 1 + 2.5 \cdot C_{vs} \quad \text{Einstein}$$

$$\mu_r = \frac{\mu_m}{\mu_l} = 1 + 2.5 \cdot C_{vs} + 10.05 \cdot C_{vs}^2 + 0.00273 \cdot e^{16.6 \cdot C_{vs}}$$

Thomas Relative Dynamic Viscosity

Relative Kinematic Viscosity

$$v_r = \frac{\rho_m \cdot \mu_m}{\rho_l \cdot \mu_l} = \frac{\rho_m}{\rho_l} \cdot \mu_r$$





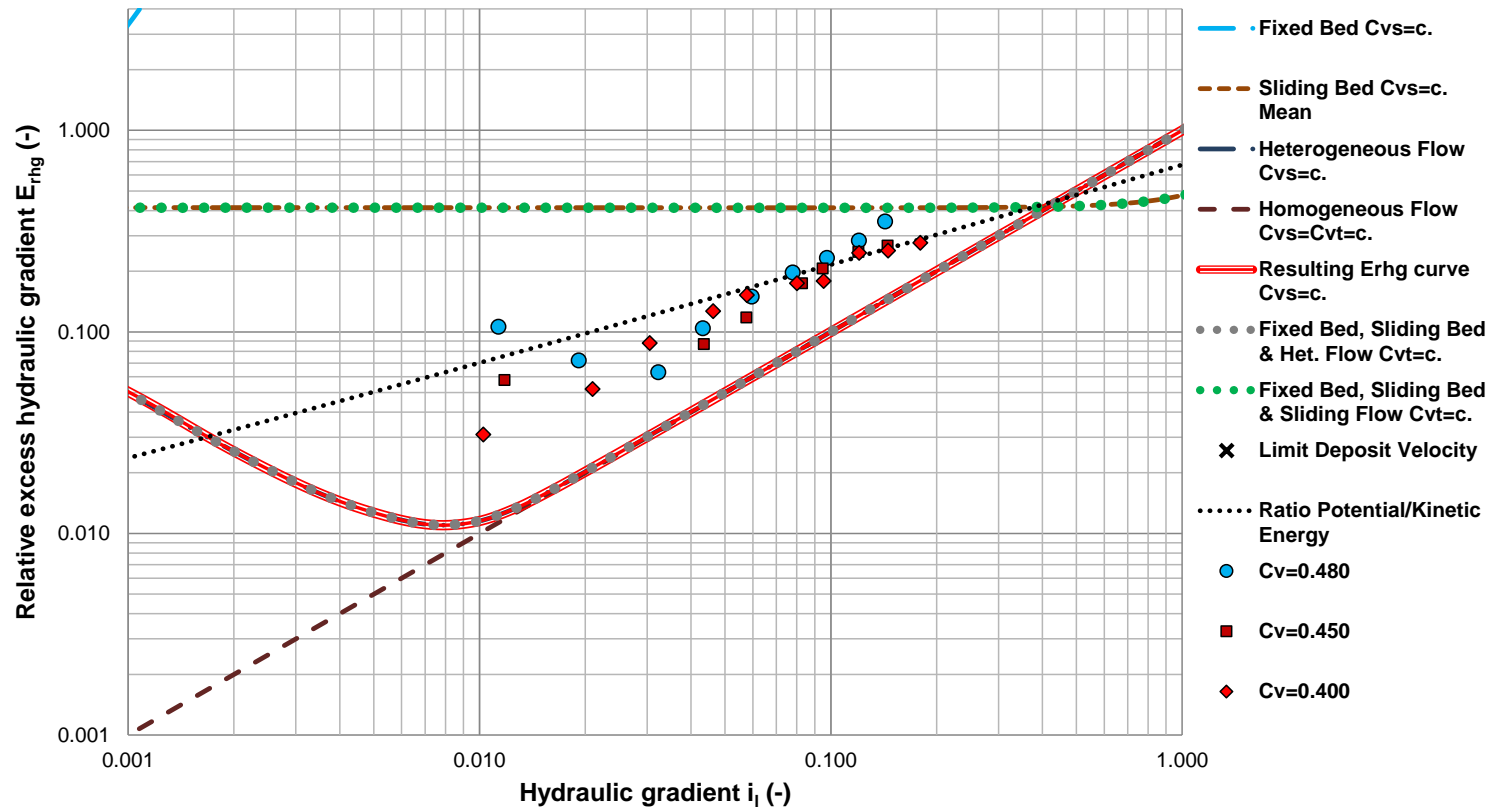
Experiments

Relative Viscosity



Solids Effect in Pure Liquid

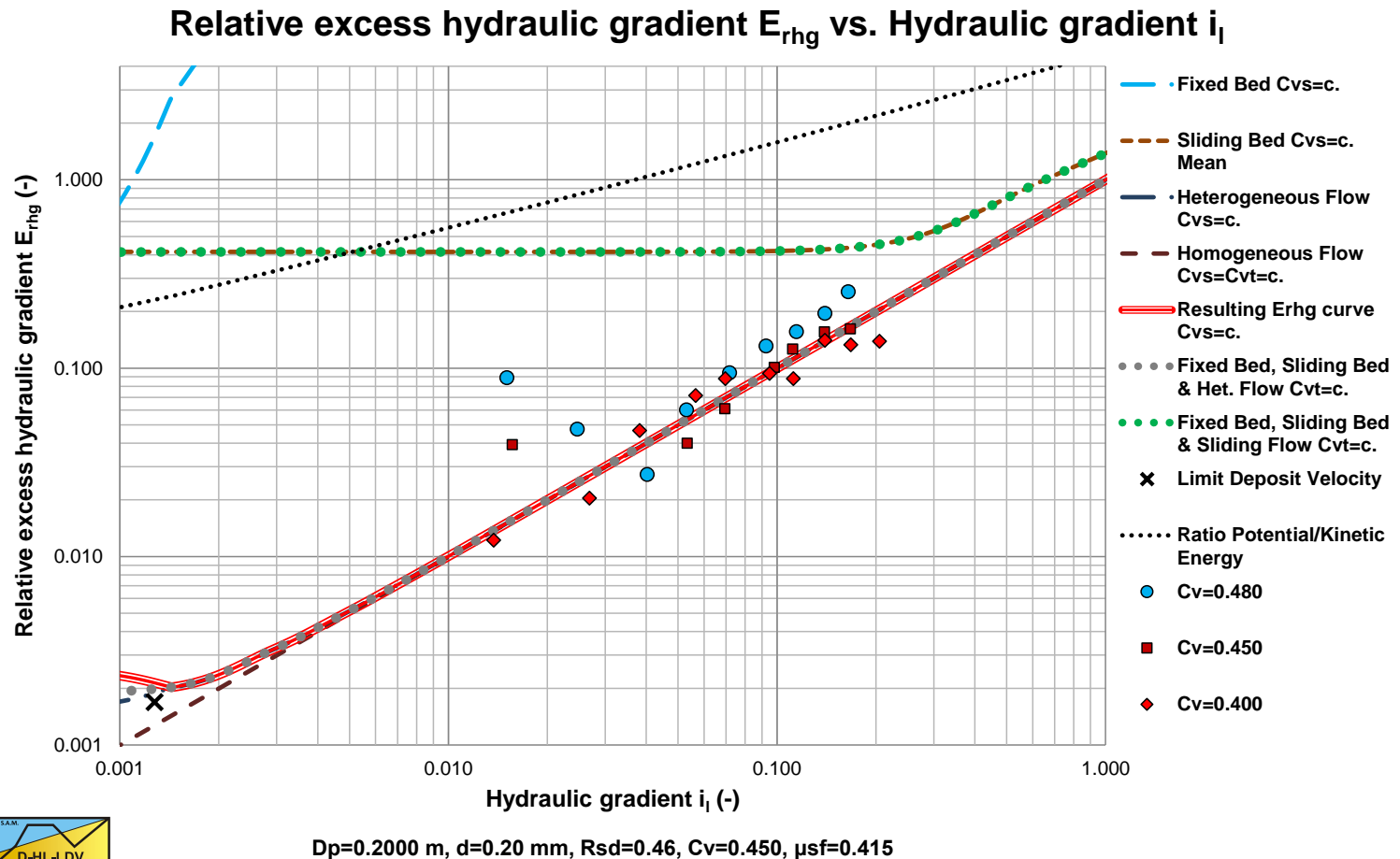
Relative excess hydraulic gradient E_{rhg} vs. Hydraulic gradient i_i



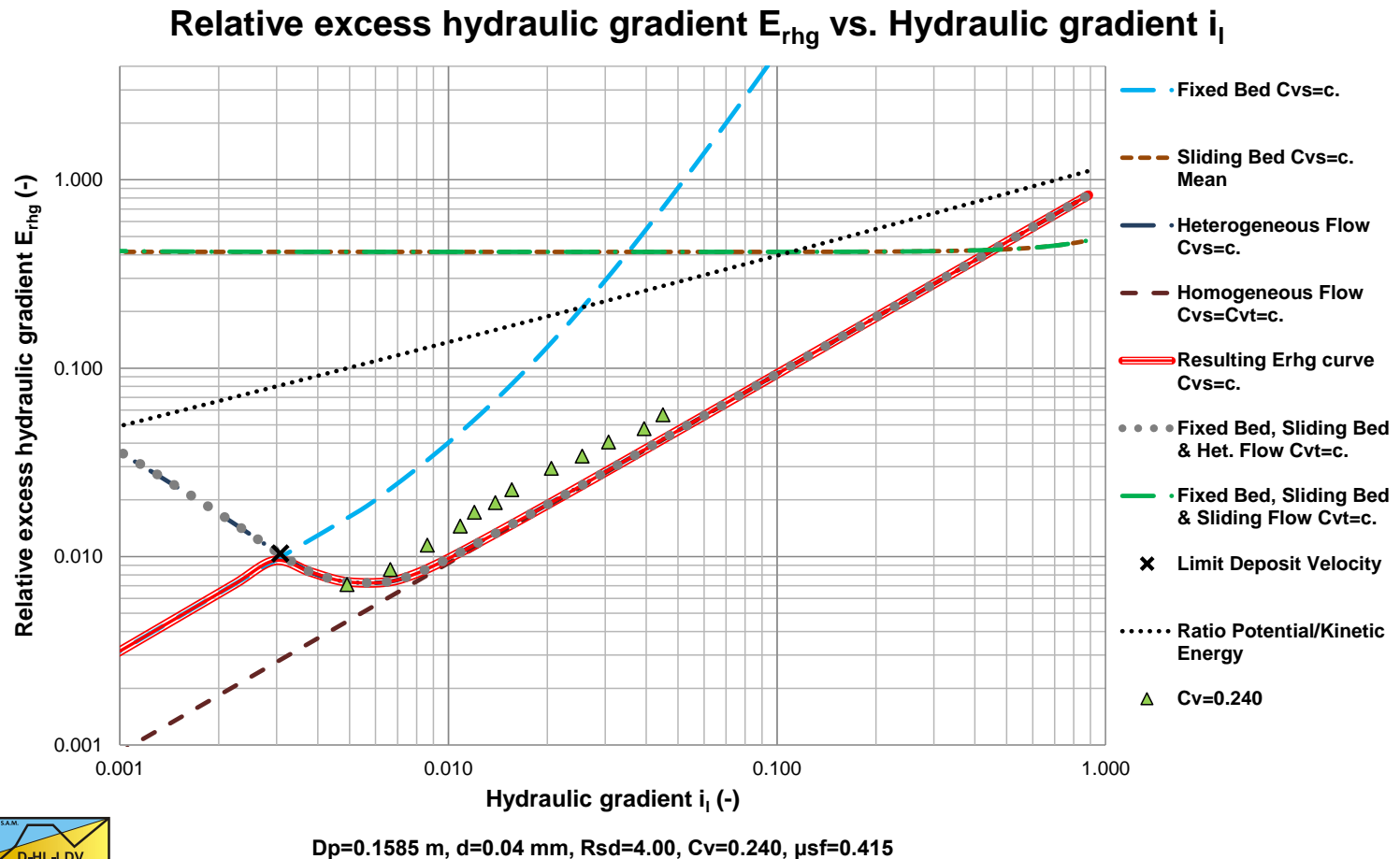
$D_p=0.2000$ m, $d=0.20$ mm, $R_{sd}=0.46$, $C_v=0.450$, $\mu_{sf}=0.415$



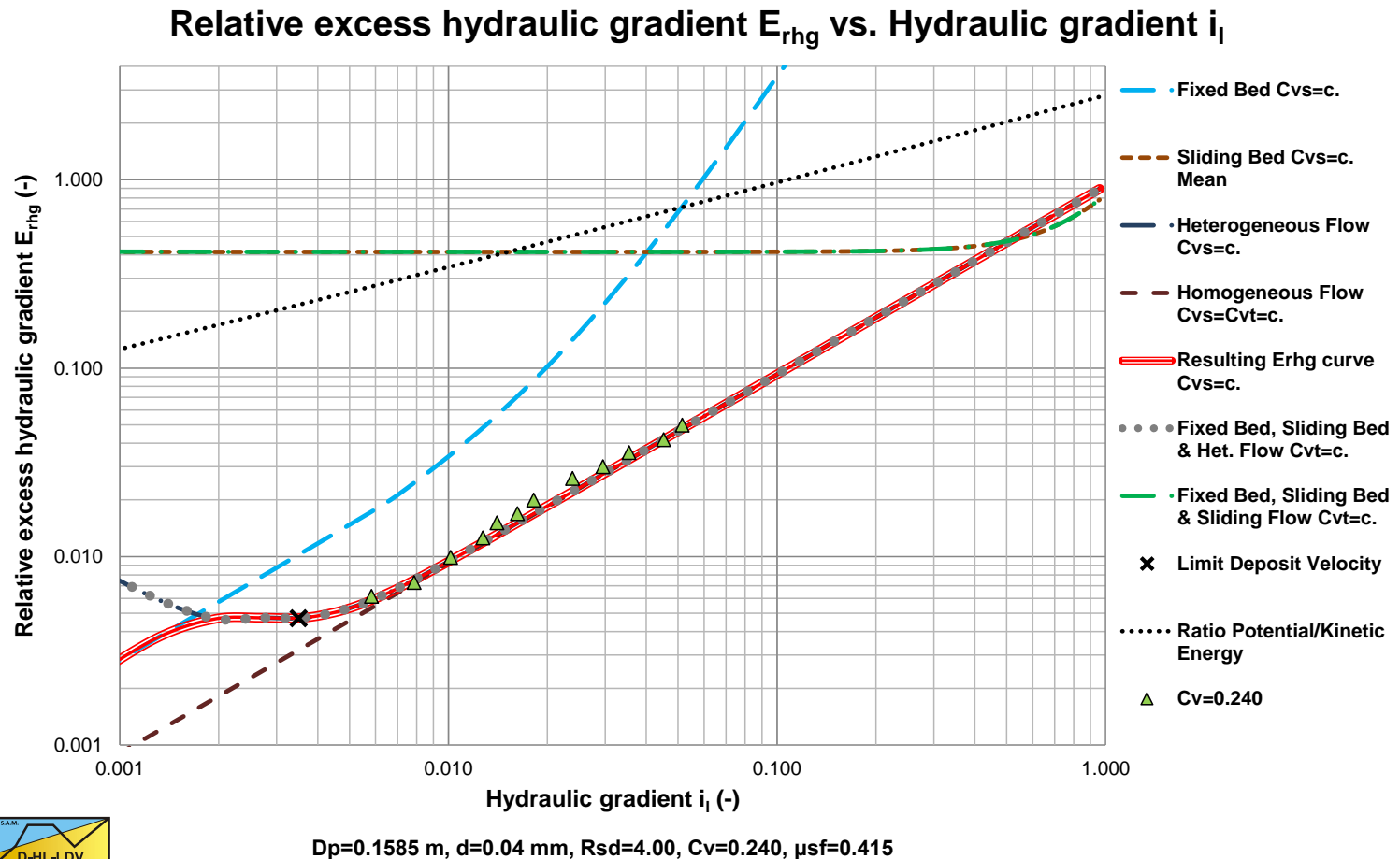
Solids Effect with Relative Viscosity



Solids Effect in Pure Liquid



Solids Effect with Relative Viscosity



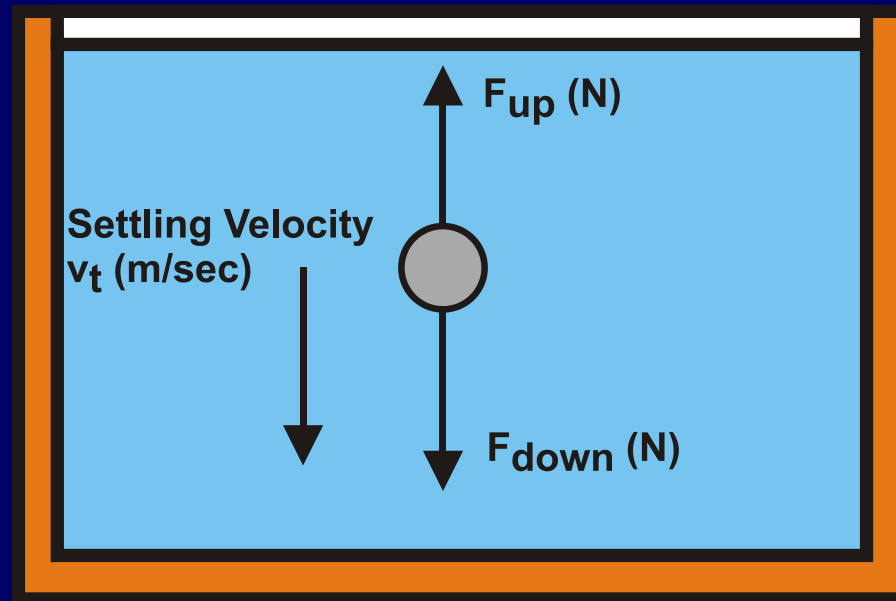


The Settling Velocity

Chapter 4



Forces on a Settling Particle



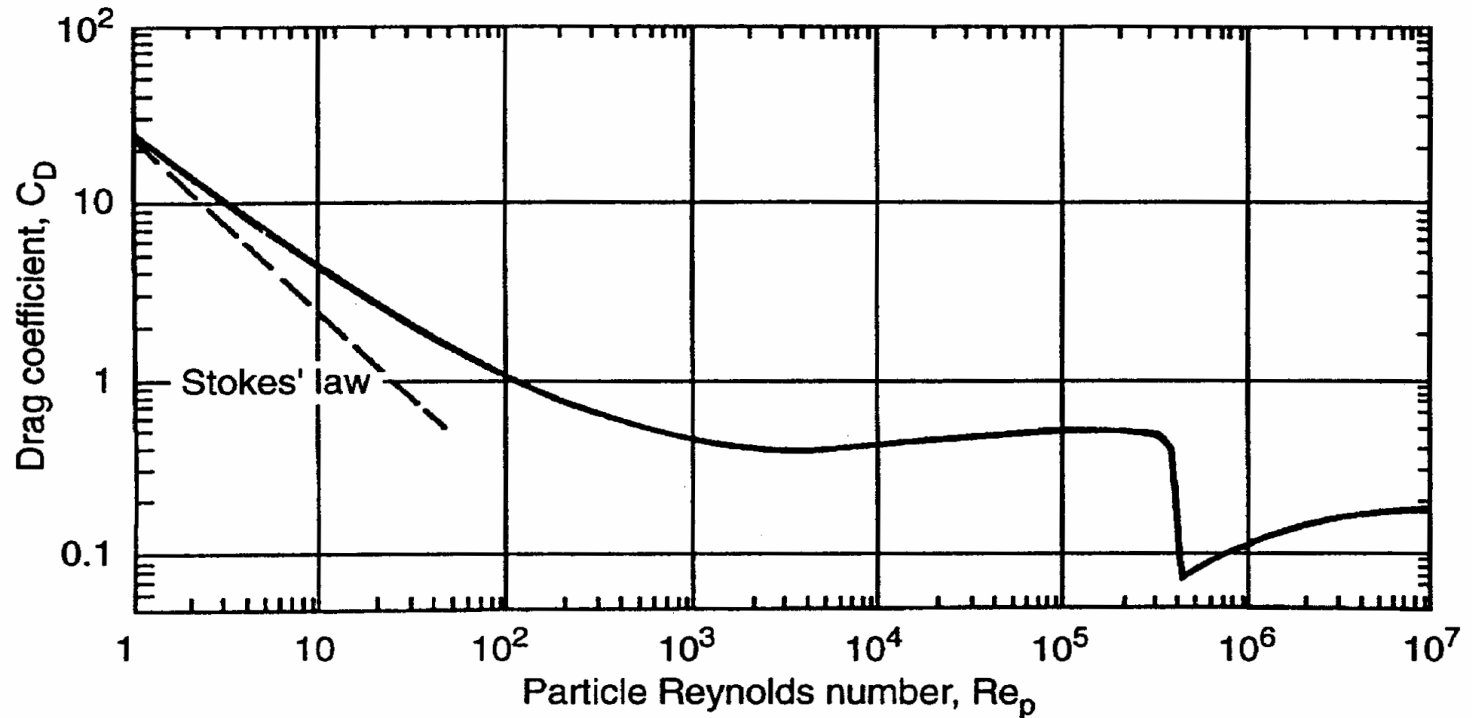
$$F_{up} = C_D \cdot \frac{1}{2} \cdot \rho_w \cdot v_t^2 \cdot A$$

$$v_t = \sqrt{\frac{4 \cdot g \cdot (\rho_q - \rho_w) \cdot d \cdot \psi}{3 \cdot \rho_w \cdot C_D}}$$

$$F_{down} = (\rho_q - \rho_w) \cdot g \cdot V \cdot \psi$$



Standard Drag Coefficient Curve for Spheres



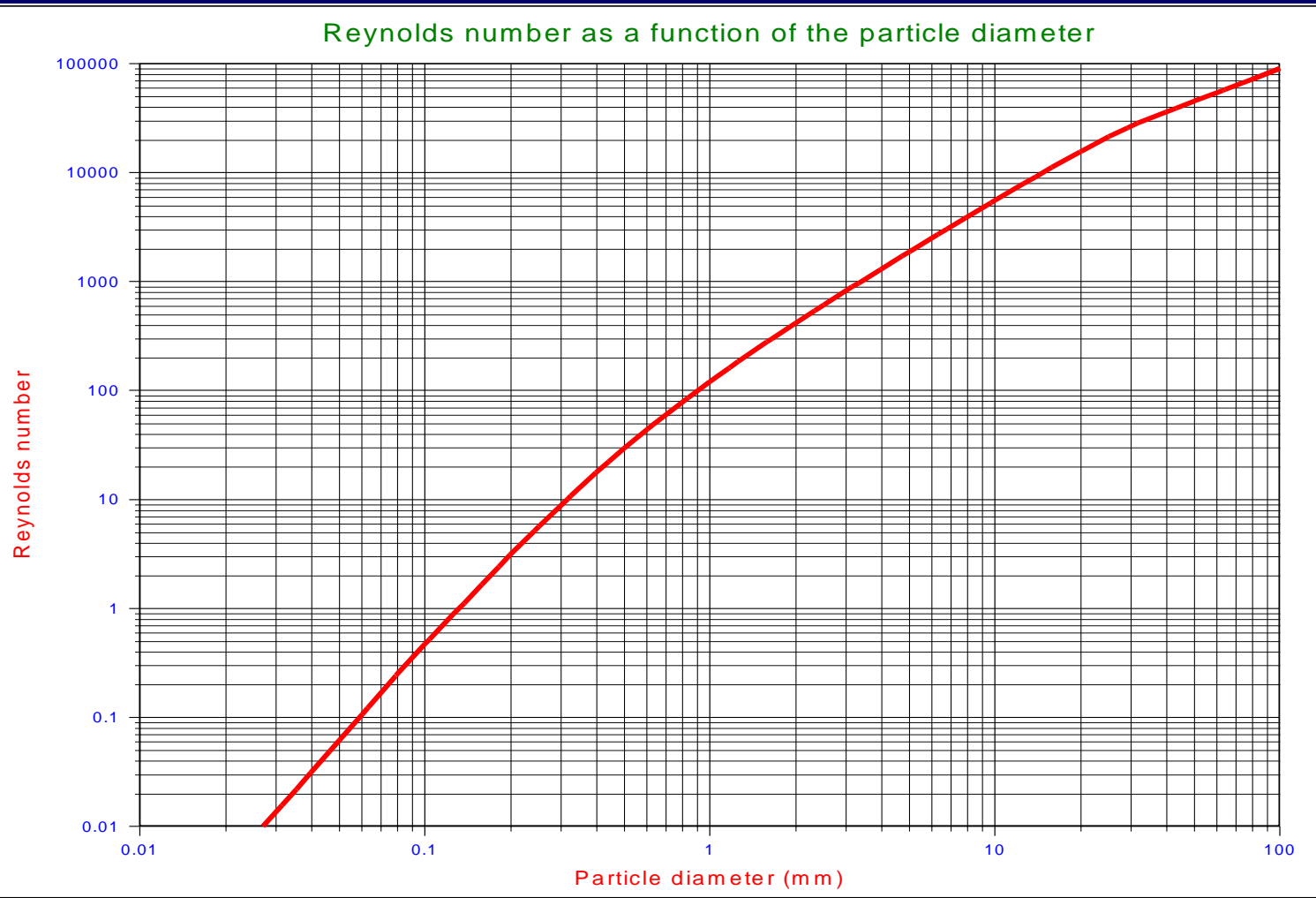
$$Re_p < 1 \quad \Rightarrow \quad C_D = \frac{24}{Re_p}$$

$$Re_p > 2000 \quad \Rightarrow \quad C_D = 0.445$$

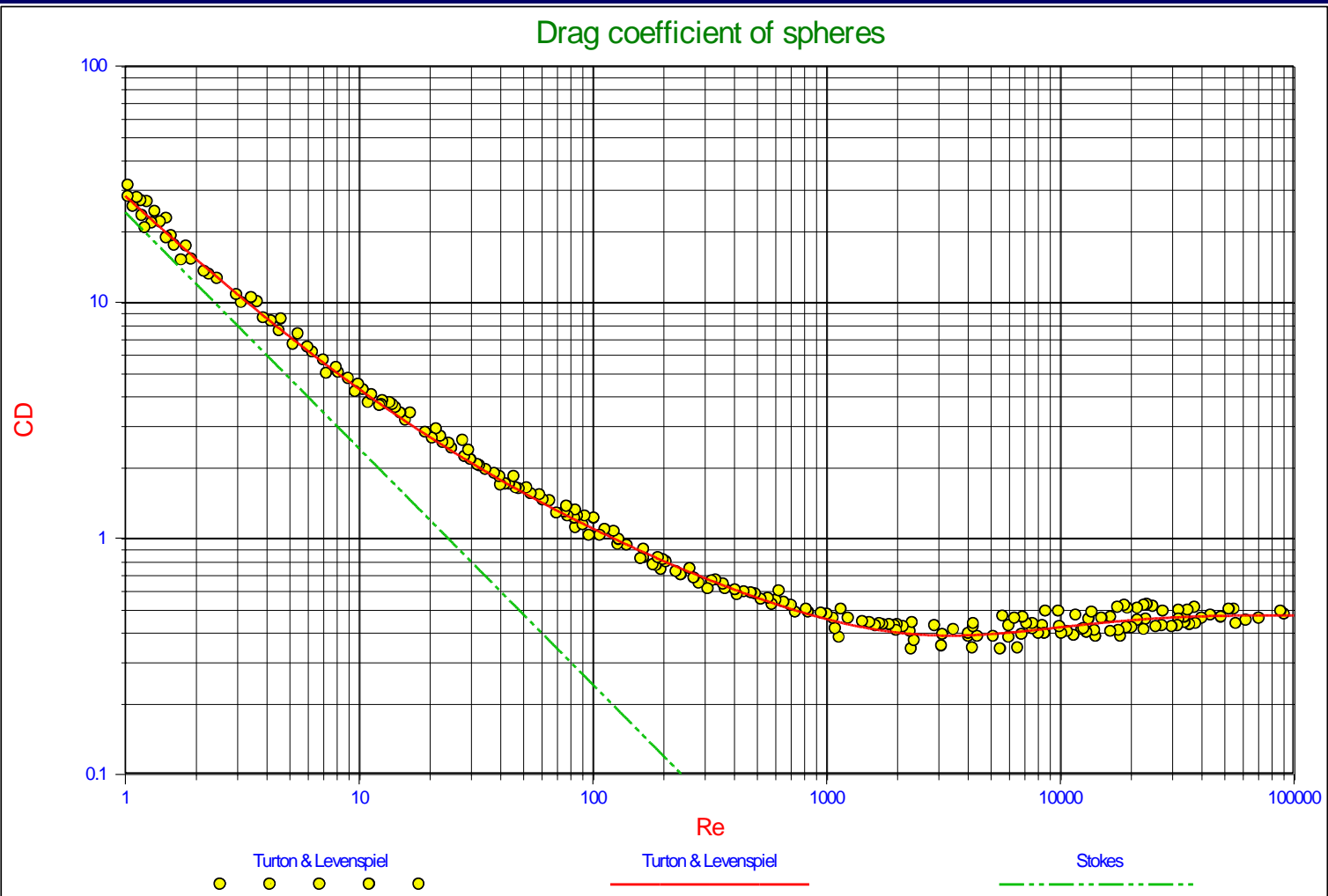
$$1 < Re_p < 2000 \quad \Rightarrow \quad C_D = \frac{24}{Re_p} + \frac{3}{\sqrt{Re_p}} + 0.34$$



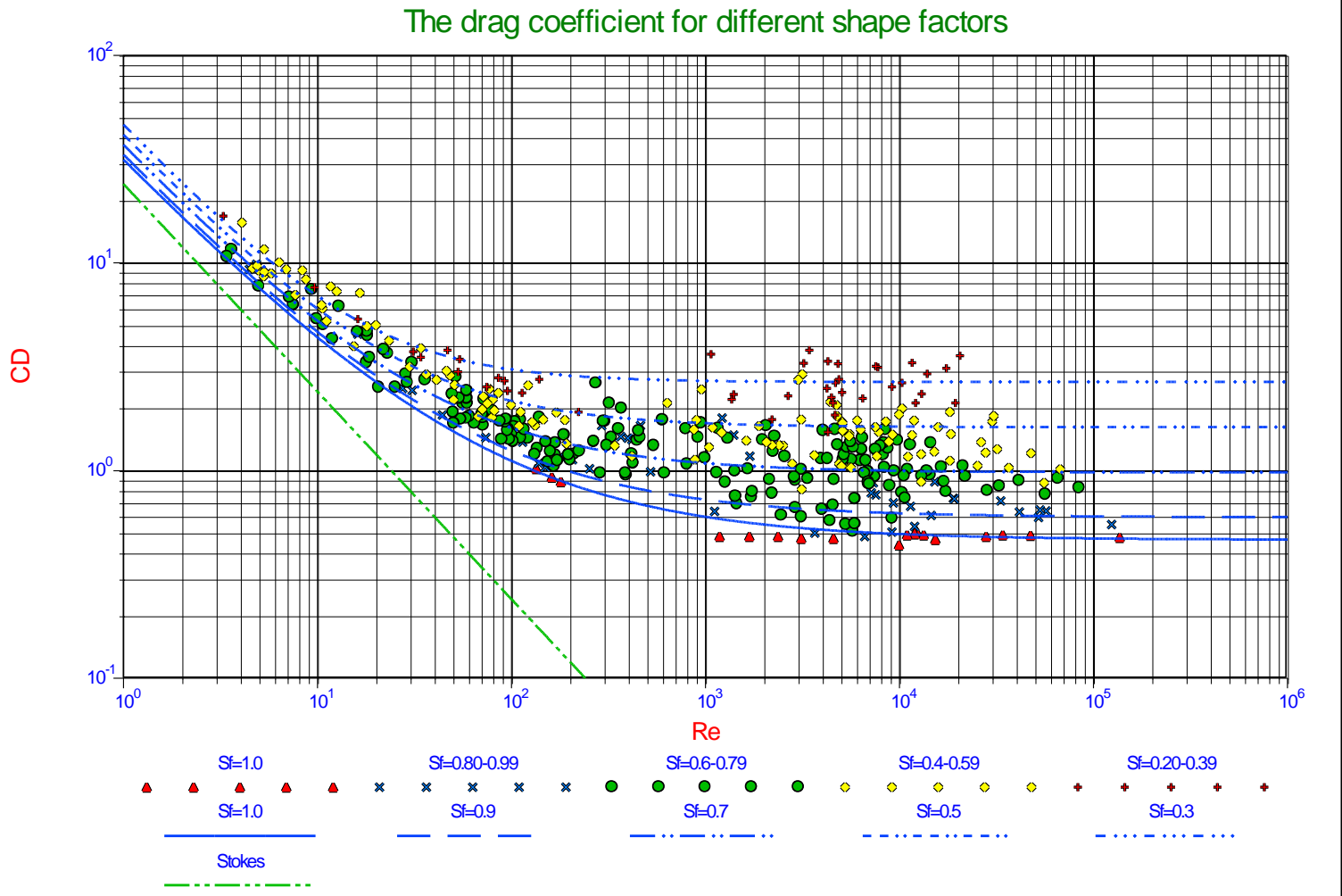
The Reynolds Number as a Function of the Particle Diameter



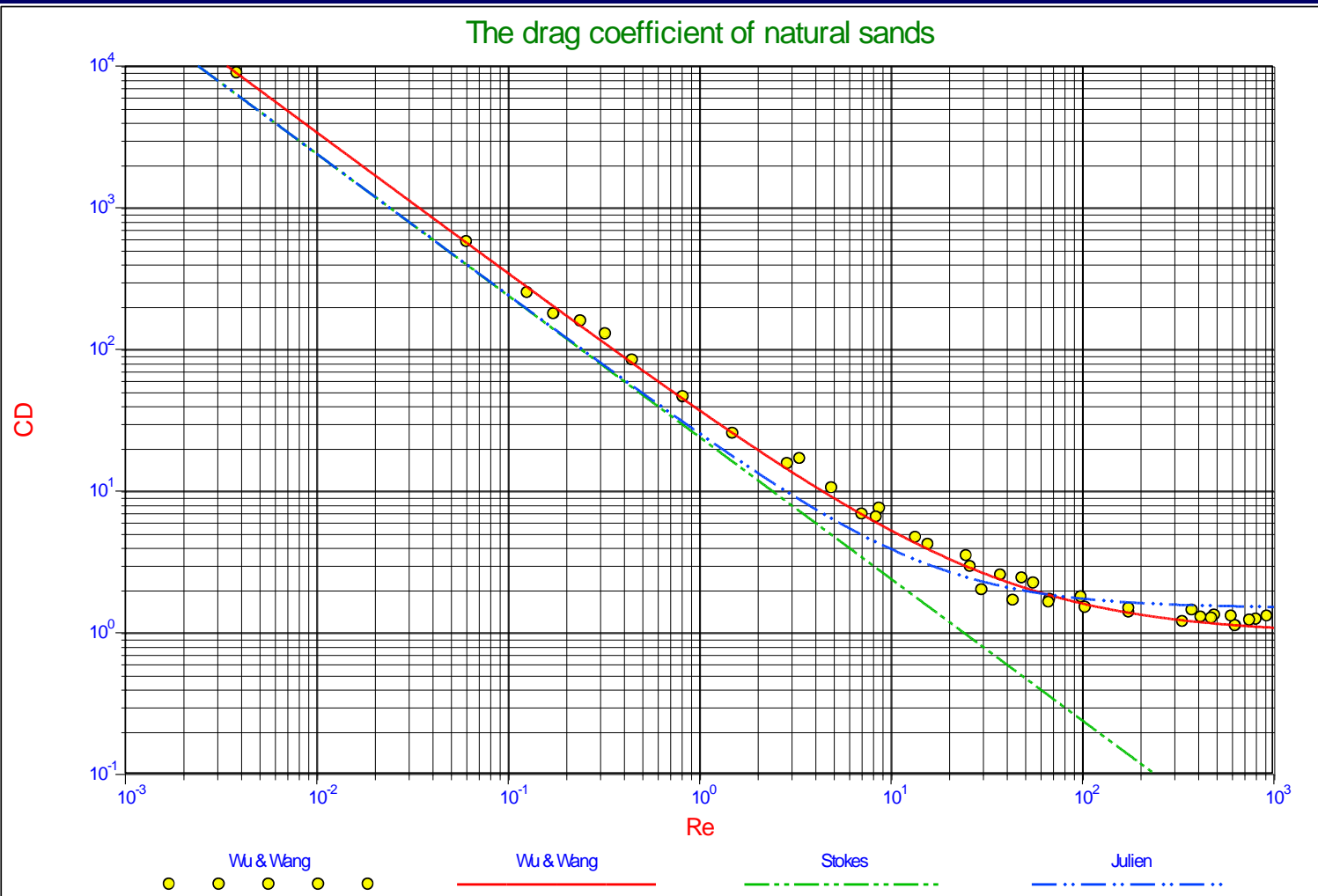
The Drag Coefficient as a Function of the Particle Reynolds Number, Spheres



The Drag Coefficient as a Function of the Particle Reynolds Number, Shapes



The Drag Coefficient as a Function of the Particle Reynolds Number, Sands



The Settling Velocity of Individual Particles

Laminar flow, $d < 0.1$ mm, according to Stokes.

$$v_t = 424 \cdot R_{sd} \cdot d^2$$

Transition zone, $d > 0.1$ mm and $d < 1$ mm, according to Budryck.

$$v_t = 8.925 \cdot \frac{\left(\sqrt{(1 + 95 \cdot R_{sd} \cdot d^3)} - 1 \right)}{d}$$

Turbulent flow, $d > 1$ mm, according to Rittinger.

$$v_t = 87 \cdot \sqrt{R_{sd} \cdot d}$$

With the relative density R_{sd} defined as:

$$R_{sd} = \frac{\rho_s - \rho_l}{\rho_l}$$

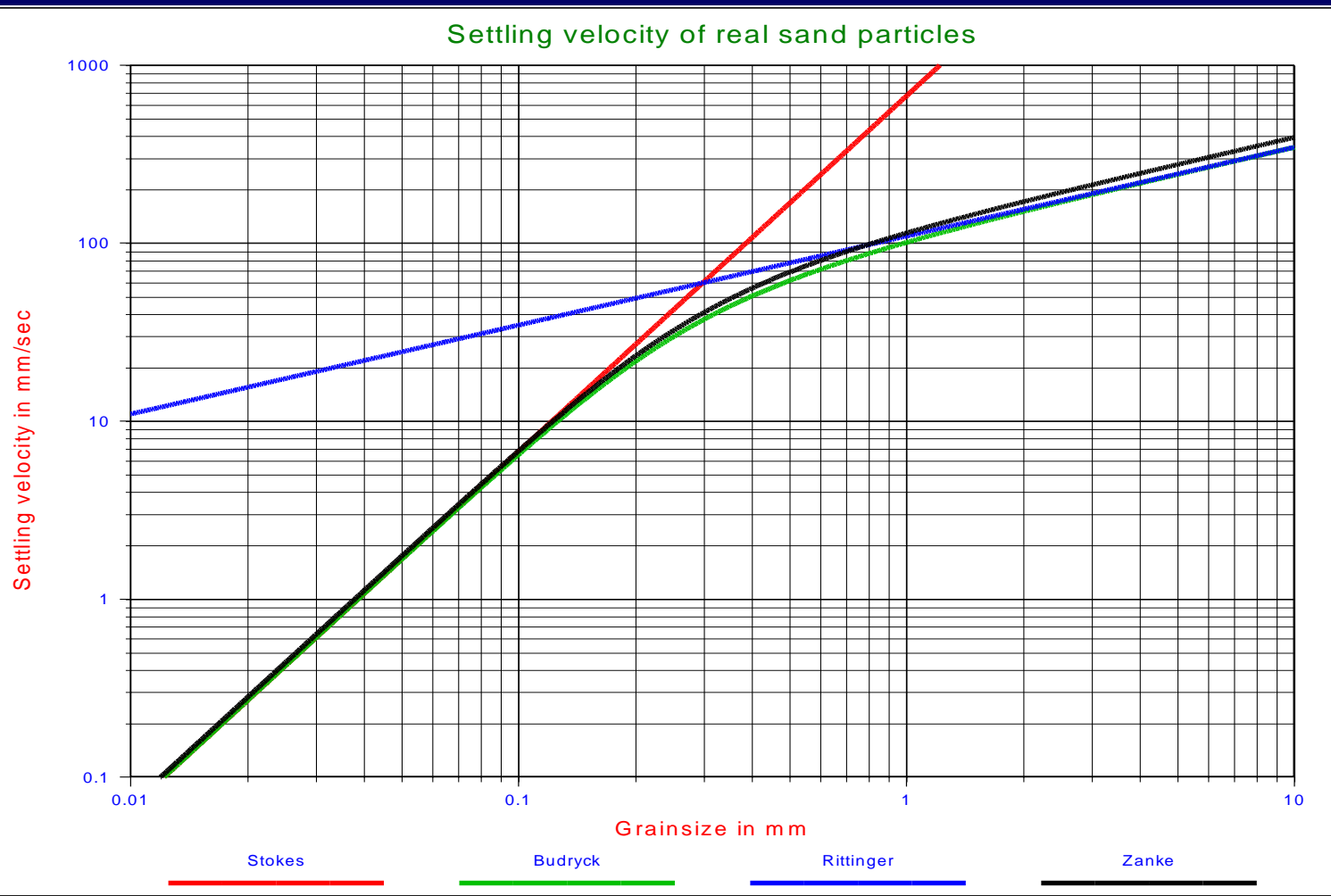


The Settling Velocity of Individual Particles according to Zanke

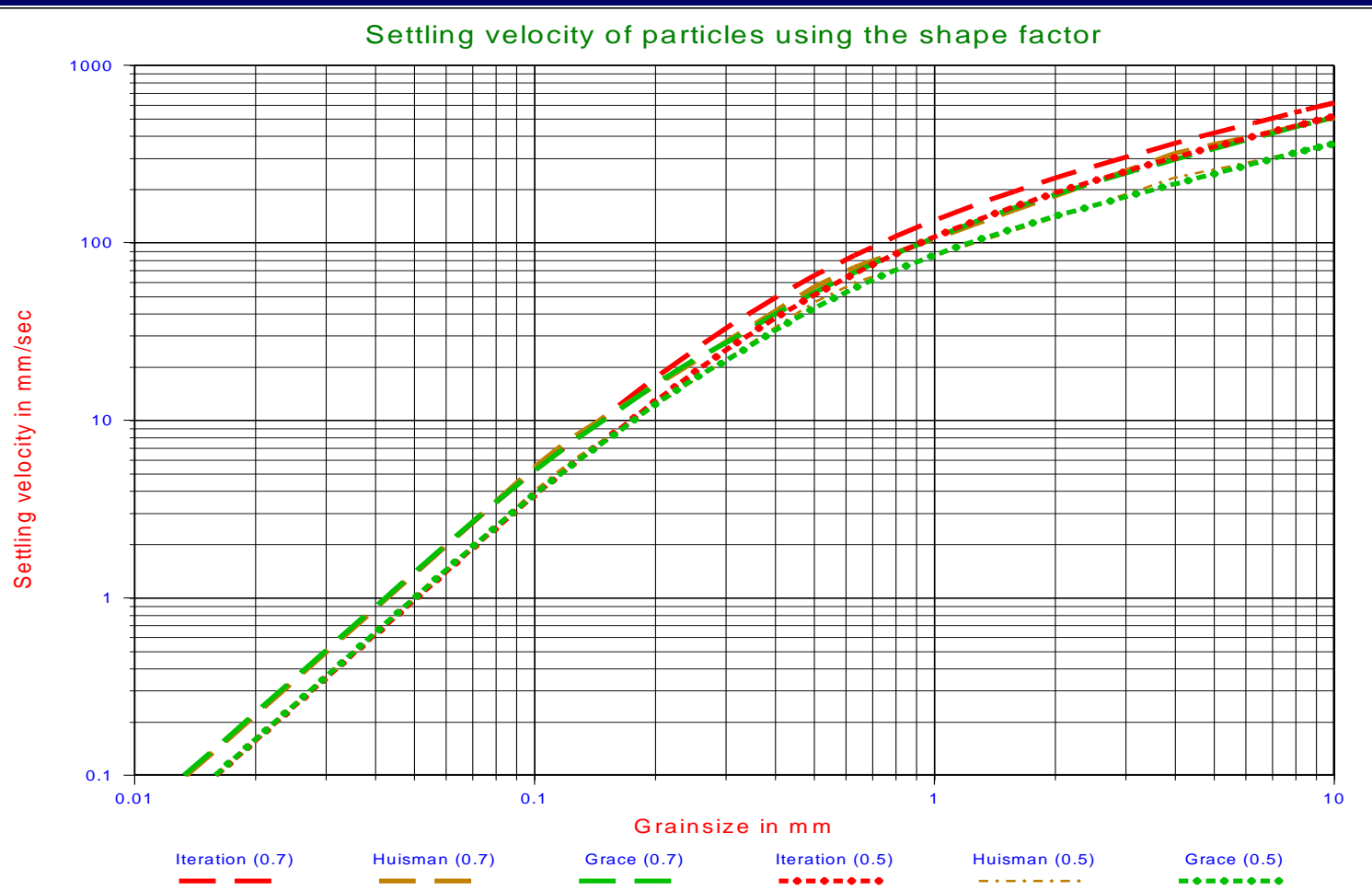
$$v_t = \frac{10 \cdot v_l}{d} \cdot \left(\sqrt{1 + \frac{R_{sd} \cdot g \cdot d^3}{100 \cdot v_l^2}} - 1 \right)$$



The Settling Velocity of Individual Particles



The Settling Velocity of Individual Particles using the Shape Factor



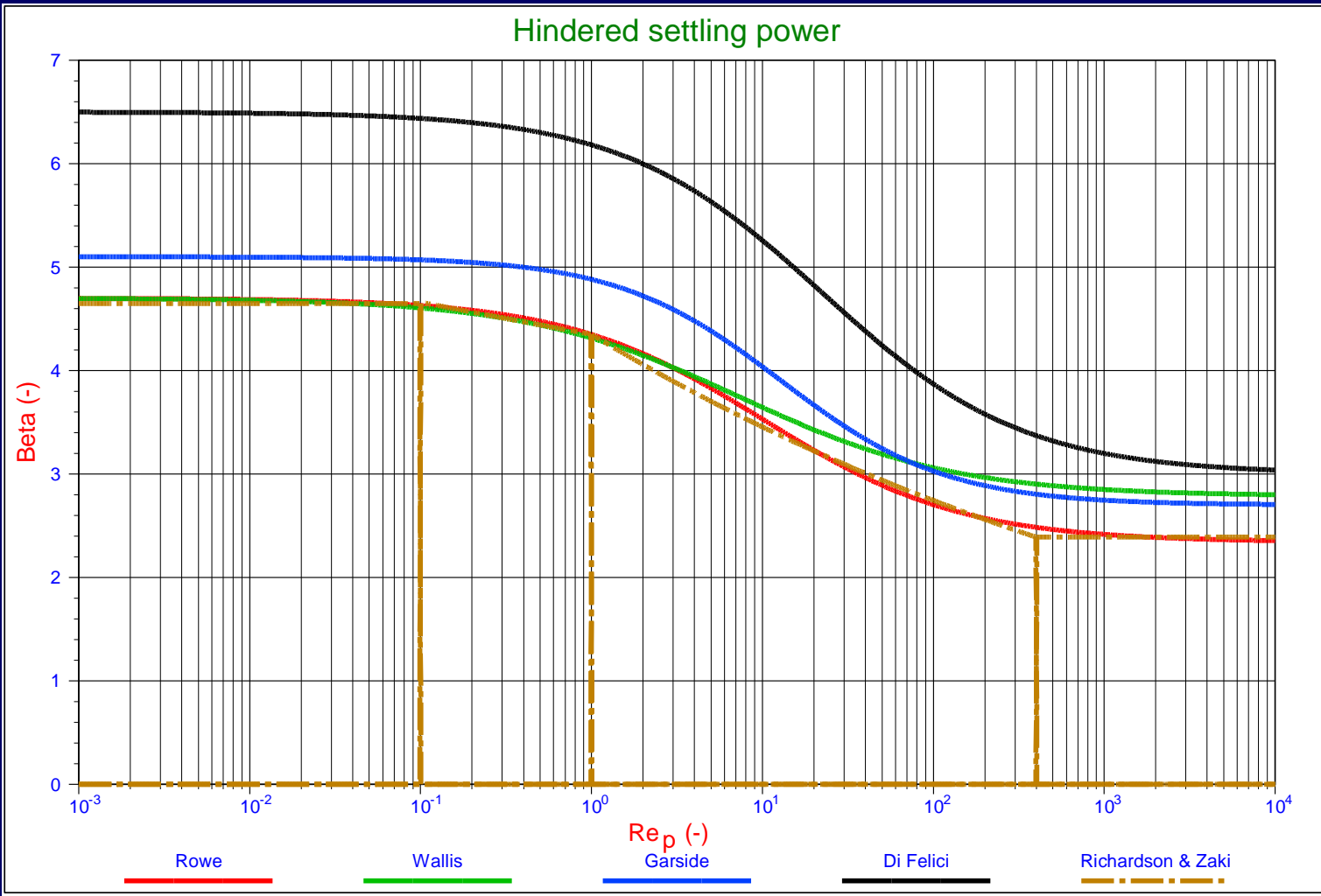
Hindered Settling (Rowe)

$$v_{th} = v_t \cdot (1 - C_v)^\beta$$

$$\beta = \frac{4.7 + 0.41 \cdot \text{Re}_p^{0.75}}{1 + 0.175 \cdot \text{Re}_p^{0.75}}$$



The Hindered Settling Power according to Several Researchers



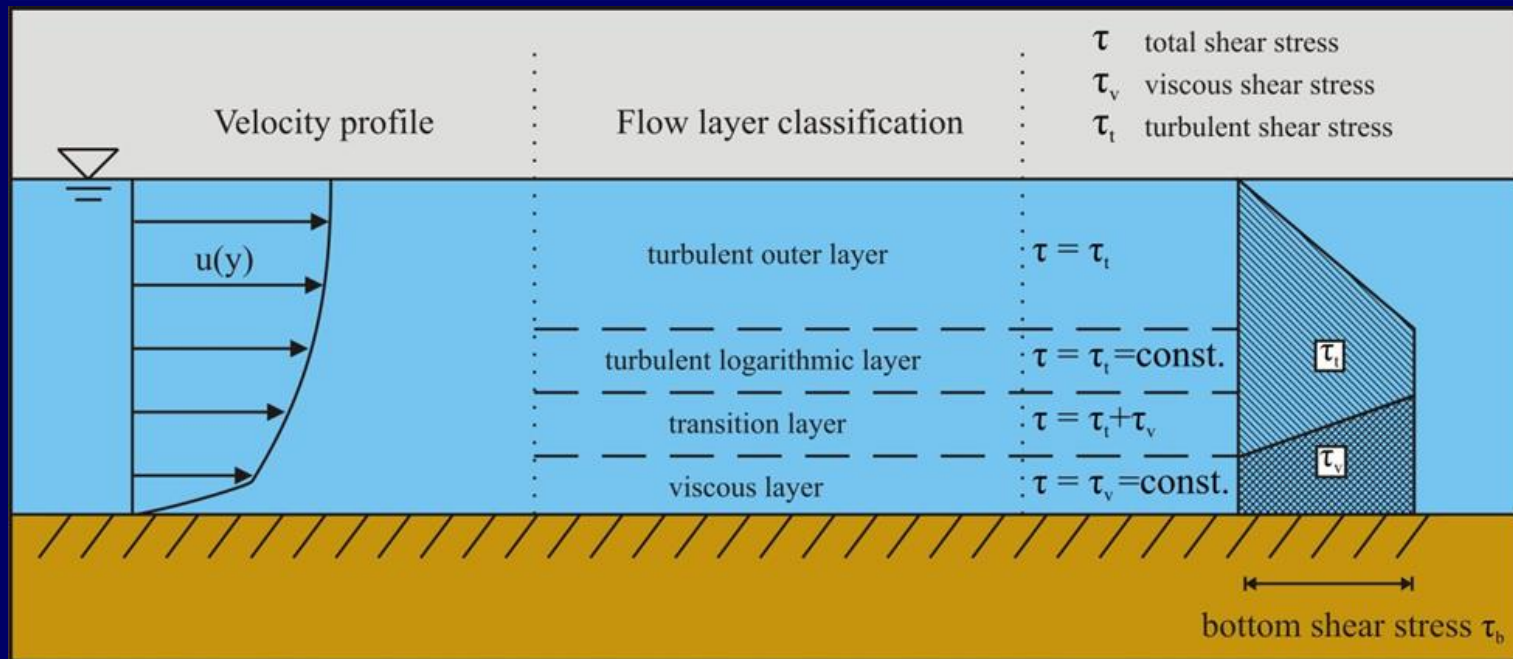


Velocity Distribution

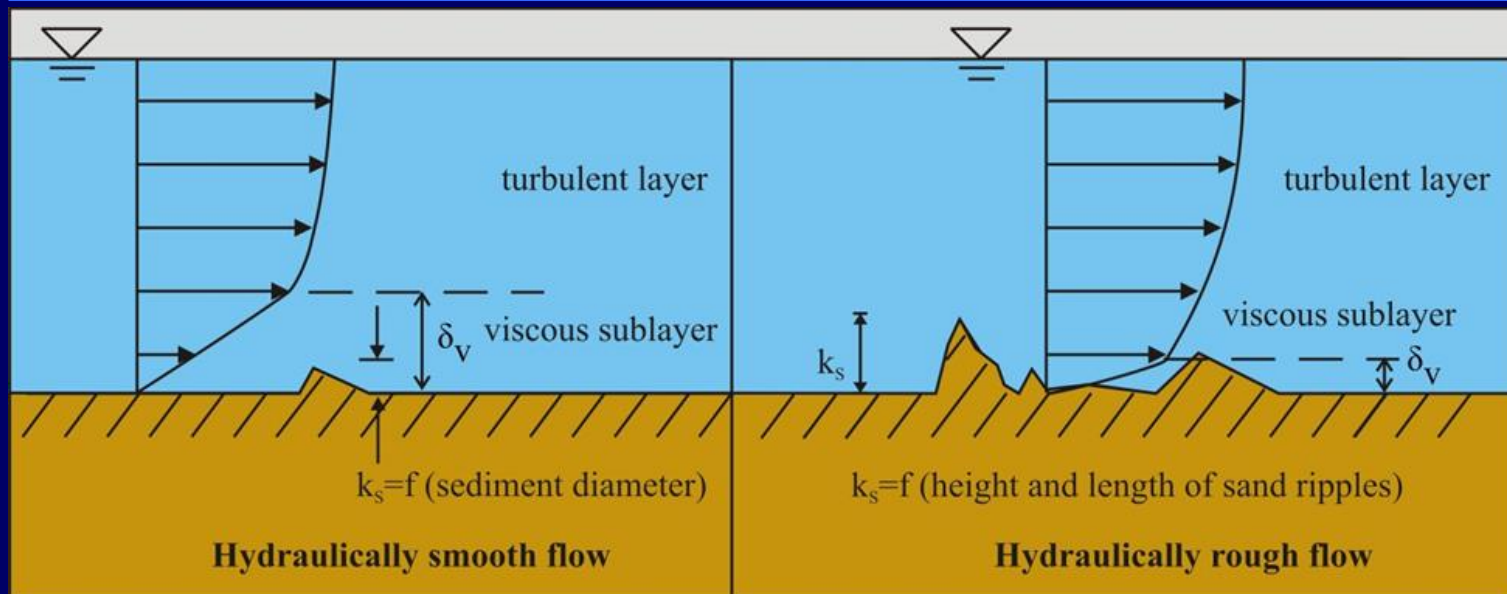
Chapter 5



Classification of Flow Layers



Engineering Classification



Velocity distribution

Viscous sublayer

$$u(z) = \frac{\tau_b}{\rho_l} \cdot \frac{z}{\nu_l} = \frac{u_*^2}{\nu_l} \cdot z$$

Turbulent layer

$$u(z) = \frac{u_*}{\kappa} \ln \left(\frac{z}{z_0} \right)$$



Friction Velocity

The bottom shear stress is often represented by friction velocity, defined by:

$$u_* = \sqrt{\frac{\tau_b}{\rho}}$$

$$u_*^2 = \frac{\lambda_1}{8} \cdot U^2 = \frac{\lambda_1}{8} \cdot v_{1s}^2$$

The term *friction velocity* comes from the fact that: $\sqrt{\tau_b / \rho_1}$

has the same unit as velocity and it has something to do with friction force.

Theoretical viscous sub layer thickness: $\delta_v = 11.6 \cdot \frac{v_1}{u_*}$

Velocity at top of viscous sub layer: $u(\delta_v) = \frac{u_*^2}{v_1} \cdot 11.6 \cdot \frac{v_1}{u_*} = 11.6 \cdot u_*$





Existing Models

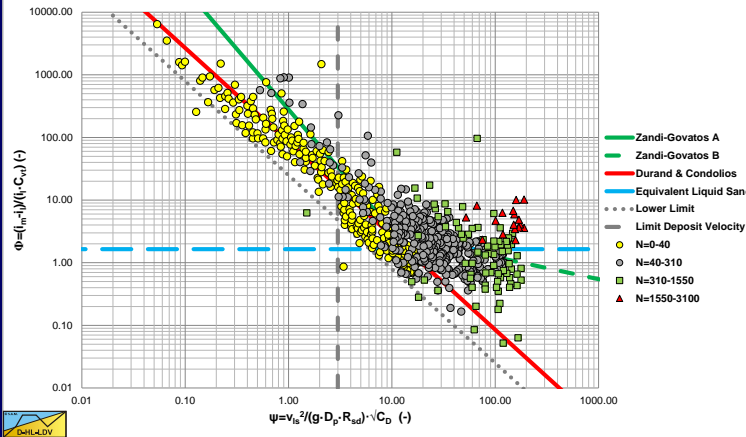
Chapter 6



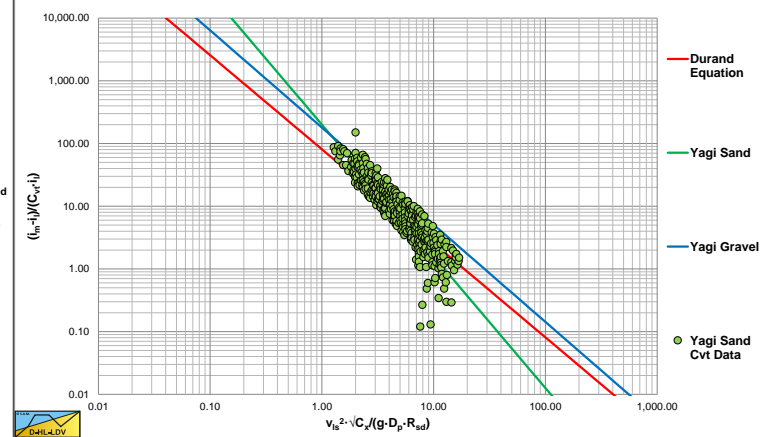
Zandi & Govatos, Yagi et al. & Babcock



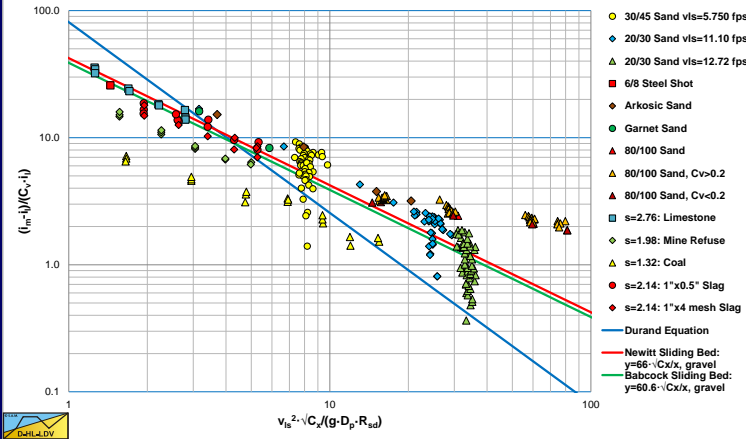
Zandi-Govatos (1967) on Durand coordinates



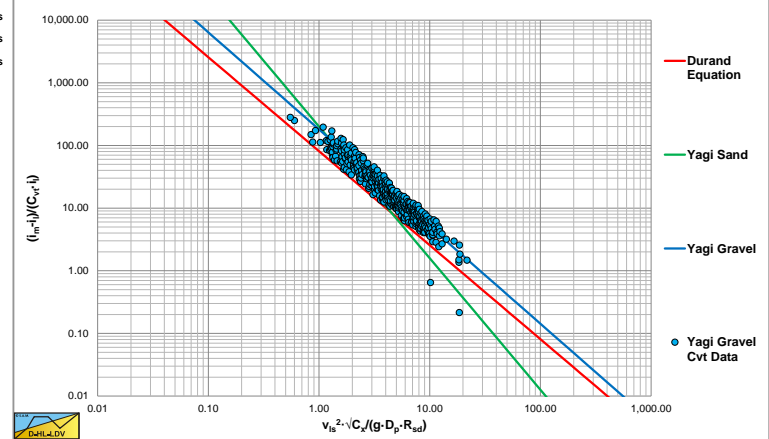
Durand Gradient vs. the Durand Coordinate, Yagi et al. (1972)



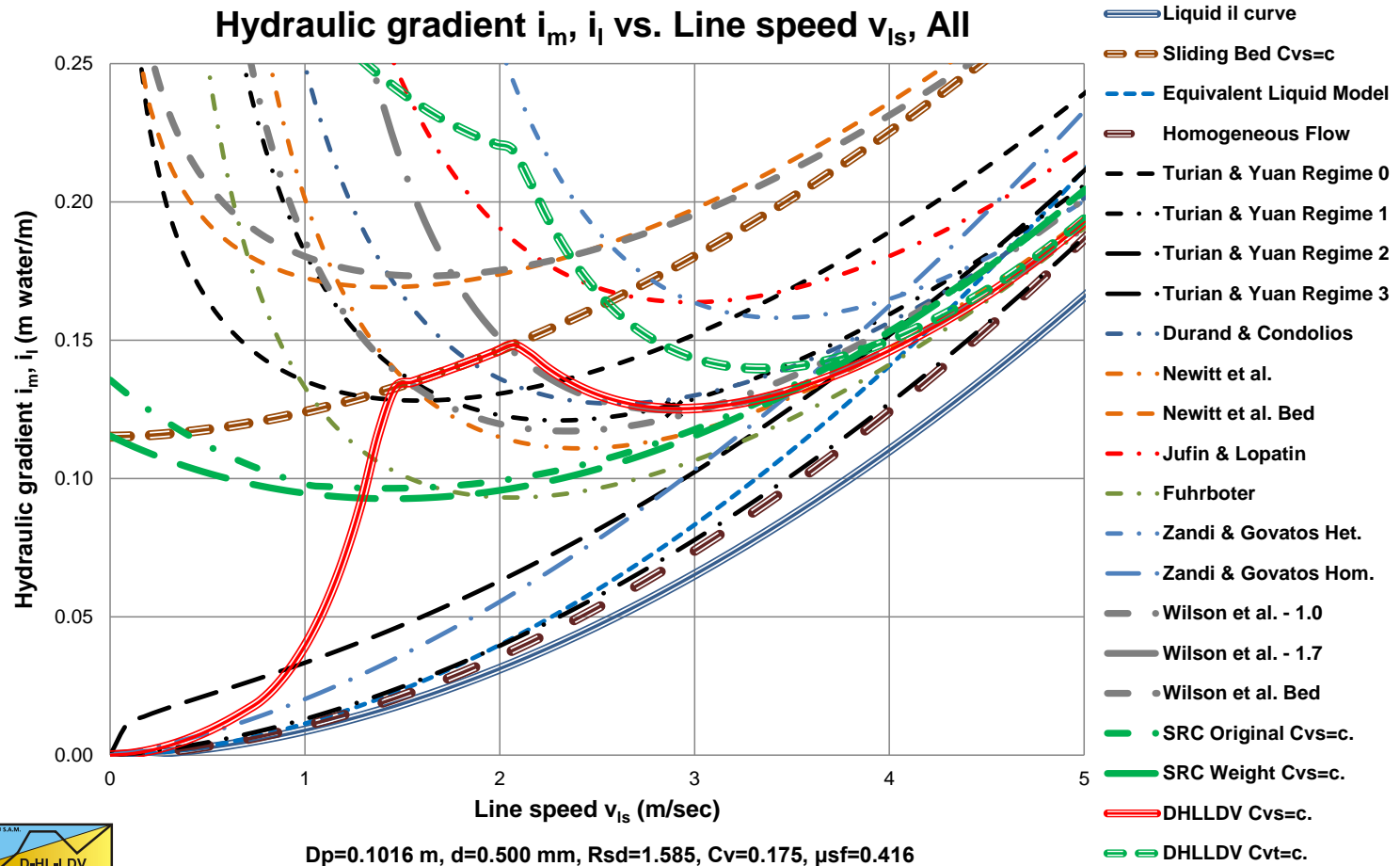
Durand Gradient vs. the Durand Coordinate, Babcock (1970)



Durand Gradient vs. the Durand Coordinate, Yagi et al. (1972)



22 Models i_m - v_{ls} graph



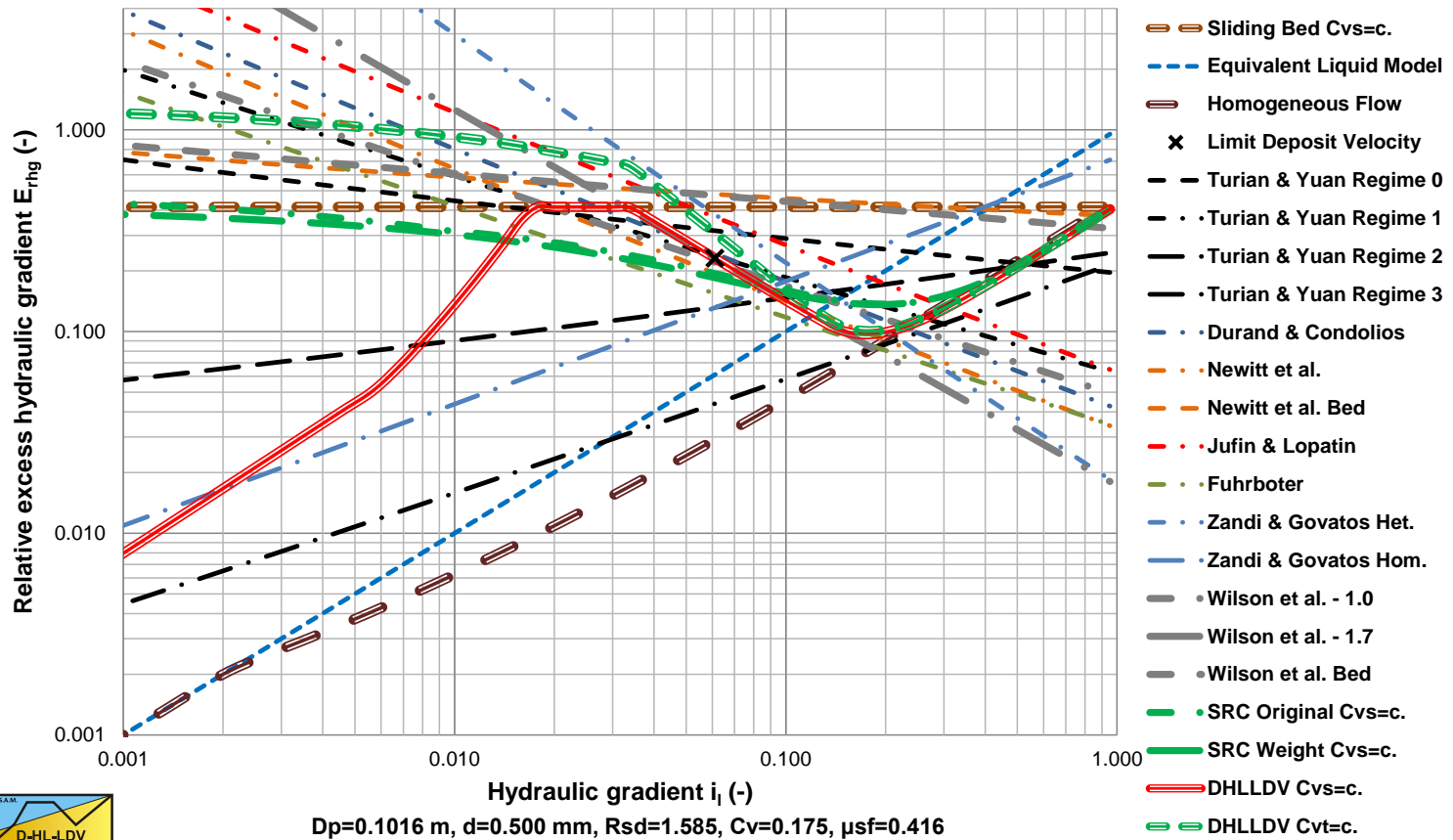
For small pipe diameters the models are still “close”. For large diameter pipes the difference is much much more.

Delft University of Technology – Offshore & Dredging Engineering



22 Models E_{rhg} - i_1 graph

Relative excess hydraulic gradient E_{rhg} vs. Hydraulic gradient i_1



This graph organizes the models better, but there is still a lot of difference between the models.

Delft University of Technology – Offshore & Dredging Engineering



The Elephant of Wilson





Existing Models Analysis



Types of Models

- There are many empirical models, mainly for heterogeneous flow, some for sliding bed and homogeneous flow
- Most empirical models add one term to the Darcy-Weisbach equation, often based on Froude numbers
- There is the equivalent liquid model (ELM) for homogeneous flow
- There are some 2 layer and 3 layer models for transport with a stationary or sliding bed or sheet flow, Wilson, Doron & Barnea, SRC Model, Matousek
- The 2 layer and 3 layer models are closed with empirical equations for the bed shear stress and the concentration distribution



Problem Analysis

- There is no overall model connecting the different flow regimes (maybe except Newitt et al.)
- There are no generic models for identifying the different flow regimes
- Sometimes the solids effect depends on the hydraulic gradient of the liquid, sometimes it does not.
- Often the solids effect has a fixed ratio between parameters, like the Froude number, forcing a certain behavior
- The influence of the pipe diameter differs a lot from model to model
- The influence of the particle diameter differs less
- The influence of the volumetric concentration is not always clear



Existing Equations Depending on i_1

$$\Delta p_m = \Delta p_l \cdot (1 + \Phi \cdot C_{vt}) \quad \text{with:} \quad \Phi = \frac{i_m - i_l}{i_l \cdot C_{vt}} = \frac{\Delta p_m - \Delta p_l}{\Delta p_l \cdot C_{vt}}$$

Durand, Condolios & Gibert based on Froude numbers

$$\Phi = K \cdot \psi^{-3/2} = K \cdot \left(\frac{v_{ls}^2}{g \cdot D_p \cdot R_{sd}} \cdot \sqrt{C_x} \right)^{-3/2} \quad \text{with:} \quad K \approx 85$$

Newitt et al. based on potential energy losses

$$\Delta p_m = \Delta p_l \cdot \left(1 + K_1 \cdot (g \cdot D_p \cdot R_{sd}) \cdot v_t \cdot C_{vt} \cdot \left(\frac{1}{v_{ls}} \right)^3 \right) \quad K_1 = 1100$$

Jufin & Lopatin empirical large diameters

$$\Delta p_m = \Delta p_l \cdot \left(1 + 2 \cdot \left(\frac{v_{\min}}{v_{ls}} \right)^3 \right) \Rightarrow v_{\min} = 5.5 \cdot (C_{vt} \cdot \psi^* \cdot D_p)^{1/6}$$



Existing Equations Independent of i_1

Fuhrboter medium diameters

$$\Delta p_m = \Delta p_l + \rho_l \cdot g \cdot \Delta L \cdot \frac{S_k}{v_{ls}} \cdot C_{vs}$$

$$i_m - i_l = \frac{S_k}{v_{ls}} \cdot C_{vs} \quad \Rightarrow \quad E_{rhg} = \frac{i_m - i_l}{R_{sd} \cdot C_{vs}} = \frac{S_k}{R_{sd} \cdot v_{ls}}$$

Wilson heterogeneous empirical (Stratification Ratio)

$$\Delta p_m = \Delta p_l + \frac{\mu_{sf}}{2} \cdot \rho_l \cdot g \cdot R_{sd} \cdot \Delta L \cdot \left(\frac{v_{50}}{v_{ls}} \right)^M \cdot C_{vt}$$

$$i_m - i_l = \frac{\mu_{sf}}{2} \cdot R_{sd} \cdot \left(\frac{v_{50}}{v_{ls}} \right)^M \cdot C_{vt} \quad \Rightarrow \quad E_{rhg} = \frac{\mu_{sf}}{2} \cdot \left(\frac{v_{50}}{v_{ls}} \right)^M = R$$



Existing Equations Summary

All equations have the solids effect in just one term, limiting the possibilities to get a high correlation with experimental data.

The first 3 equations multiply the solids effect with the Darcy Weisbach equation, making it dependent on the Darcy-Weisbach friction coefficient from the Moody diagram.

$$\Delta p_m = \Delta p_l \cdot (1 + \Phi \cdot C_{vt}) \quad \text{with:} \quad \Phi = \frac{i_m - i_l}{i_l \cdot C_{vt}} = \frac{\Delta p_m - \Delta p_l}{\Delta p_l \cdot C_{vt}}$$

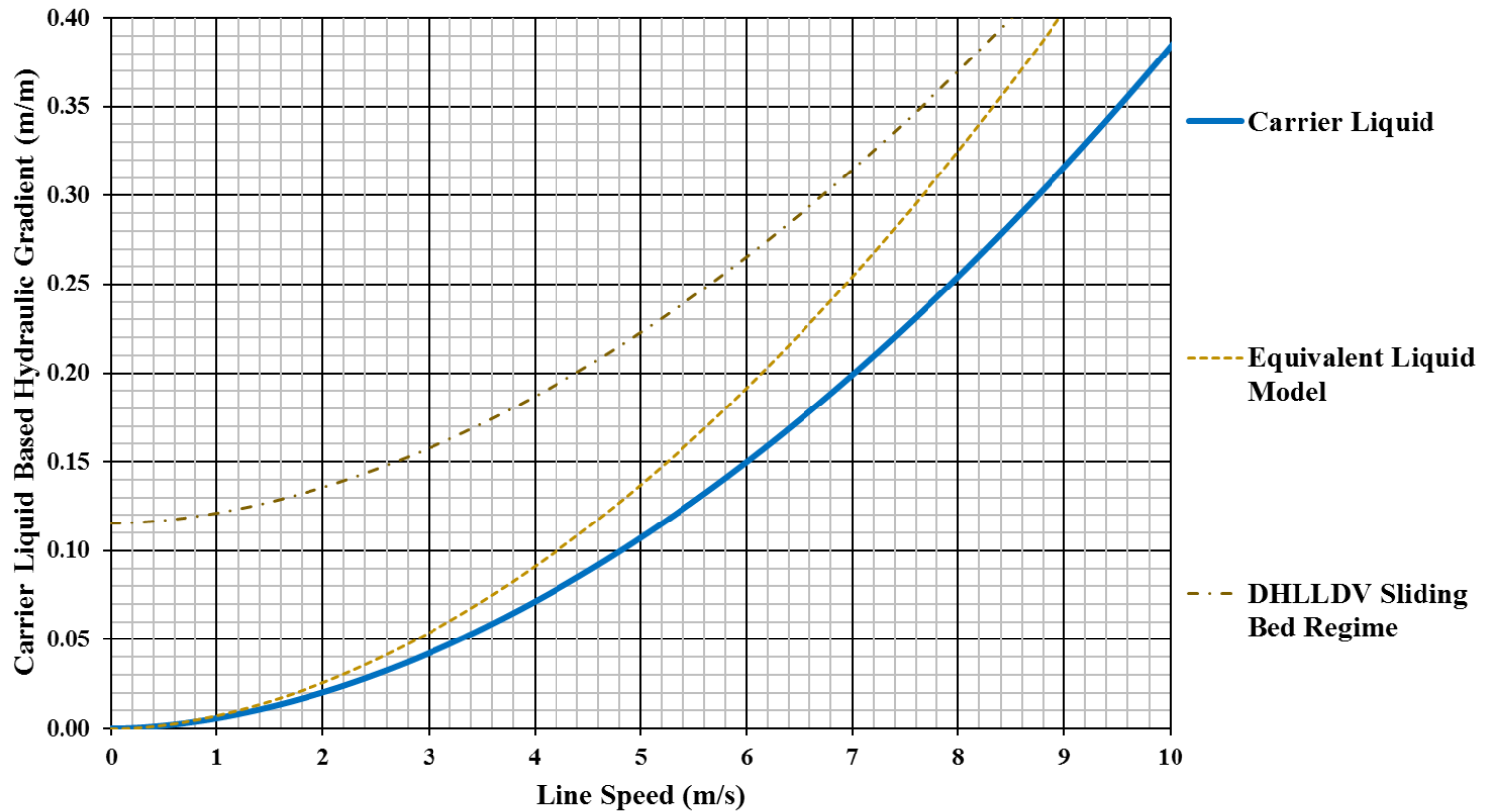
$$E_{rhg} = \frac{i_m - i_l}{R_{sd} \cdot C_{vt}} = \frac{i_l \cdot \Phi \cdot C_{vt}}{R_{sd} \cdot C_{vt}} = \frac{i_l \cdot \Phi}{R_{sd}}$$

The Wilson & Fuhrboter equations have an independent solids effect.



Reference System i_m-v_{ls} graph

Carrier Liquid Based Hydraulic Gradients Uniform & Graded Solids, C_{vs}

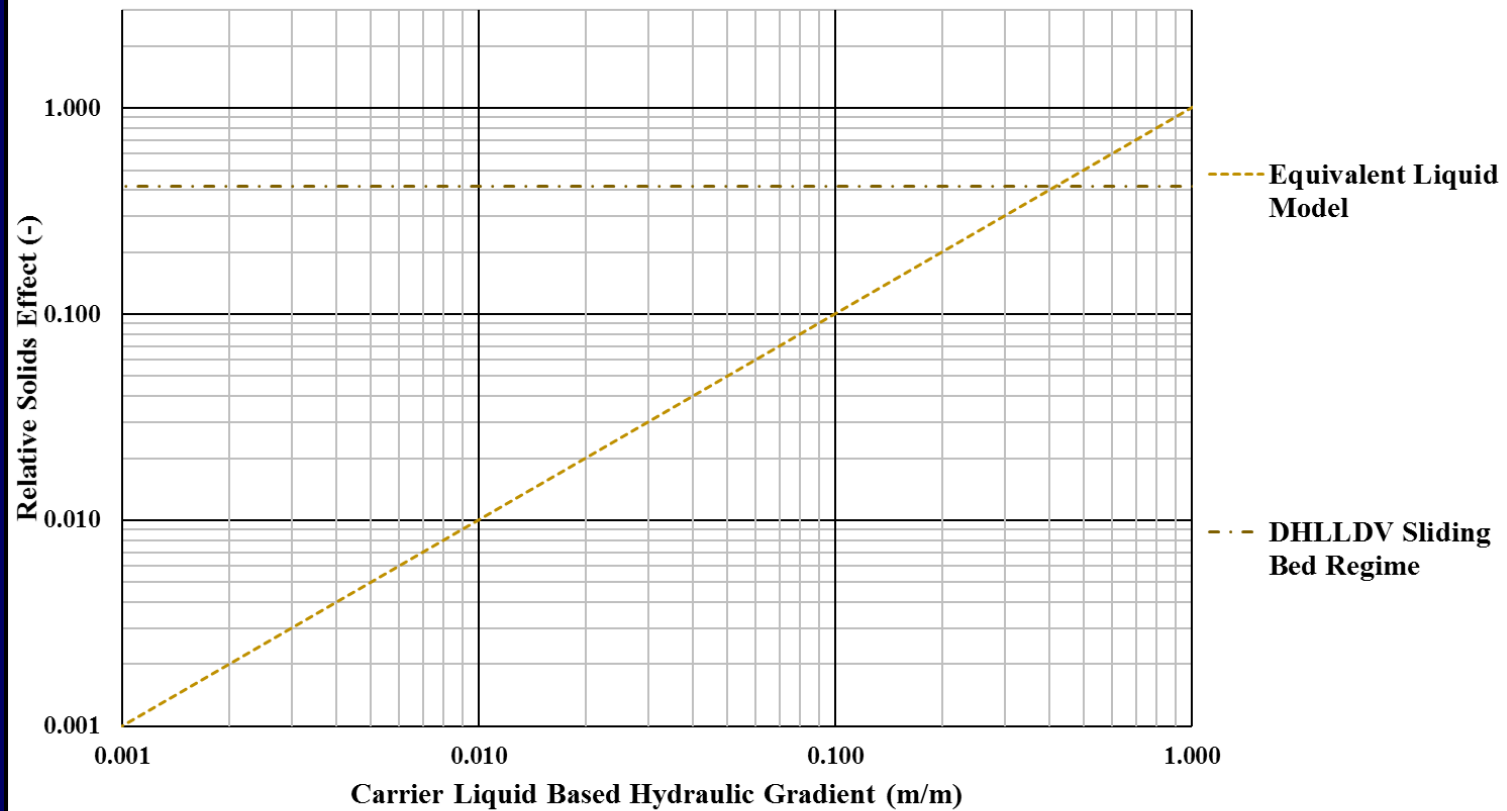


$D_p=0.1524$ m, $d=1.000$ mm, $R_{sd}=1.585$, $C_{vs}=0.175$, $\mu_{sf}=0.416$, $\rho_{cl}=1.025$ ton/m³, $C_{vb}=0.55$, $\theta=0.00^\circ$



Reference System $E_{rhg}-i_l$ graph

Carrier Liquid Based Relative Solids Effect Uniform & Graded Solids, C_{vs}

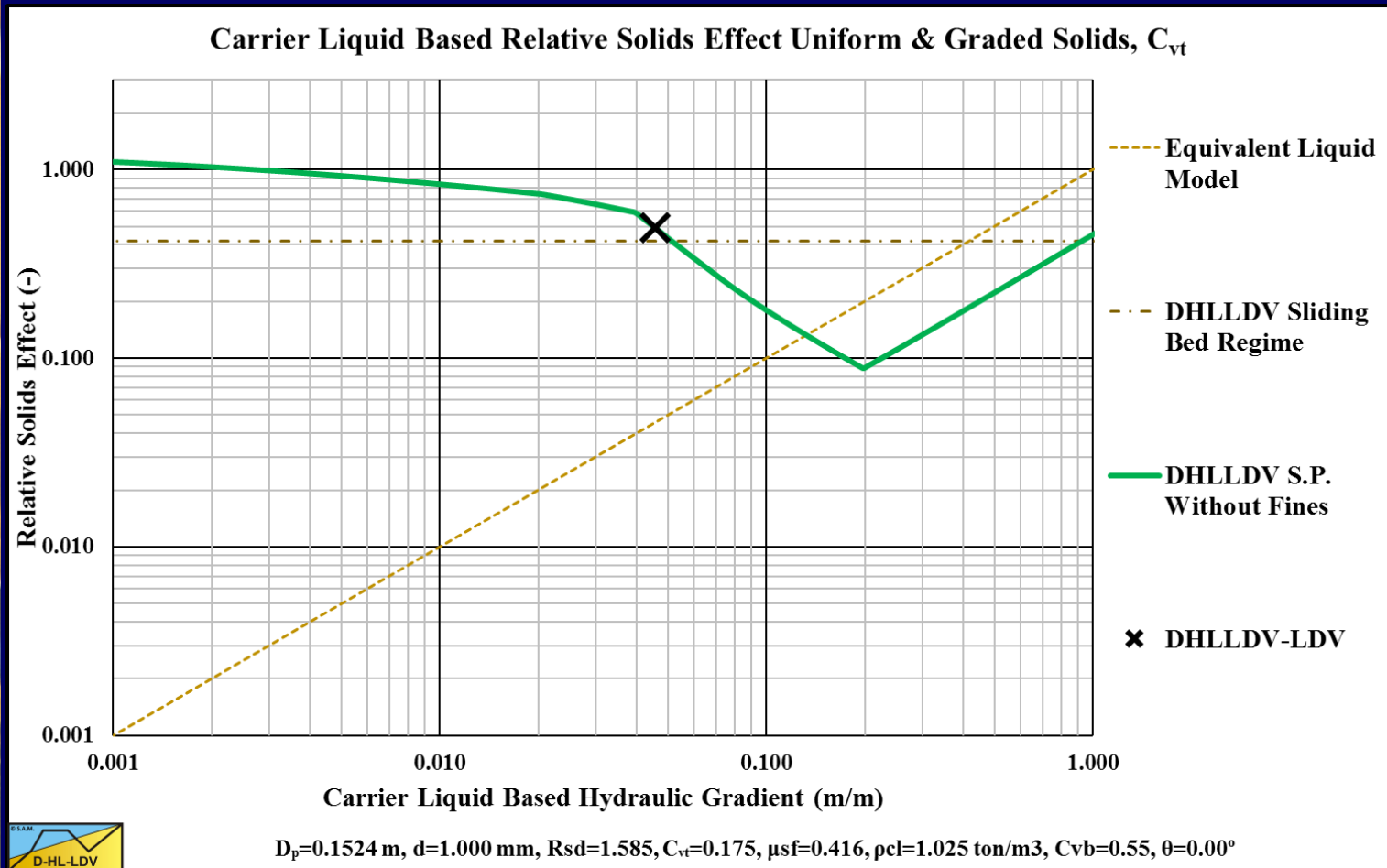


$D_p=0.1524$ m, $d=1.000$ mm, $R_{sd}=1.585$, $C_{vs}=0.175$, $\mu_{sf}=0.416$, $\rho_{cl}=1.025$ ton/m³, $C_{vb}=0.55$, $\theta=0.00^\circ$

This graph organizes the models better.



Resulting $E_{rhg}-i_l$ graph shape

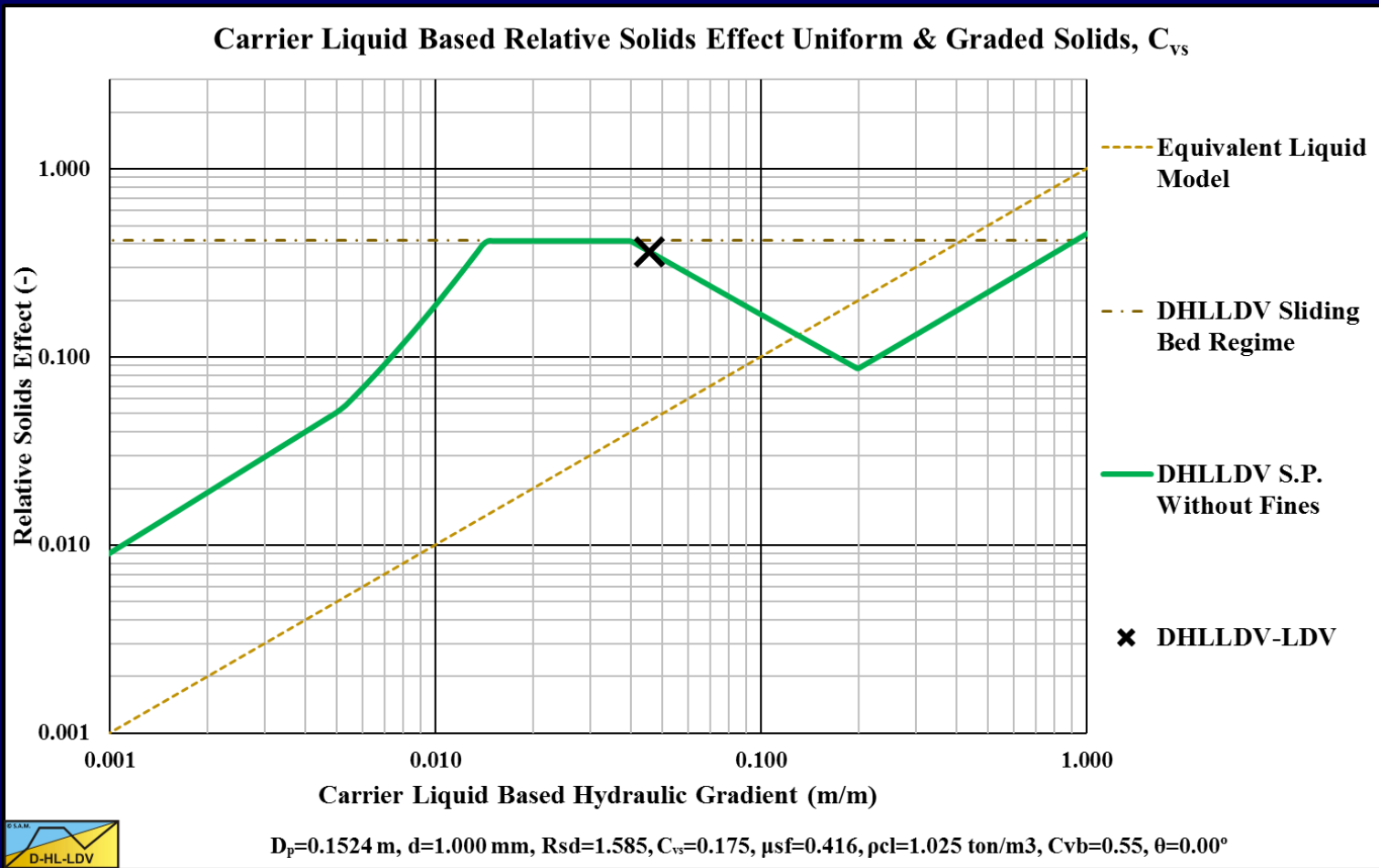


The shape of the relative solids effect curve for constant transport concentration.

Delft University of Technology – Offshore & Dredging Engineering



Resulting $E_{rhg}-i_l$ graph shape

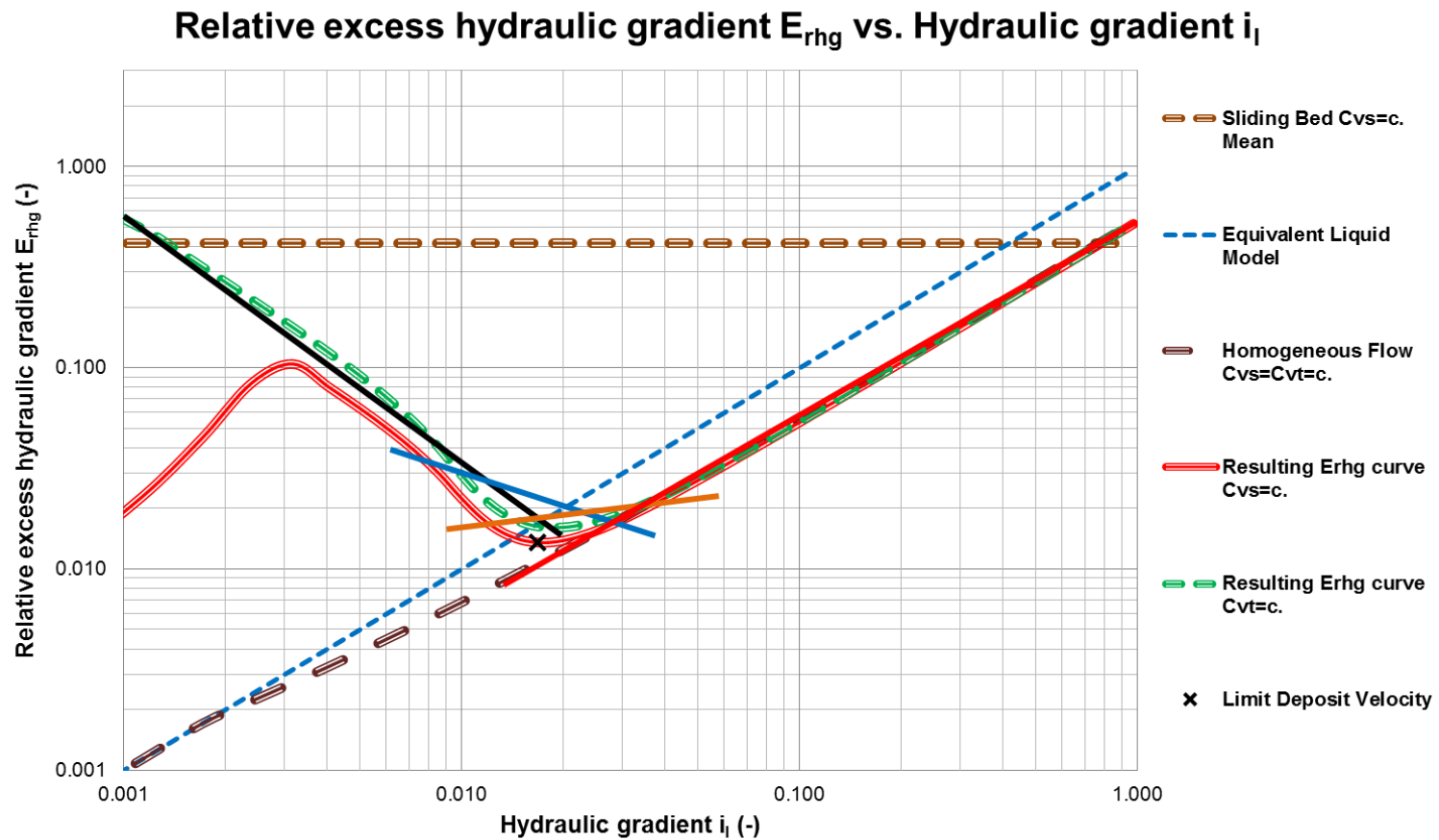


The shape of the relative solids effect curve for constant spatial concentration.

Delft University of Technology – Offshore & Dredging Engineering



Different Models Fine Sand

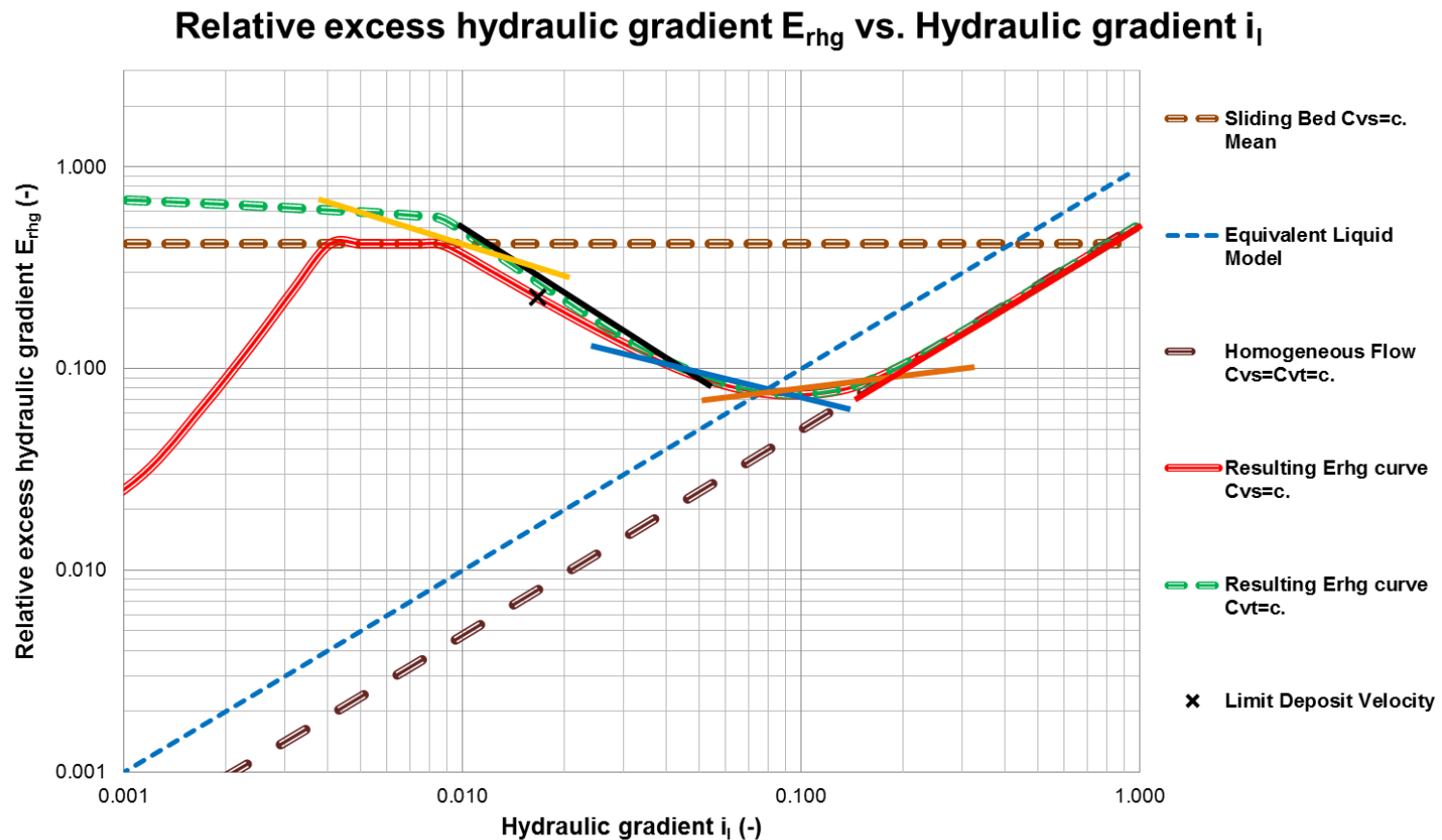


$D_p=0.7620$ m, $d=0.200$ mm, $R_{sd}=1.585$, $C_v=0.300$, $\mu_{sf}=0.416$

4 possible models: Black heterogeneous, blue pseudo homogeneous, light brown pseudo homogeneous & red homogeneous.



Different Models Coarse Sand & Gravel

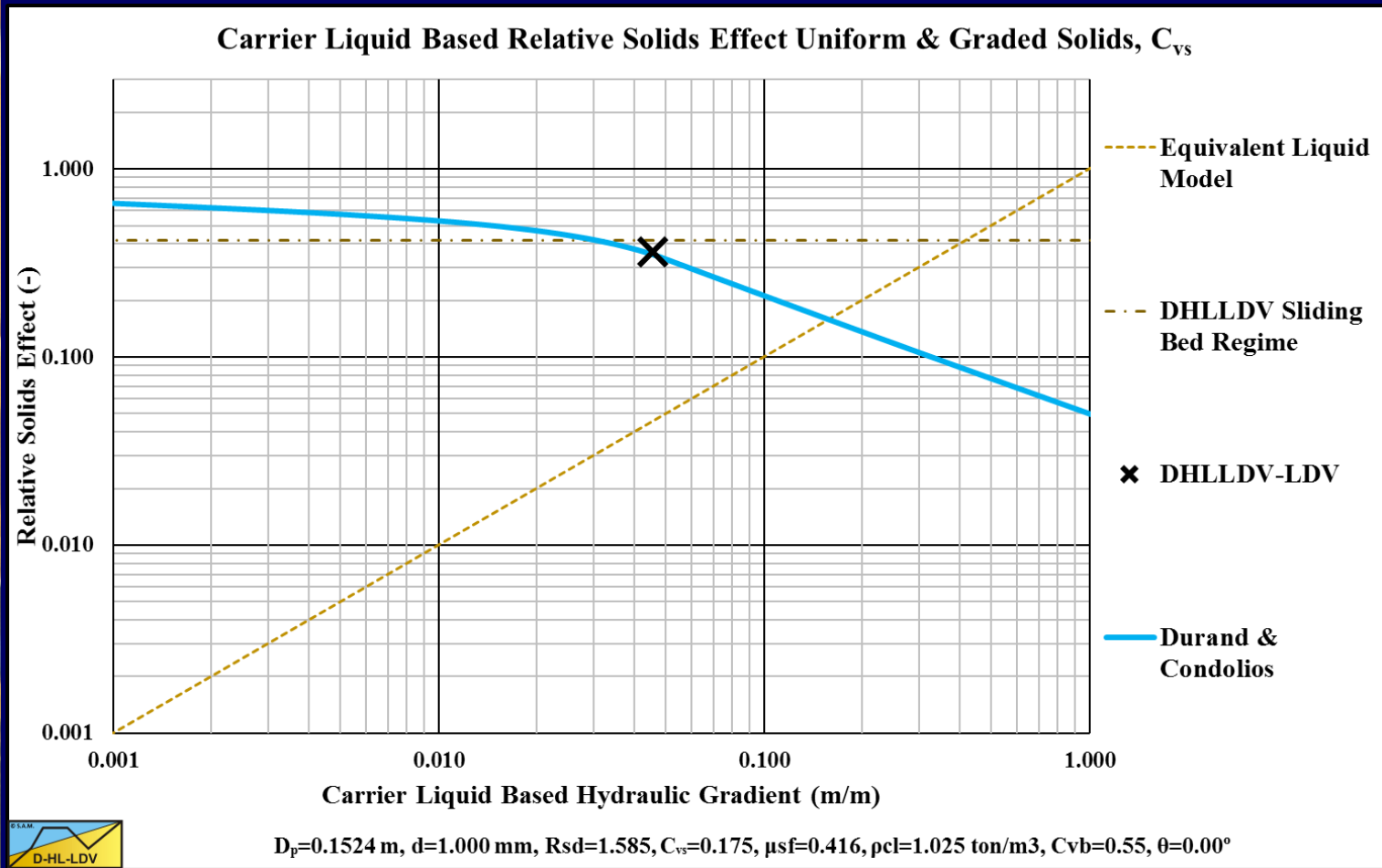


$D_p=0.7620$ m, $d=2.000$ mm, $R_{sd}=1.585$, $C_v=0.300$, $\mu_{sf}=0.416$

5 possible models: Orange SB/He, black He, blue pseudo Ho, light brown pseudo Ho & red Ho.



Adding Durand & Condolios to the graph

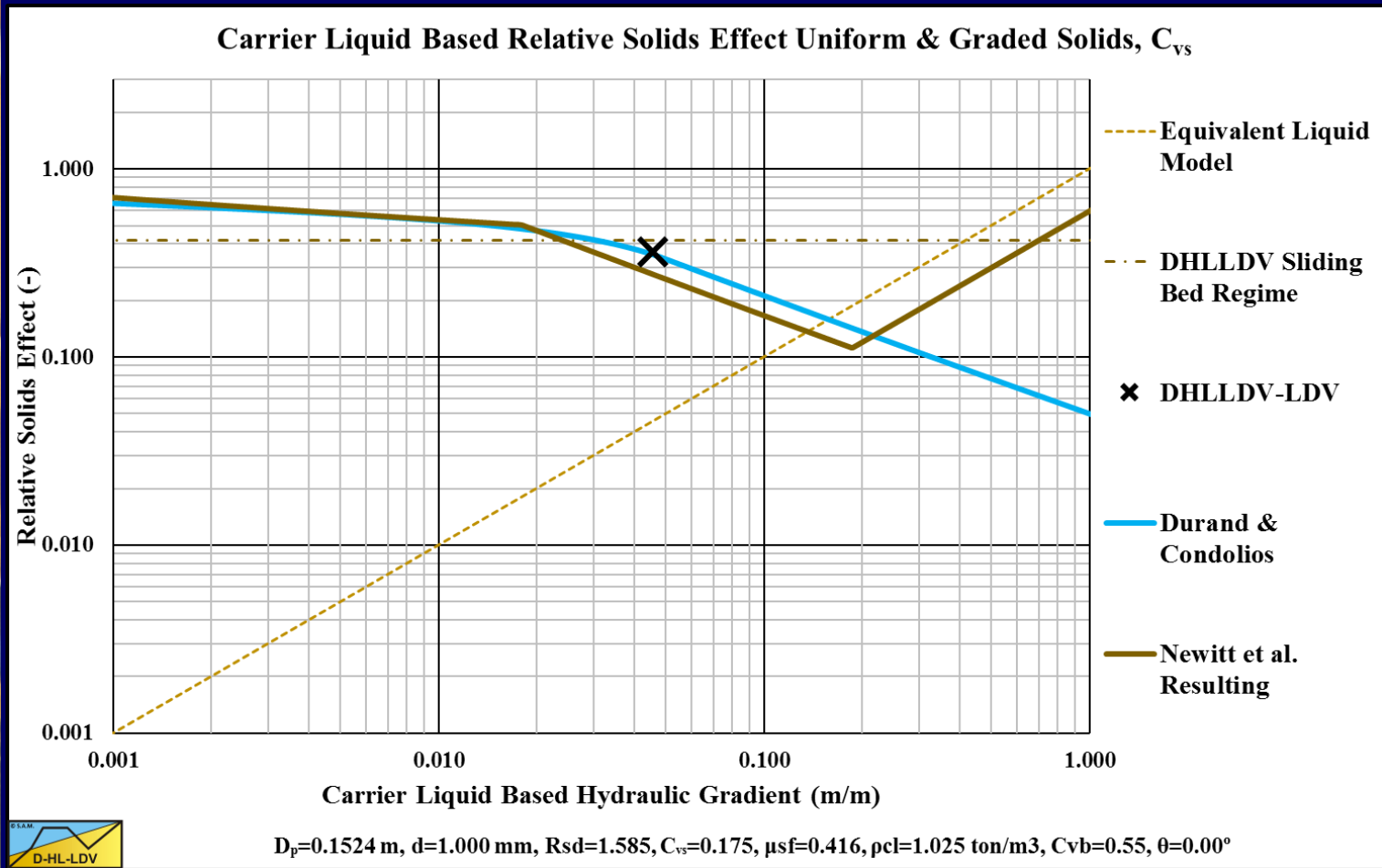


Durand & Condolios (1953) including constant Froude number below the Limit Deposit Velocity.

Delft University of Technology – Offshore & Dredging Engineering



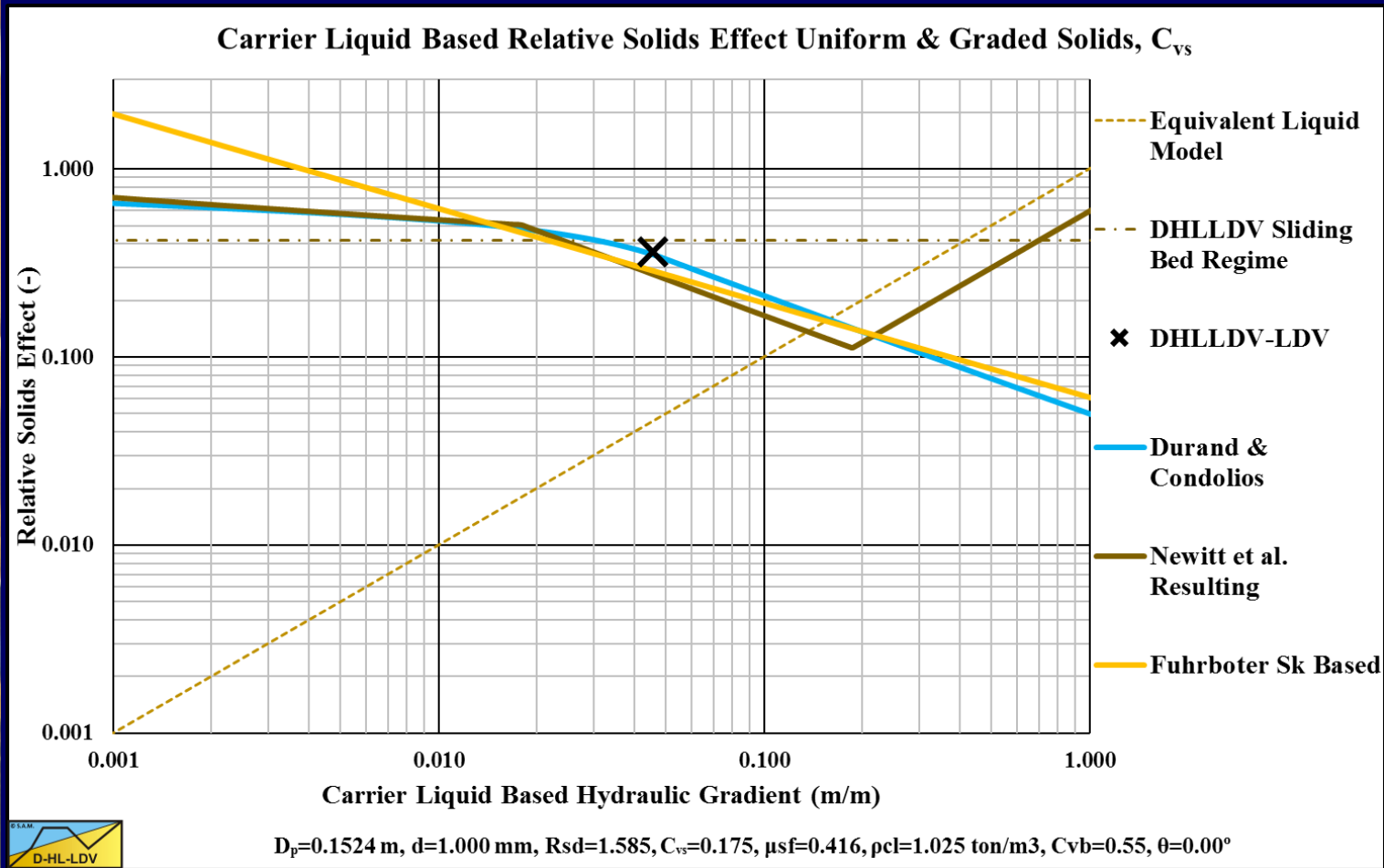
Adding Newitt et al. to the graph



Newitt et al. (1955) 3 flow regimes.



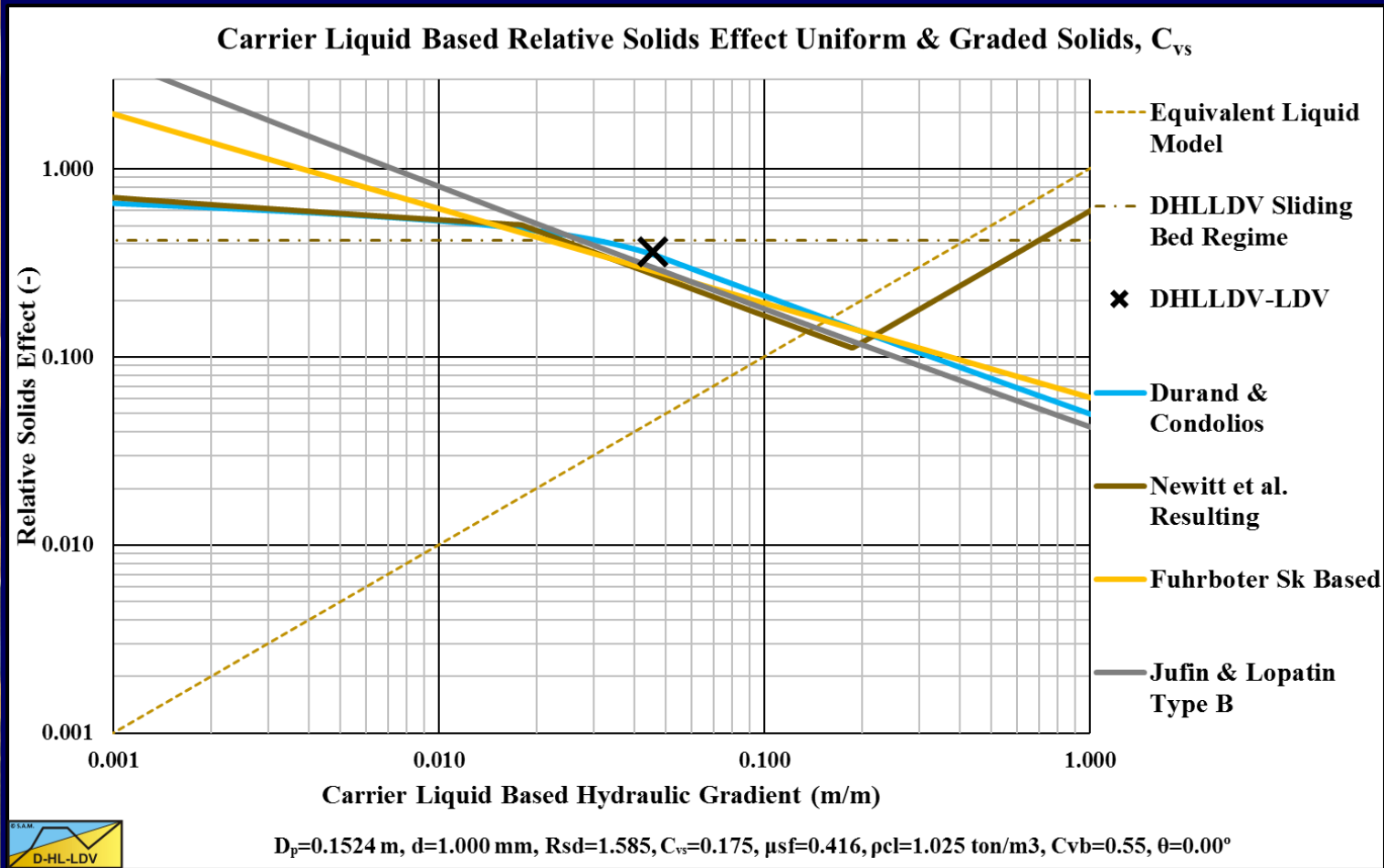
Adding Fuhrboter to the graph



Fuhrboter (1961) only heterogeneous flow regime.



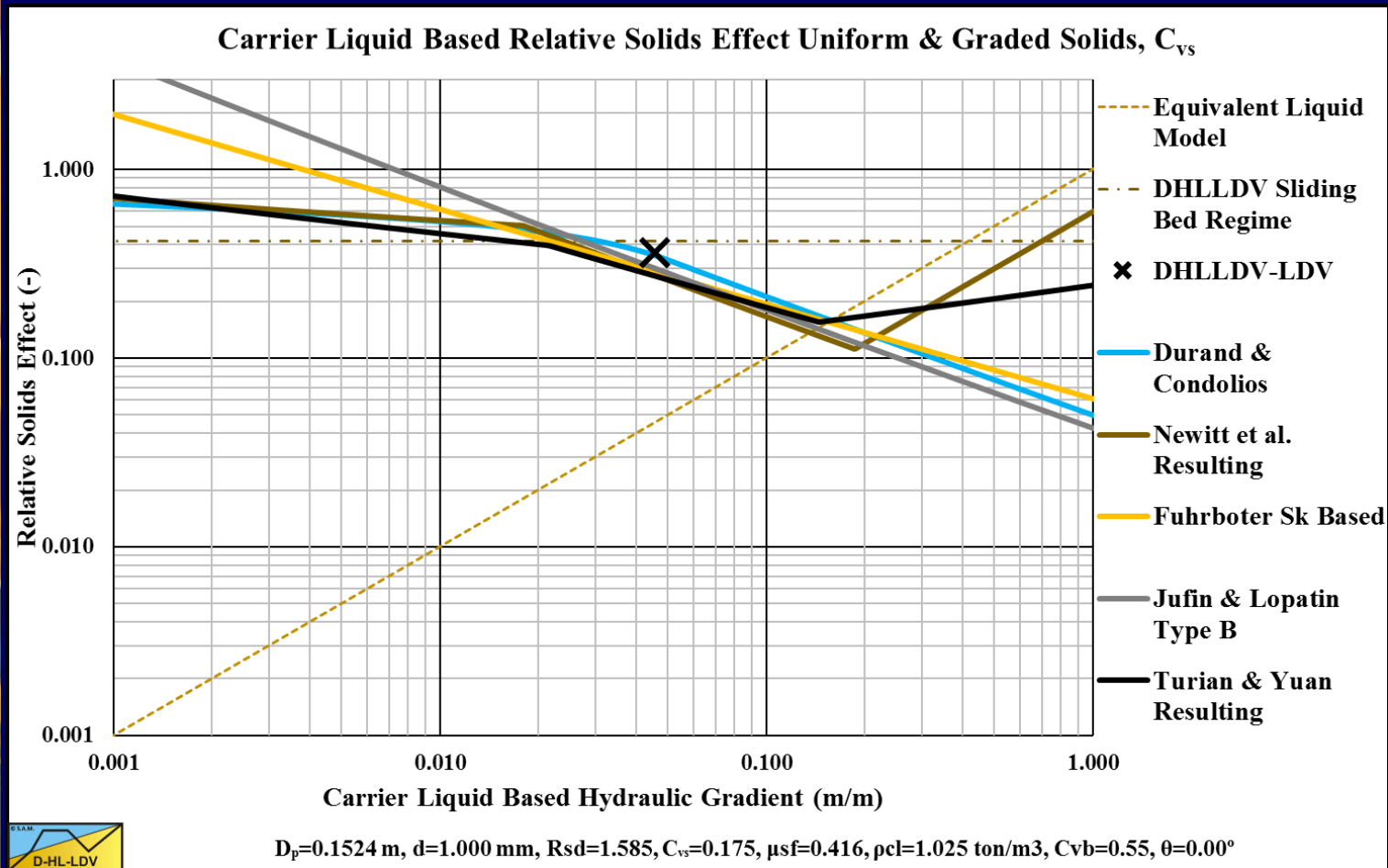
Adding Jufin-Lopatin to the graph



Jufin & Lopatin (1966) only heterogeneous flow regime.



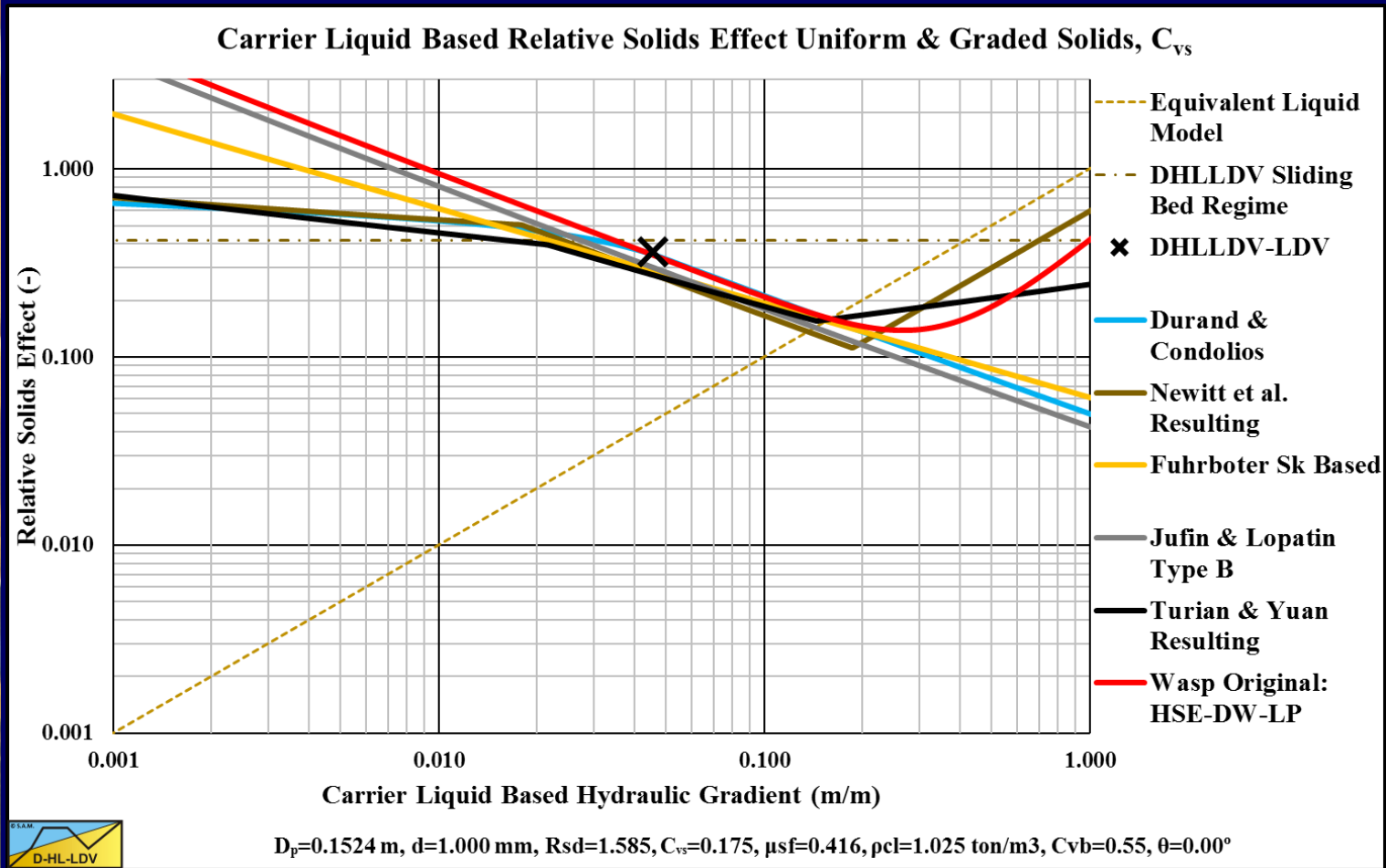
Adding Turian & Yuan to the graph



Turian & Yuan (1977) all flow regimes.



Adding Wasp to the graph

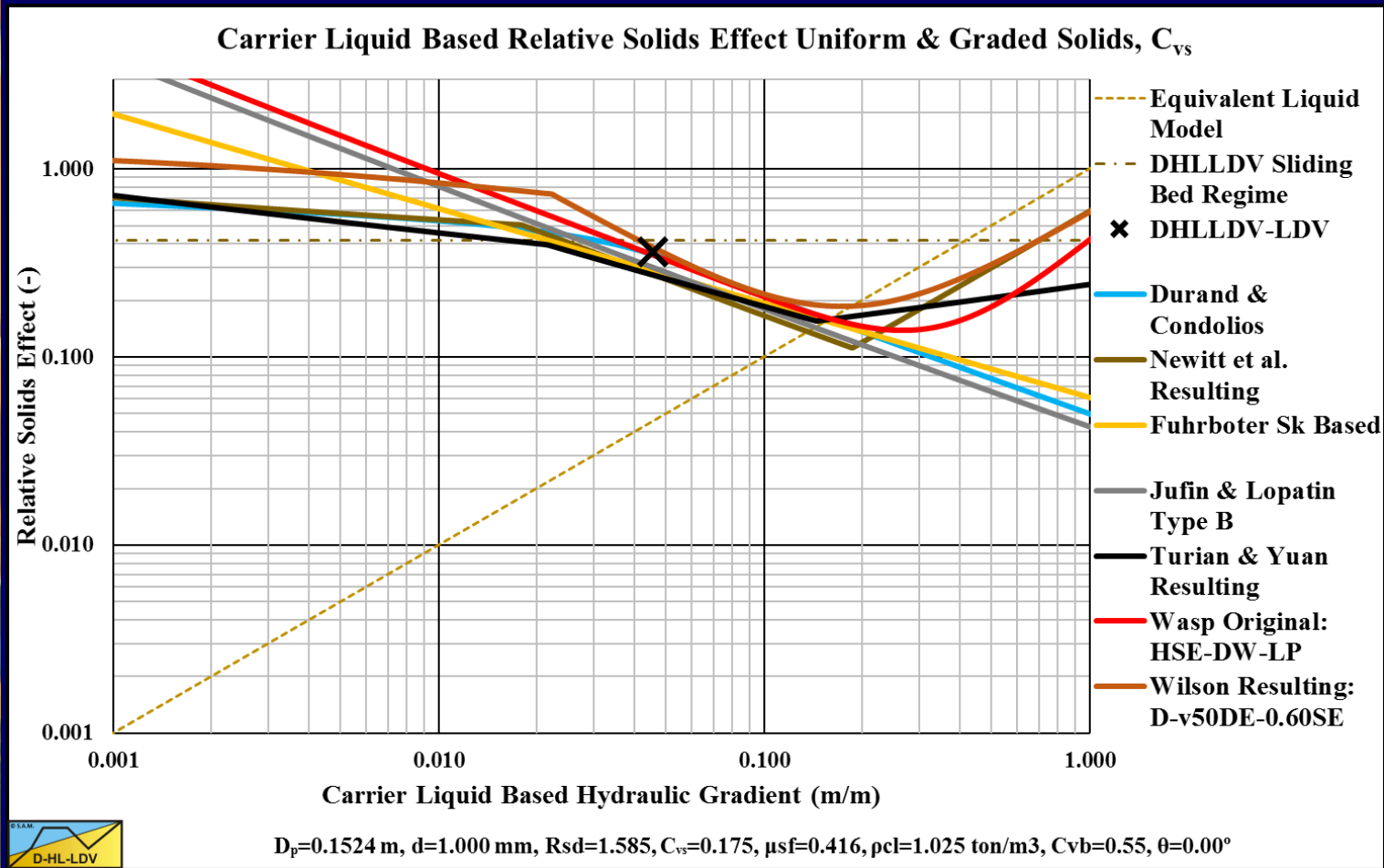


Original Wasp (1963) model with hindered settling, only the heterogeneous & homogeneous flow regimes.

Delft University of Technology – Offshore & Dredging Engineering



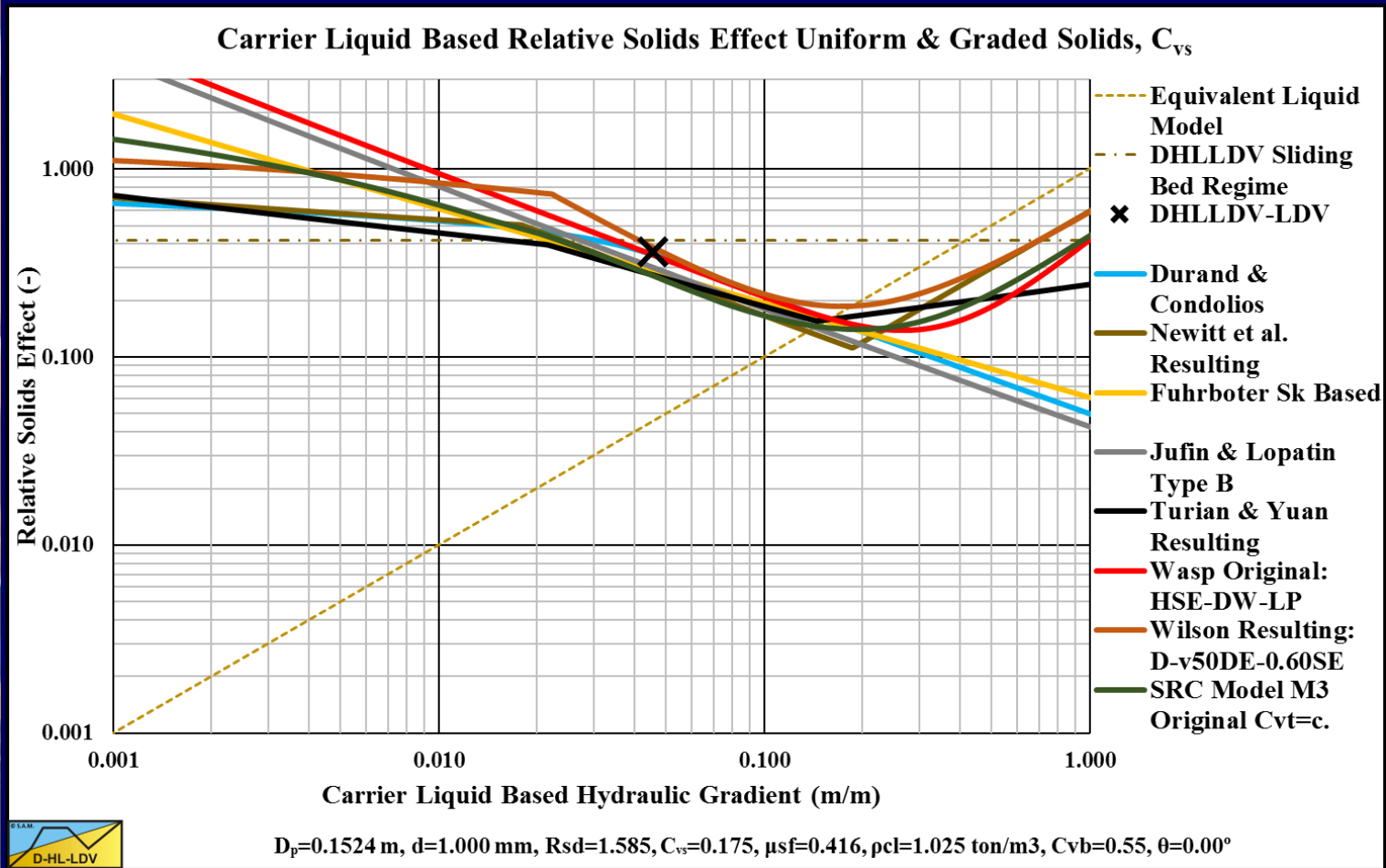
Adding Wilson et al. to the graph



Wilson et al. (1979) all flow regimes.



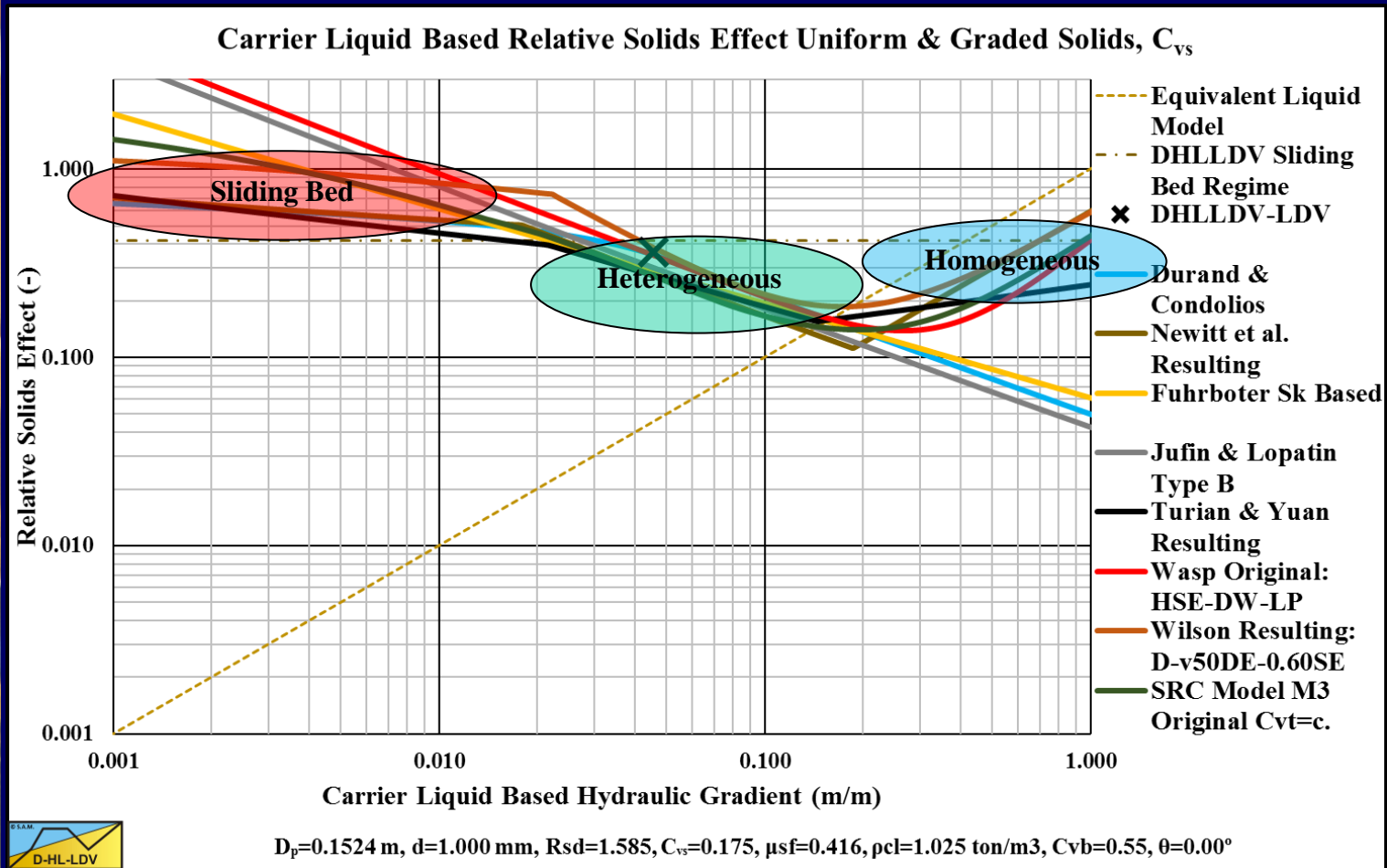
Adding the SRC model to the graph



SRC model (2004) all flow regimes.



Conclusions

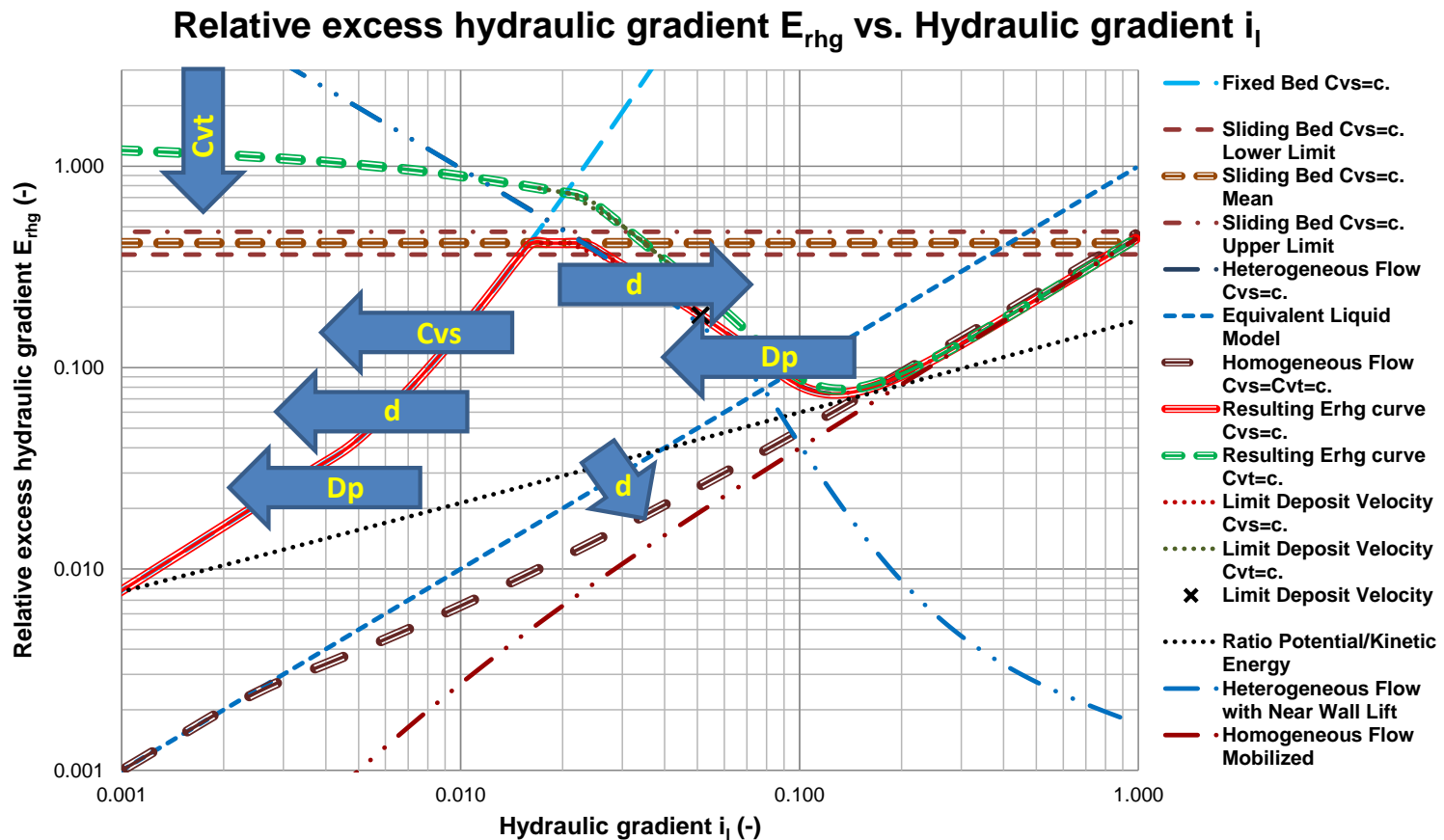


All models based on experiments in small diameter pipes and mainly in the heterogeneous flow regime.

Delft University of Technology – Offshore & Dredging Engineering



How To Read The Graph? ($D_p=6$ inch)



$D_p=0.1524$ m, $d=0.500$ mm, $R_{sd}=1.585$, $C_v=0.175$, $\mu_{sf}=0.416$

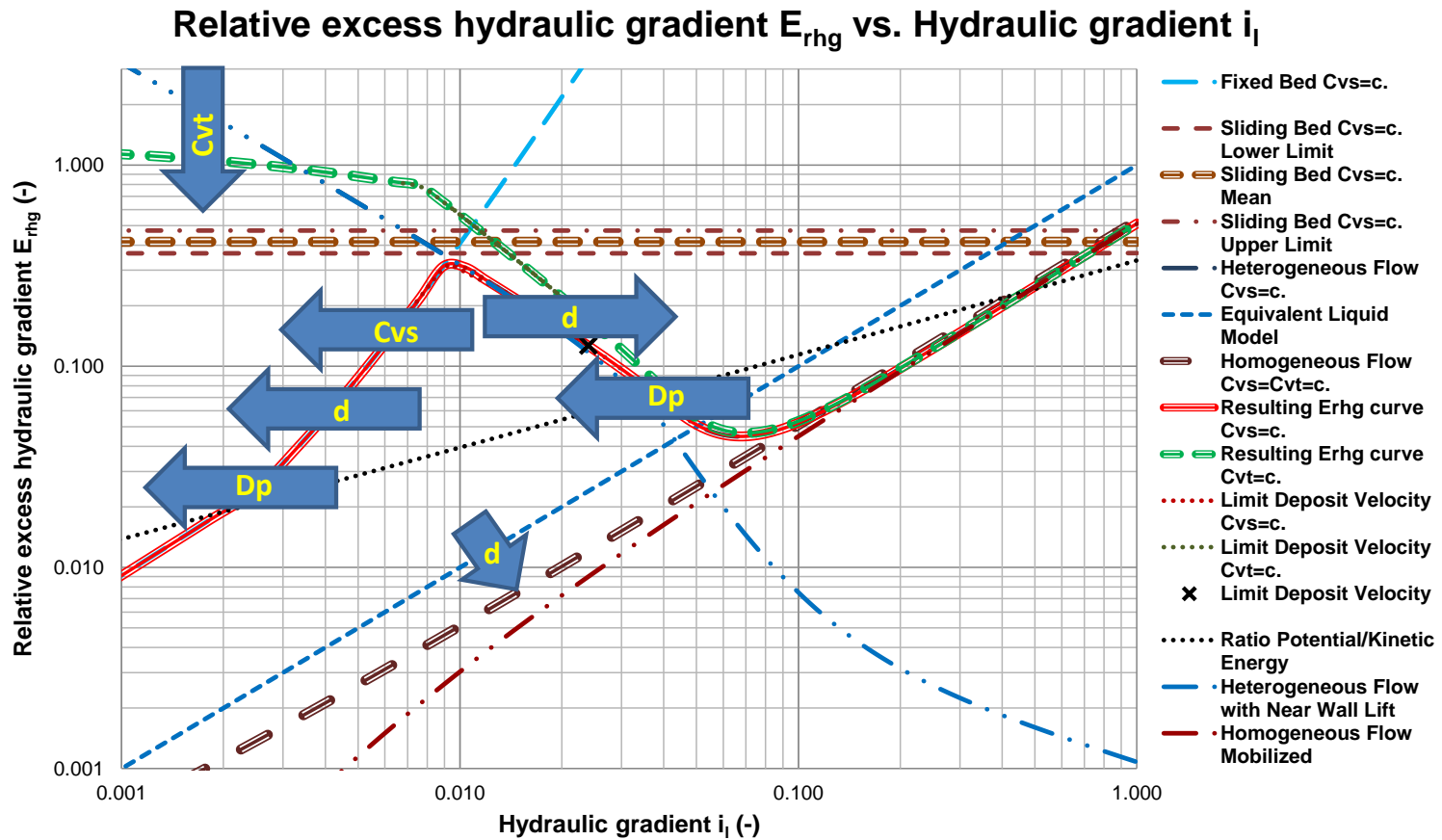
$$i_1 = \frac{\Delta p_1}{\rho_1 \cdot g \cdot \Delta L} = \frac{\lambda_1 \cdot v_{ls}^2}{2 \cdot g \cdot D_p}$$

Hydraulic Gradient
Relative Excess H.G.

$$E_{rhg} = \frac{i_m - i_1}{R_{sd} \cdot C_v}$$



How To Read The Graph? ($D_p=30$ inch)



$D_p=0.7620$ m, $d=1.000$ mm, $R_{sd}=1.585$, $C_v=0.175$, $\mu_{sf}=0.416$

$$i_1 = \frac{\Delta p_1}{\rho_1 \cdot g \cdot \Delta L} = \frac{\lambda_1 \cdot v_{ls}^2}{2 \cdot g \cdot D_p}$$

Hydraulic Gradient
Relative Excess H.G.

$$E_{rhg} = \frac{i_m - i_1}{R_{sd} \cdot C_v}$$



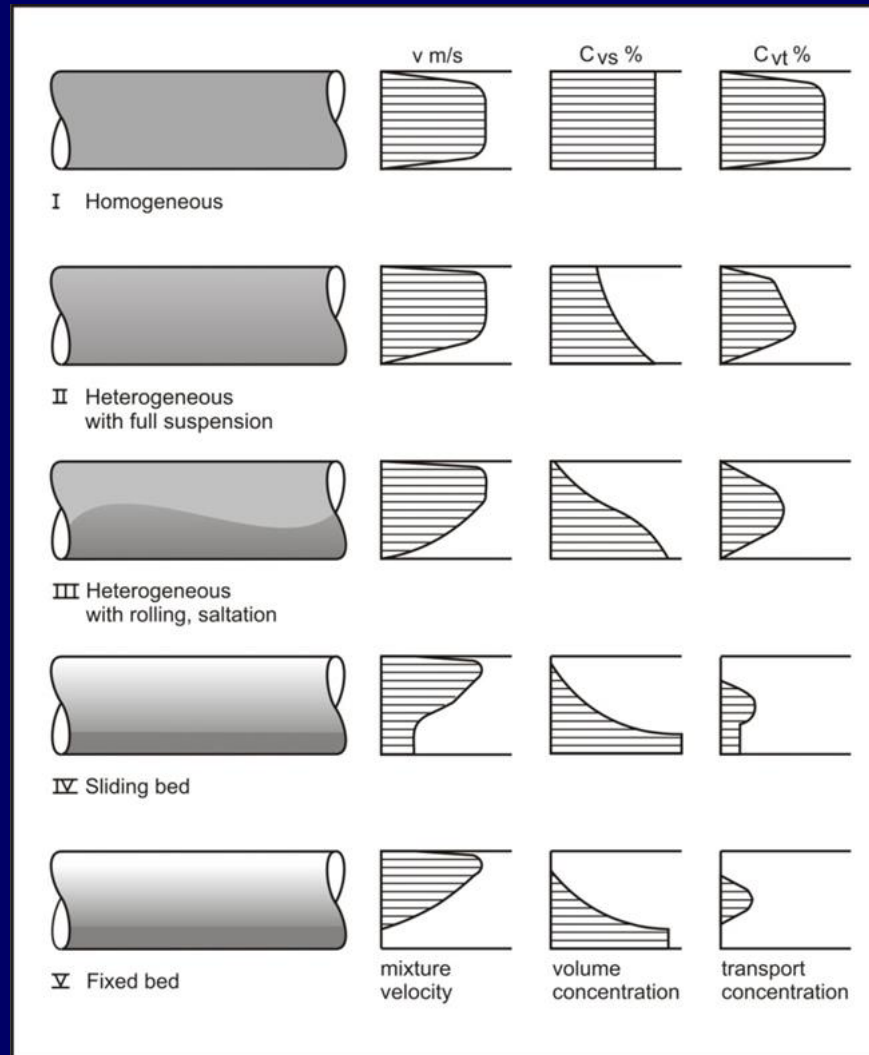


Flow Regimes History

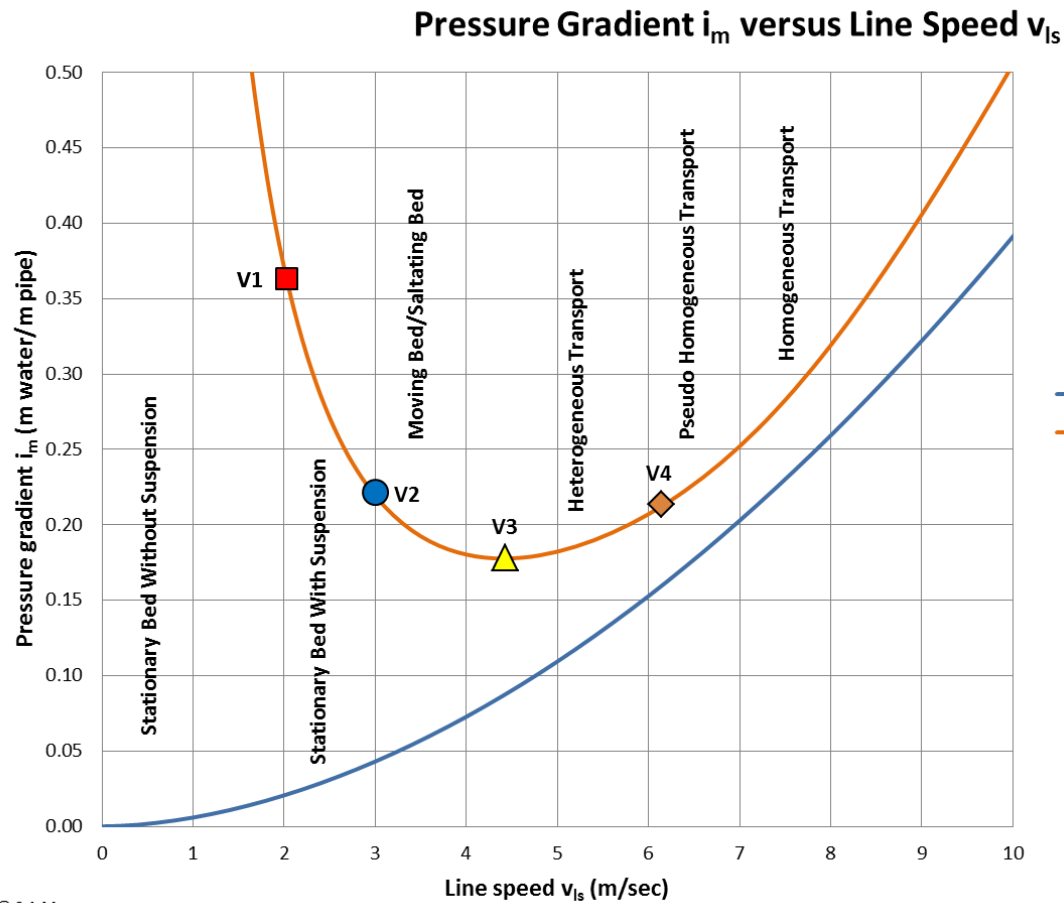
Chapter 1



Regimes History



Abulnaga (2002)

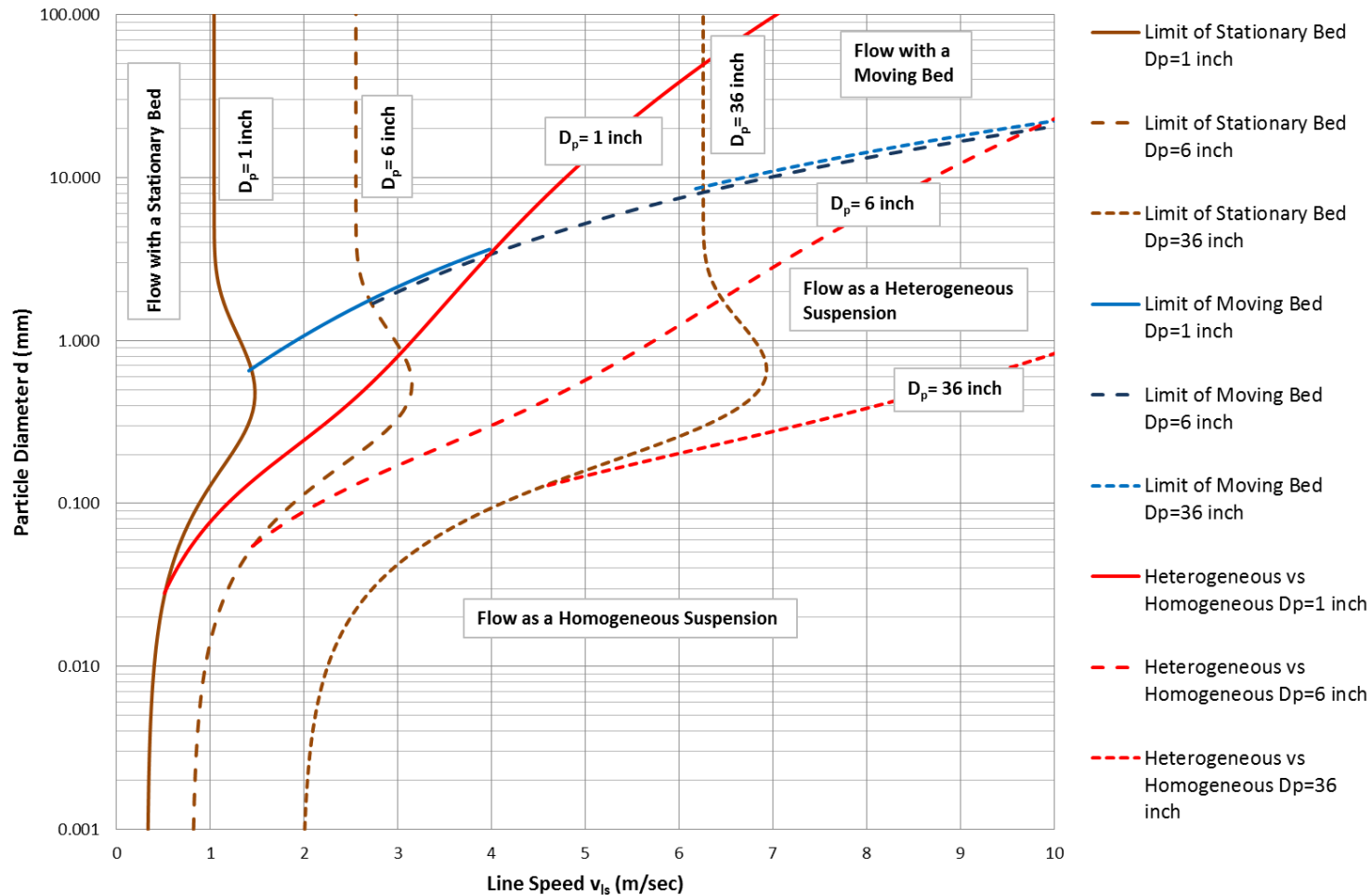


© S.A.M.



Miedema (2013), Inspired by Newitt et al.

Flow Regimes according to Newitt et al. (1955) & Durand & Condolios (1952)



© S.A.M.

Not concentration dependent

Delft University of Technology – Offshore & Dredging Engineering





Flow Regime Identification

Chapter 7.2



Starting Points DHLLDV Framework

**Constant Spatial Volumetric
Concentration**

Uniform Sand & Gravels

Newtonian Liquid



Starting Points

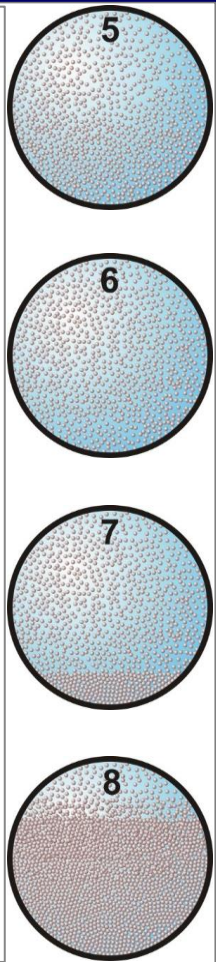
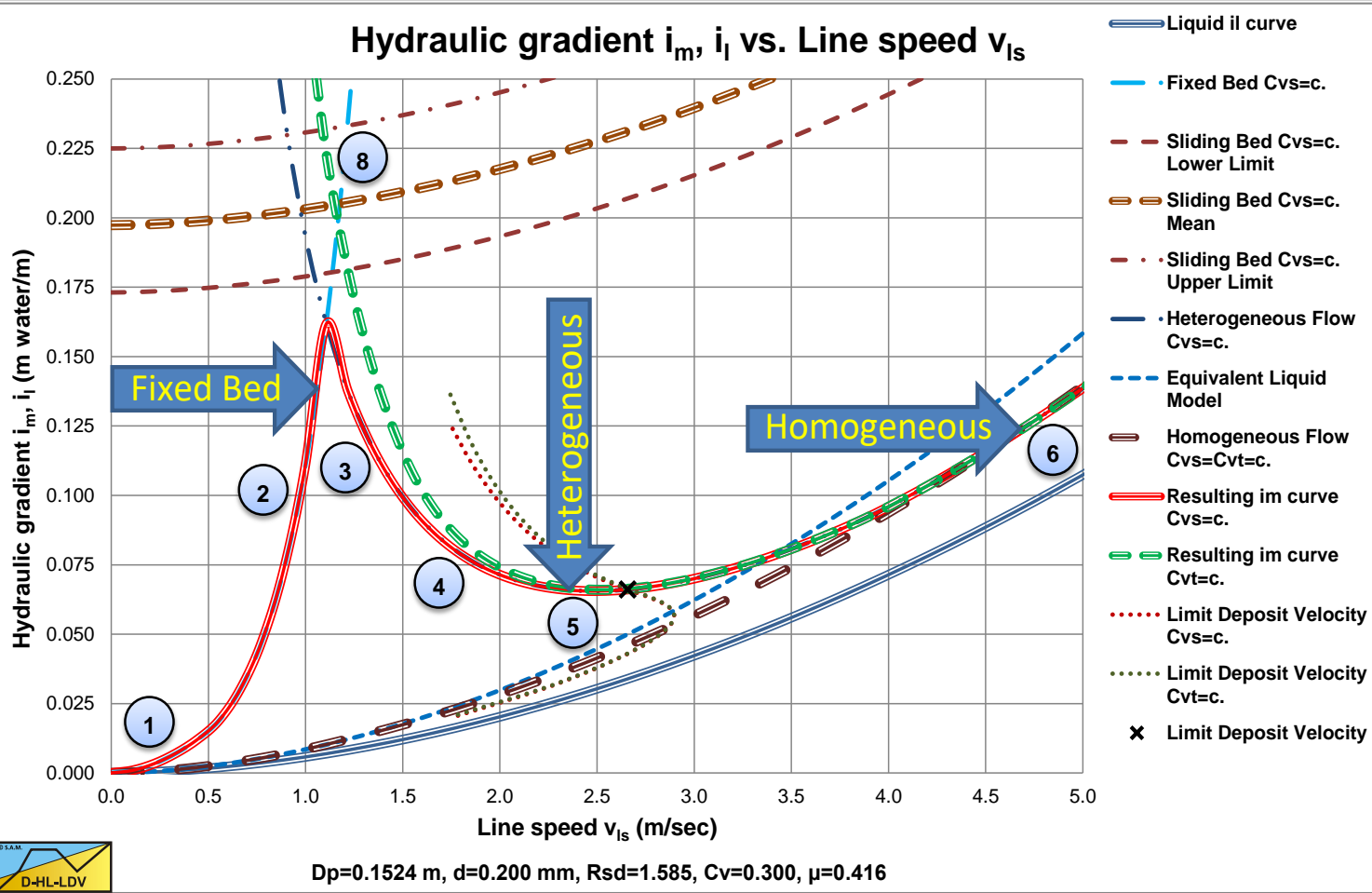
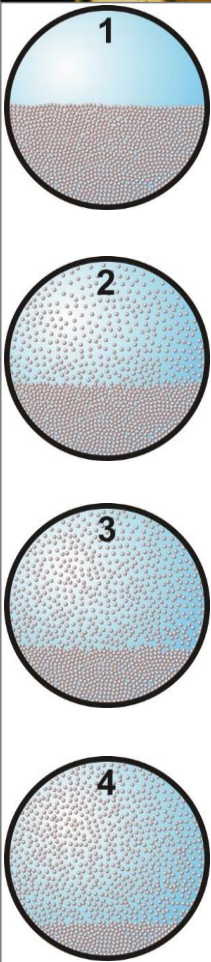
The 5 main flow regimes are identified based on their dominating behavior regarding energy dissipation.

1. The fixed bed regime is identified based on shear stresses at the liquid-fixed bed interface (sheet flow).
2. The sliding bed regime is identified based on sliding friction energy losses.
3. The heterogeneous flow regime is identified based on potential and kinetic energy losses.
4. The homogeneous flow regime is identified based on energy losses in turbulent eddies and viscous friction.
5. The sliding flow regime is identified based on sliding friction, potential and kinetic energy losses.

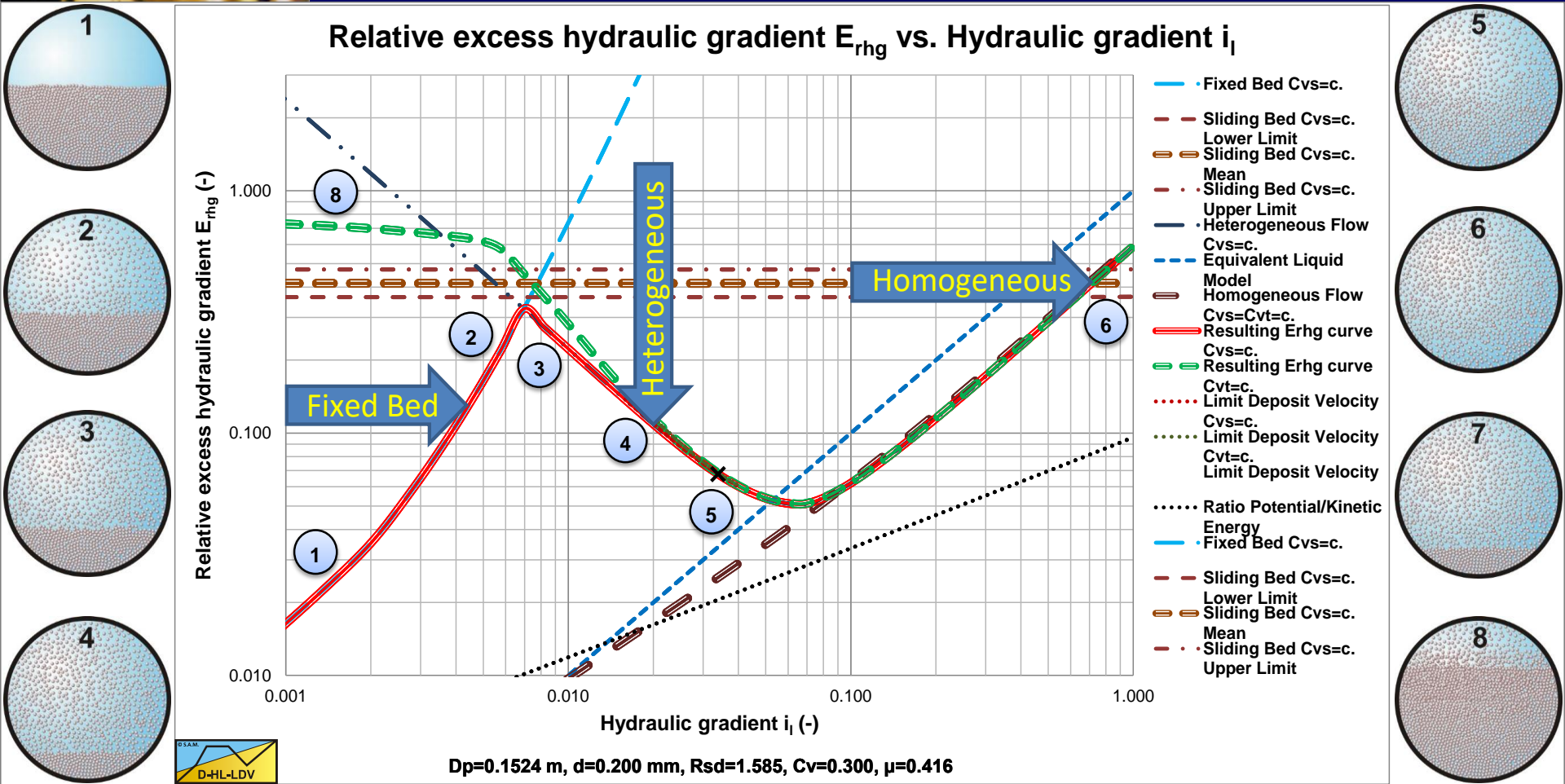
At flow regime transitions, a mix of two flow regimes will be present.



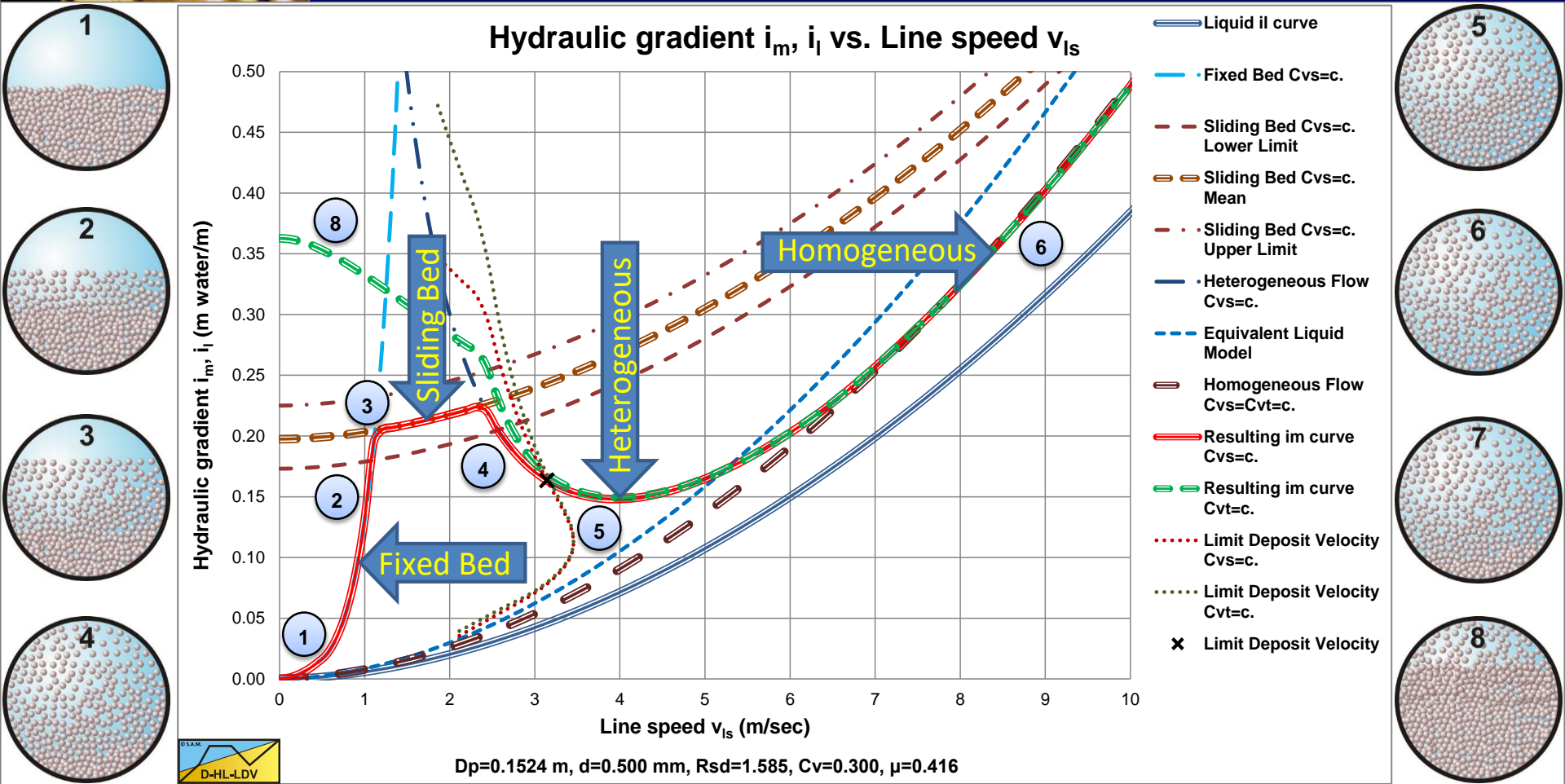
Small Particles, Scenario L1 & R1, $i_m - v_{Is}$



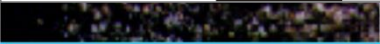
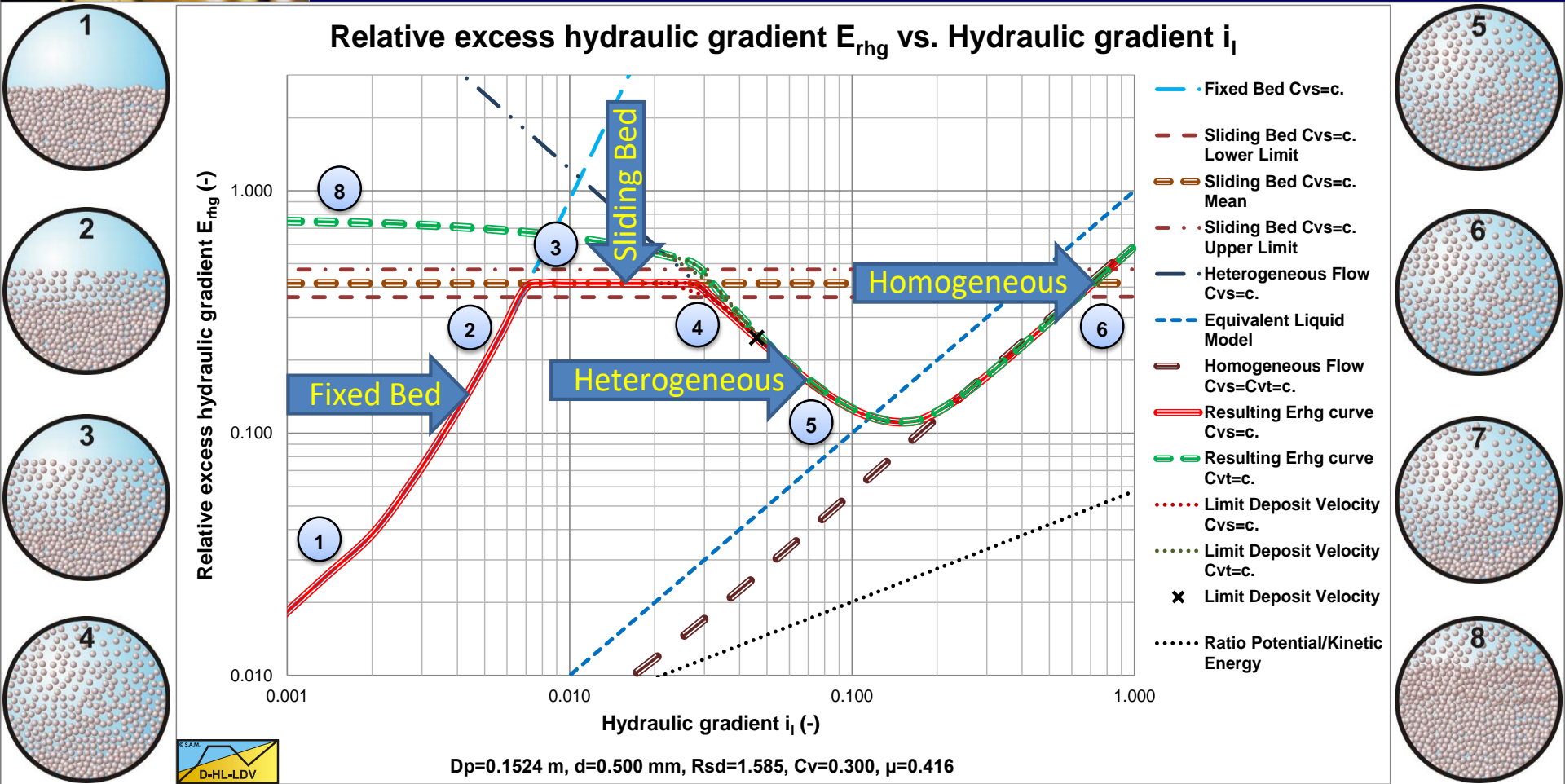
Small Particles, Scenario L1 & R1, $E_{rhg}-i_i$



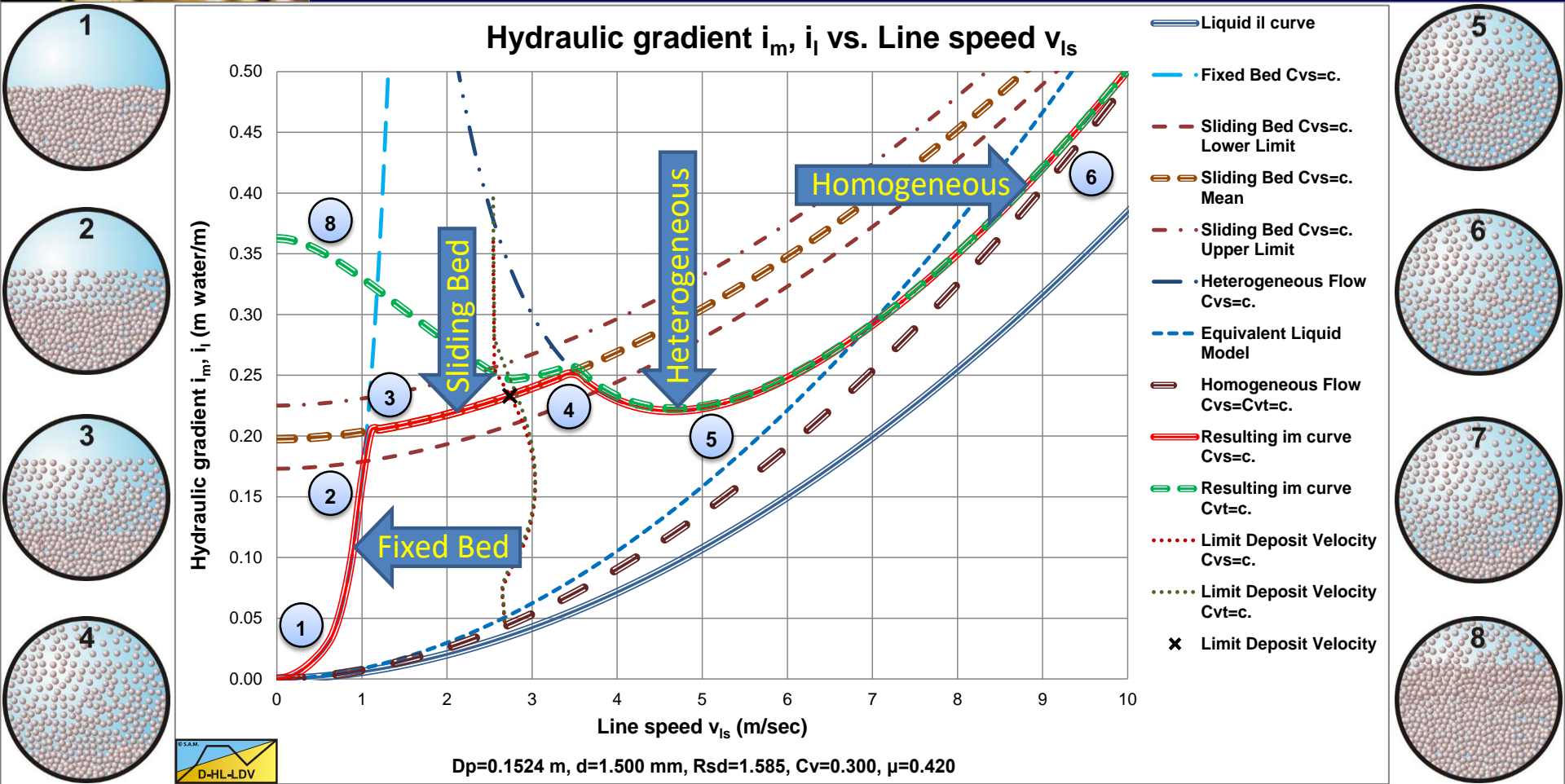
Medium Part., Scenario L2A & R2A, i_m-v_{Is}



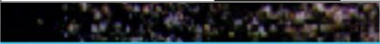
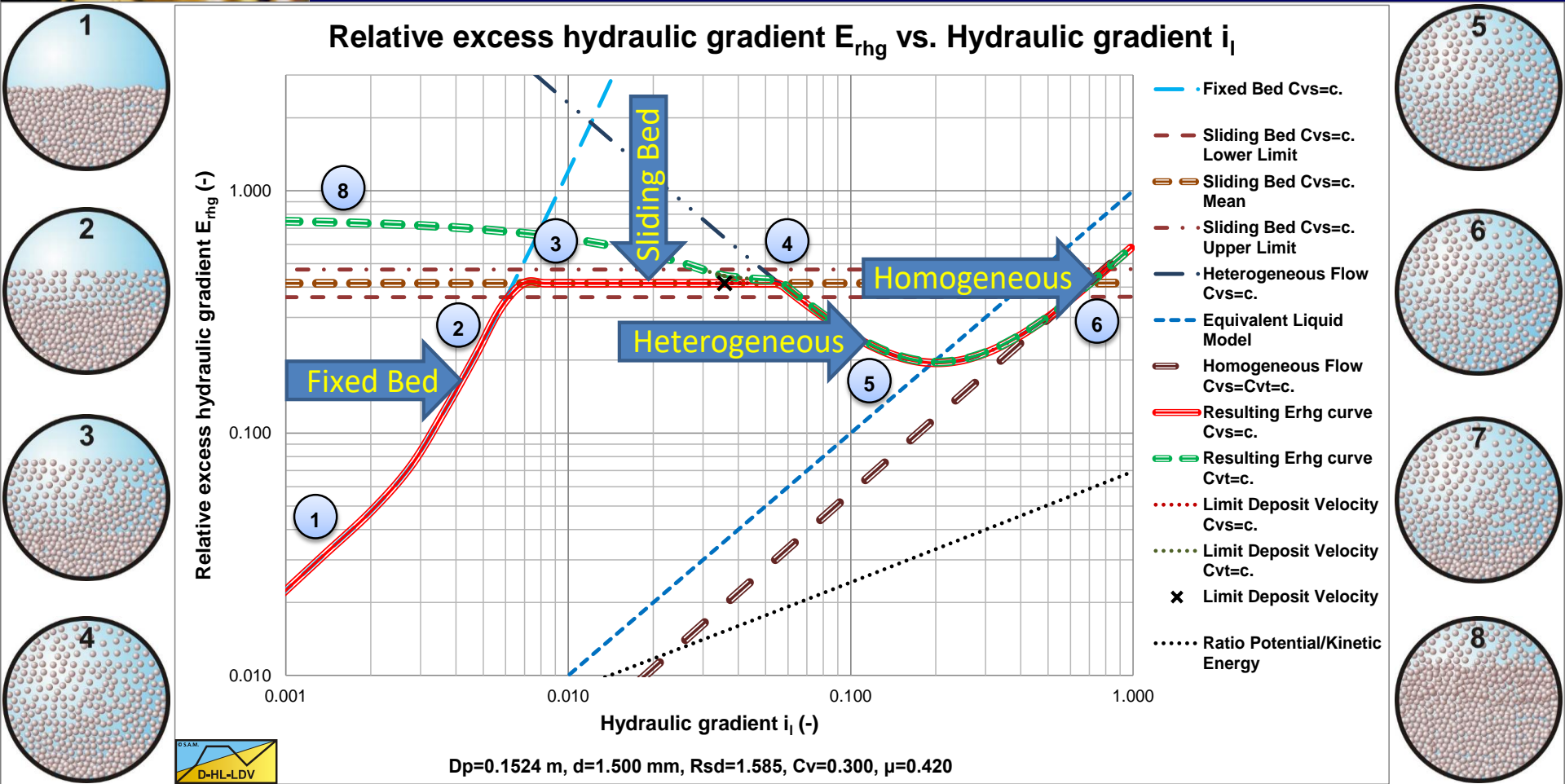
Medium Part., Scenario L2A & R2A, $E_{rhg}-i_i$



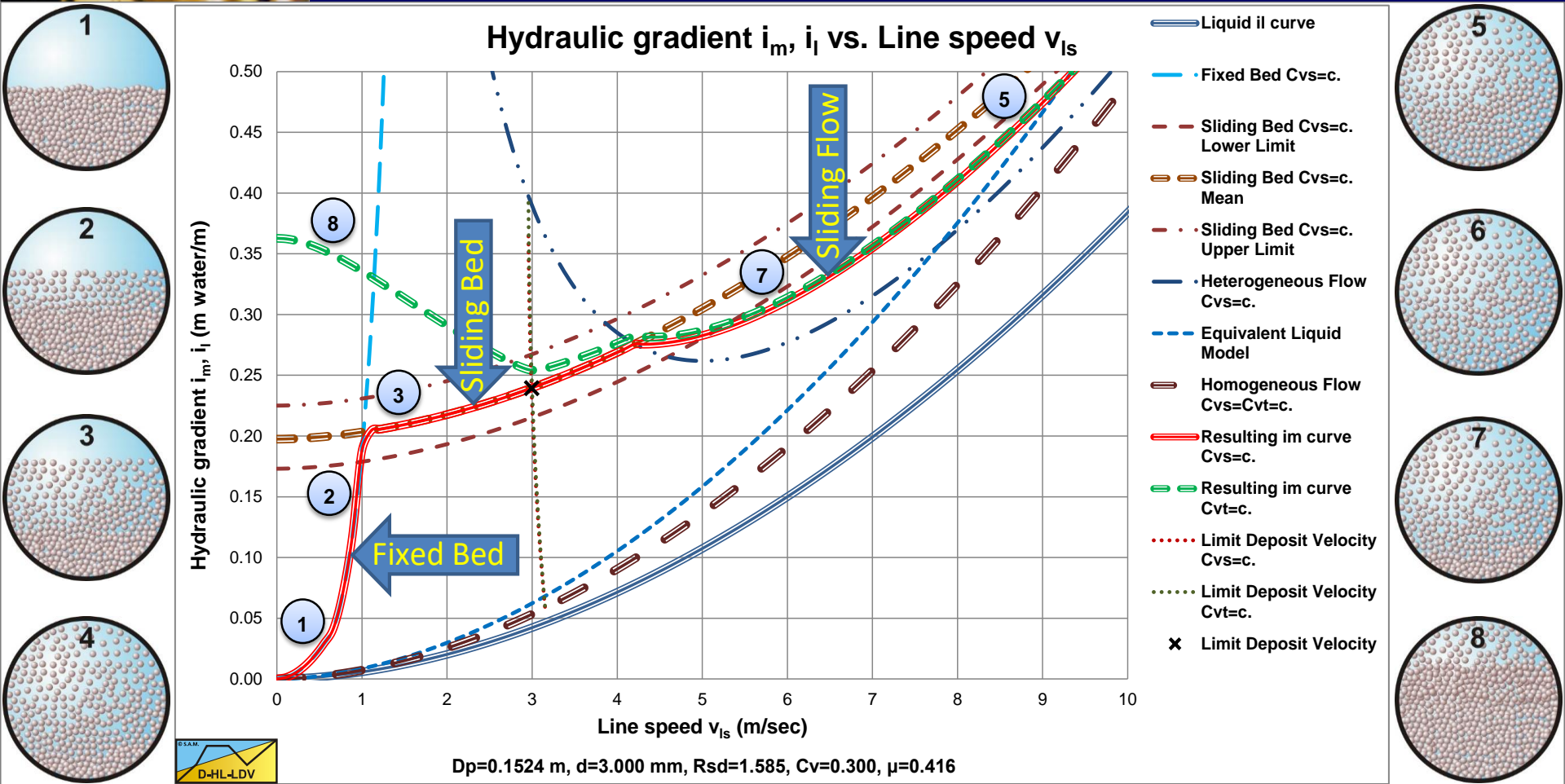
Large Part., Scenario L2B & R2B, i_m-v_{Is}



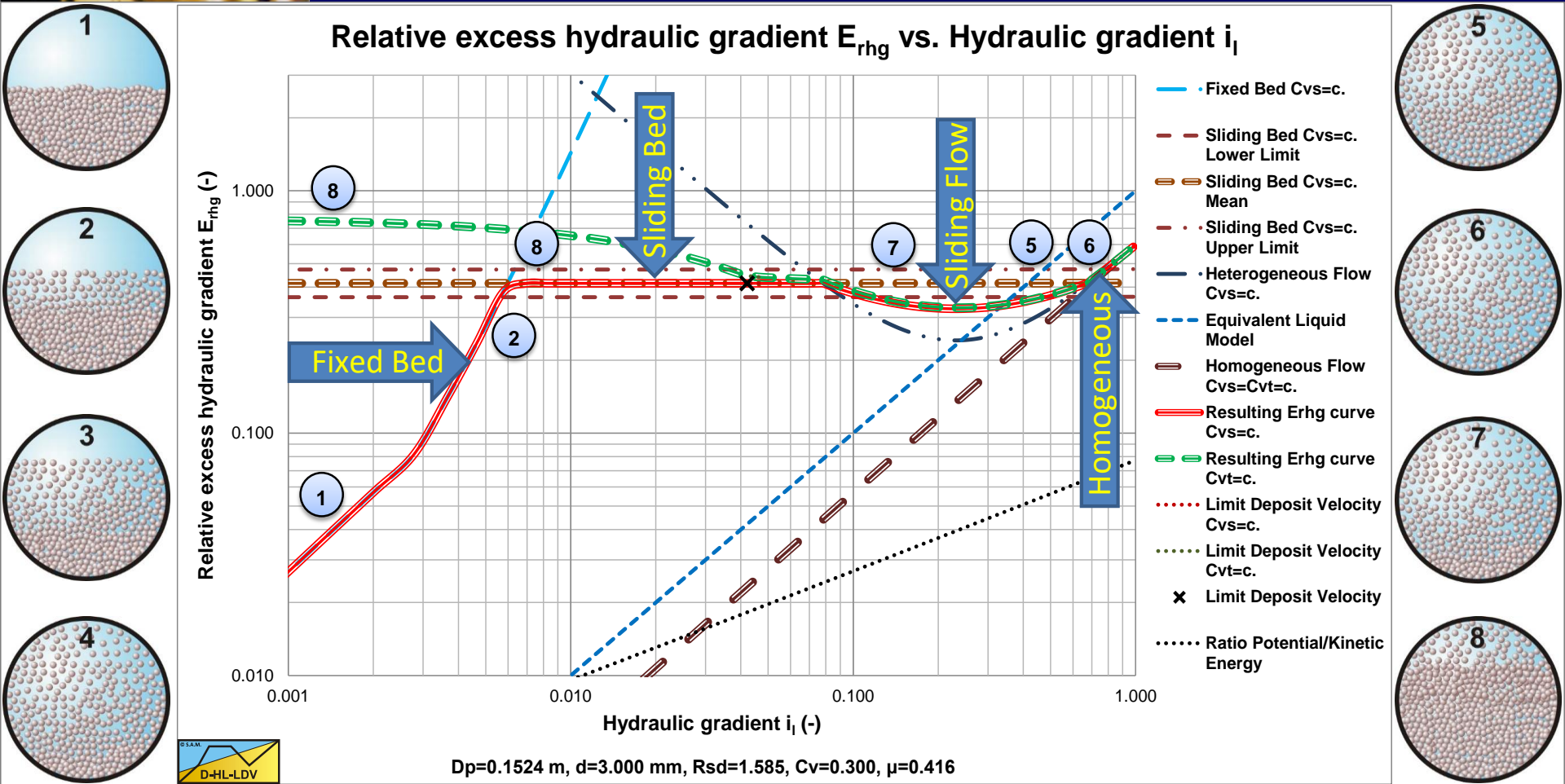
Large Part., Scenario L2B & R2B, $E_{rhg}-i_1$



Very Large Part., Scenario L3 & R3, $i_m - v_{ls}$



Very Large Part., Scenario L3 & R3, $E_{rhg}-i_1$



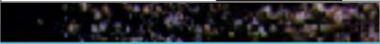
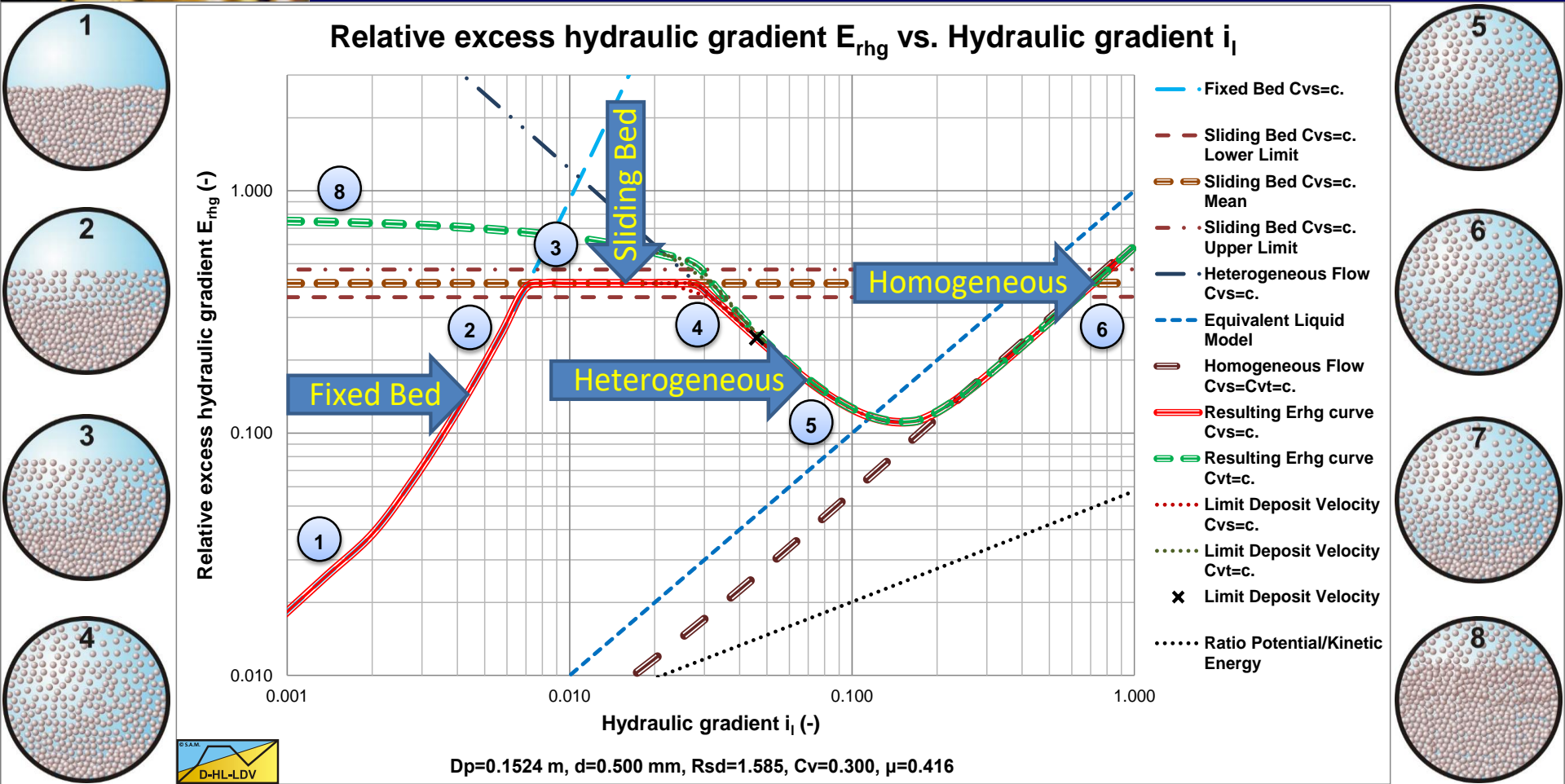


Stationary/Fixed Bed Regime

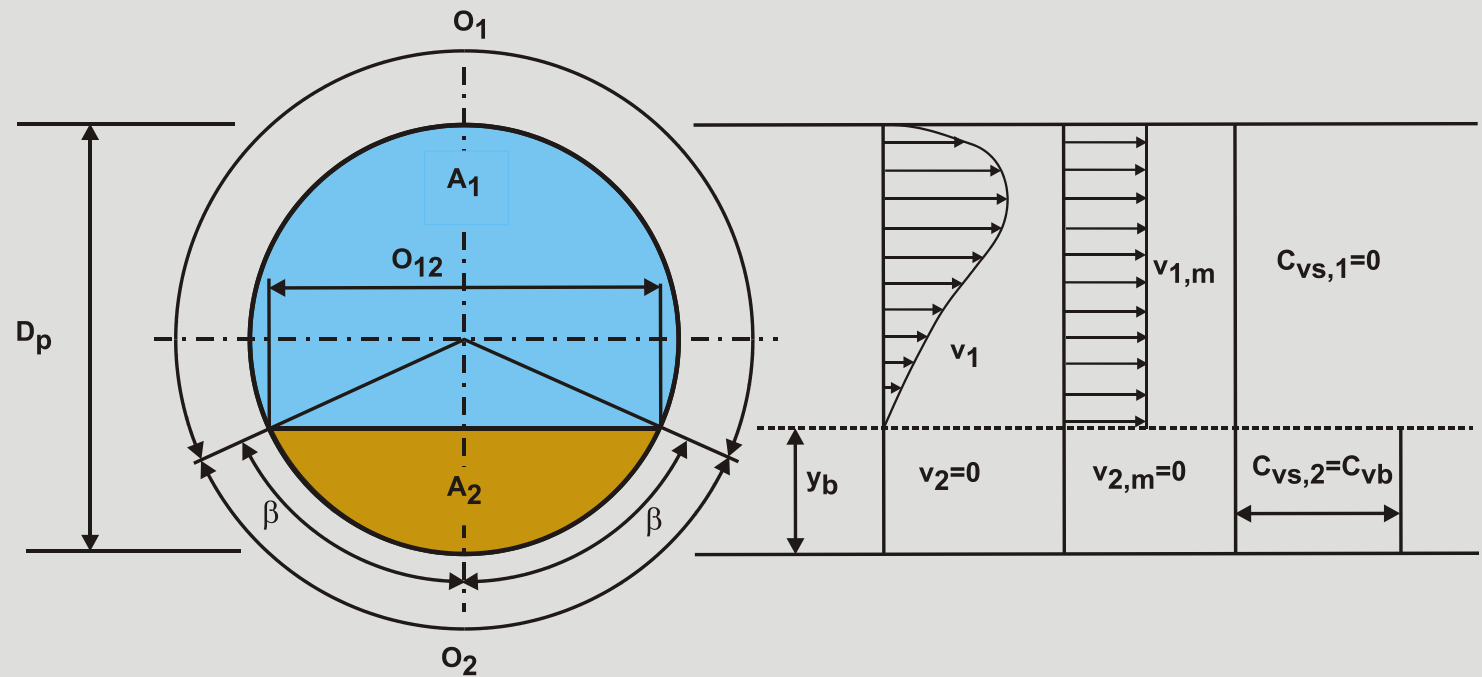
Chapter 7.3 & 8.3



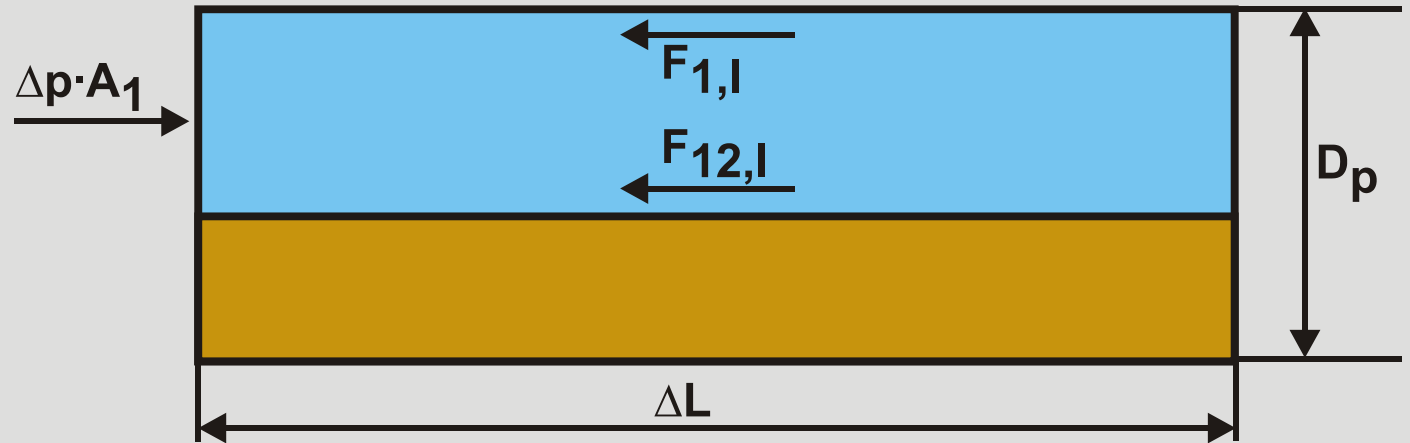
Flow Regimes



Definitions



Equilibrium of Forces



$$\Delta p = \Delta p_2 = \Delta p_1 = \frac{\tau_{1,l} \cdot O_1 \cdot \Delta L + \tau_{12,l} \cdot O_{12} \cdot \Delta L}{A_1} = \frac{F_{1,l} + F_{12,l}}{A_1}$$



Shear Stresses

$$\tau_{1,l} = \frac{\lambda_1}{4} \cdot \frac{1}{2} \cdot \rho_1 \cdot v_1^2 \quad \text{with:} \quad \lambda_1 = \frac{1.325}{\left(\ln \left(\frac{0.27 \cdot \varepsilon}{D_H} + \frac{5.75}{Re^{0.9}} \right) \right)^2} \quad \text{and} \quad Re = \frac{v_1 \cdot D_H}{\nu_1}$$

$$\tau_{12,l} = \frac{\lambda_{12}}{4} \cdot \frac{1}{2} \cdot \rho_1 \cdot v_1^2 \quad \text{with:} \quad \lambda_{12} = \frac{\alpha \cdot 1.325}{\left(\ln \left(\frac{0.27 \cdot d}{D_H} + \frac{5.75}{Re^{0.9}} \right) \right)^2} \quad \text{and} \quad Re = \frac{v_1 \cdot D_H}{\nu_1}$$

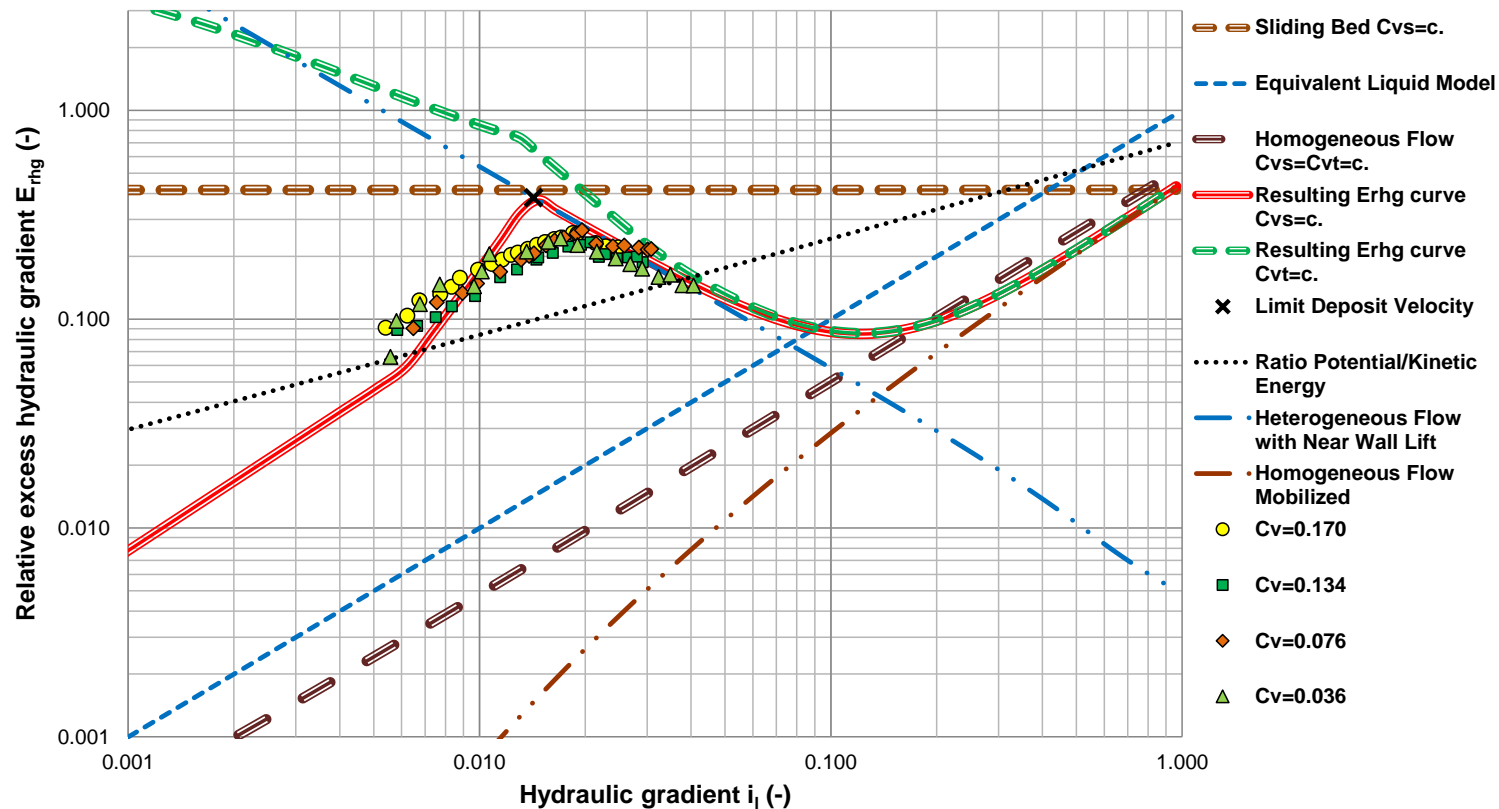
$$\lambda_{12} = 0.83 \cdot \lambda_1 + 0.37 \cdot \left(\frac{(v_1 - v_2)}{\sqrt{2 \cdot g \cdot D_H \cdot R_{sd}}} \right)^{2.73} \cdot \left(\frac{\rho_s \cdot \frac{\pi}{6} \cdot d^3}{\rho_1 \cdot l^3} \right)^{0.094} = 0.83 \cdot \lambda_1 + 0.37 \cdot Fr_{DC}^{2.73} \cdot \left(\frac{m_p}{\rho_1} \right)^{0.094}$$

$$\Delta p = \Delta p_2 = \Delta p_1 = \frac{\tau_{1,l} \cdot O_1 \cdot \Delta L + \tau_{12,l} \cdot O_{12} \cdot \Delta L}{A_1} = \frac{F_{1,l} + F_{12,l}}{A_1}$$



Kazanskij (1980), $C_{vs}=0.036$

Relative excess hydraulic gradient E_{rhg} vs. Hydraulic gradient i_i

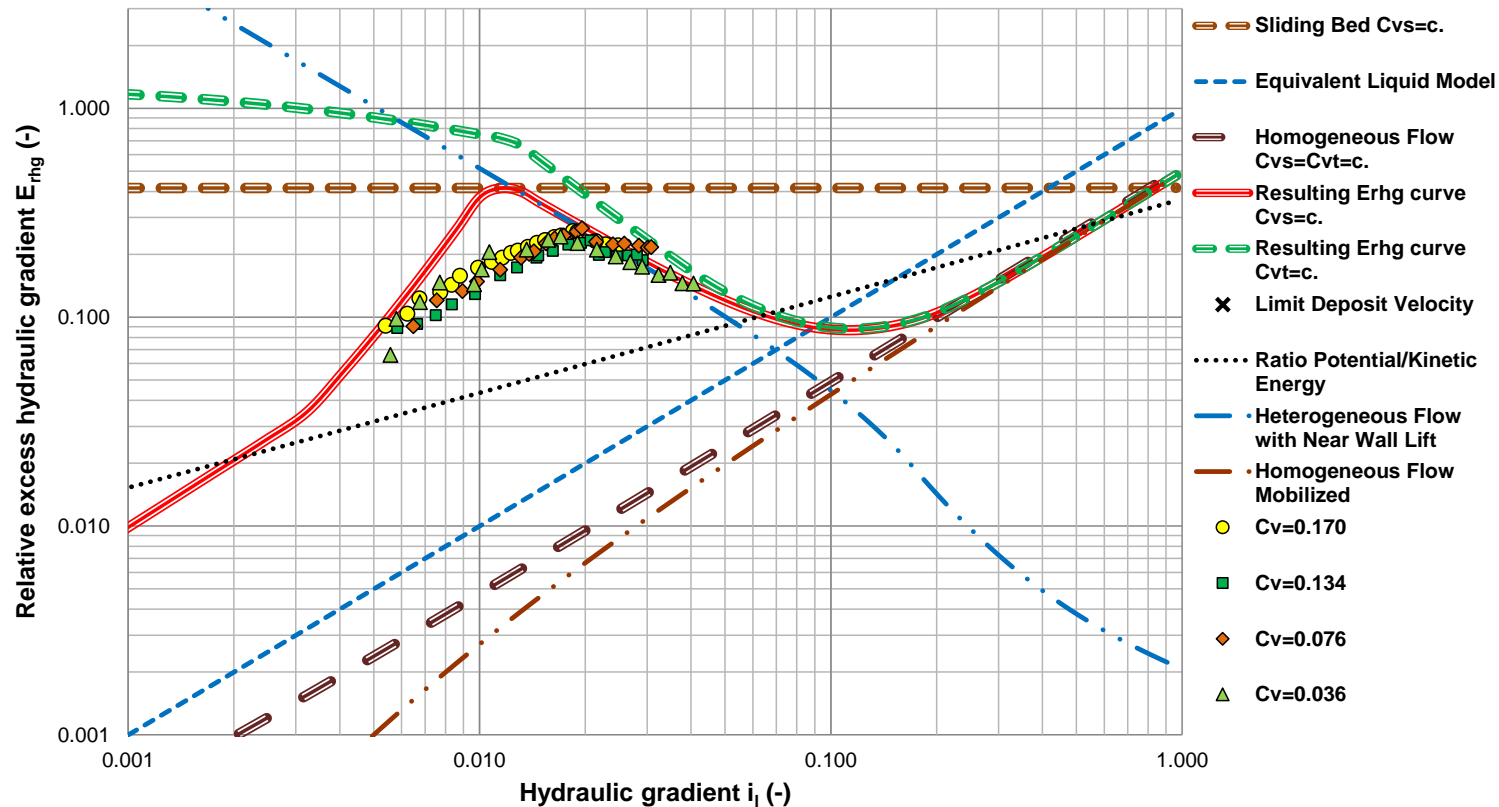


$D_p=0.5000$ m, $d=1.500$ mm, $R_{sd}=1.585$, $C_v=0.036$, $\mu_{sf}=0.416$



Kazanskij (1980), $C_{vs}=0.17$

Relative excess hydraulic gradient E_{rhg} vs. Hydraulic gradient i_i



$D_p=0.5000$ m, $d=1.500$ mm, $R_{sd}=1.585$, $C_v=0.170$, $\mu_{sf}=0.416$



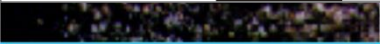
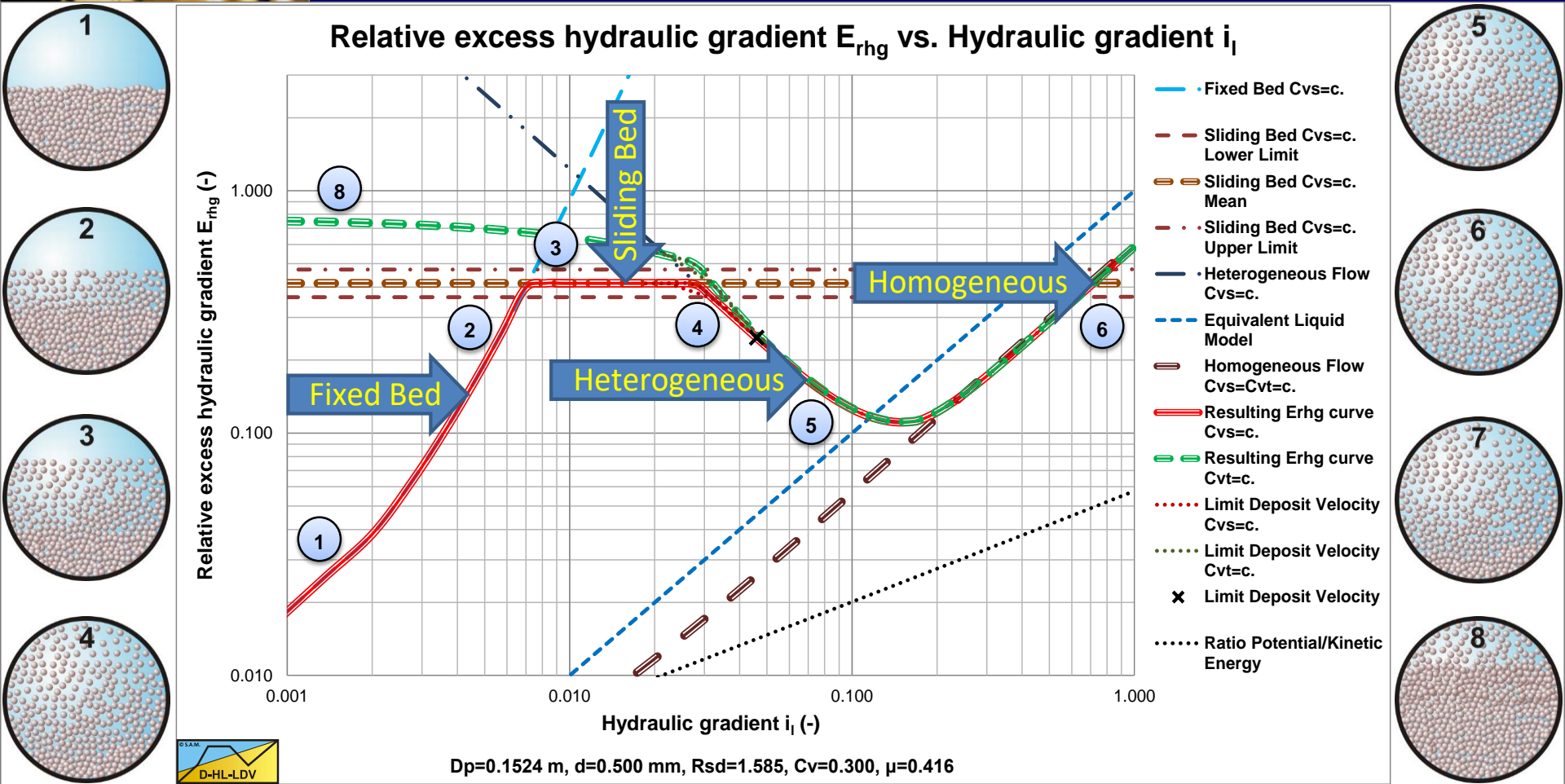


Sliding Bed Regime

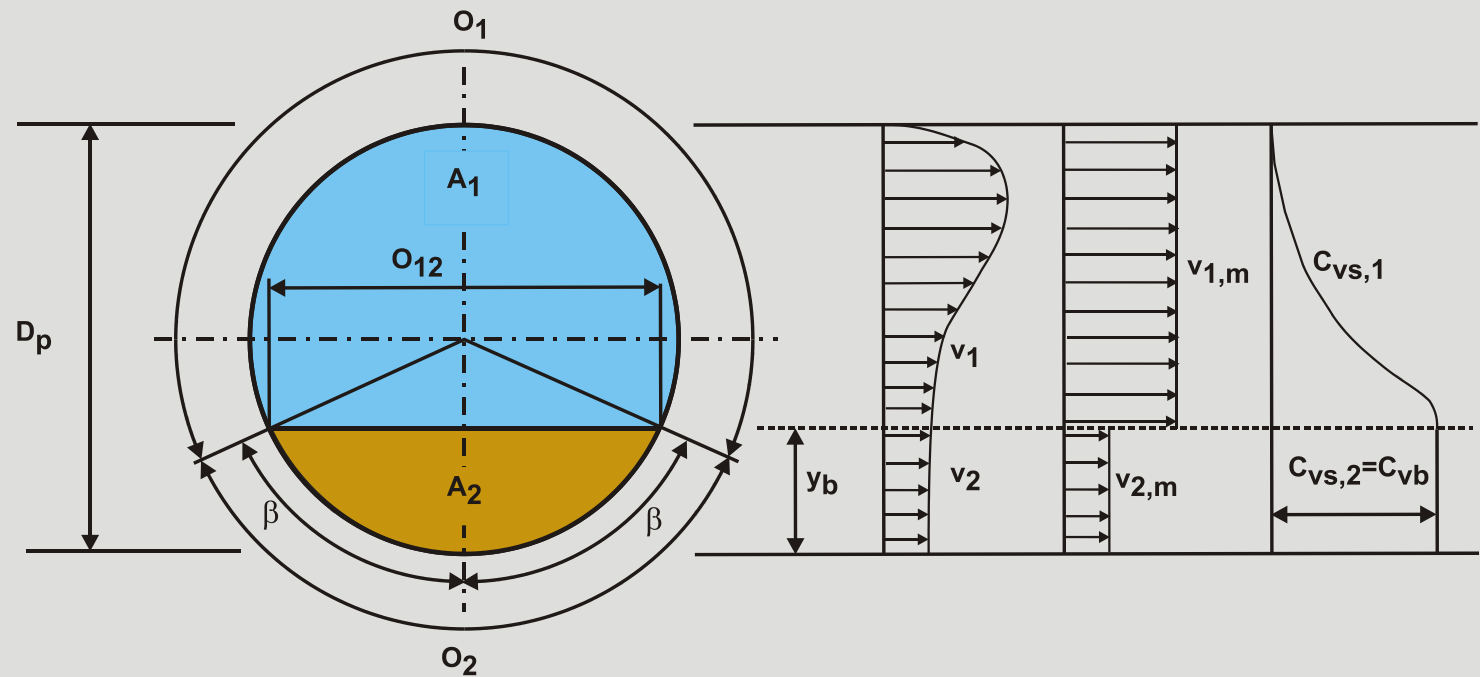
Chapter 7.4 & 8.4



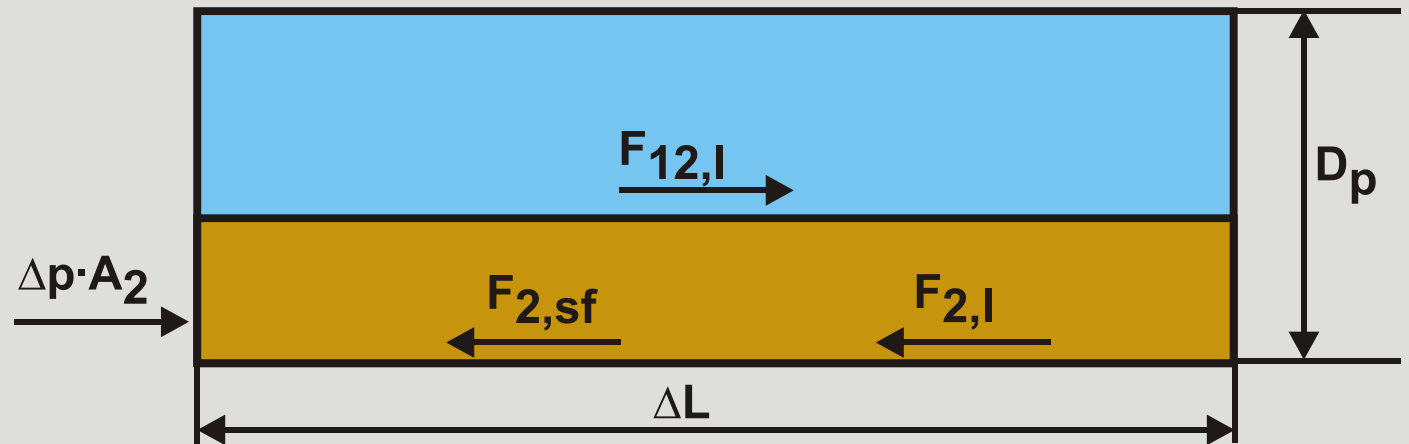
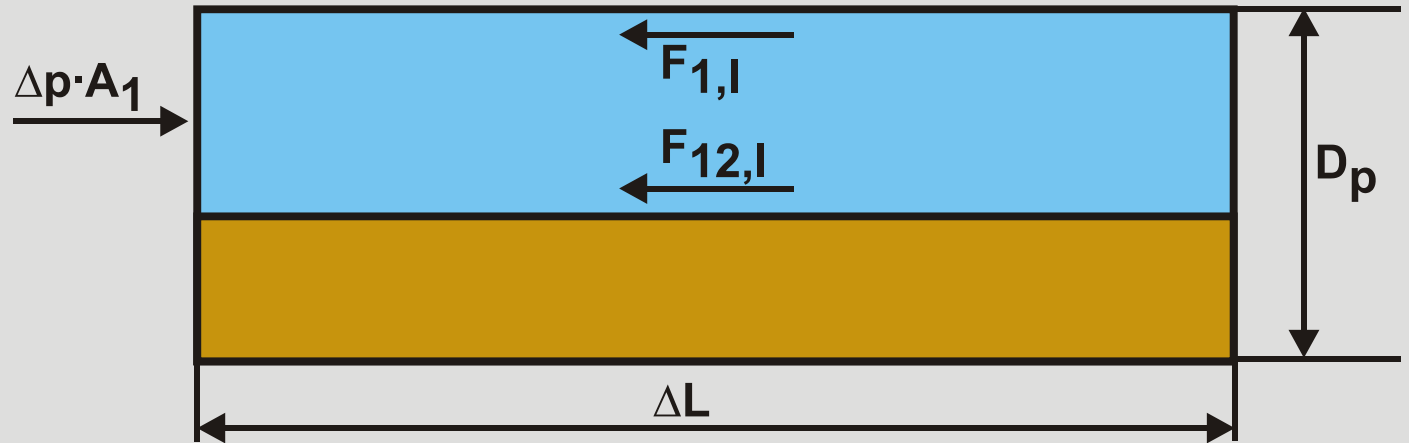
Flow Regimes



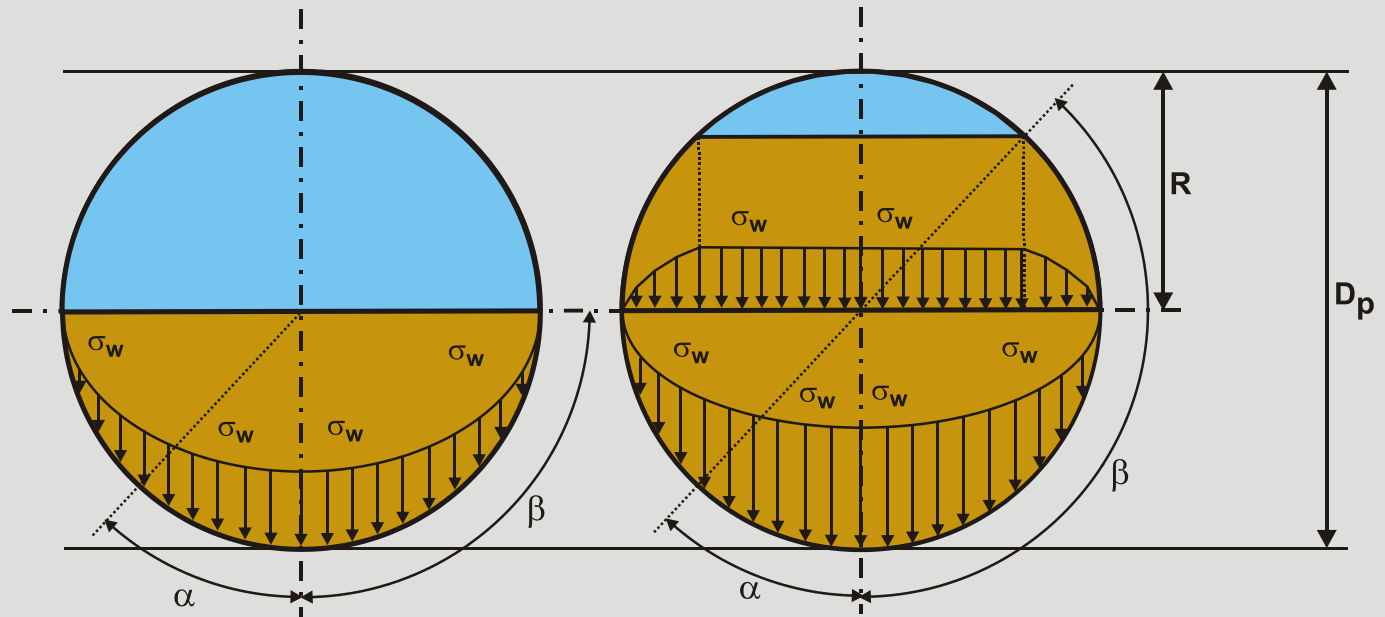
Definitions



Equilibrium of Forces



The Submerged Weight Approach

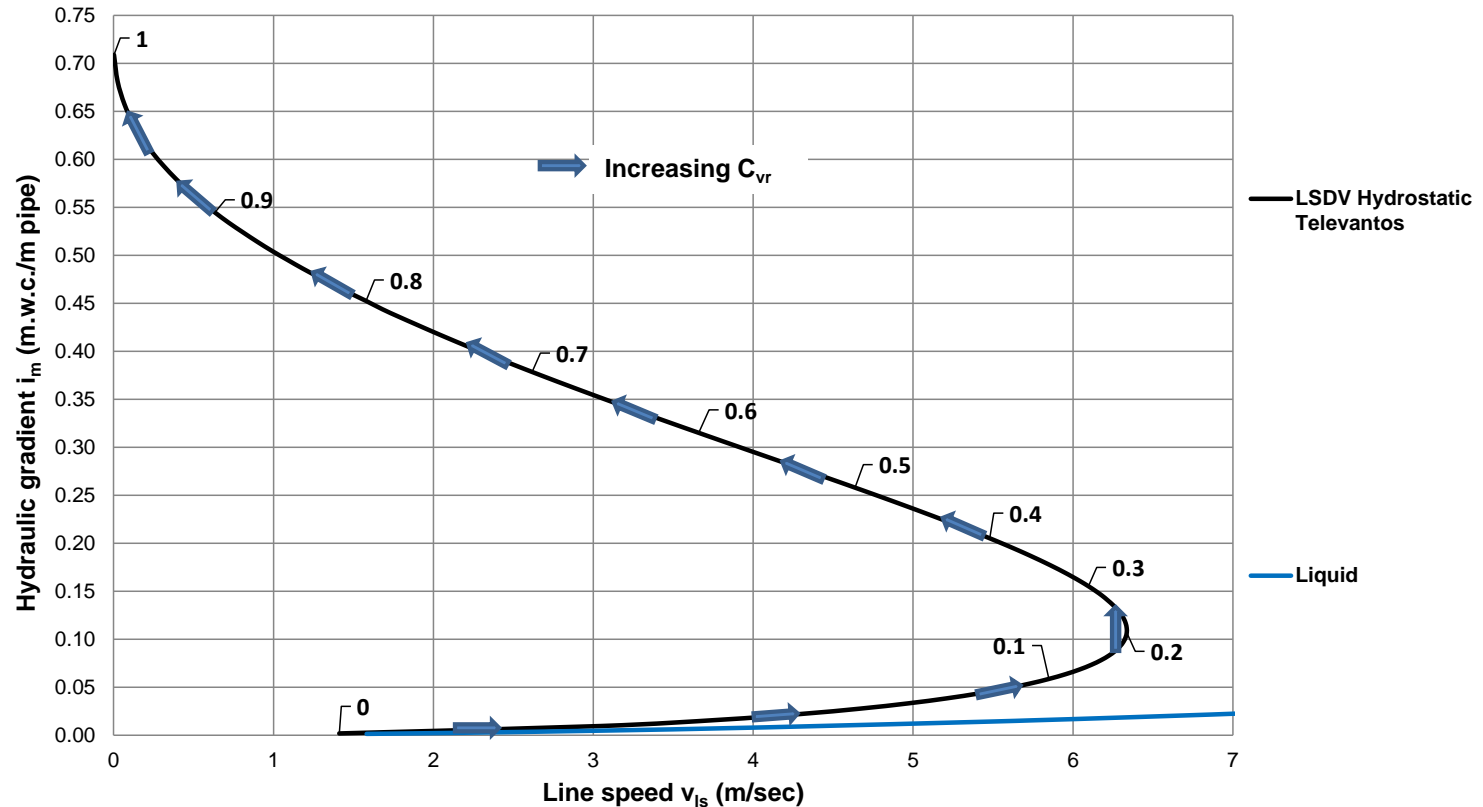


$$F_{sf} = \mu_{sf} \cdot \rho_l \cdot g \cdot \Delta L \cdot R_{sd} \cdot C_{vb} \cdot \frac{(\beta - \sin(\beta) \cdot \cos(\beta))}{\pi} \cdot A_p$$



The Limit of Stationary Deposit Velocity

Hydraulic gradient i_m vs. line speed v_{ls} , $C_{vr} = C_{vs}/C_{vb}$

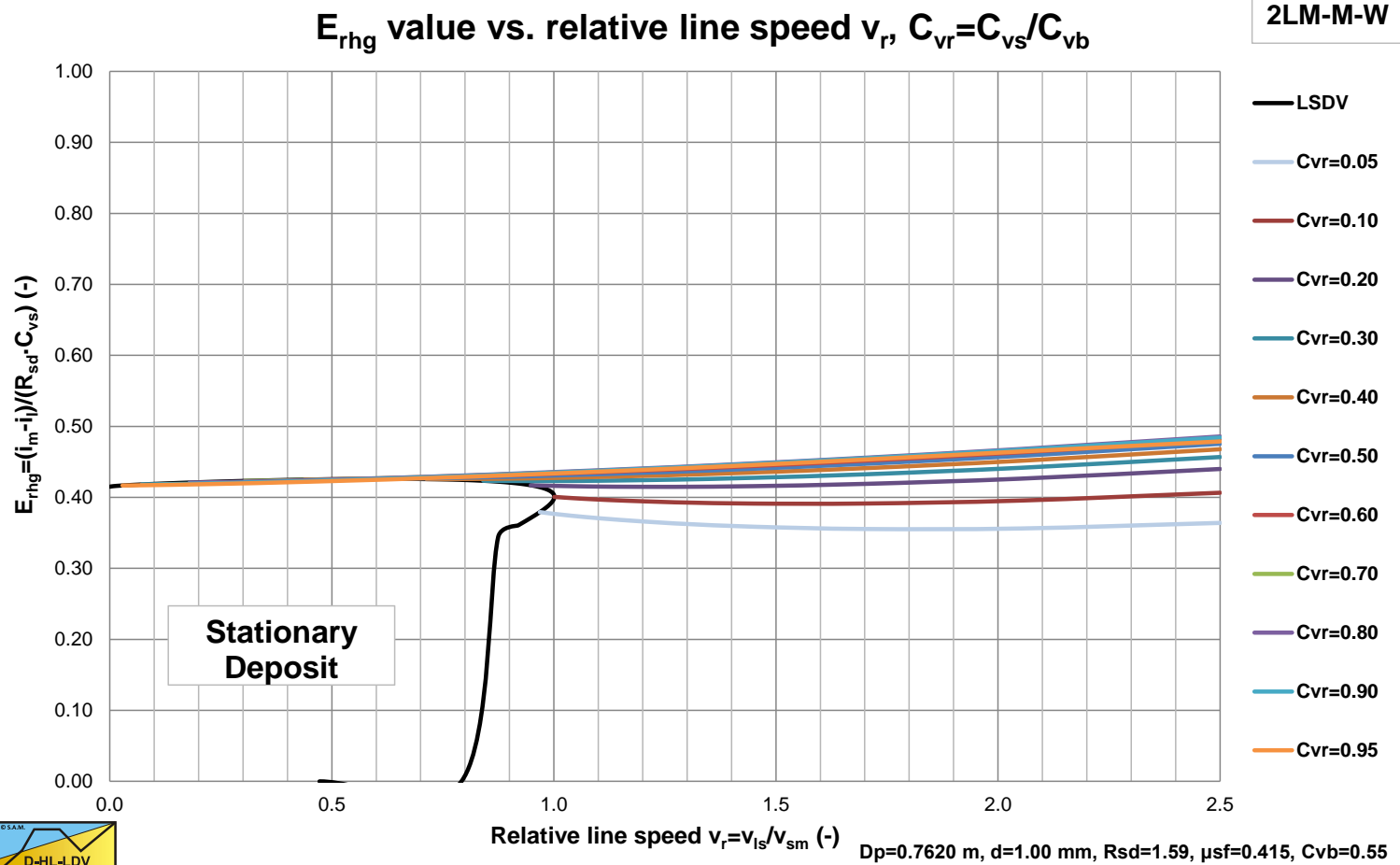


$D_p=0.7620$ m, $d=0.50$ mm, $R_{sd}=1.585$, $\mu_{sf}=0.415$, $C_{vb}=0.55$

$$F_{2,sf} + F_{2,l} = F_{12,sf} + \Delta p \cdot A_2$$



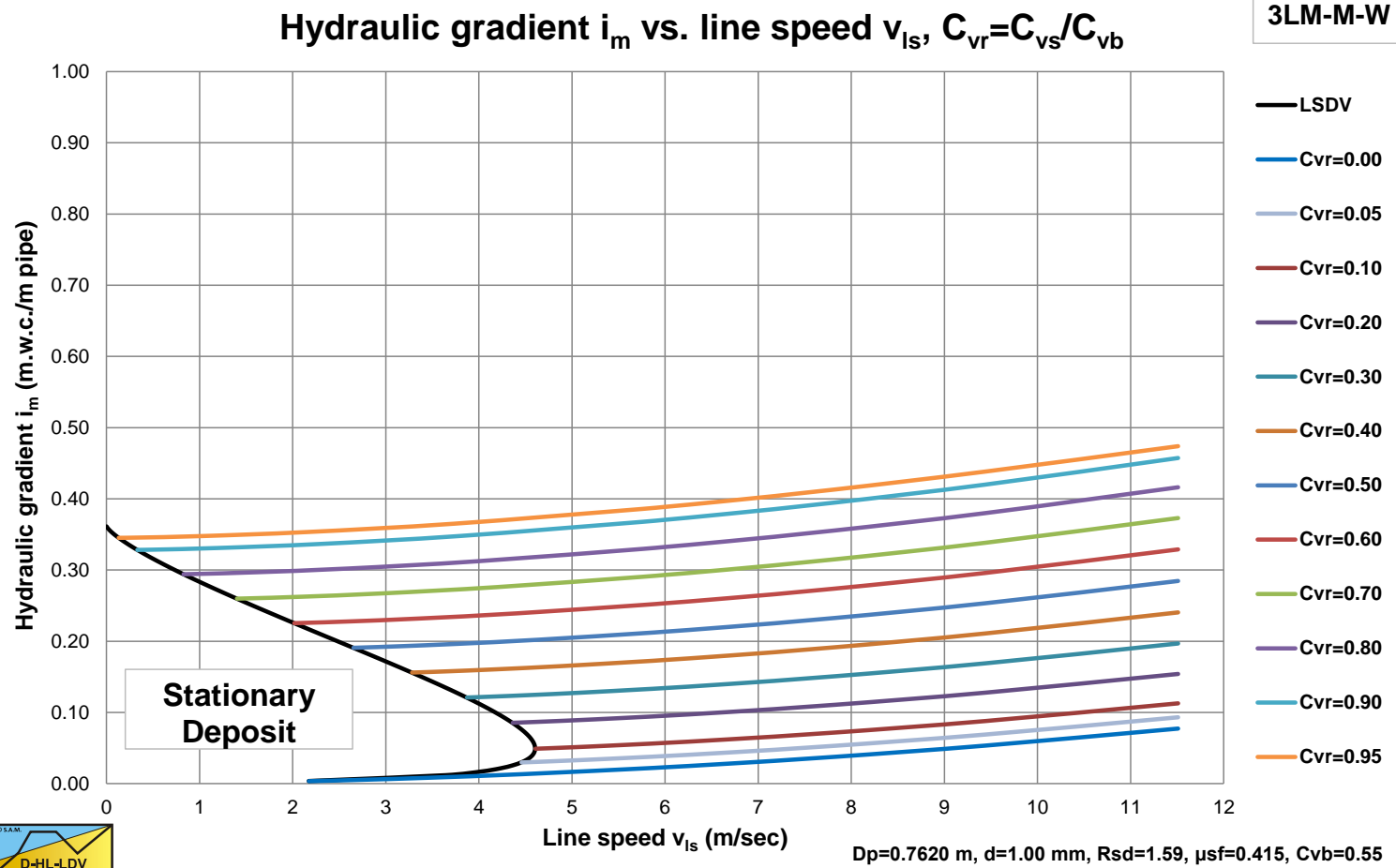
The E_{rhg} Value is almost μ_{sf}



$$E_{rhg} = \frac{i_m - i_l}{R_{sd} \cdot C_{vs}} = \mu_{sf} \quad \text{and} \quad i_m - i_l = \mu_{sf} \cdot R_{sd} \cdot C_{vs}$$



Resulting Hydraulic Gradient Graph, C_{vs}

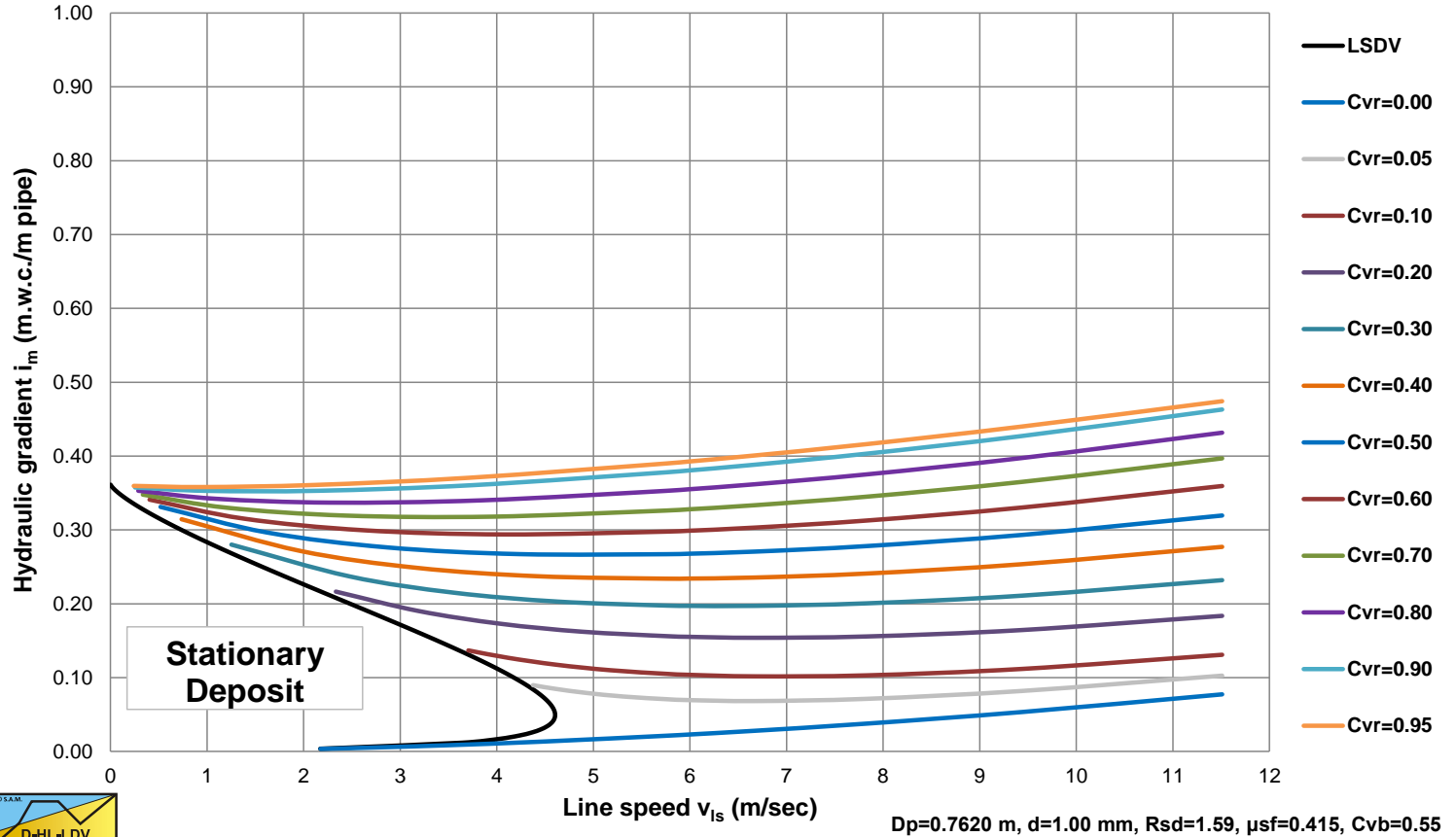


Resulting Hydraulic Gradient Graph, C_{vt}



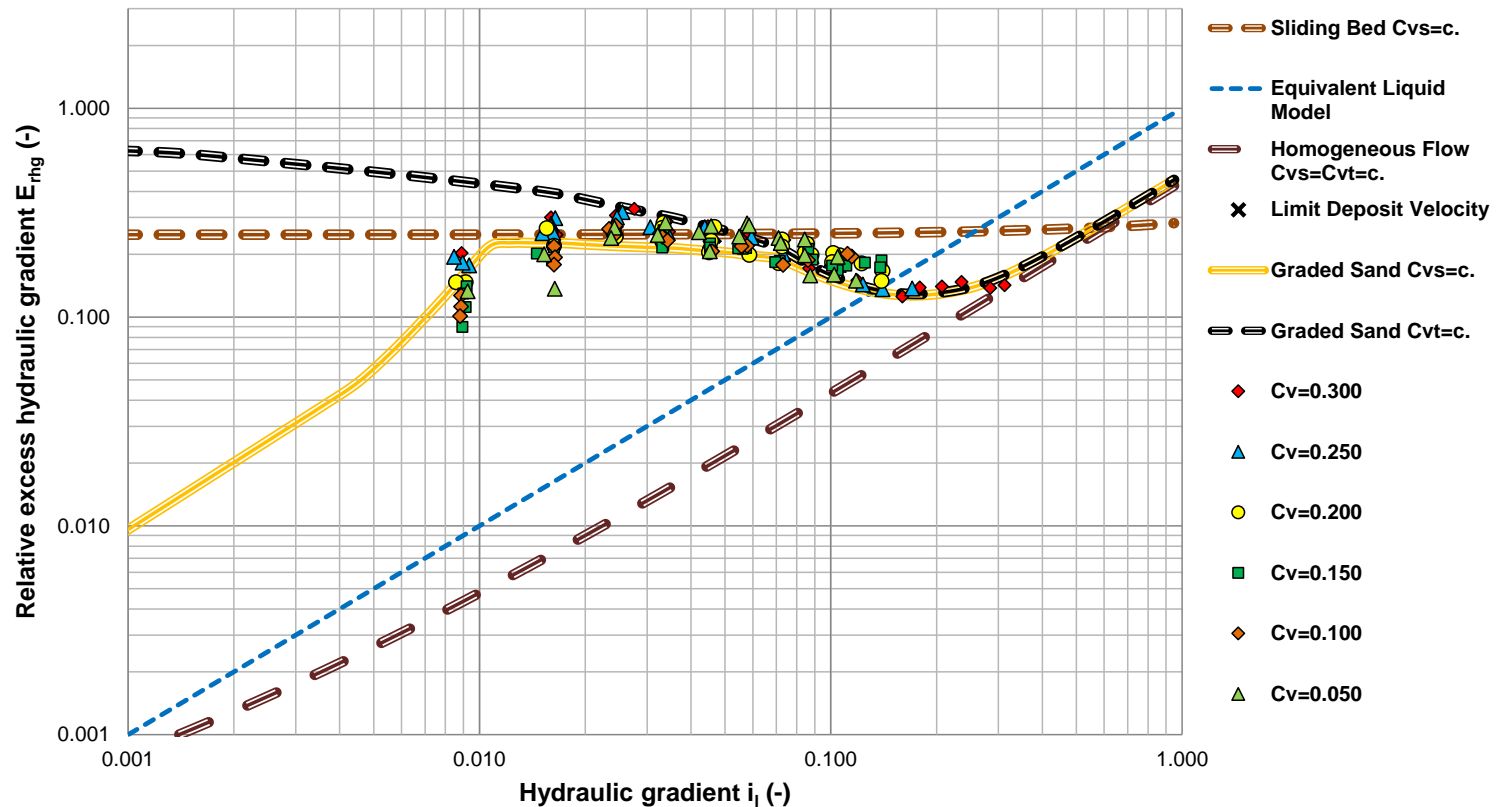
Hydraulic gradient i_m vs. line speed v_{ls} , $C_{vr} = C_{vt} / C_{vb}$

3LM-M-W



Wiedenroth (1967), Medium Sand

Relative excess hydraulic gradient E_{rhg} vs. Hydraulic gradient i_1

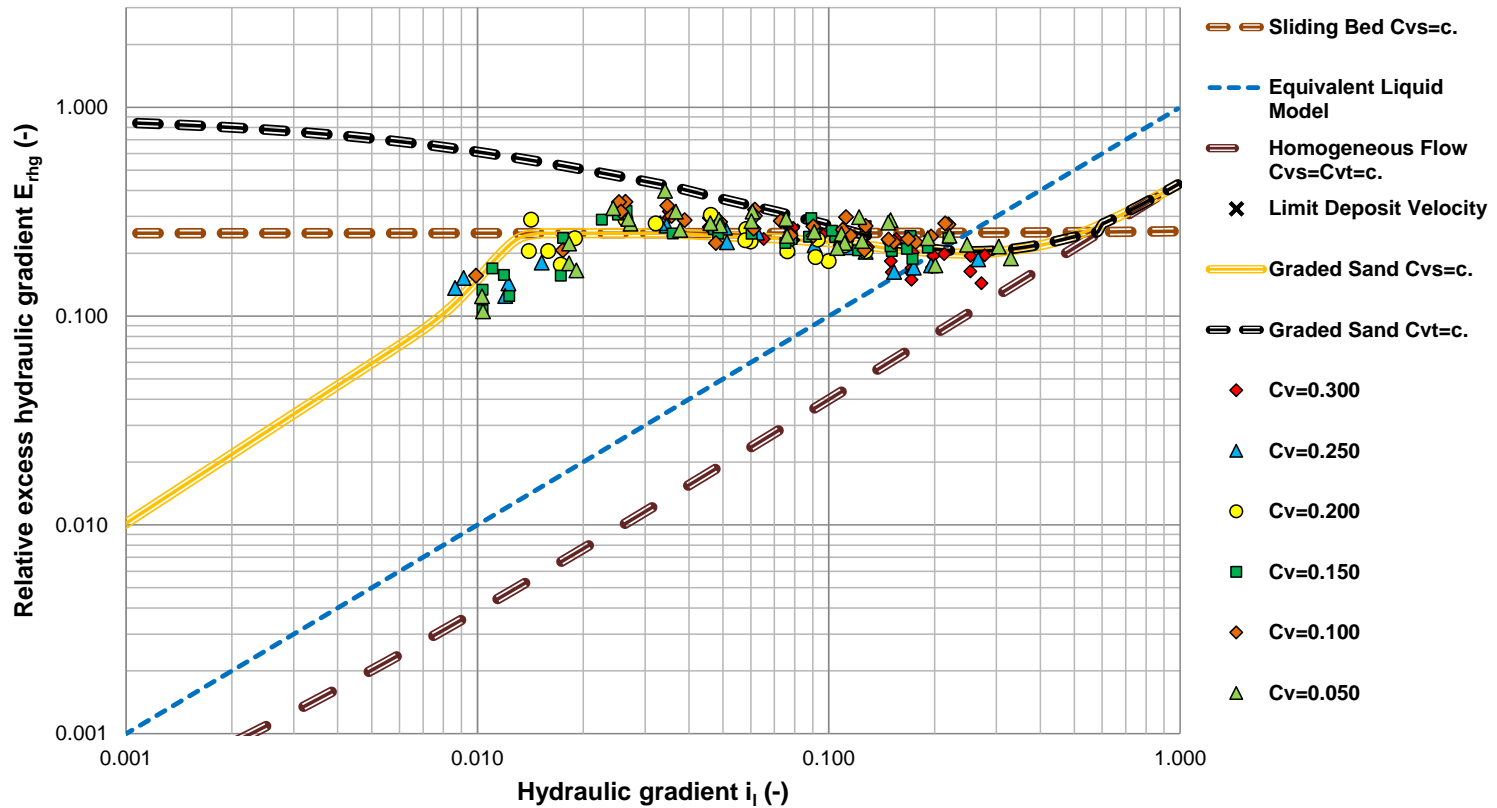


$D_p=0.1250$ m, $d=0.900$ mm, $Rsd=1.585$, $Cv=0.200$, $\mu_{sf}=0.250$



Wiedenroth (1967), Coarse Sand

Relative excess hydraulic gradient E_{rhg} vs. Hydraulic gradient i_1



$D_p=0.1250$ m, $d=2.200$ mm, $R_{sd}=1.585$, $C_v=0.150$, $\mu_{sf}=0.250$



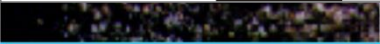
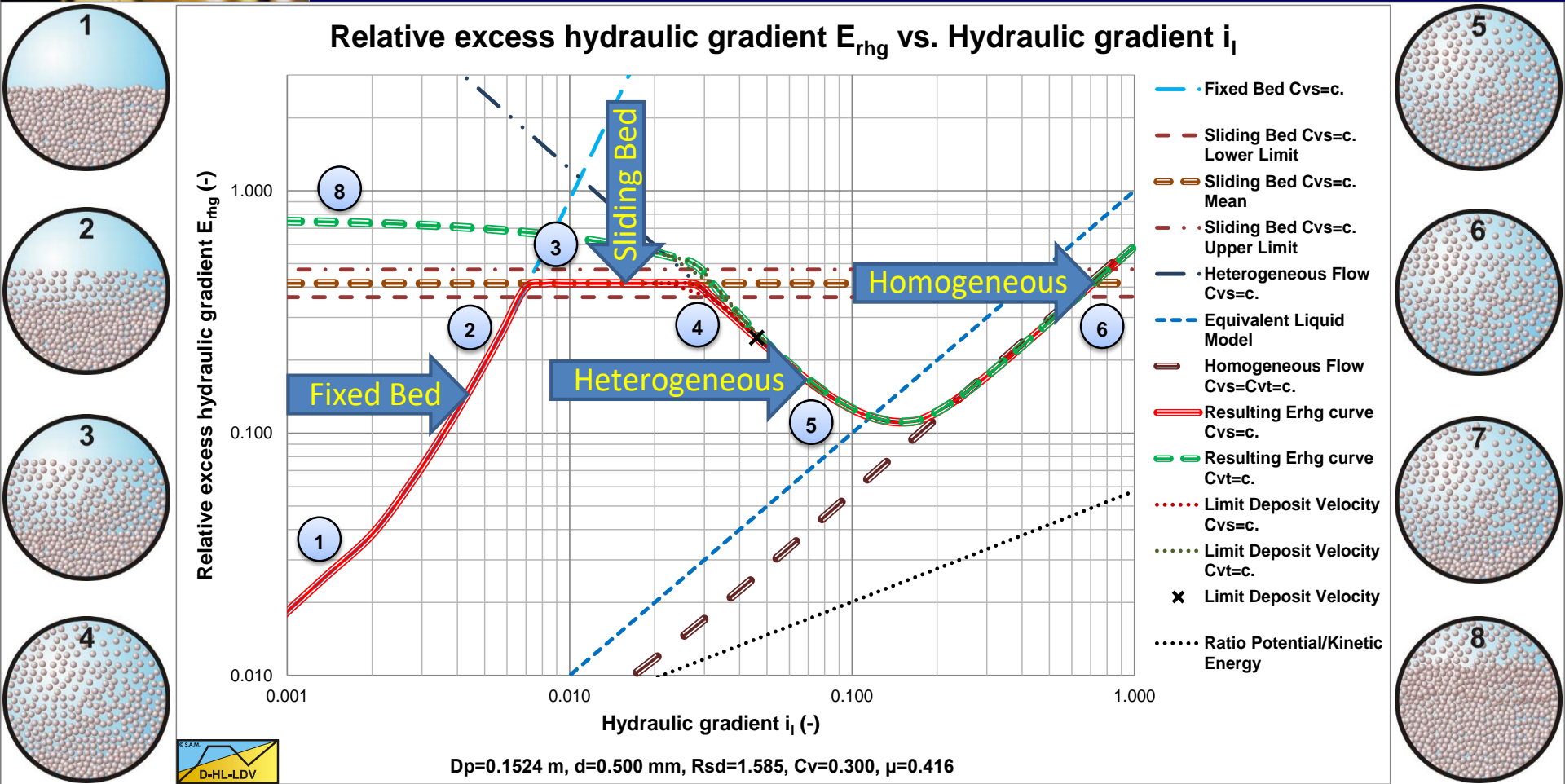


Heterogeneous Flow Regime

Chapter 7.5 & 8.5



Flow Regimes



Energy Dissipation

Energy Dissipation by:

- Turbulence Viscous Dissipation (Darcy Weisbach)
- Potential Energy Losses (Hindered Settling Velocity)
- Kinetic Energy Losses (Collisions)

$$\Delta p_m = \Delta p_{l,visc} + \Delta p_{s,pot} + \Delta p_{s,kin} = \Delta p_{l,visc} \cdot \left(1 + \frac{\Delta p_{s,pot}}{\Delta p_{l,visc}} + \frac{\Delta p_{s,kin}}{\Delta p_{l,visc}} \right)$$

$$\frac{\Delta p_m}{\Delta L} = \lambda_1 \cdot \frac{1}{D_p} \cdot \frac{1}{2} \cdot \rho_l \cdot v_{ls}^2 + \rho_l \cdot g \cdot R_{sd} \cdot C_{vs} \cdot \left(\frac{v_t \cdot (1 - C_{vs} / \kappa_C)^\beta}{v_{ls}} \right) + \rho_l \cdot g \cdot R_{sd} \cdot C_{vs} \cdot \left(\frac{v_{sl}}{v_t} \right)^2$$

$$\Delta p_m = \Delta p_l \cdot \left(1 + \frac{(2 \cdot g \cdot R_{sd} \cdot D_p)}{\lambda_1} \cdot C_{vs} \cdot \frac{1}{v_{ls}^2} \cdot \left(\frac{v_t \cdot (1 - C_{vs} / \kappa_C)^\beta}{v_{ls}} + \left(\frac{v_{sl}}{v_t} \right)^2 \right) \right)$$

Slip



Turbulent Energy Dissipation

$$\Delta p_1 = \lambda_1 \cdot \frac{\Delta L}{D_p} \cdot \frac{1}{2} \cdot \rho_1 \cdot v_{ls}^2$$

$$i_1 = i_w = \frac{\Delta p_1}{\rho_1 \cdot g \cdot \Delta L} = \frac{\lambda_1 \cdot v_{ls}^2}{2 \cdot g \cdot D_p}$$

$$\lambda_1 = \frac{1.325}{\left(\ln \left(\frac{\varepsilon}{3.7 \cdot D_p} + \frac{5.75}{Re^{0.9}} \right) \right)^2} = \frac{0.25}{\left(\log_{10} \left(\frac{\varepsilon}{3.7 \cdot D_p} + \frac{5.75}{Re^{0.9}} \right) \right)^2}$$



Potential Energy Dissipation

Incorporating hindered settling, assuming the concentration is not uniform and using the spatial volumetric concentration, this gives:

$$E_{\text{rgh,pot}} = \frac{v_t}{v_{\text{ls}}} \cdot \left(1 - \frac{C_{\text{vs}}}{0.175 \cdot (1 + \beta)} \right)^\beta$$

The denominator of $0.175 \cdot (1 + \beta)$ gives a factor 1 for very small particles with $\beta=4.7$, assuming a uniform concentration, and a factor 0.6 for very large particles with $\beta=2.39$, assuming the average position of particles is at 30% of the pipe diameter from the bottom.



Kinetic Energy Dissipation

The number of collisions per unit of time will be constant or decrease with increasing line speed due to the increase of the momentum of the particles.

The number of collisions per unit of pipeline length will thus be reversely proportional to the line speed to a power between 1 and 2.

Energy per interaction/collision is:

$$\Delta E_{s,kin,p} = m \cdot v_{ls} \cdot v_{sl} \quad \Rightarrow \quad v_{sl} = \frac{\Delta E_{s,kin,p}}{m \cdot v_{ls}}$$

Giving a contribution to the relative excess hydraulic gradient of:

$$E_{rhg} = \left(\frac{v_{sl}}{v_t} \right)^2$$



Three Influence Factors of Slip

1. Ratio thickness viscous sub-layer to particle diameter, lubrication effect
2. Angle of attack, collision impact
3. Particle Froude number, collision impact

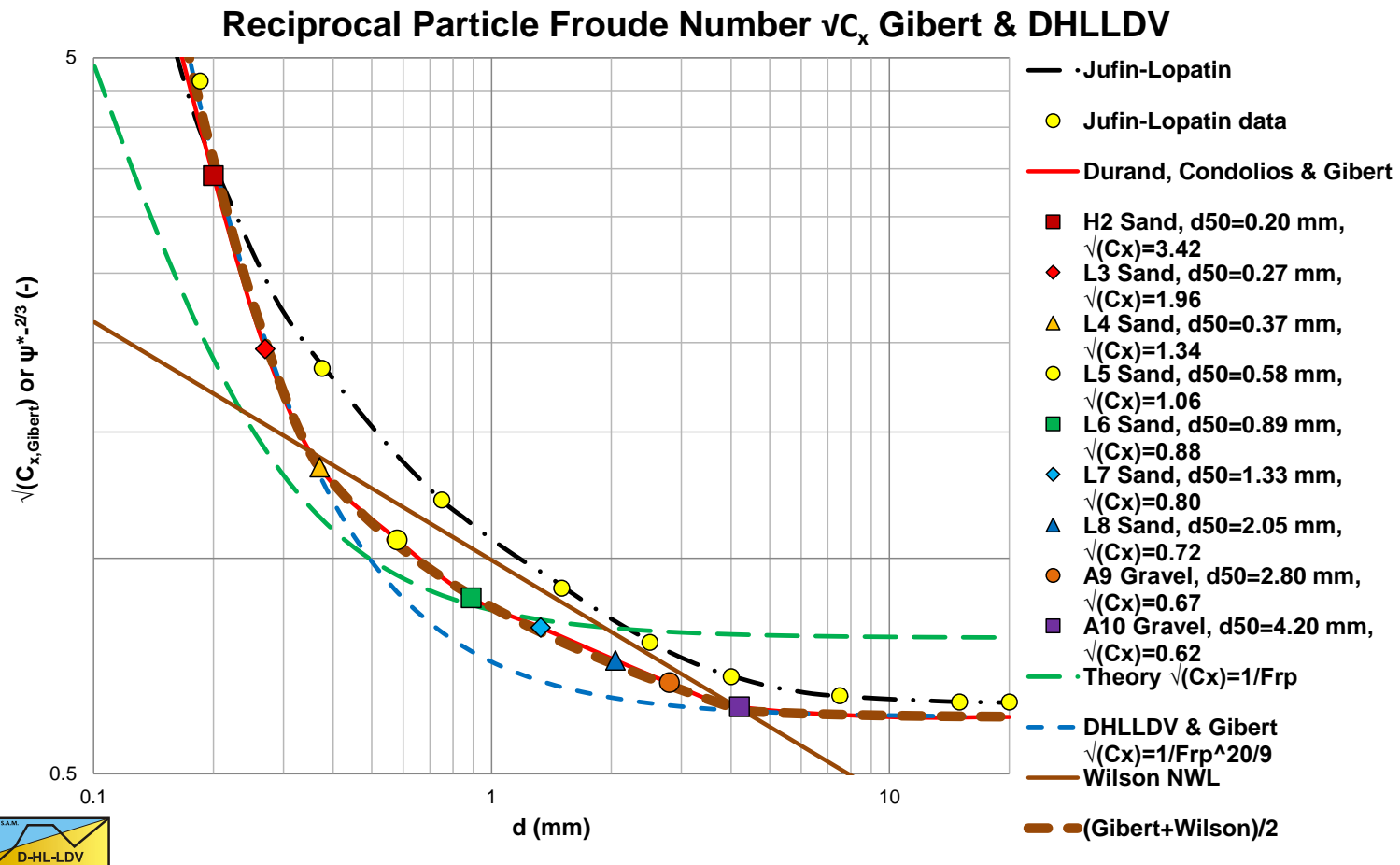
Ratio: $\left(\frac{\delta_v}{d} \right)$

Angle of attack: $\left(\frac{v_t}{11.6 \cdot u_*} \right)$

Particle Froude number: $\left(\frac{v_t}{\sqrt{g \cdot d}} \right)$



Particle Froude Number, Gibert (1960), $\sqrt{C_x}$



$$\Delta p_m = \Delta p_l \cdot (1 + \Phi \cdot C_{vs}) \quad \text{with:} \quad \Phi = 85 \cdot \left(\frac{v_{ls}^2 \cdot \sqrt{C_x}}{g \cdot D_p \cdot R_{sd}} \right)^{-3/2}$$



Relative Slip Squared

$$\left(\frac{v_{sl}}{v_t}\right)^2 = 8.5^2 \cdot \left(\frac{1}{\lambda_1}\right) \cdot \left(\frac{v_t}{\sqrt{g \cdot d}}\right)^{20/3} \cdot \left(\frac{(v_1 \cdot g)^{1/3}}{v_{ls}}\right)^2$$

$$= \frac{8.5^2}{8} \cdot \left(\frac{v_t}{\sqrt{g \cdot d}}\right)^{20/3} \cdot \left(\frac{(v_1 \cdot g)^{1/3}}{\sqrt{\lambda_1 / 8} \cdot v_{ls}}\right)^2$$





=



+



The pressure losses are:
viscous losses + the
sedimentation capability
(potential energy) + the
collision impact times the
collision intensity (kinetic
energy)

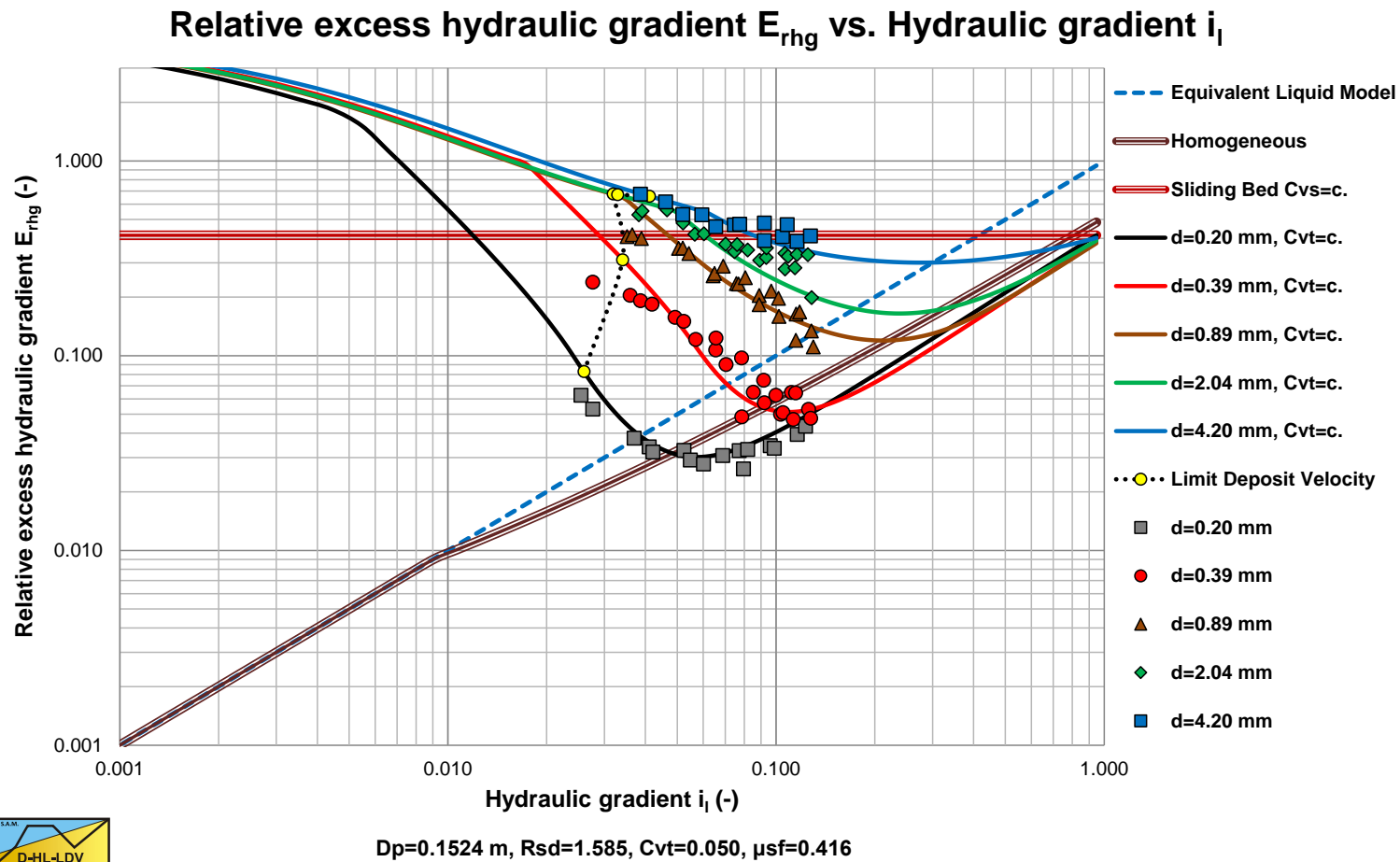
+



X



Verification & Validation, Durand et al.

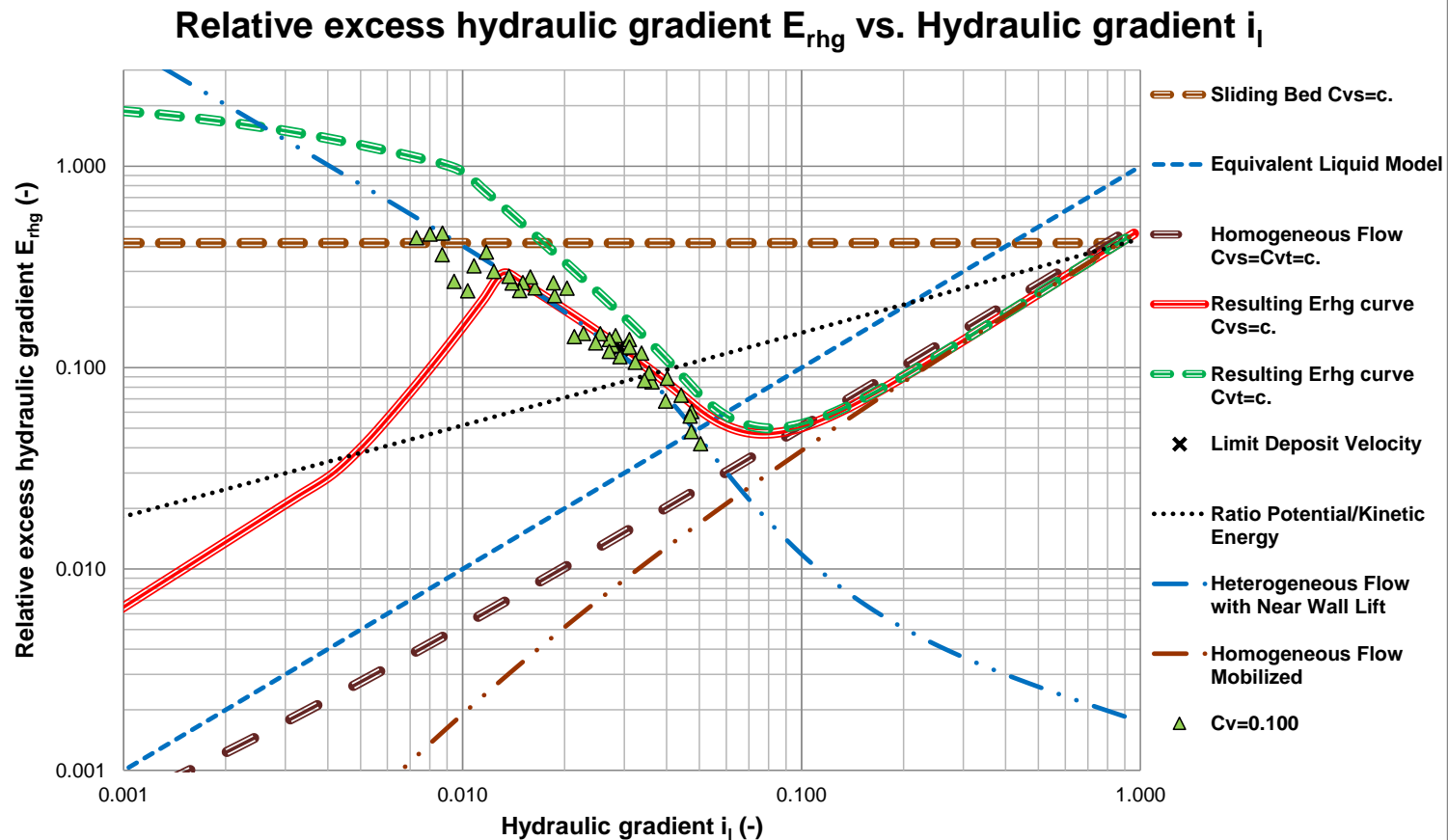


Durand & Condolios (1952)

Delft University of Technology – Offshore & Dredging Engineering



Verification & Validation, Clift et al.



$D_p=0.4400$ m, $d=0.680$ mm, $Rsd=1.585$, $Cv=0.100$, $\mu_{sf}=0.416$

Clift (1982)

Delft University of Technology – Offshore & Dredging Engineering



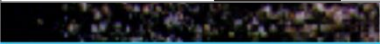
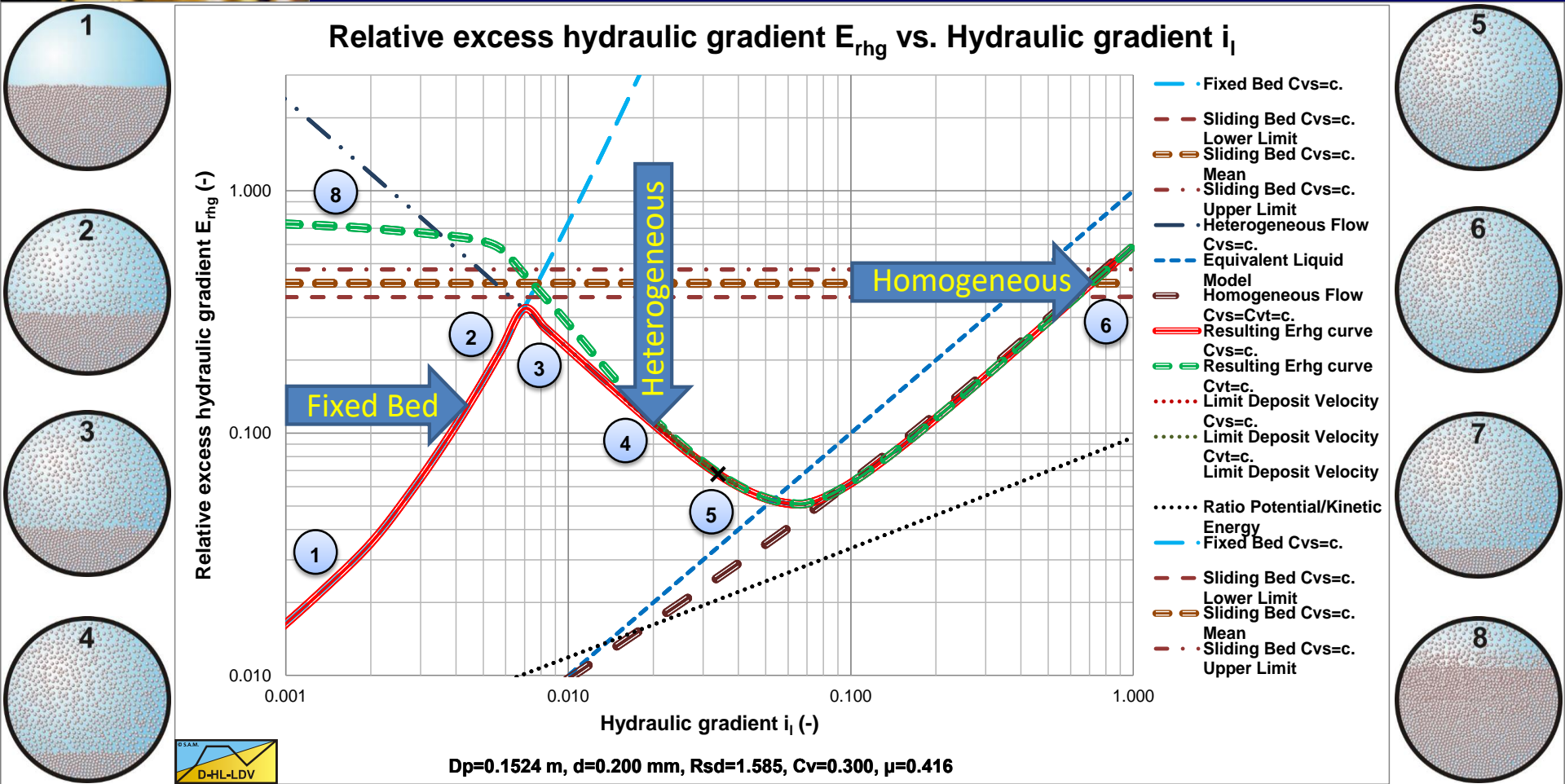


Homogeneous Flow Regime

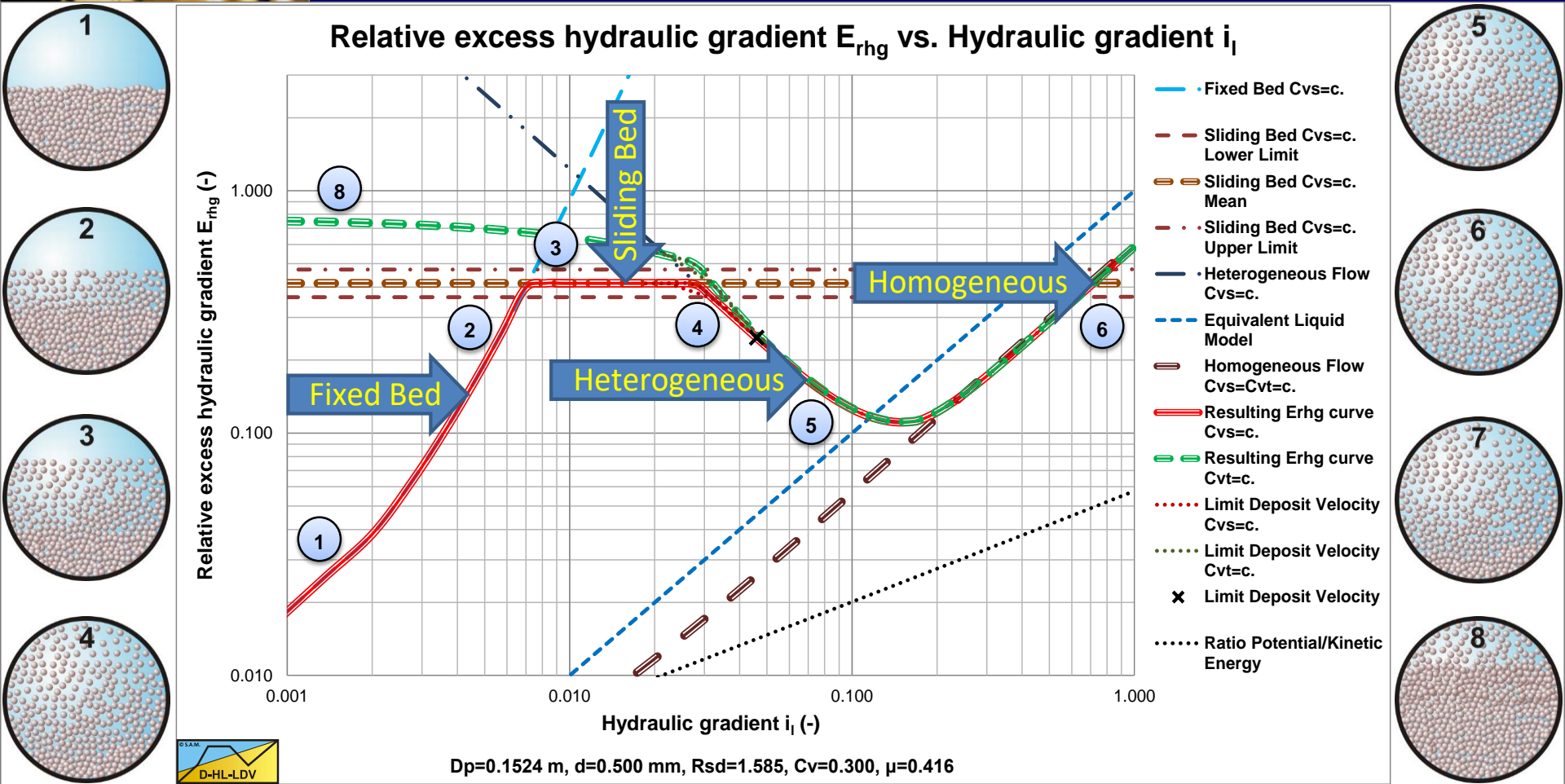
Chapter 7.6 & 8.6



Flow Regimes, Fine Particles



Flow Regimes, Medium/Coarse Particles



The Equivalent Liquid Model (ELM)

$$\Delta p_m = \lambda_1 \cdot \frac{\Delta L}{D_p} \cdot \frac{1}{2} \cdot \rho_m \cdot v_{ls}^2$$

$$\begin{aligned} i_m &= \frac{\Delta p_m}{\rho_l \cdot g \cdot \Delta L} = \frac{\rho_m}{\rho_l} \cdot \frac{\lambda_1 \cdot v_{ls}^2}{2 \cdot g \cdot D_p} \\ &= i_1 \cdot (1 + R_{sd} \cdot C_{vs}) \end{aligned}$$

$$E_{rhg} = \frac{i_m - i_1}{R_{sd} \cdot C_{vs}} = i_1$$



Phenomena

- **Very fine particles:** The liquid properties have to be adjusted. The ELM can be used with the adjusted liquid properties.
- **Fine particles:** The ELM can be used with the original liquid properties. At high line speeds the lubrication effect will be mobilized.
- **Medium/Coarse particles:** The lubrication effect is mobilized, due to a particle poor viscous sub-layer. This gives a reduction of the solids effect in the ELM.



Very Fine Particles

$$d_{\text{lim}} = \sqrt{\frac{\text{Stk} \cdot 9 \cdot \rho_l \cdot v_l \cdot D_p}{\rho_s \cdot v_{\text{ls,ldv}}}} \approx \sqrt{\frac{\text{Stk} \cdot 9 \cdot \rho_l \cdot v_l \cdot D_p}{\rho_s \cdot 7.5 \cdot D_p^{0.4}}} \quad X=1$$

$$\rho_x = \rho_l + \rho_l \cdot \frac{X \cdot C_{\text{vs}} \cdot R_{\text{sd}}}{(1 - C_{\text{vs}} + C_{\text{vs}} \cdot X)}$$

$$C_{\text{vs},x} = \frac{X \cdot C_{\text{vs}}}{(1 - C_{\text{vs}} + C_{\text{vs}} \cdot X)} \quad \text{and} \quad C_{\text{vs},r} = (1 - X) \cdot C_{\text{vs}}$$

$$\mu_x = \mu_l \cdot \left(1 + 2.5 \cdot C_{\text{vs},x} + 10.05 \cdot C_{\text{vs},x}^2 + 0.00273 \cdot e^{16.6 \cdot C_{\text{vs},x}} \right)$$

$$v_x = \frac{\mu_x}{\rho_x} \quad \text{and} \quad R_{\text{sd},x} = \frac{\rho_s - \rho_x}{\rho_x}$$



Fine Particles

$$E_{\text{rhg}} = \frac{i_m - i_l}{R_{\text{sd}} \cdot C_{\text{vs}}} = i_l \cdot \left(1 - \frac{1 + R_{\text{sd}} \cdot C_{\text{vs}} - \left(\frac{A_{C_v}}{\kappa} \cdot \ln \left(\frac{\rho_m}{\rho_l} \right) \cdot \sqrt{\frac{\lambda_l}{8}} + 1 \right)^2}{R_{\text{sd}} \cdot C_{\text{vs}} \cdot \left(\frac{A_{C_v}}{\kappa} \cdot \ln \left(\frac{\rho_m}{\rho_l} \right) \cdot \sqrt{\frac{\lambda_l}{8}} + 1 \right)^2} \right) \cdot \left(1 - \left(\frac{\delta_v}{d} \right) \right)$$

$$E_{\text{rhg}} = \frac{i_m - i_l}{R_{\text{sd}} \cdot C_{\text{vs}}} = i_l \cdot \left(1 - (1 - \alpha_E) \cdot \left(1 - \left(\frac{\delta_v}{d} \right) \right) \right)$$

$$i_m = i_l + i_l \cdot R_{\text{sd}} \cdot C_{\text{vs}} \cdot \left(1 - (1 - \alpha_E) \cdot \left(1 - \left(\frac{\delta_v}{d} \right) \right) \right)$$

$$\left(\frac{\delta_v}{d} \right) = \text{max}=1 \quad \Rightarrow \quad i_m = i_l + i_l \cdot R_{\text{sd}} \cdot C_{\text{vs}} = i_l \cdot (1 + R_{\text{sd}} \cdot C_{\text{vs}}) \quad \text{ELM}$$

$$\left(\frac{\delta_v}{d} \right) = 0 \quad \Rightarrow \quad i_m = i_l + i_l \cdot R_{\text{sd}} \cdot C_{\text{vs}} \cdot \alpha_E = i_l \cdot (1 + R_{\text{sd}} \cdot C_{\text{vs}} \cdot \alpha_E)$$



Medium/Coarse Particles

$$E_{\text{rhg}} = i_l \cdot \frac{1 + R_{\text{sd}} \cdot C_{\text{vs}} - \left(\frac{A_{C_v}}{\kappa} \cdot \ln \left(\frac{\rho_m}{\rho_l} \right) \cdot \sqrt{\frac{\lambda_1}{8} + 1} \right)^2}{R_{\text{sd}} \cdot C_{\text{vs}} \cdot \left(\frac{A_{C_v}}{\kappa} \cdot \ln \left(\frac{\rho_m}{\rho_l} \right) \cdot \sqrt{\frac{\lambda_1}{8} + 1} \right)^2} = \alpha_E \cdot i_l$$

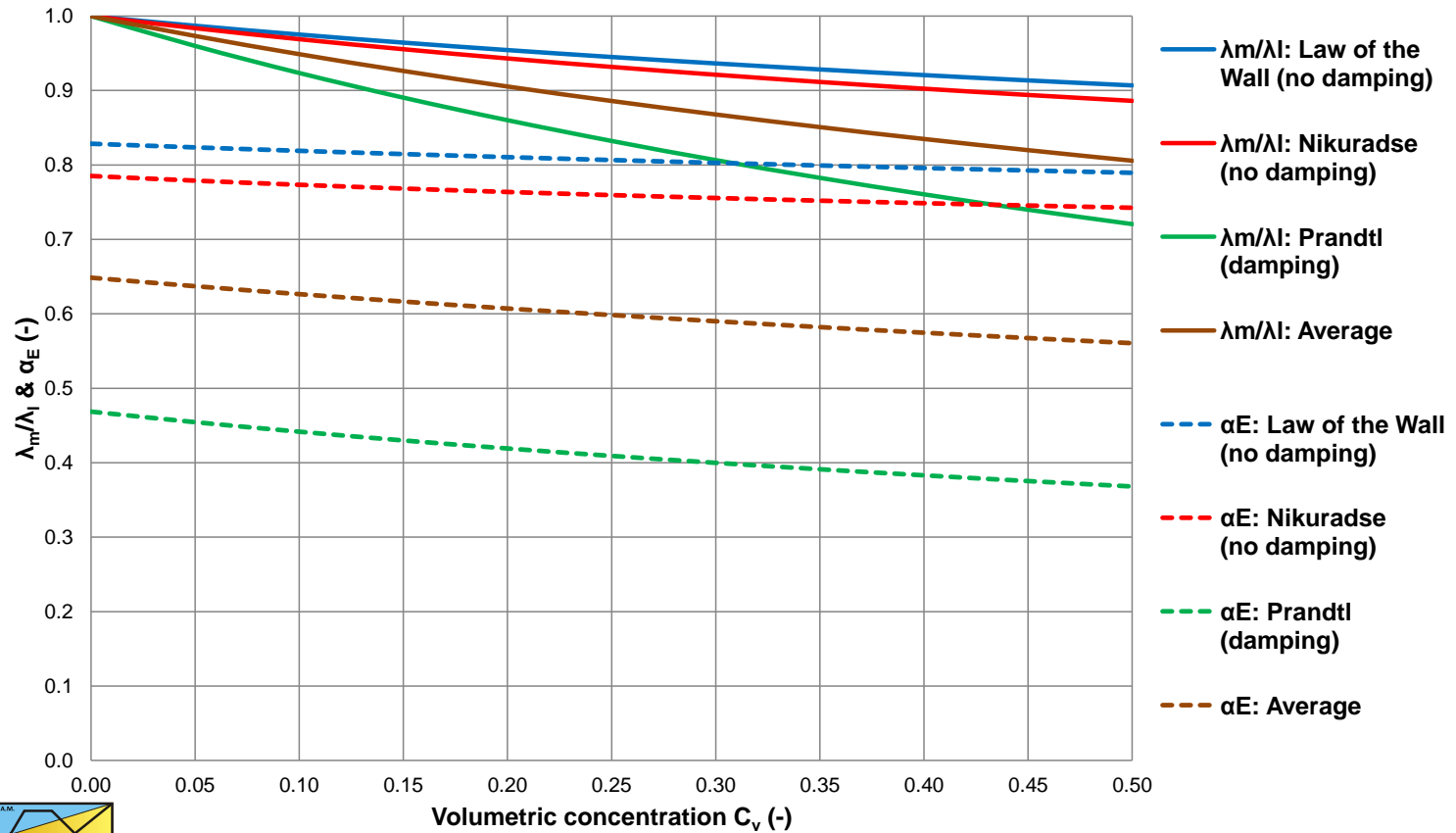
$$i_m = i_l + i_l \cdot \frac{1 + R_{\text{sd}} \cdot C_{\text{vs}} - \left(\frac{A_{C_v}}{\kappa} \cdot \ln \left(\frac{\rho_m}{\rho_l} \right) \cdot \sqrt{\frac{\lambda_1}{8} + 1} \right)^2}{\left(\frac{A_{C_v}}{\kappa} \cdot \ln \left(\frac{\rho_m}{\rho_l} \right) \cdot \sqrt{\frac{\lambda_1}{8} + 1} \right)^2}$$

$$p_m = p_l + p_l \cdot \frac{1 + R_{\text{sd}} \cdot C_{\text{vs}} - \left(\frac{A_{C_v}}{\kappa} \cdot \ln \left(\frac{\rho_m}{\rho_l} \right) \cdot \sqrt{\frac{\lambda_1}{8} + 1} \right)^2}{\left(\frac{A_{C_v}}{\kappa} \cdot \ln \left(\frac{\rho_m}{\rho_l} \right) \cdot \sqrt{\frac{\lambda_1}{8} + 1} \right)^2}$$

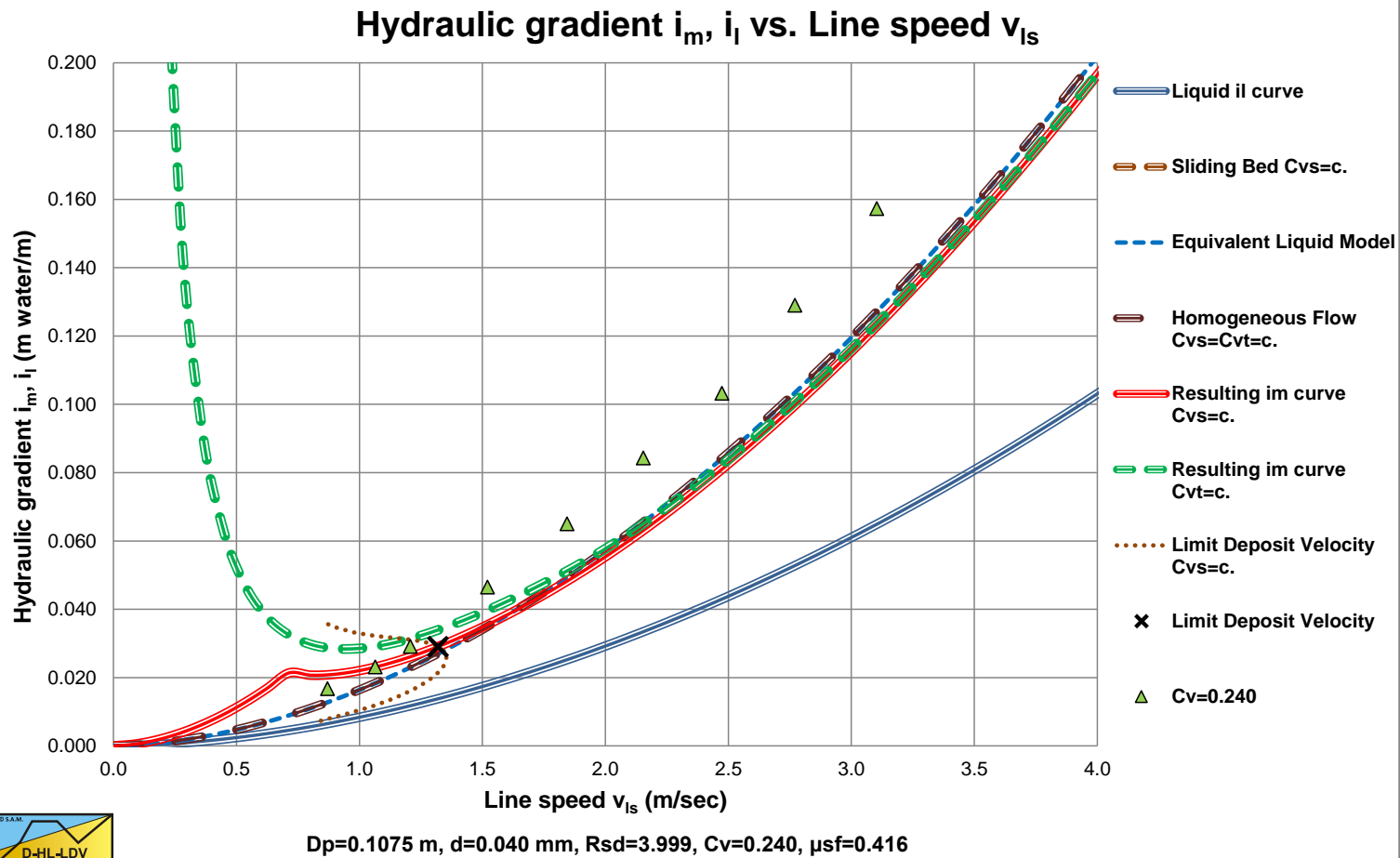


Lubrication Factor α_E

λ_m/λ_l & α_E vs. Volumetric concentration C_v



Very Fine Particles

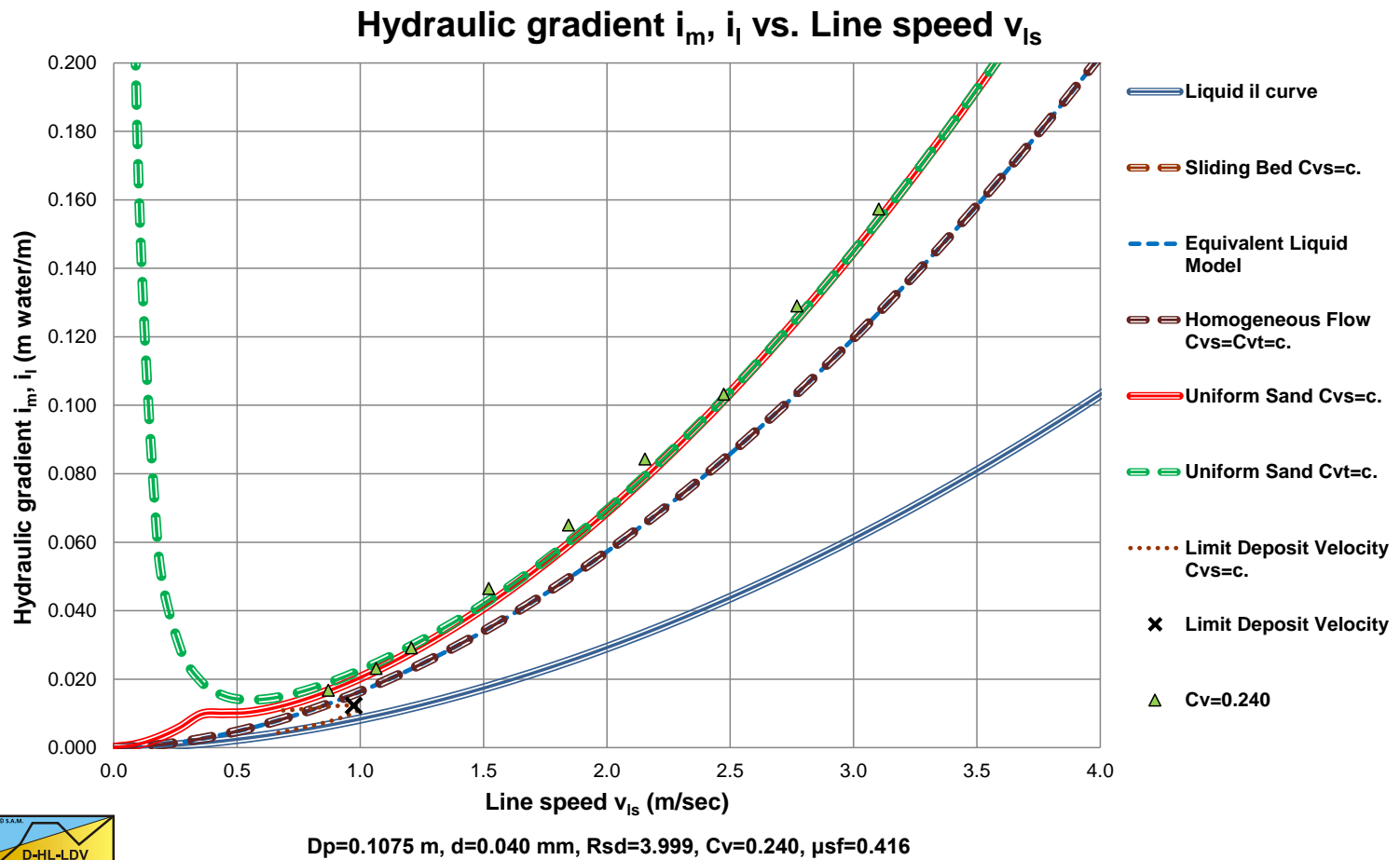


Thomas (1976)

Delft University of Technology – Offshore & Dredging Engineering



Very Fine Particles, with Thomas (1965)



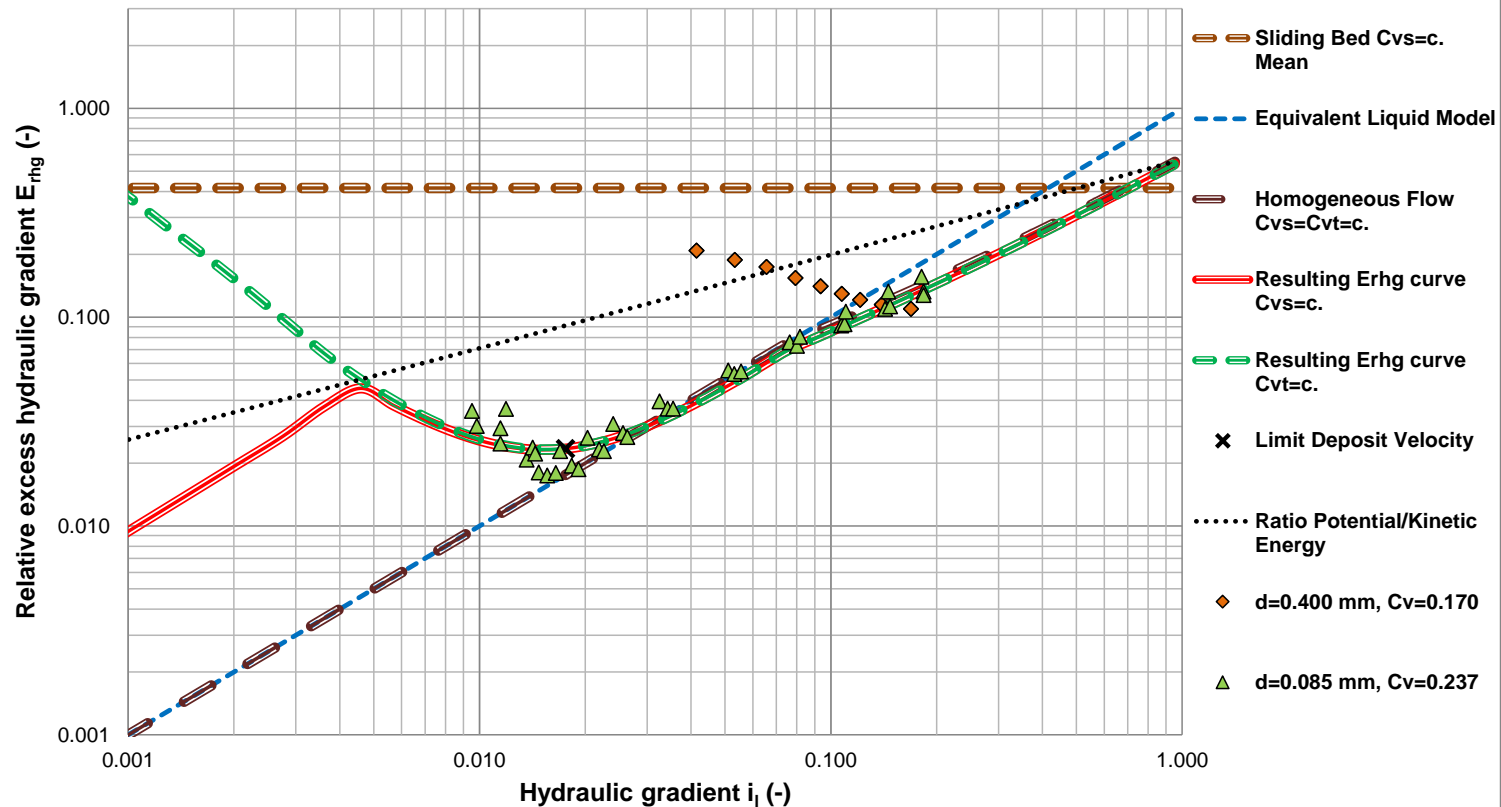
Thomas (1976) Adjusted Liquid Properties

Delft University of Technology – Offshore & Dredging Engineering



Fine Particles

Relative excess hydraulic gradient E_{rhg} vs. Hydraulic gradient i_1



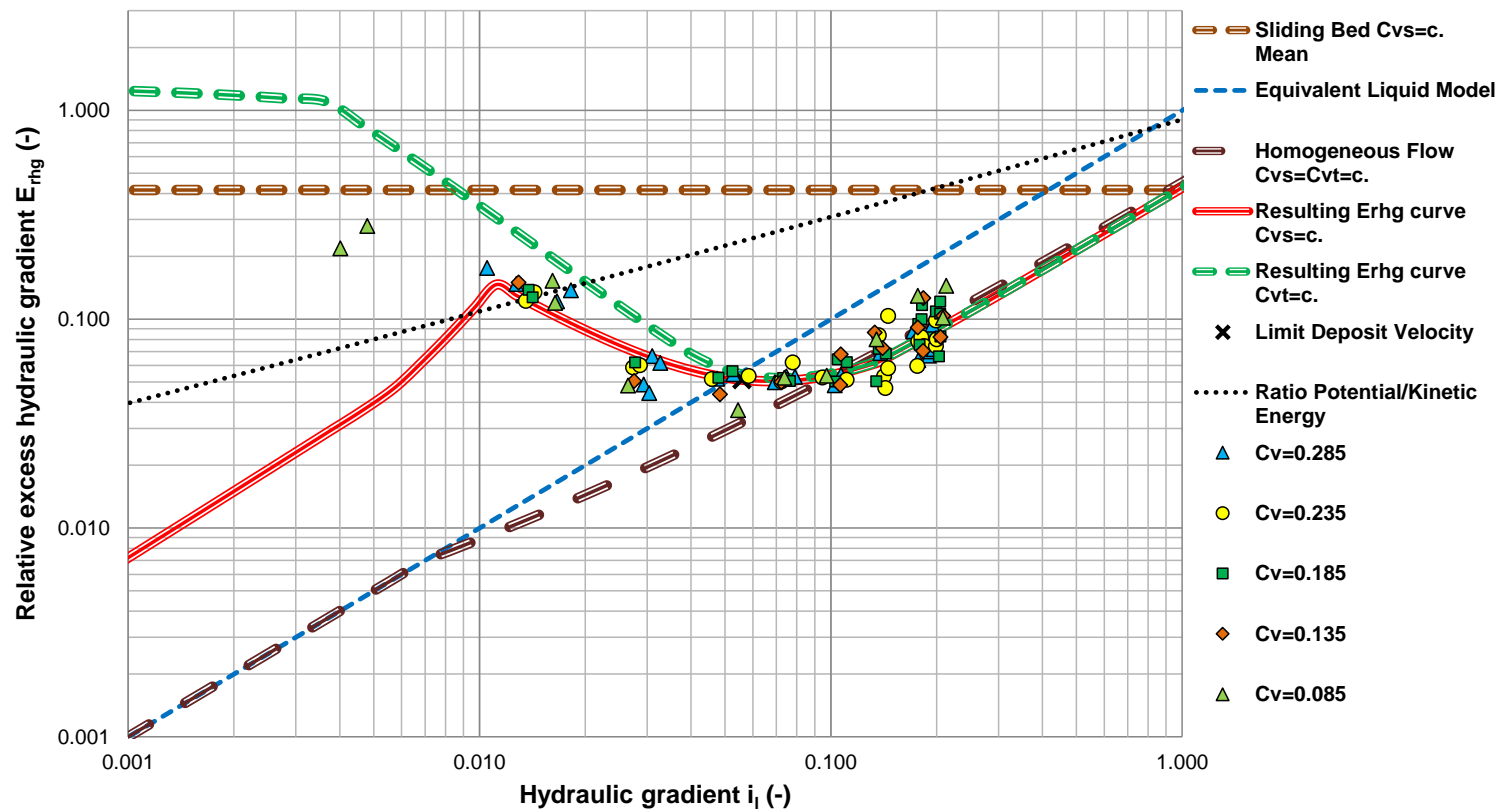
$D_p=0.1016$ m, $d=0.085$ mm, $Rsd=1.585$, $Cv=0.237$, $\mu sf=0.416$

Whitlock (2004)



Medium/Coarse Particles

Relative excess hydraulic gradient E_{rhg} vs. Hydraulic gradient i_1



$D_p=0.1000$ m, $d=0.280$ mm, $Rsd=1.585$, $Cv=0.175$, $\mu_{sf}=0.416$

Blythe & Czarnotta (1995)

Delft University of Technology – Offshore & Dredging Engineering



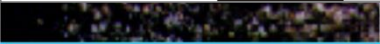
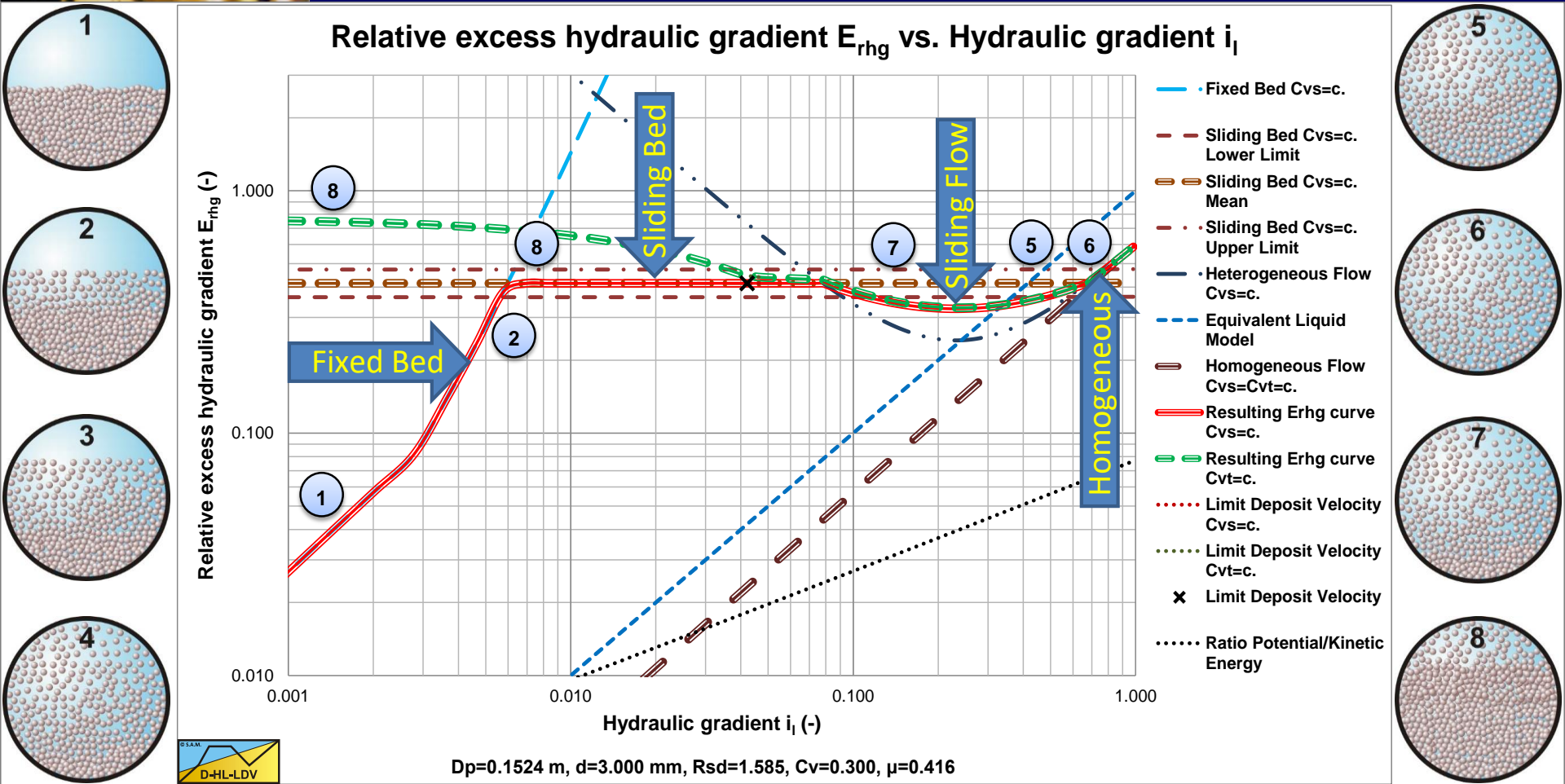


Sliding Flow Regime

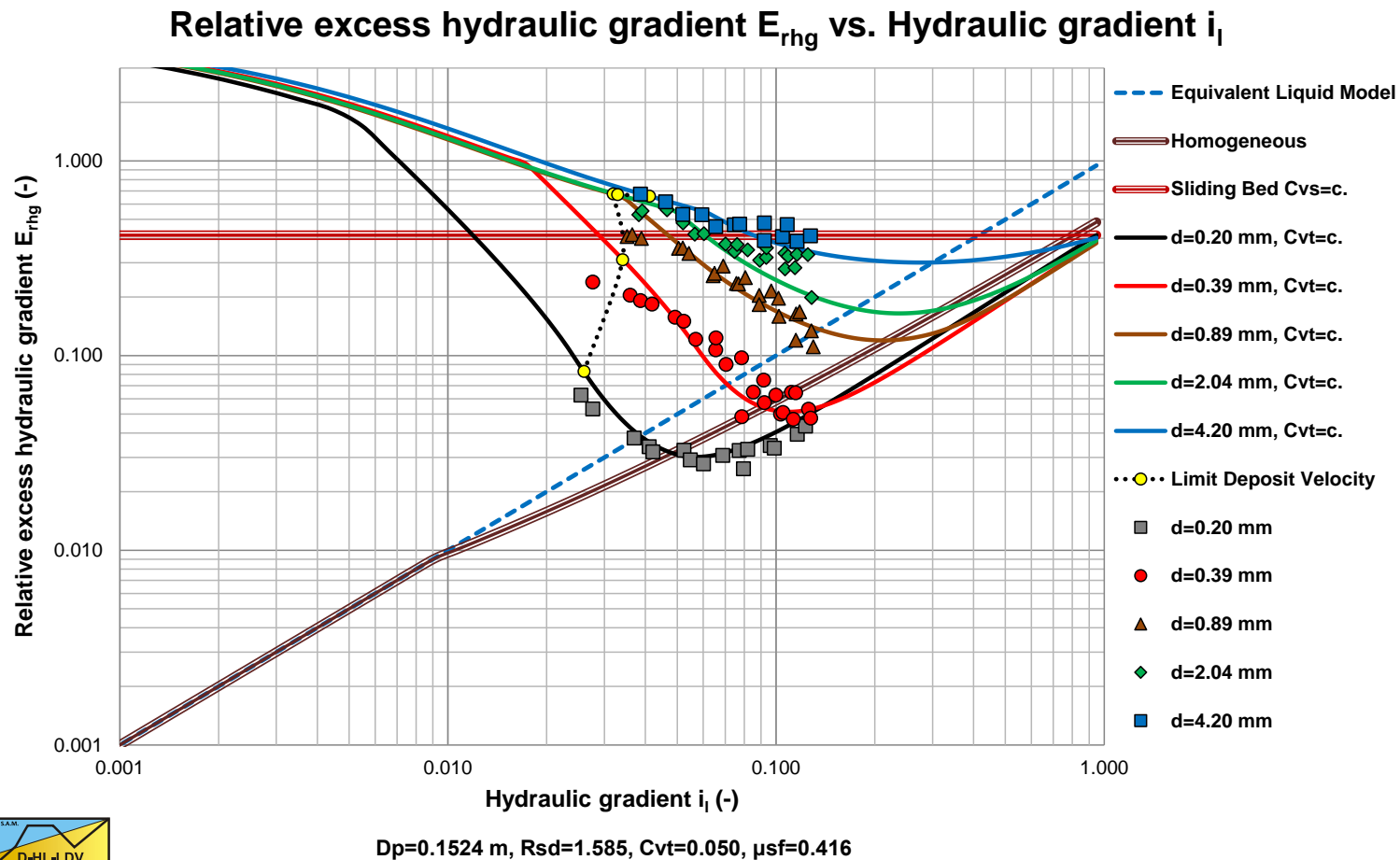
Chapter 7.7 & 8.8



Flow Regimes



Verification & Validation, Durand

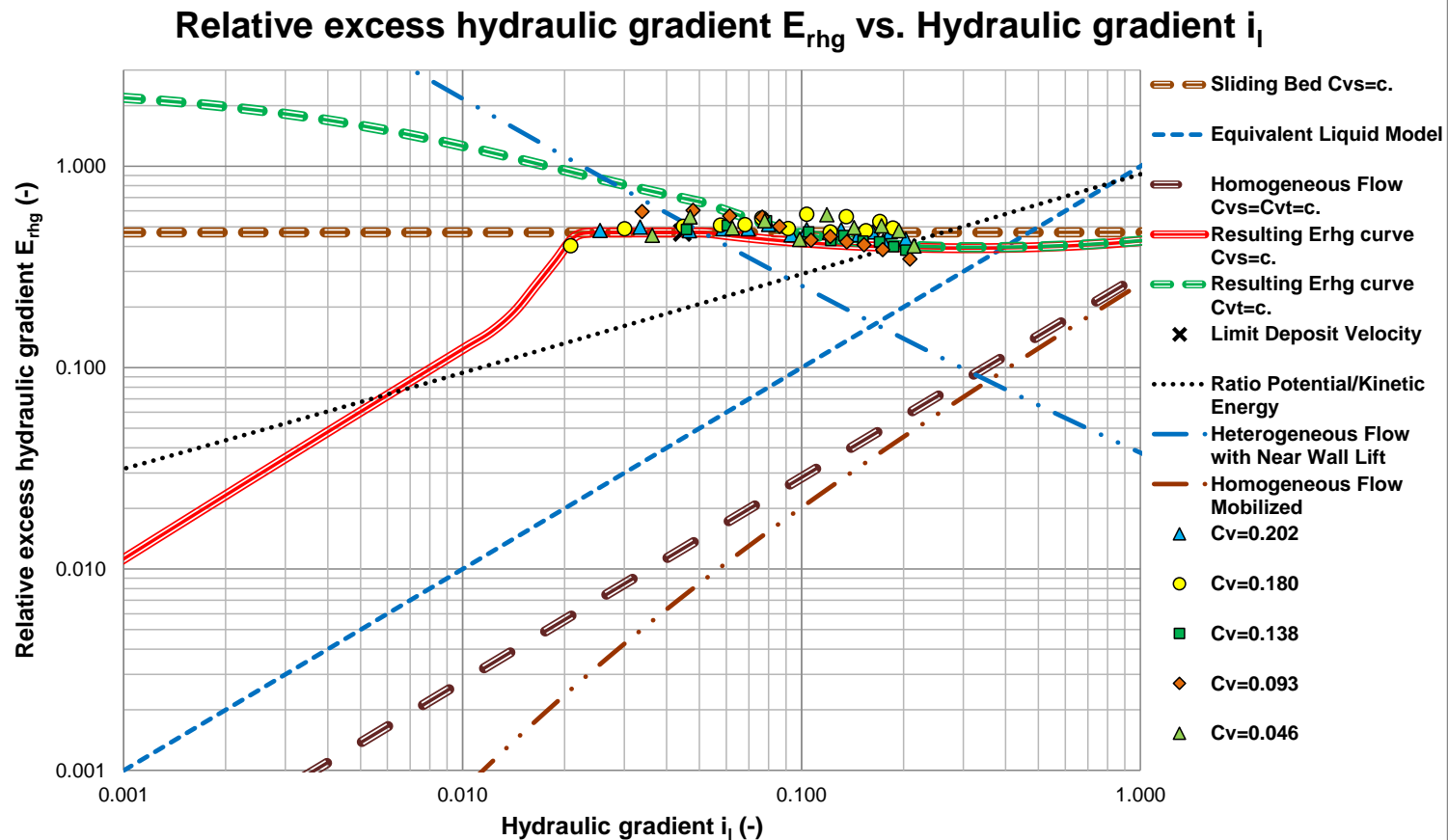


Durand, Condolios & Gibert (1952-1960)

Delft University of Technology – Offshore & Dredging Engineering



Verification & Validation, Boothroyde

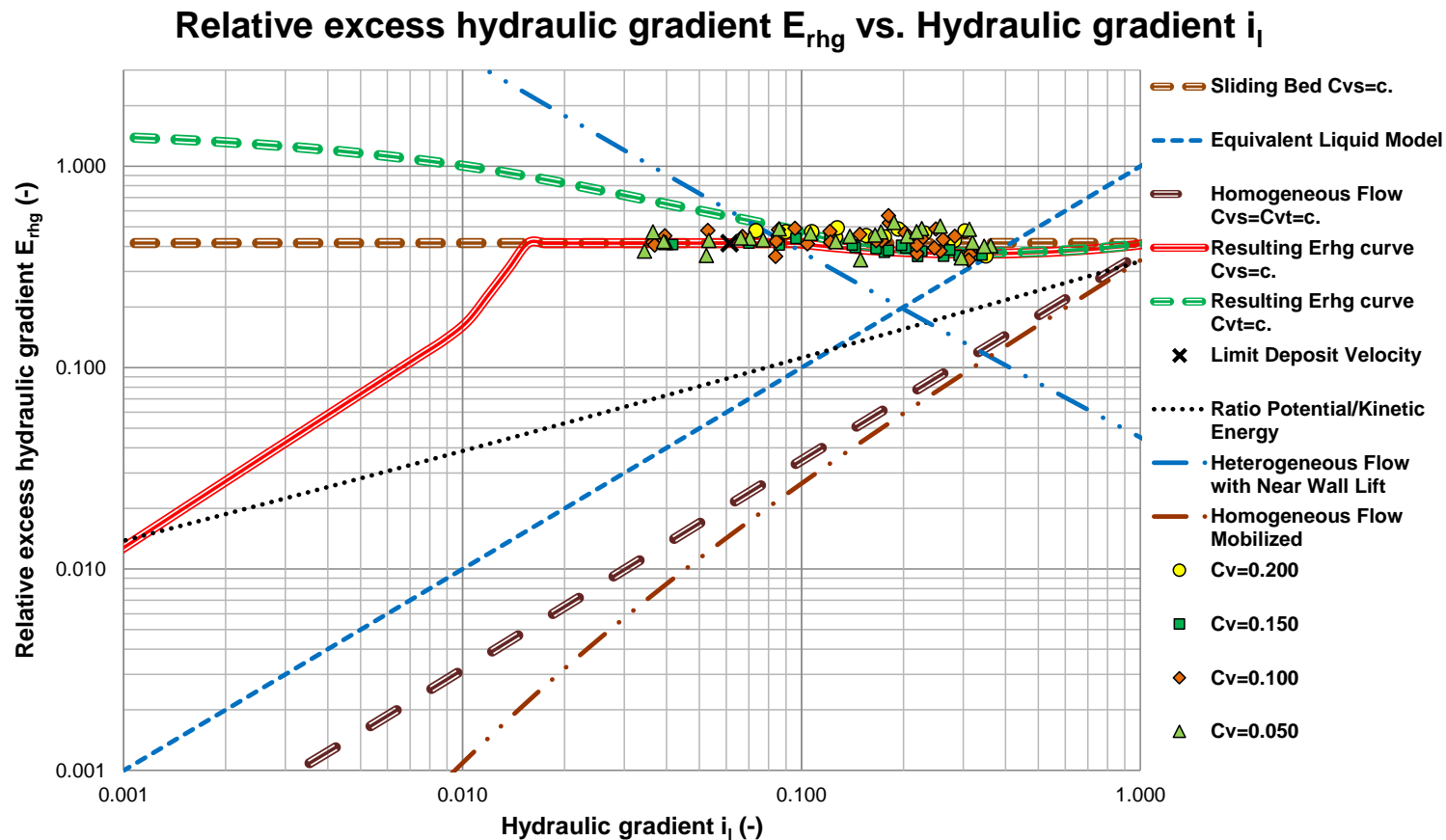


$D_p=0.2000$ m, $d=10.000$ mm, $Rsd=1.732$, $Cv=0.100$, $\mu_{sf}=0.470$

Boothroyde et al. (1979)



Verification & Validation, Wiedenroth

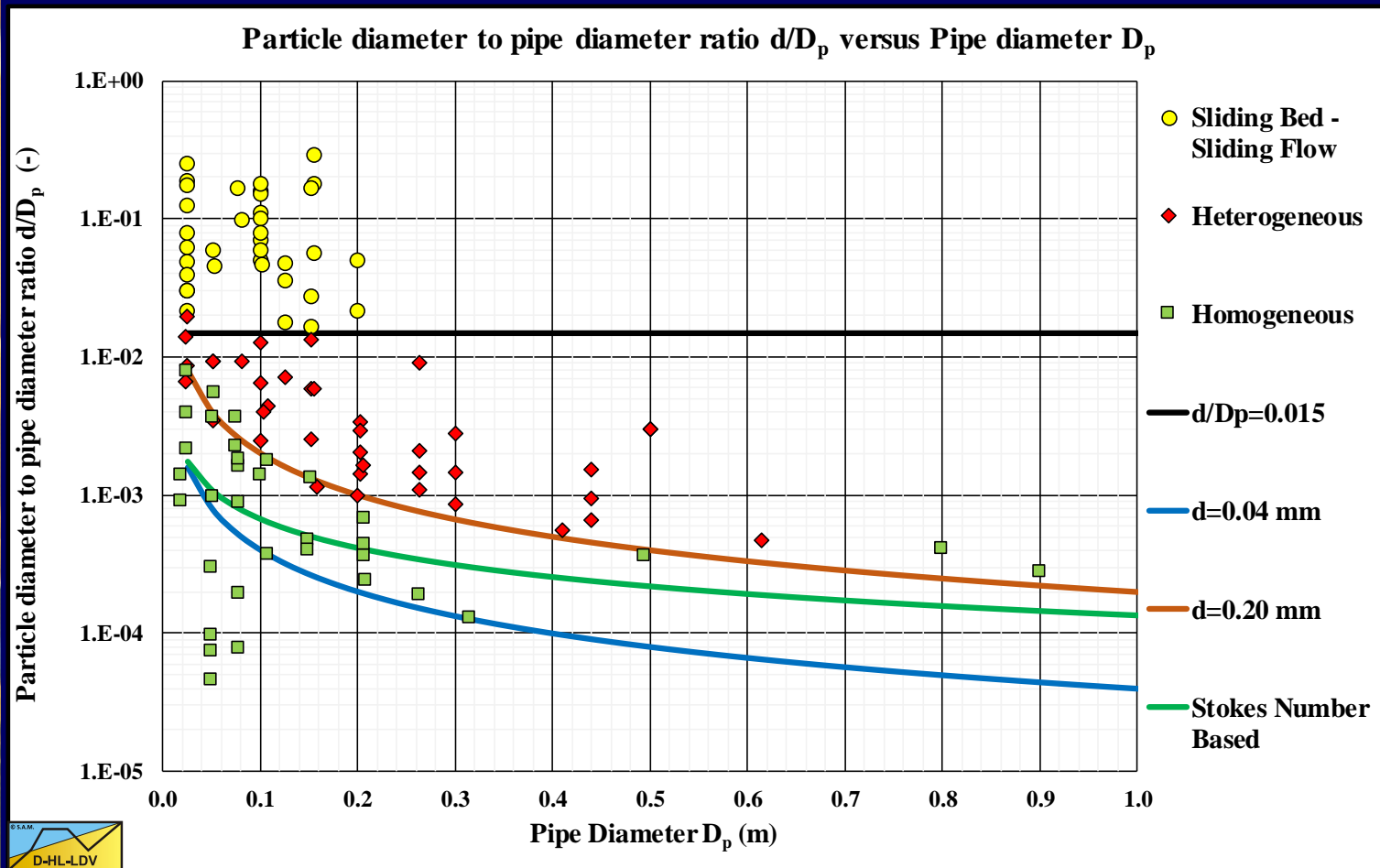


$D_p=0.1250$ m, $d=5.950$ mm, $Rsd=1.585$, $Cv=0.150$, $\mu_{sf}=0.416$

Wiedenroth (1967)



Verification & Validation, All



Phenomena

If the particle diameter to pipe diameter ratio is larger than about 0.015, the particles will not be suspended anymore, but stay in a fast flowing sort of bed, behaving according to a sliding bed.

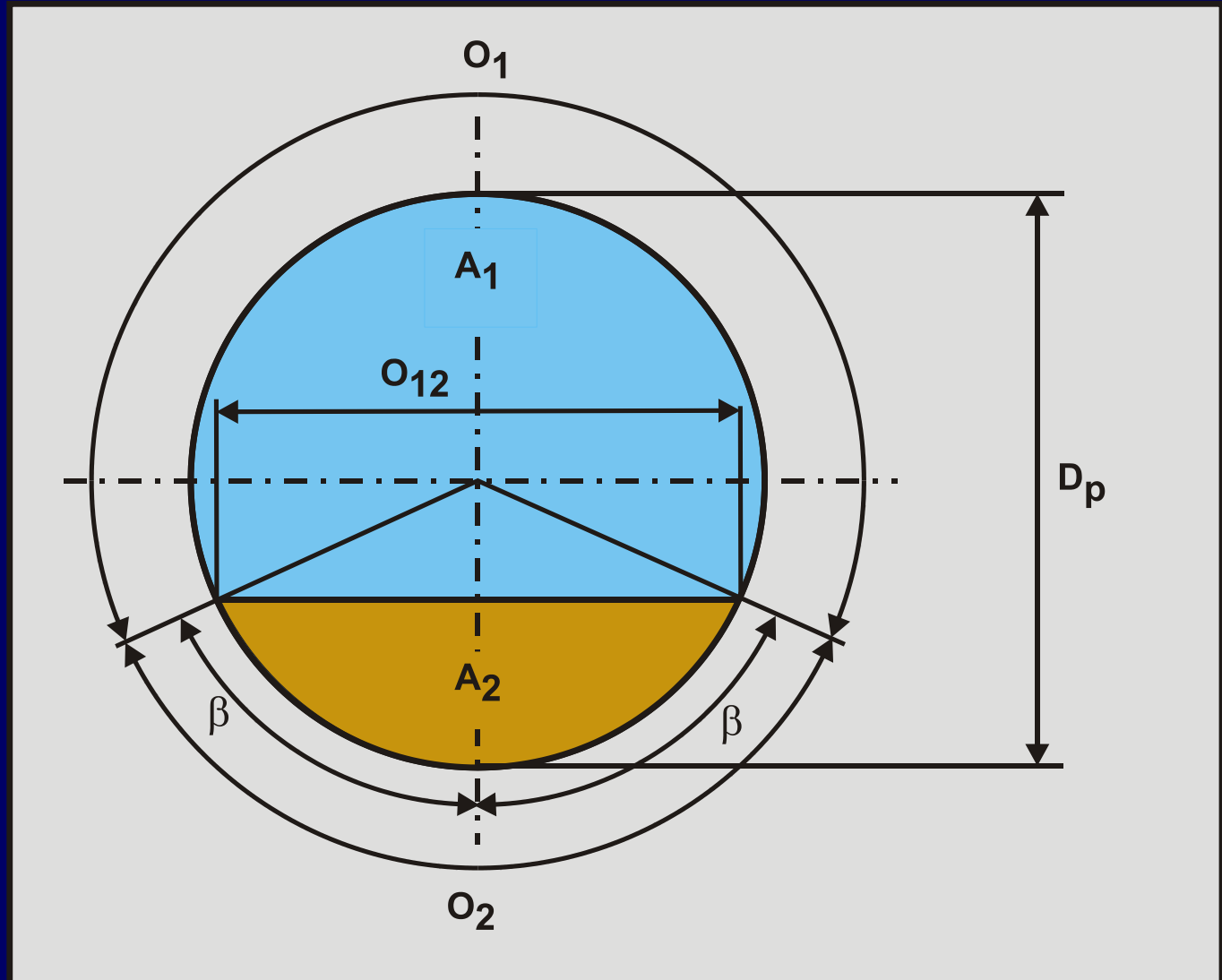
For $0.0075 < d/D_p < 0.03$ there is a transition from heterogeneous behavior to sliding flow behavior.

Above $d/D_p = 0.03$ sliding flow is fully mobilized.

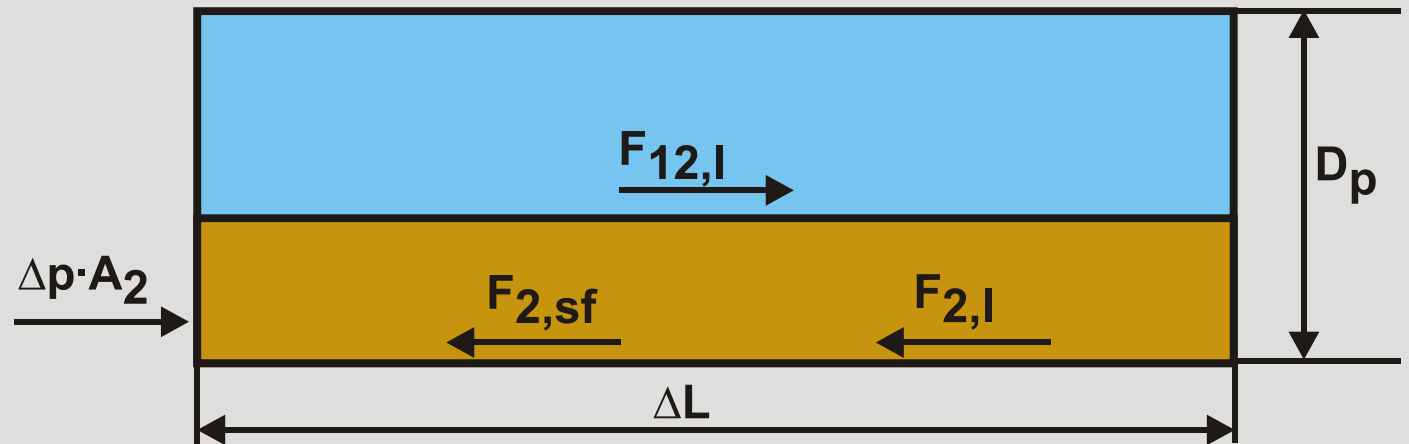
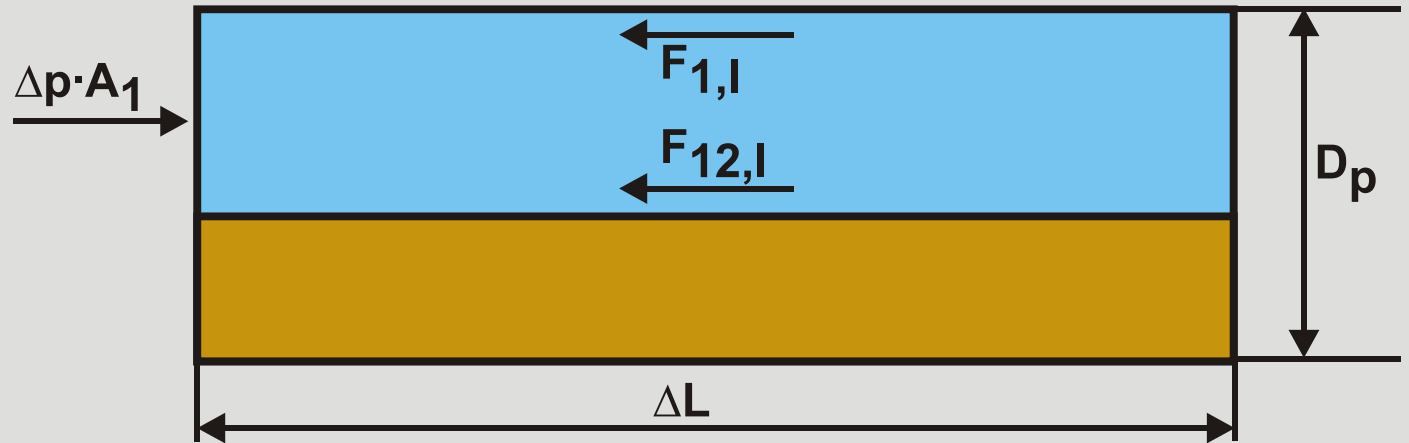
The higher the line speed the smaller the concentration of the flowing particles at the bottom of the pipe.



Definitions



Equilibrium of Forces



Derivation d/D_p Factor 1

Deposition = Suspension

Criterion: $v_t = u_*$

Equilibrium of forces on layer above the sliding bed

$$F_{12,l} + F_{1,l} = \Delta p \cdot A_1$$

$$\rho_l \cdot u_*^2 \cdot D_p \cdot \sin(\beta) \cdot \Delta L + \alpha_\tau \cdot \rho_l \cdot u_*^2 \cdot D_p \cdot (\pi - \beta) \cdot \Delta L$$

$$= \Delta p \cdot A_p \cdot (1 - C_{vr})$$

$$\Delta p = \frac{\rho_l \cdot u_*^2 \cdot D_p \cdot \Delta L \cdot (\sin(\beta) + \alpha_\tau \cdot (\pi - \beta))}{A_p \cdot (1 - C_{vr})}$$



Derivation d/D_p Factor 2

Equilibrium of forces the bed

$$F_{12,1} + \Delta p \cdot A_2 = F_{2,sf} + F_{2,l} \quad F_{2,l} = \text{small and is neglected here}$$

$$\rho_l \cdot u_*^2 \cdot D_p \cdot \sin(\beta) \cdot \Delta L + \Delta p \cdot A_p \cdot C_{vr} = \mu_{sf} \cdot (\rho_s - \rho_l) \cdot g \cdot A_p \cdot C_{vs} \cdot \Delta L$$

$$\rho_l \cdot u_*^2 \cdot D_p \cdot \sin(\beta) + \frac{\rho_l \cdot u_*^2 \cdot D_p \cdot (\sin(\beta) + \alpha_\tau \cdot (\pi - \beta))}{(1 - C_{vr})} \cdot C_{vr}$$

$$= \mu_{sf} \cdot (\rho_s - \rho_l) \cdot g \cdot A_p \cdot C_{vs}$$

$$\frac{\rho_l \cdot u_*^2 \cdot D_p \cdot (\sin(\beta) + \alpha_\tau \cdot (\pi - \beta)) \cdot C_{vr}}{(1 - C_{vr})} = \mu_{sf} \cdot (\rho_s - \rho_l) \cdot g \cdot A_p \cdot C_{vs}$$



Derivation d/D_p Factor 3

Equilibrium of forces the bed

$$\frac{\rho_l \cdot u_*^2 \cdot D_p \cdot (\sin(\beta) + \alpha_\tau \cdot (\pi - \beta) \cdot C_{vr})}{(1 - C_{vr})} = \mu_{sf} \cdot (\rho_s - \rho_l) \cdot g \cdot A_p \cdot C_{vs}$$

$$u_*^2 = \frac{\mu_{sf} \cdot (\rho_s - \rho_l) \cdot g \cdot A_p \cdot C_{vb} \cdot C_{vr} \cdot (1 - C_{vr})}{\rho_l \cdot D_p \cdot (\sin(\beta) + \alpha_\tau \cdot (\pi - \beta) \cdot C_{vr})}$$

$$u_*^2 = \frac{\pi}{4} \cdot \frac{\mu_{sf} \cdot R_{sd} \cdot g \cdot D_p \cdot C_{vb} \cdot C_{vr} \cdot (1 - C_{vr})}{(\sin(\beta) + \alpha_\tau \cdot (\pi - \beta) \cdot C_{vr})}$$



Derivation d/D_p Factor 4

Friction velocity squared

$$u_*^2 = \frac{\pi}{4} \cdot \frac{\mu_{sf} \cdot R_{sd} \cdot g \cdot D_p \cdot C_{vb} \cdot C_{vr} \cdot (1 - C_{vr})}{(\sin(\beta) + \alpha_\tau \cdot (\pi - \beta) \cdot C_{vr})}$$

Settling velocity

$$v_t = \sqrt{\frac{4}{3} \cdot \frac{R_{sd} \cdot g \cdot d \cdot \psi}{C_D}} \quad \Rightarrow \quad v_t^2 = \frac{4}{3} \cdot \frac{R_{sd} \cdot g \cdot d \cdot \psi}{C_D}$$

\Rightarrow

$$\frac{4}{3} \cdot \frac{R_{sd} \cdot g \cdot d \cdot \psi}{C_D} = \frac{\pi}{4} \cdot \frac{\mu_{sf} \cdot R_{sd} \cdot g \cdot D_p \cdot C_{vb} \cdot C_{vr} \cdot (1 - C_{vr})}{(\sin(\beta) + \alpha_\tau \cdot (\pi - \beta) \cdot C_{vr})}$$



Derivation d/D_p Factor 5

With wall shear stress

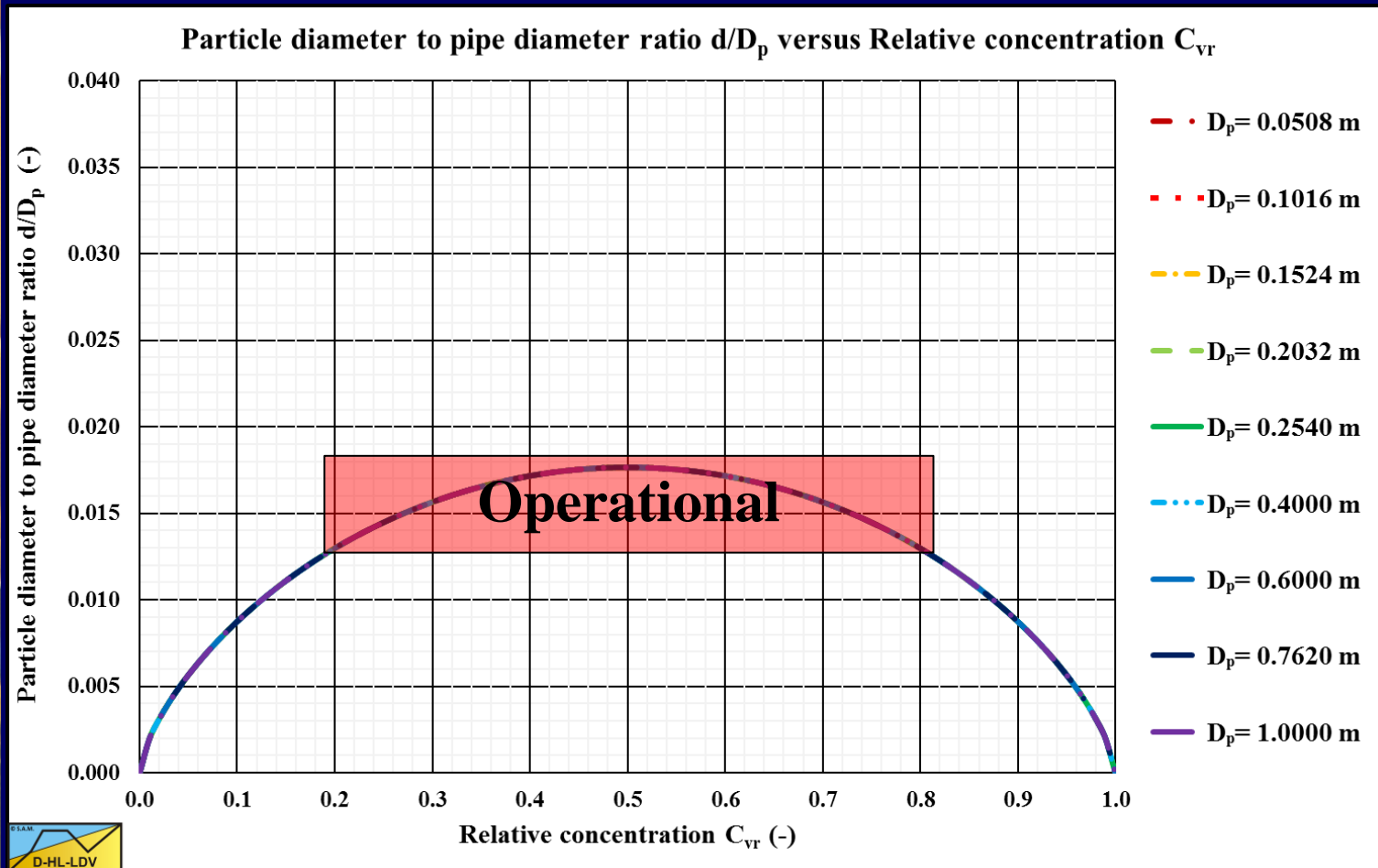
$$\frac{d}{D_p} = \frac{3 \cdot \pi \cdot C_D}{16 \cdot \psi} \cdot \frac{\mu_{sf} \cdot C_{vb} \cdot C_{vr} \cdot (1 - C_{vr})}{(\sin(\beta) + \alpha_\tau \cdot (\pi - \beta) \cdot C_{vr})}$$

Without wall shear stress

$$\frac{d}{D_p} = \frac{3 \cdot \pi \cdot C_D}{16 \cdot \psi} \cdot \frac{\mu_{sf} \cdot C_{vb} \cdot C_{vr} \cdot (1 - C_{vr})}{\sin(\beta)}$$



Particle to Pipe Diameter Ratio, Spheres

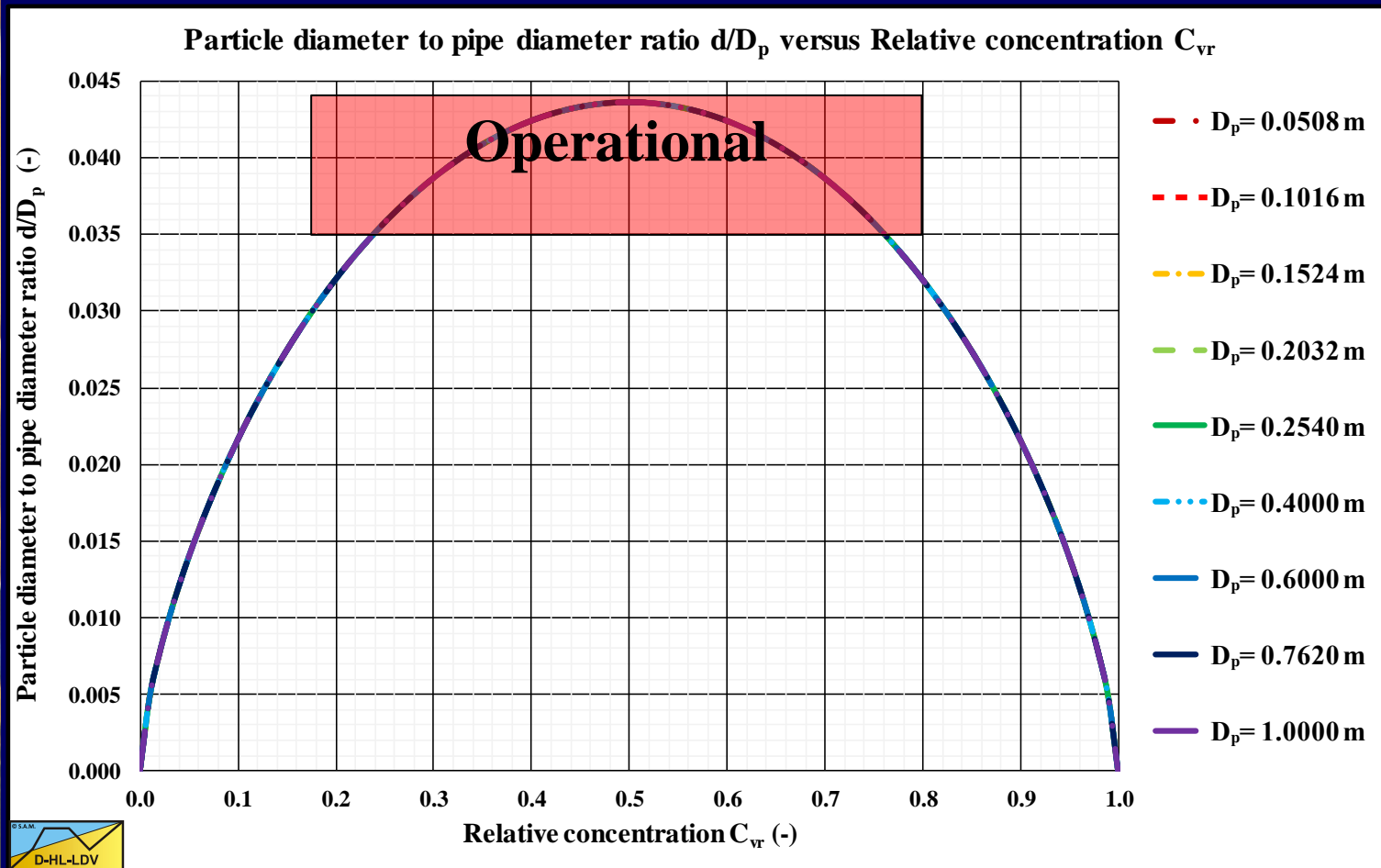


d/D_p ratio for spheres without τ_1 , matching Wilson & Sellgren (0.013-0.018).

Delft University of Technology – Offshore & Dredging Engineering



Particle to Pipe Diameter Ratio, Gravels



d/D_p ratio for gravels without τ_1 , higher than Wilson & Sellgren (0.013-0.018).

Delft University of Technology – Offshore & Dredging Engineering

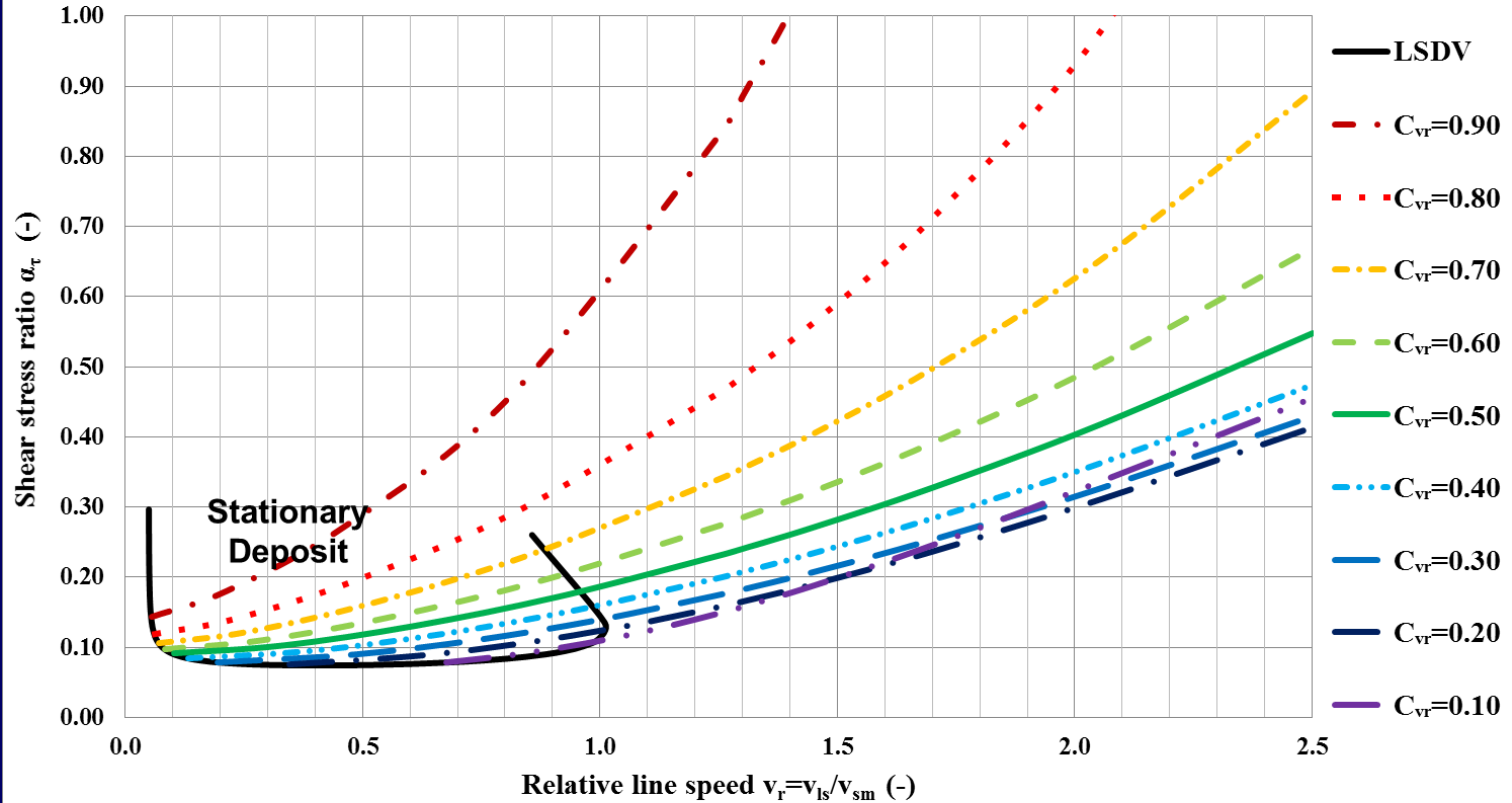


Shear Stress Ratio



Shear stress ratio α_τ vs. relative line speed v_r , $C_{vr} = C_{vt}/C_{vb}$

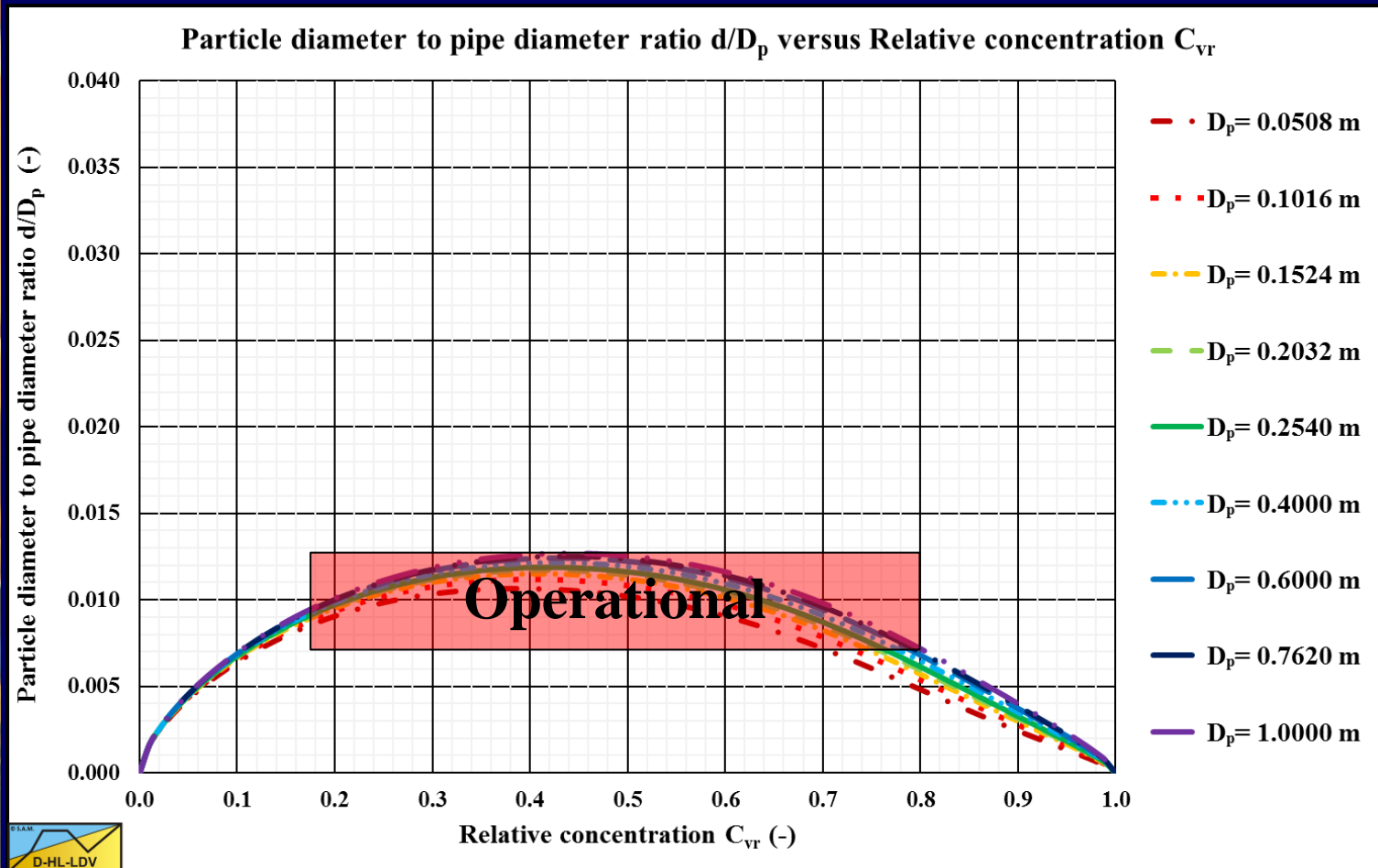
3LM-D-W



$D_p=0.7620$ m, $d=1.000$ mm, $R_{sd}=1.585$, $\mu_{sf}=0.416$, $C_{vb}=0.55$



Particle to Pipe Diameter Ratio, Spheres

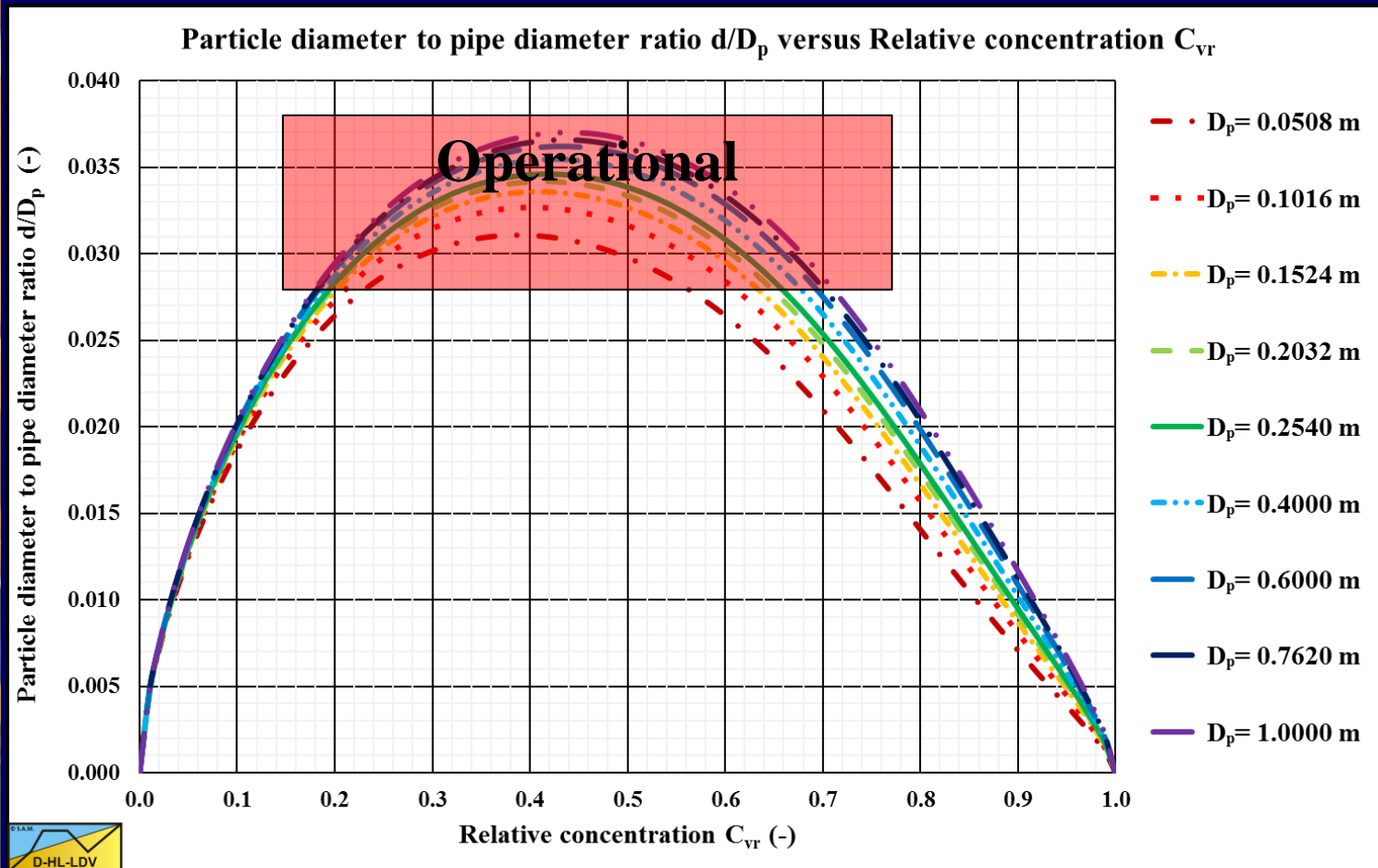


d/D_p ratio for spheres with τ_1 , still matching Wilson & Sellgren (0.013-0.018).

Delft University of Technology – Offshore & Dredging Engineering



Particle to Pipe Diameter Ratio, Gravels



d/D_p ratio for gravels with τ_1 , higher than Wilson & Sellgren (0.013-0.018).

Delft University of Technology – Offshore & Dredging Engineering



Conclusions

- It is possible to derive a more fundamental equation for the transition between the heterogeneous flow regime and the sliding flow regime based on the assumption deposition=suspension.
- This fundamental equation matches the d/D_p ratio of 0.015 closely for spheres.
- For sand and gravel particles the d/D_p ratio is closer to 0.03.
- The d/D_p ratio depends weakly on the pipe diameter and the particle diameter.
- The d/D_p ratio depends strongly on the particle shape and the particle drag coefficient.



Limit Deposit Velocity

Chapter 7.8 & 8.10



Definitions LSDV, MHGV & LDV

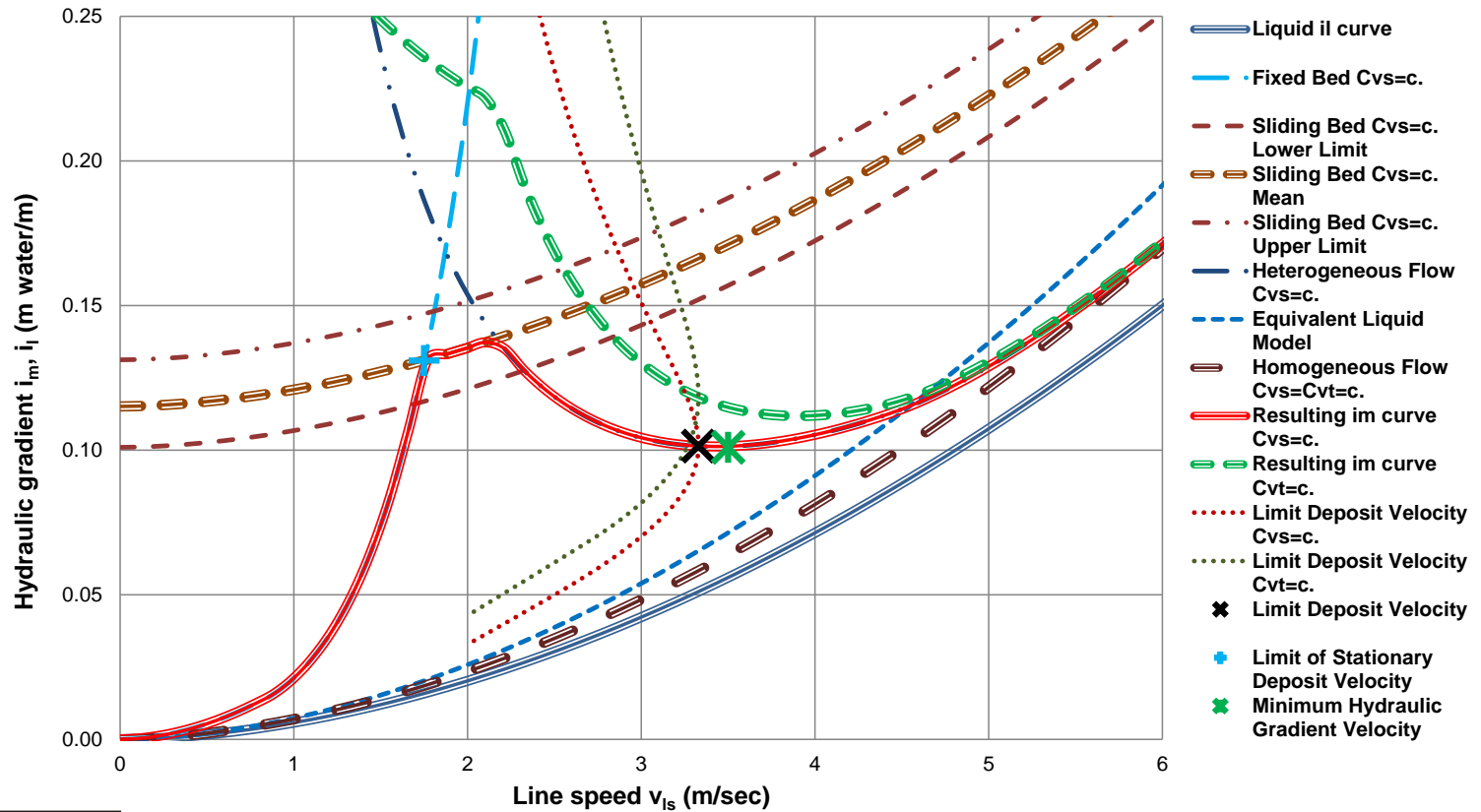
- Limit of Stationary Deposit Velocity (**LSDV**): The line speed at the start of a sliding bed. So the transition from a stationary to a sliding bed. The **LSDV** only exists above a certain particle diameter, pipe diameter and spatial volumetric concentration combination.
- Minimum Hydraulic Gradient Velocity (**MHGV**): The line speed where the hydraulic gradient of a mixture has a minimum with constant delivered volumetric concentration.
- Limit Deposit Velocity (**LDV**): The line speed above which there is no stationary or sliding bed. So below the **LDV** there is a stationary or a sliding bed.



Definitions LSDV, MHGV & LDV

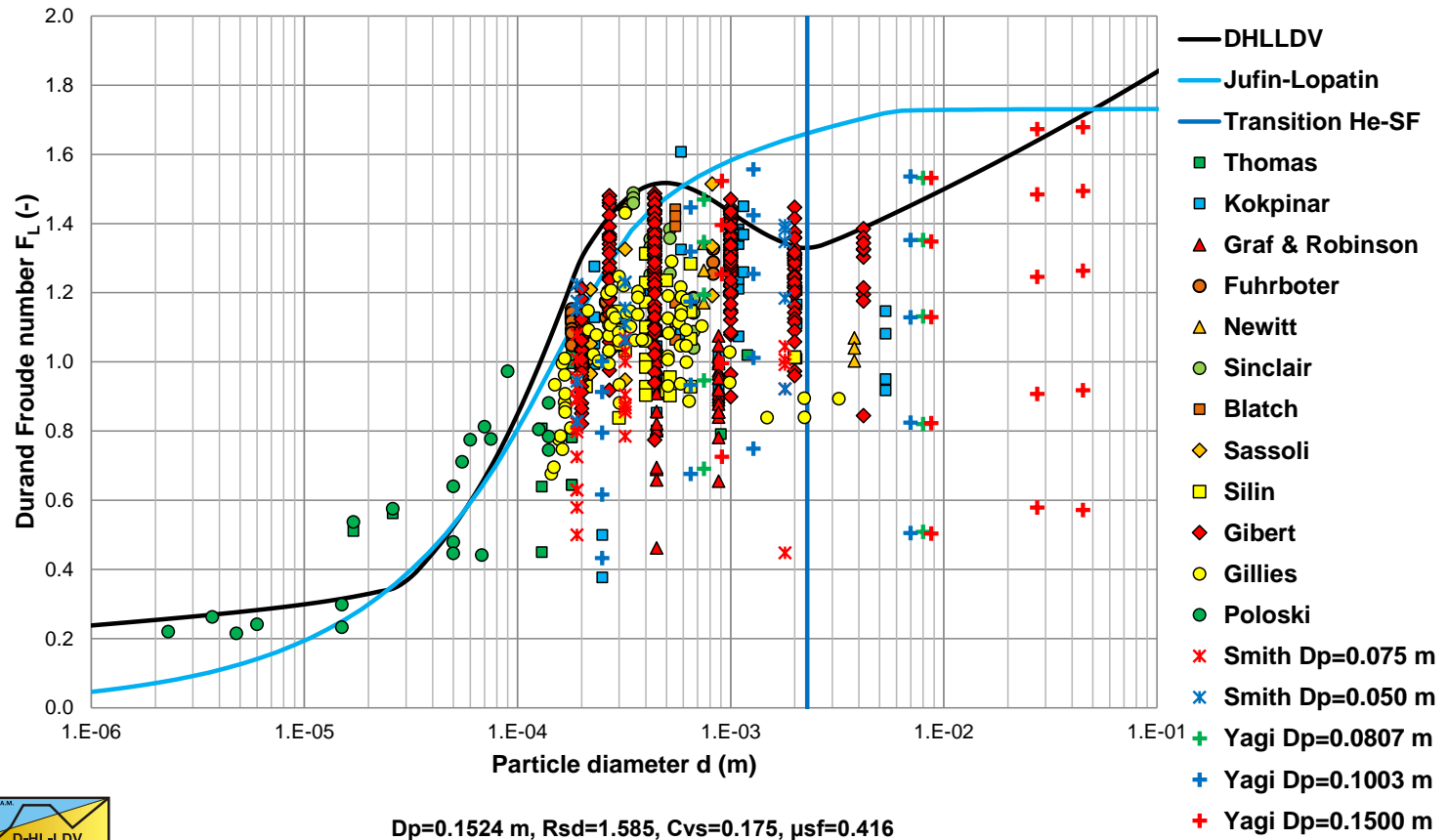


Hydraulic gradient i_m, i_l vs. Line speed v_{ls}



Experiments

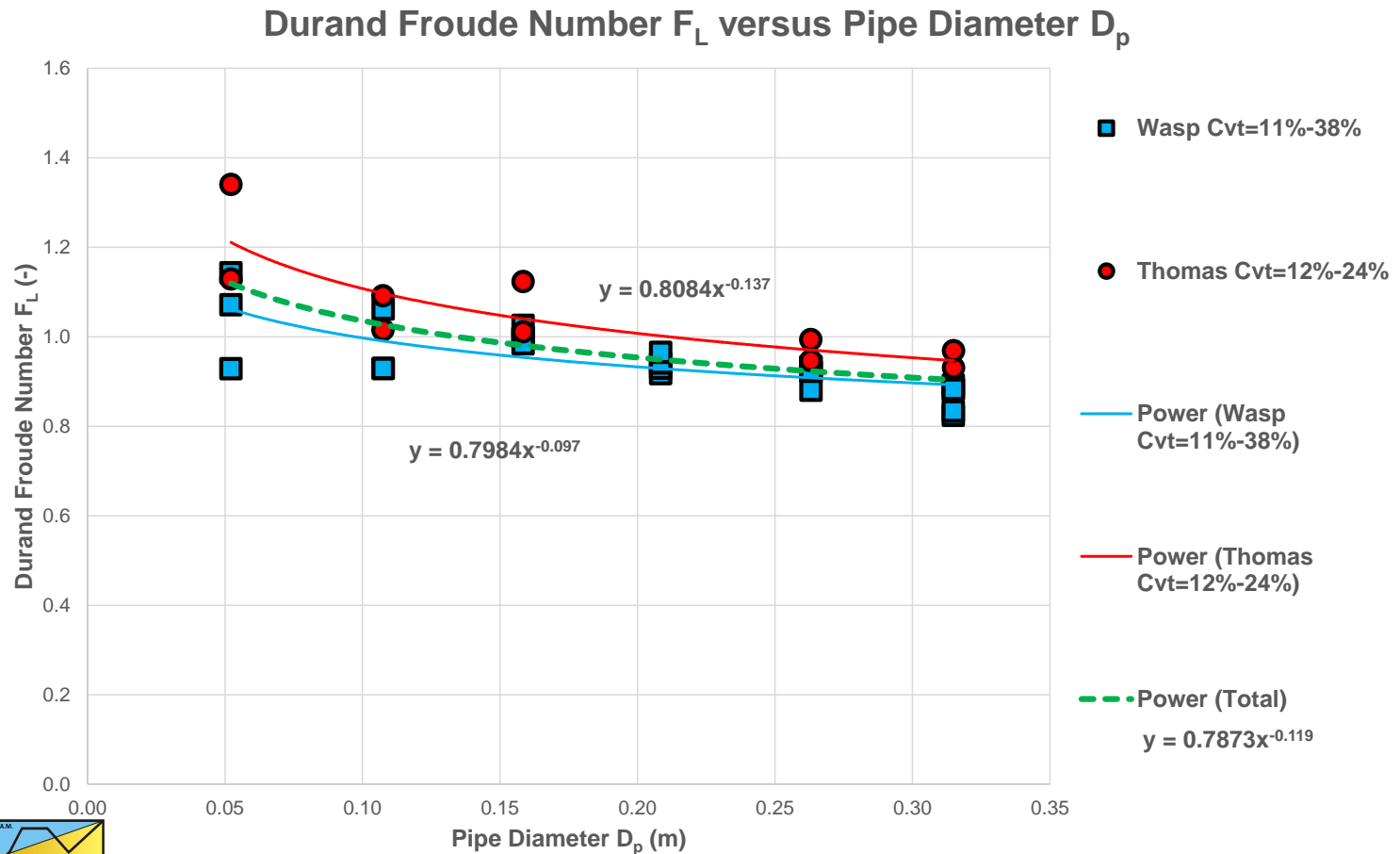
Durand Froude number F_L (-) vs. Particle diameter d (m)



$$F_L = \frac{v_{ls,ldv}}{\sqrt{2 \cdot g \cdot R_{sd} \cdot D_p}} = \frac{LDV}{\sqrt{2 \cdot g \cdot R_{sd} \cdot D_p}}$$



Influence of Pipe Diameter

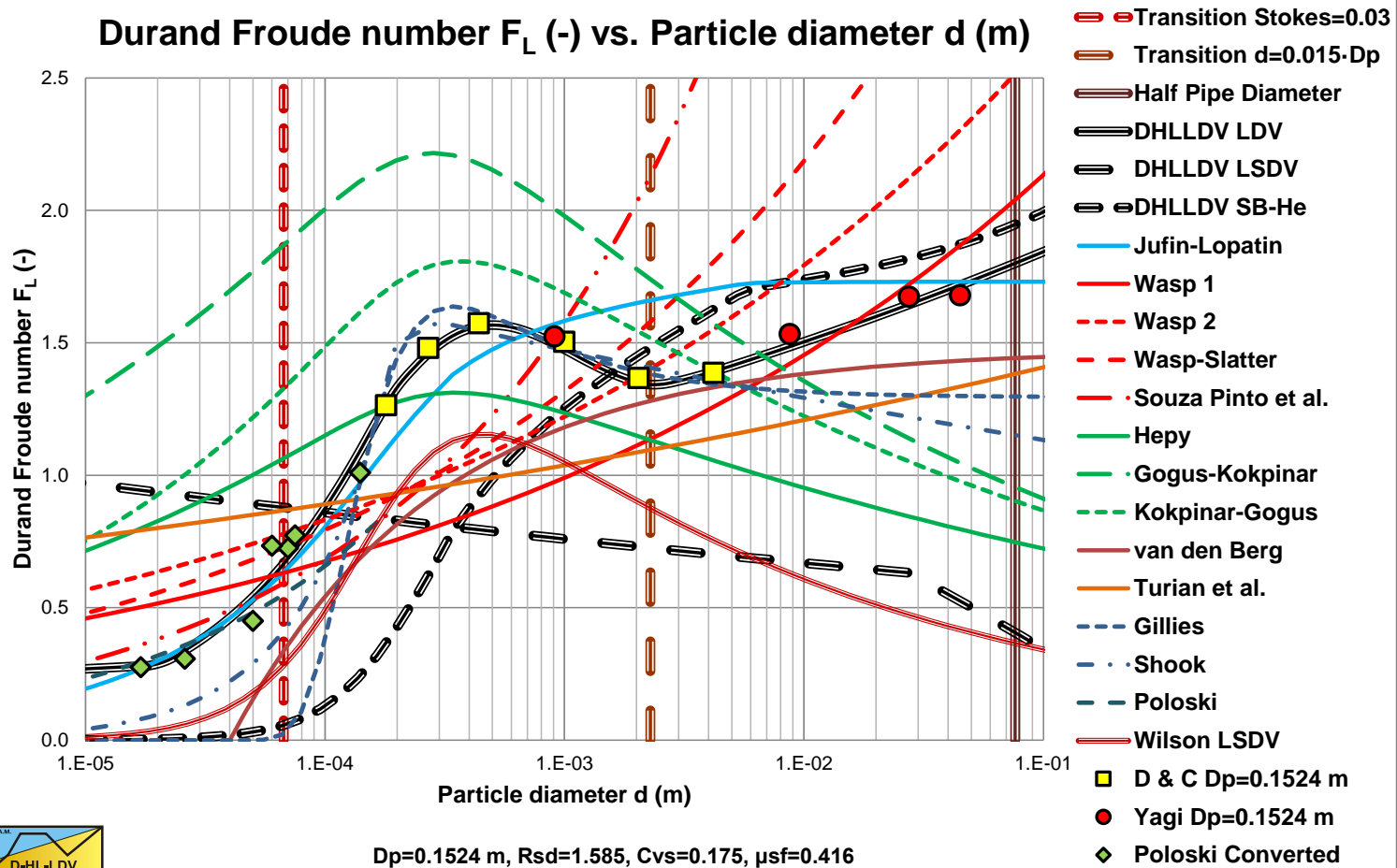


Thomas (1979) and Wasp et al. (1977)



15 Models

Durand Froude number F_L (-) vs. Particle diameter d (m)



Starting Points 1

- The pipe diameter D_p : The **LDV** is proportional to the pipe diameter D_p to a power between 1/3 and 1/2 (about 0.4) for small to large particles and a power of about 0.1 for very small particles.
- The particle diameter d : The **LDV** has a lower limit for very small particles, after which it increases to a maximum at a particle diameter of about $d = 0.5$ mm. For medium sized particles with a particle size $d > 0.5$ mm, the F_L value decreases slightly to a minimum for a particle size of about $d = 2$ mm. Above 2 mm, the F_L value will remain constant according to Durand and Condolios (1952) and Gillies (1993). For particles with $d/D_p > 0.015$, the Wilson et al. (1992) criterion for full stratified flow, the F_L value increases again.



Starting Points 2

- The relative submerged density R_{sd} : The relation between the **LDV** and the relative submerged density is not very clear, however the data shown by Kokpinar and Gogus (2001) and the conclusions of Lahiri (2009) show that the F_L value decreases with increasing solids density and thus relative submerged density R_{sd} to a power of -0.1 to -0.4 .
- The spatial volumetric concentration C_{vs} : The volumetric concentration leading to the maximum **LDV** is somewhere between 15% and 20% according to Durand and Condolios (1952). Lahiri (2009) reported a maximum at about 17.5%, while Poloski et al. (2010) derived 15%. This maximum **LDV** results from on one hand a linear increase of the sedimentation with the concentration and on the other hand a reduced sedimentation due to the hindered setting. These two counteracting phenomena result in a maximum **LDV**, which is also present in the equation of the potential energy.



5 Regions

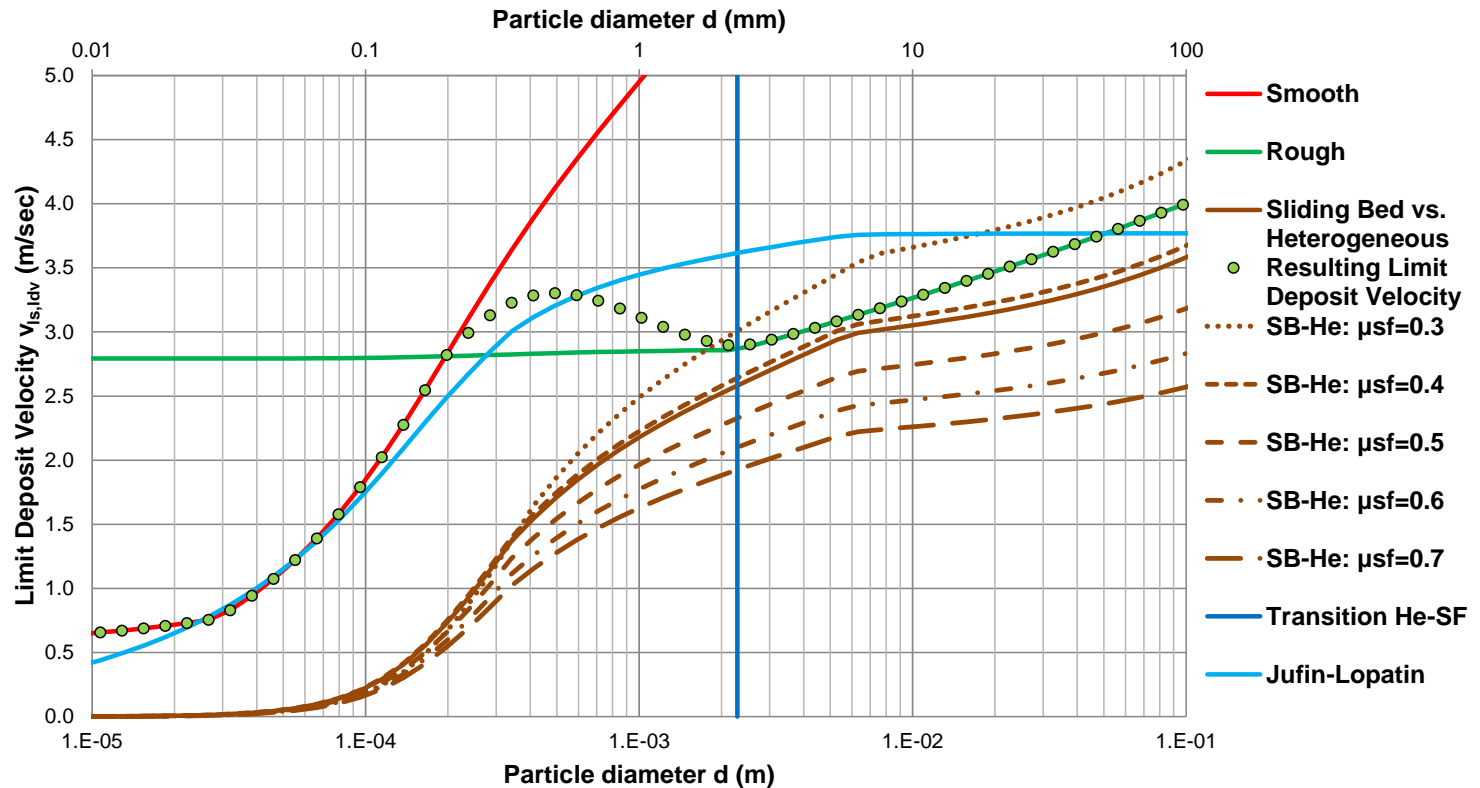
1. Very small particles, smaller than about 50% of the thickness of the viscous sub layer, giving a lower limit of the **LDV**. This is for particles up to about 0.15 mm in large pipes to 0.04 mm in very small pipes.
2. Small particles up to about 0.2 mm, a smooth bed, show an increasing **LDV** with increasing particle diameter.
3. Medium particles with a diameter from 0.2 mm up to a diameter of 2 mm, a transition zone from a smooth bed to a rough bed. First the **LDV** increases to a particle diameter of about 0.5 mm, after which it decreases slowly to an asymptotic value at a diameter of about 2 mm.
4. Large particles with a diameter larger than 2 mm, a rough bed, giving a constant **LDV**.
5. Particles with a particle diameter to pipe diameter ratio larger than about 0.015 cannot be carried by turbulent eddies, just because eddies are not large enough. This will probably result in an increasing **LDV** with the particle diameter.



Resulting LDV Curve



Limit Deposit Velocity $v_{Is,ldv}$ (m/sec) vs. Particle diameter d (m)



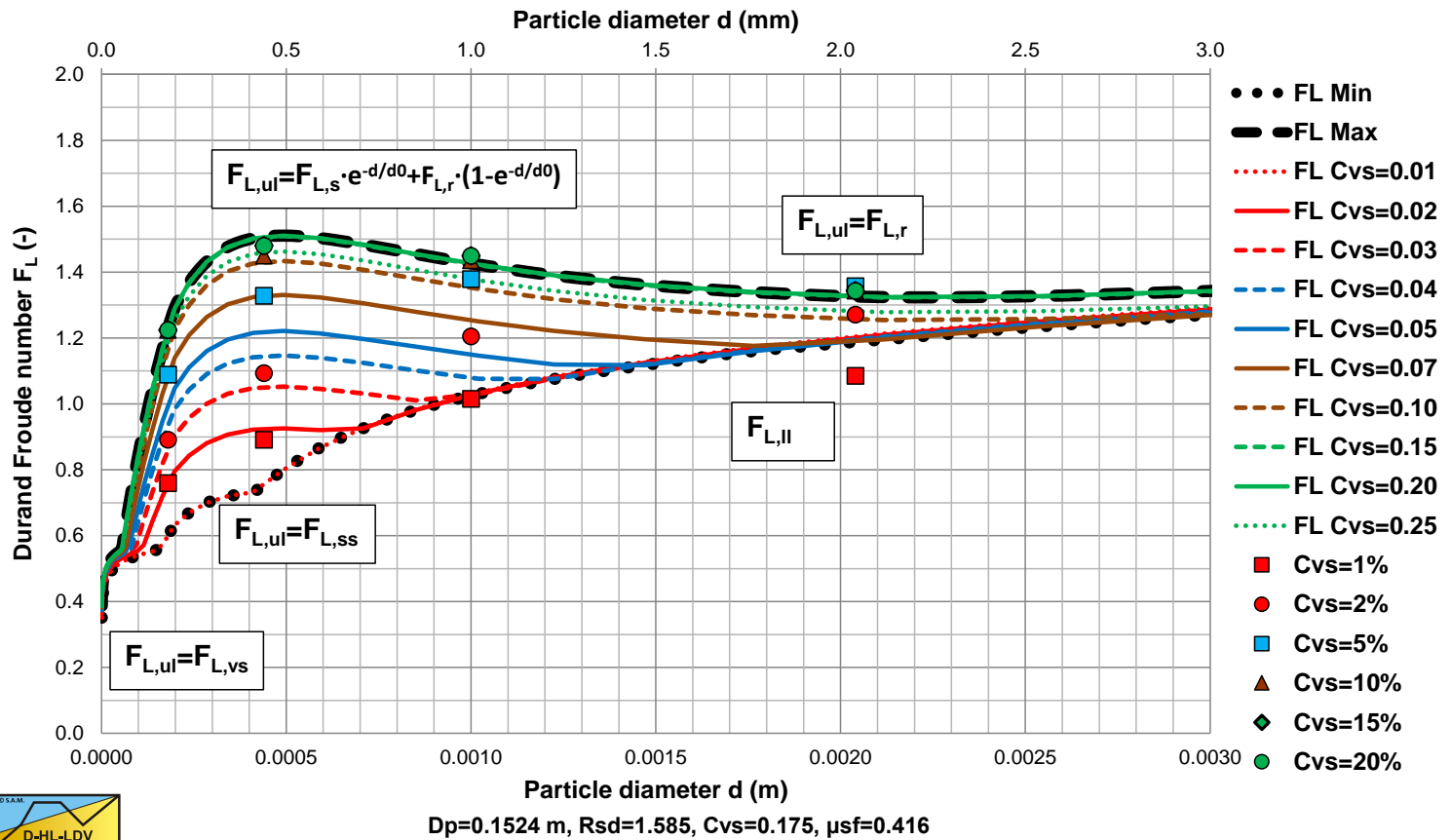
$D_p=0.1524$ m, $R_{sd}=1.585$, $C_{vs}=0.175$, $\mu_{sf}=0.416$



Comparison with Durand & Condolios



Durand Froude number F_L (-) vs. Particle diameter d (m)



Conclusions

- The Limit Deposit Velocity is modeled in 5 regions.
- Since these regions behave according to different physics it is impossible to find one equation covering the different physics.
- Sometimes a transitions region is required going from one type of physical behavior to another type of physical behavior.
- Overall the method described gives a good match with experimental data.





Slip Velocity or Holdup Function

Chapter 7.9 & 8.11



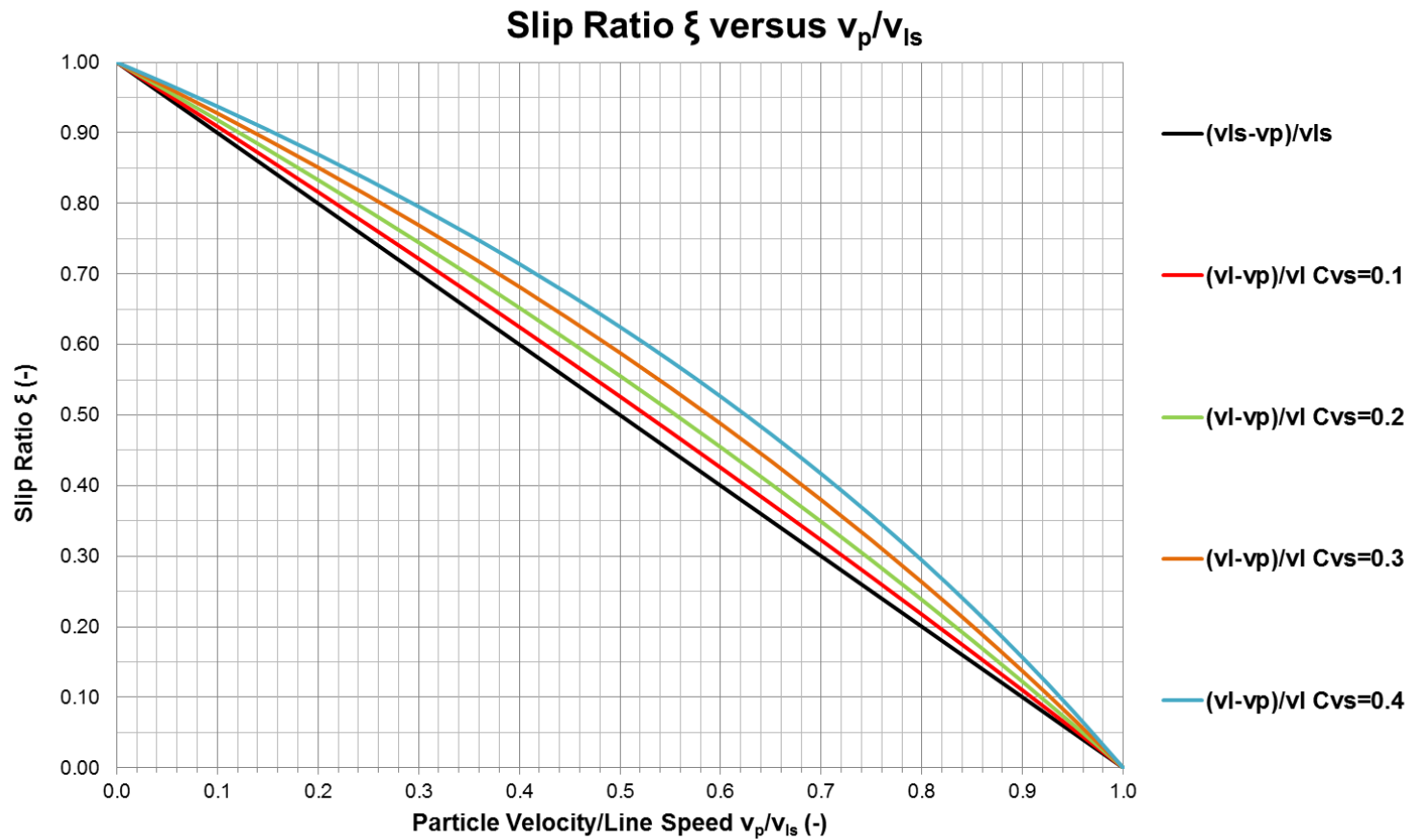
Definitions

1. Slip is the difference between the cross section averaged liquid velocity and the cross section averaged solids velocity (heterogeneous regime).
 2. Slip is the difference between the cross section averaged mixture velocity (the line speed) and the cross section averaged solids velocity (C_{vt} vs. C_{vs}).
- For low concentrations the two definitions give almost the same slip velocity.
 - For high concentrations the first definition gives a higher slip velocity than the second definition.

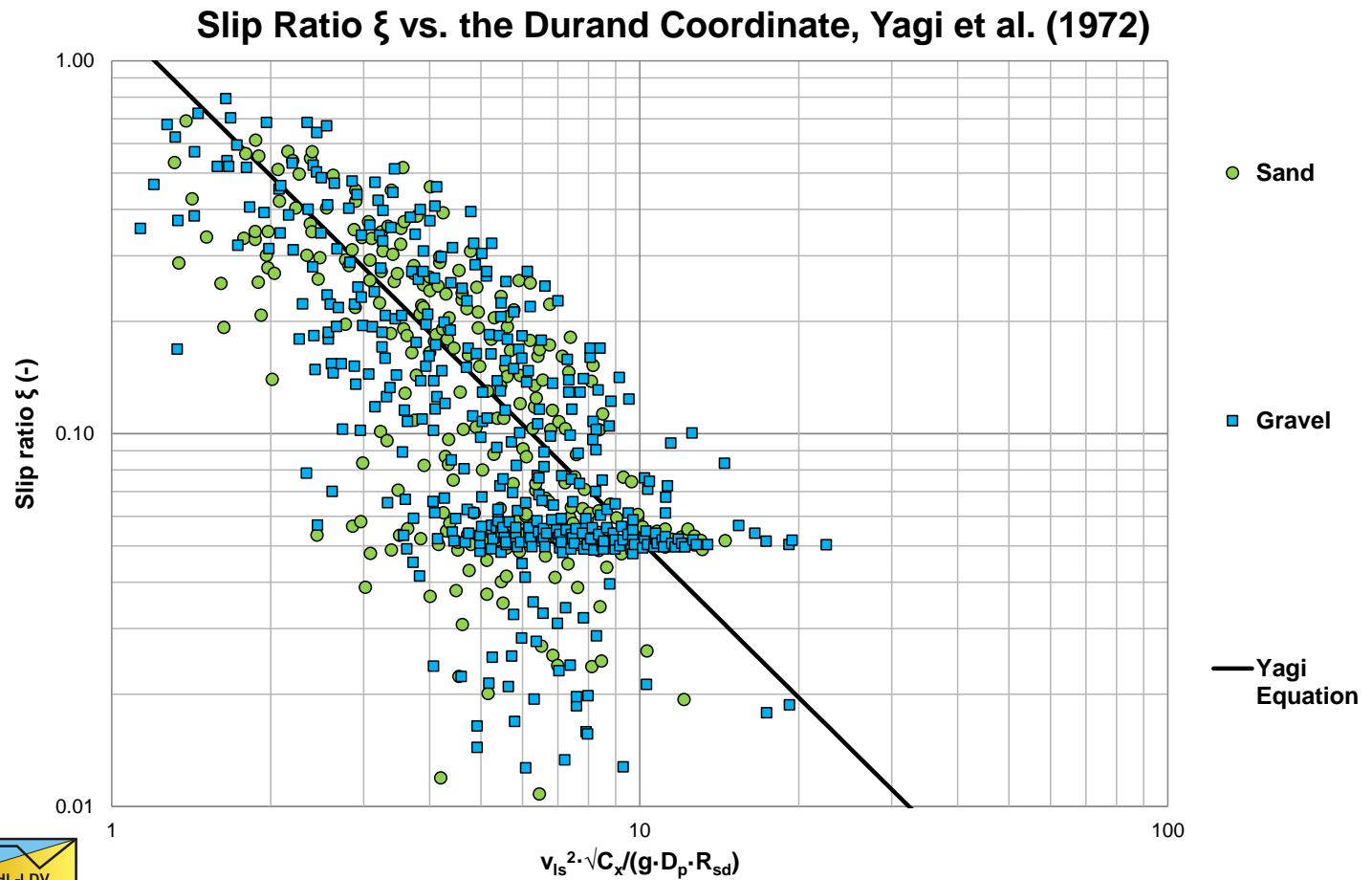
Slip Ratio is the ratio of the slip velocity to the cross sectional averaged liquid velocity or line speed.



Slip Ratio 2 Definitions

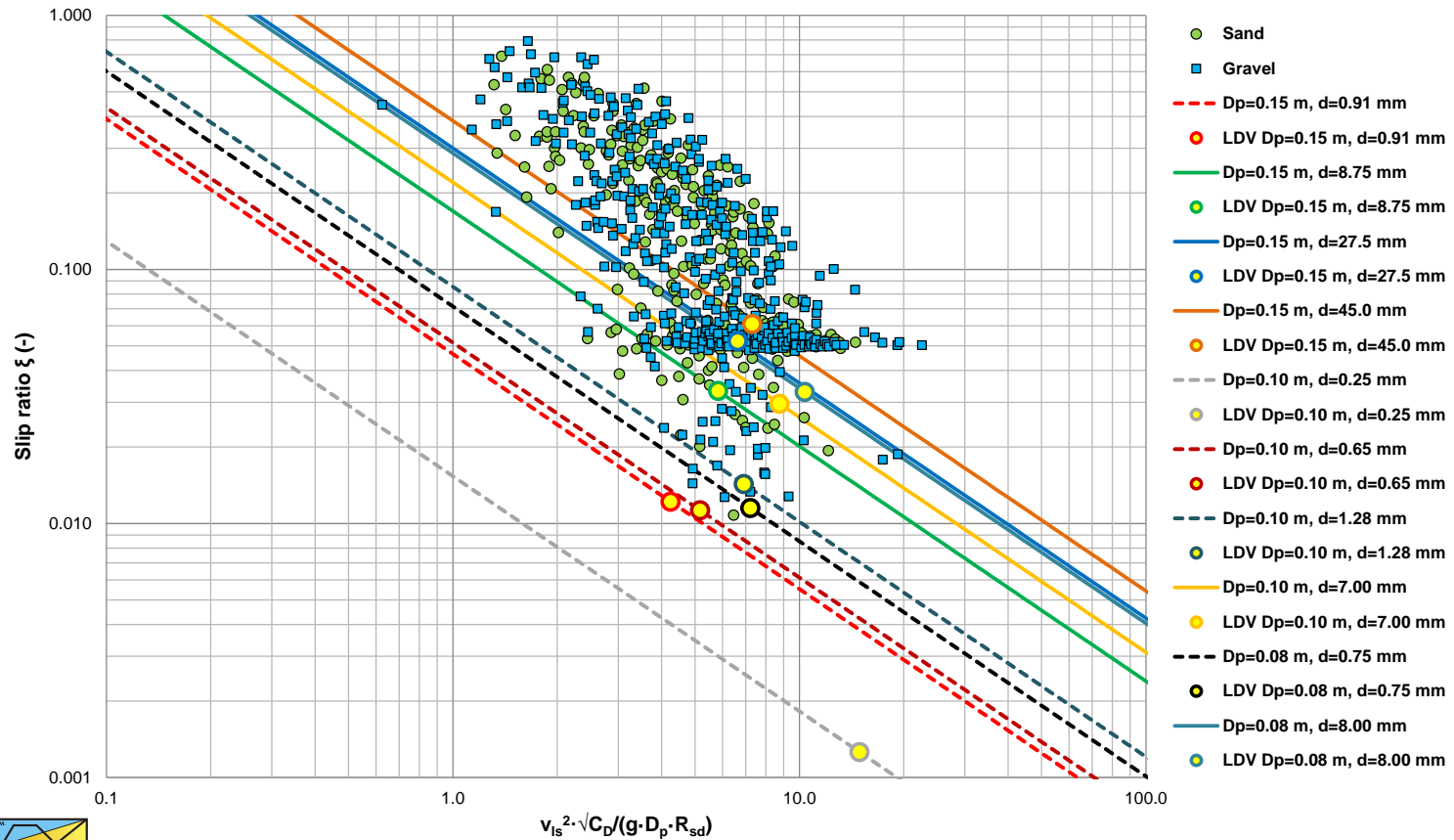


Slip Ratio Yagi et al. (1972)



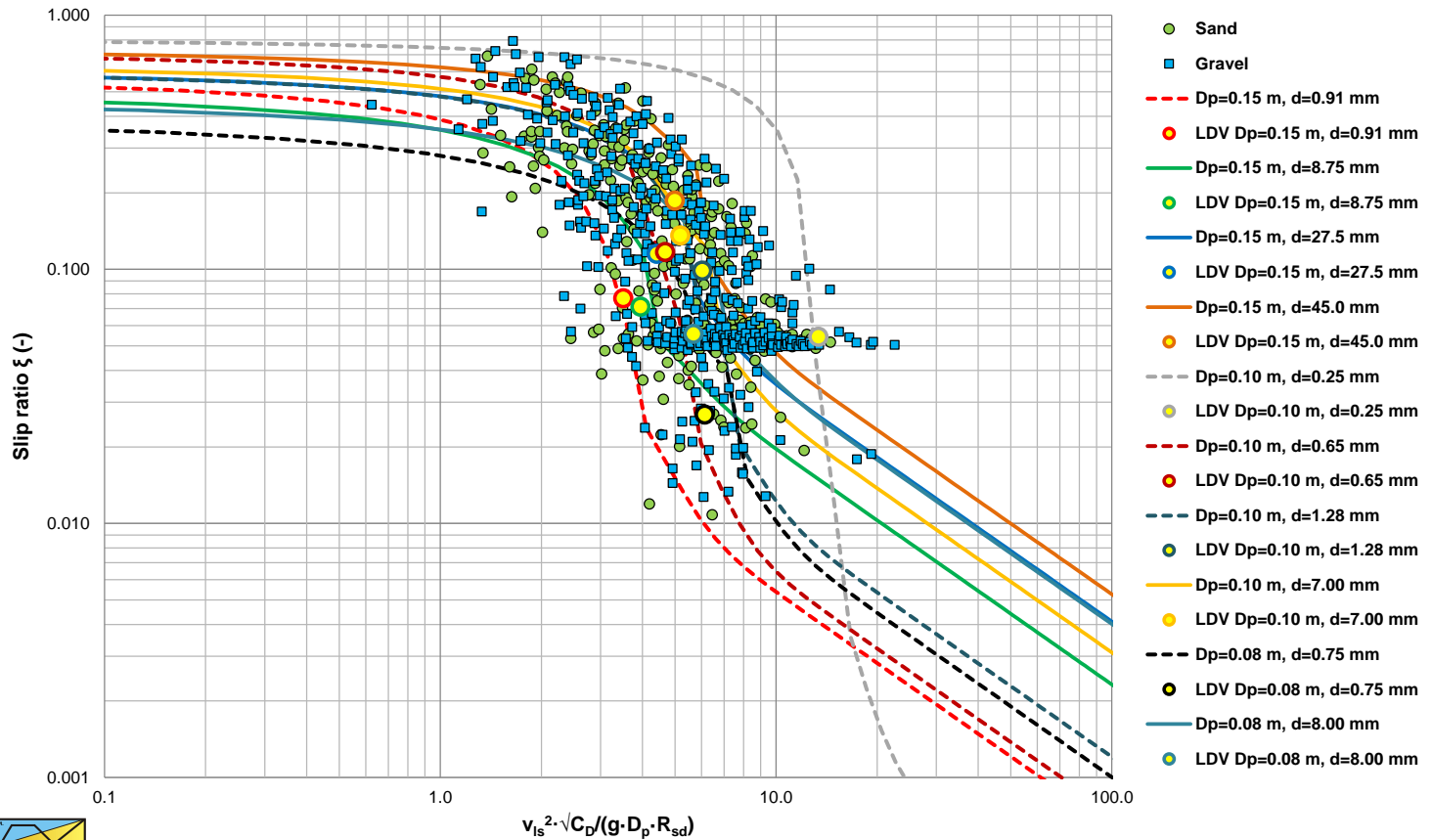
Comparison with DHLLDV Heterogeneous

Slip Ratio ξ vs. the Durand Coordinate, Yagi et al. (1972) vs. Theory



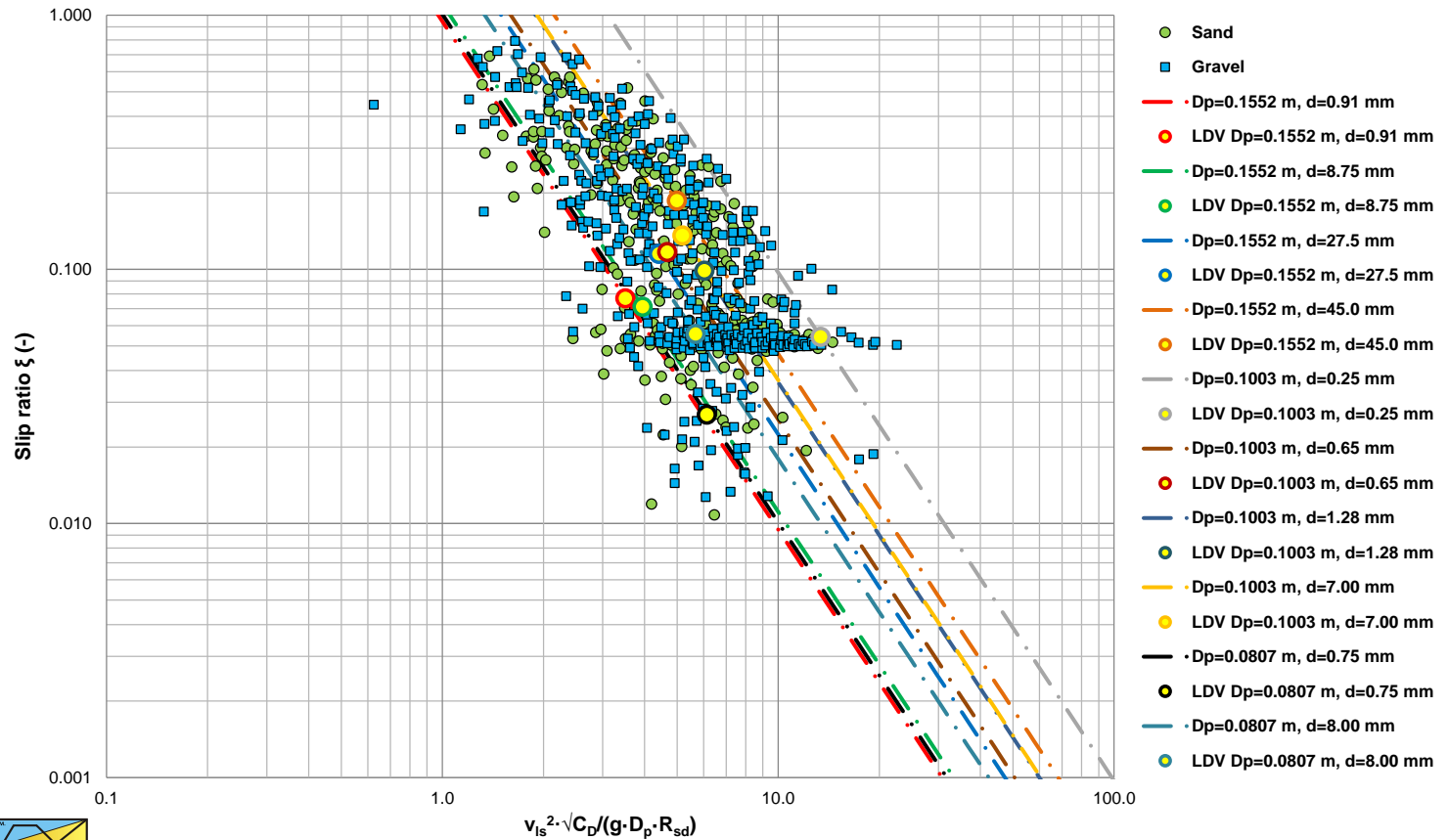
Heterogeneous + Sliding Bed

Slip Ratio ξ vs. the Durand Coordinate, Yagi et al. (1972) vs. Theory



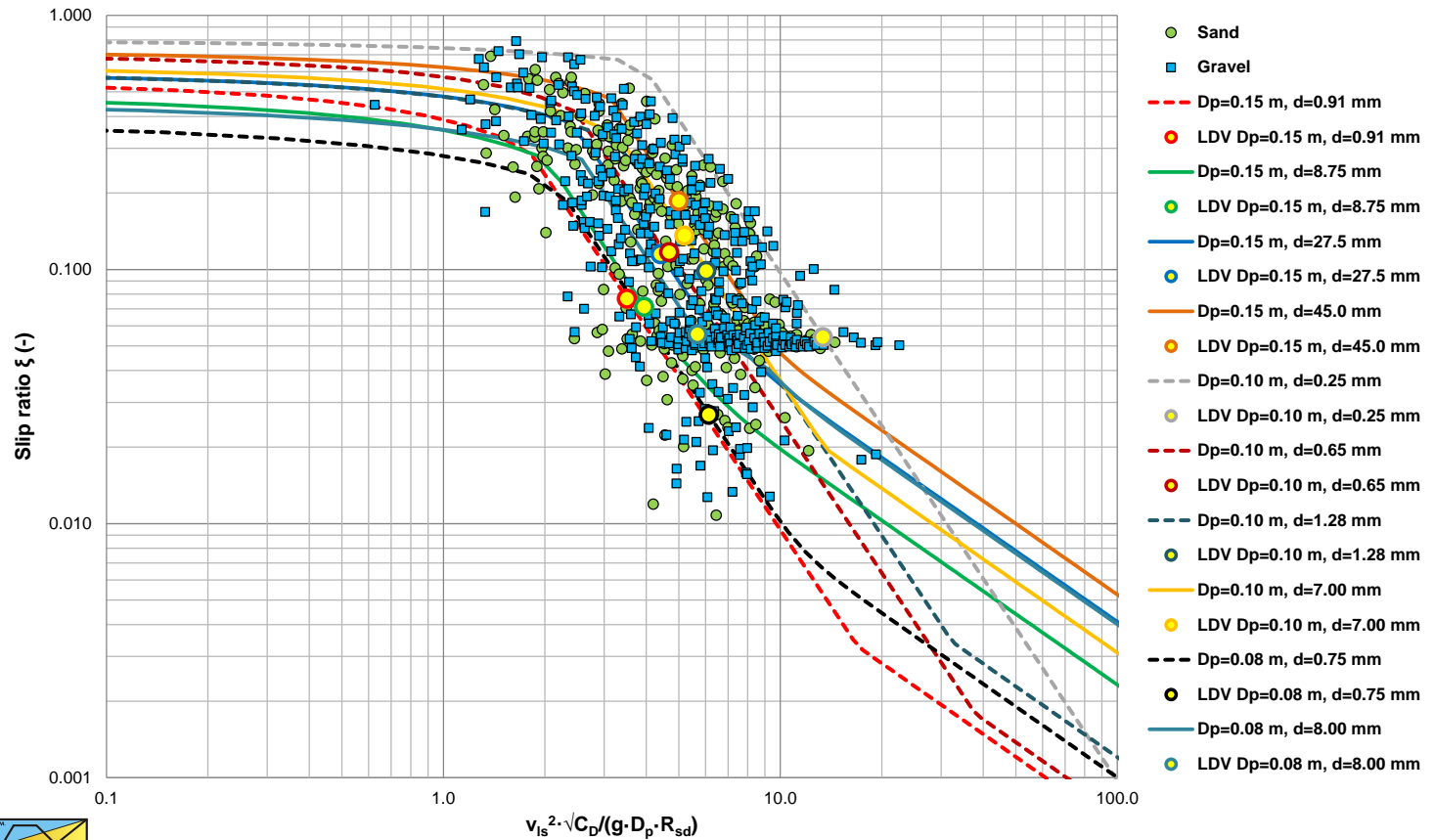
LDV Region

Slip Ratio ξ vs. the Durand Coordinate, Yagi et al. (1972) vs. Theory



Sliding Bed, LDV & He. Regions

Slip Ratio ξ vs. the Durand Coordinate, Yagi et al. (1972) vs. Theory



Slip resulting from 3LM

$$C_{vr} = \frac{C_{vt}}{C_{vb}} \quad \text{and} \quad \alpha = 0.58 \cdot C_{vr}^{-0.42}$$

$$\frac{1}{1 - \xi_{v_{ls,lsdv}}} = C_{vr}^{-0.5}$$

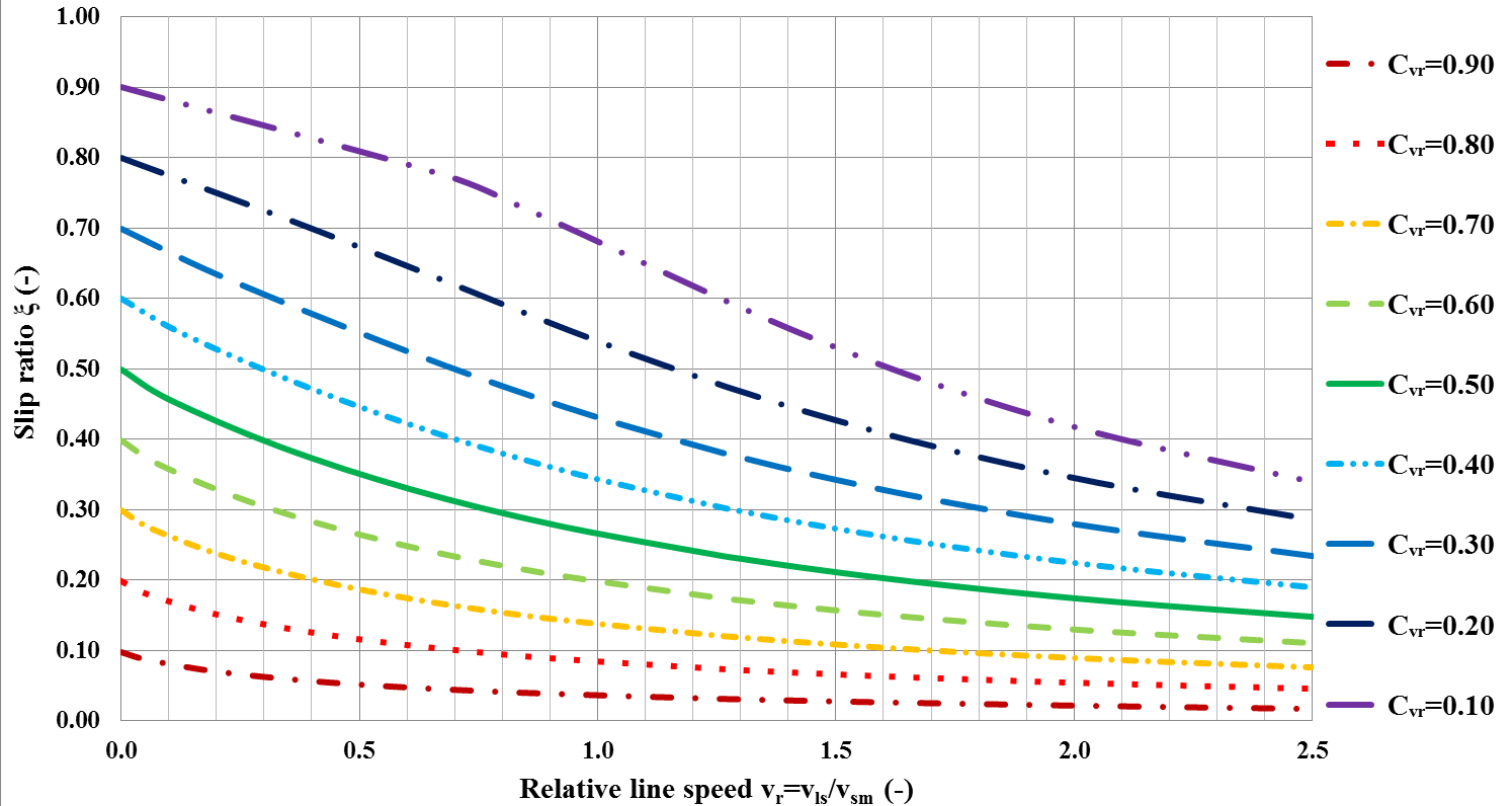
$$\xi = (1 - C_{vr}) \cdot e^{\left(-\left(0.83 + \frac{\mu_{sf}}{4} + (C_{vr} - 0.5 - 0.075 \cdot D_p)^2 + 0.025 \cdot D_p \right) \cdot D_p^{0.025} \cdot \left(\frac{v_{ls}}{v_{ls,lsdv}} \right)^\alpha \cdot C_{vr}^{0.65} \cdot \left(\frac{R_{sd}}{1.585} \right)^{0.1} \right)}$$



Slip resulting from 3LM

Slip ratio ξ vs. relative line speed v_r , $C_{vr}=C_{vt}/C_{vb}$

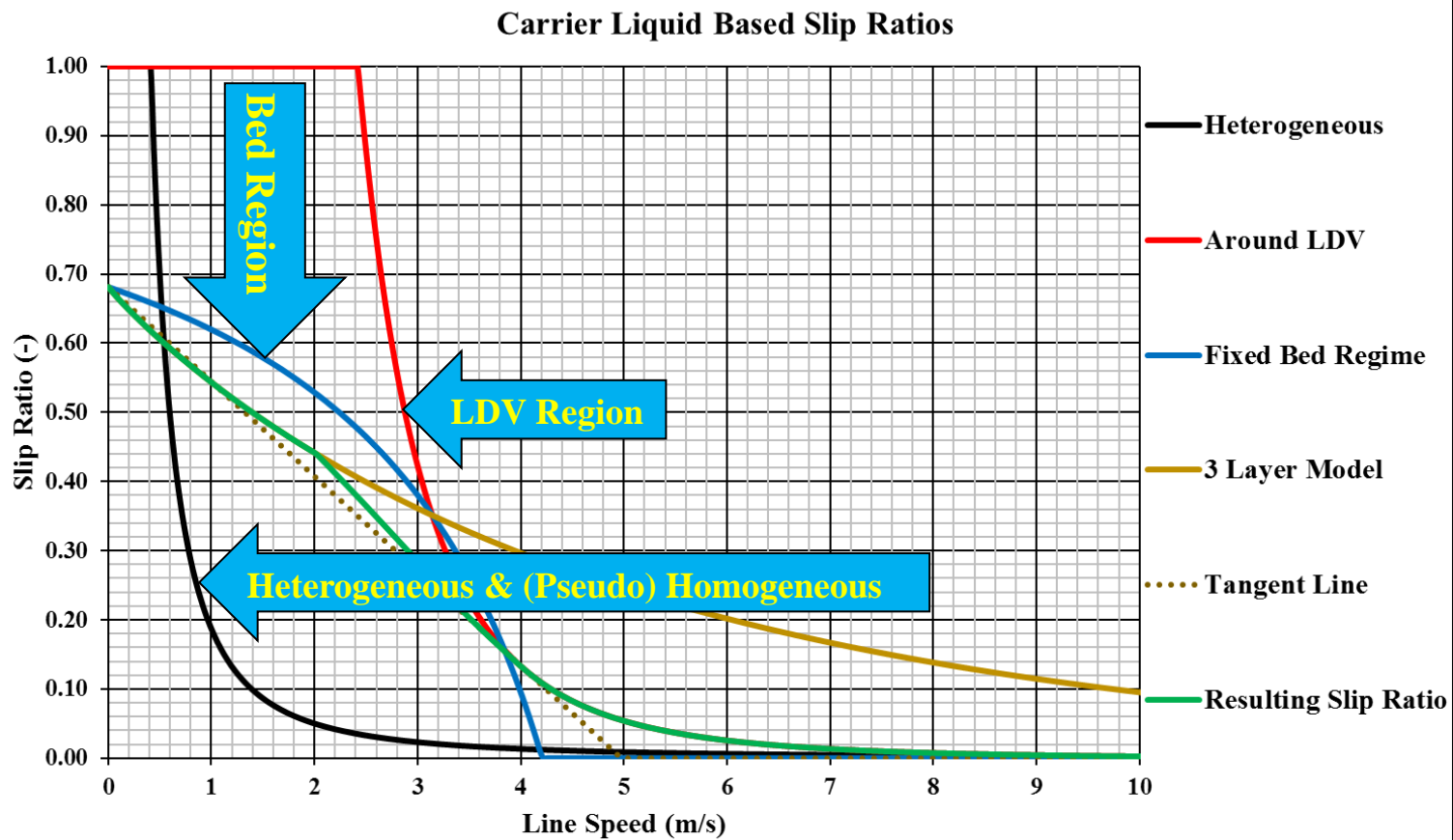
3LM-D-W



$D_p=0.1524$ m, $d=1.000$ mm, $R_{sd}=1.585$, $\mu_{sf}=0.416$, $C_{vb}=0.55$



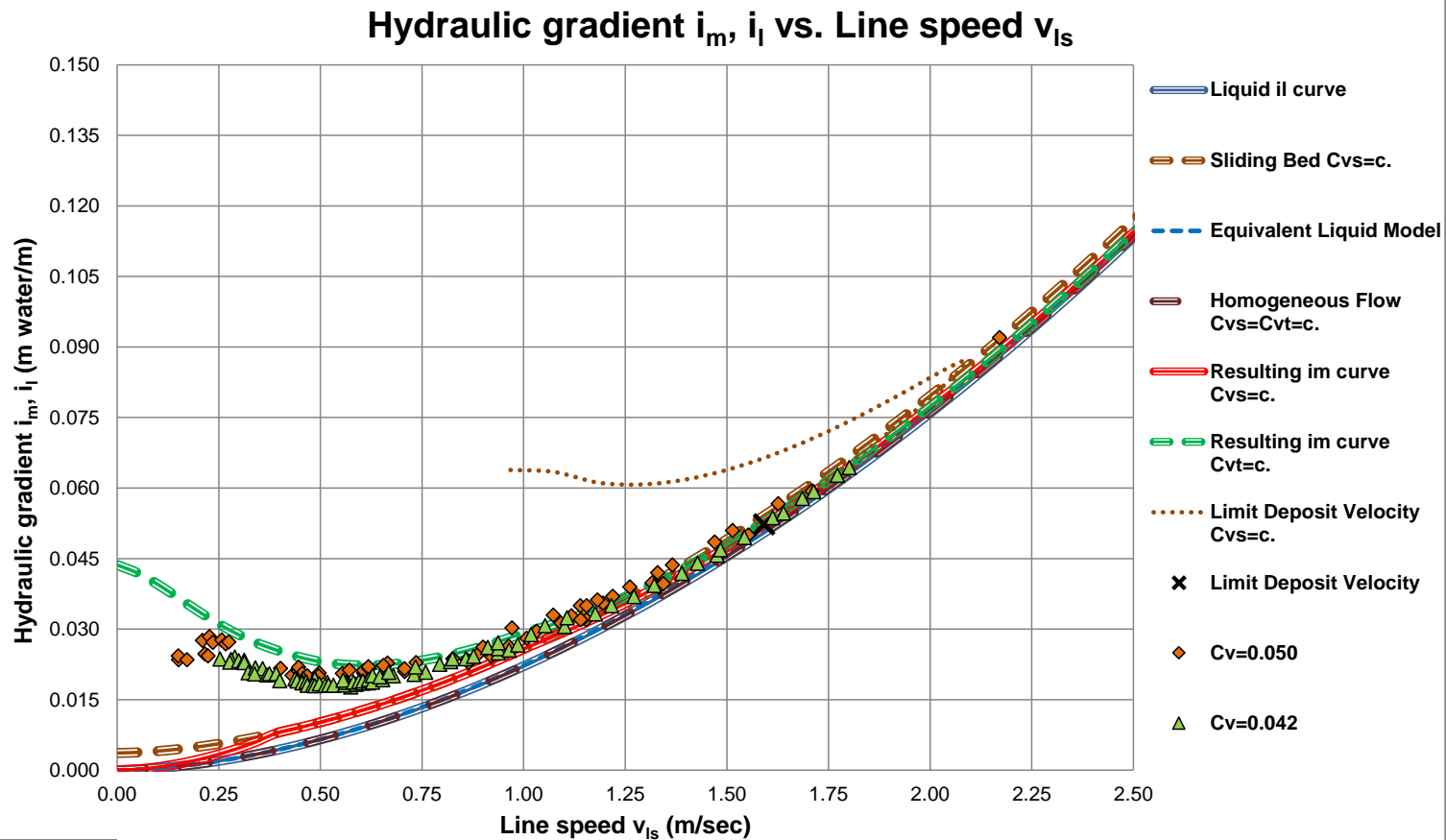
Construction Slip Ratio Curve



$D_p=0.1524$ m, $d=1.000$ mm, $R_{sd}=1.585$, $C_v=0.175$, $\mu_{sf}=0.416$, $\rho_{cl}=1.025$ ton/m³, $C_{vb}=0.55$, Fines=0.00 %, $\theta=0.00^\circ$



Doron et al. (1987), $C_{vt}=0.042-0.050$



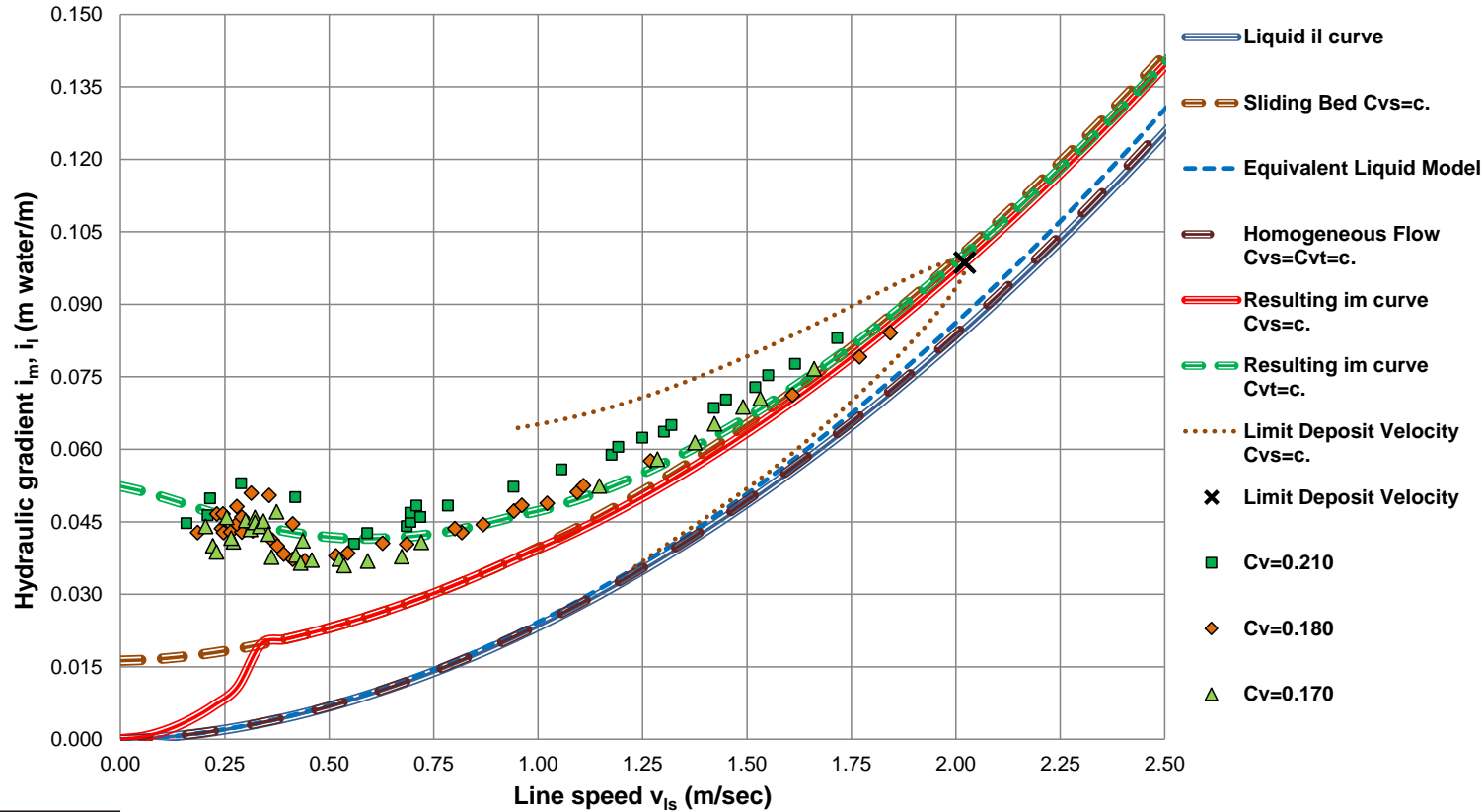
$D_p=0.0508$ m, $d=3.000$ mm, $R_{sd}=0.210$, $C_v=0.042$, $\mu_{sf}=0.416$



Doron et al. (1987), $C_{vt}=0.17-0.21$



Hydraulic gradient i_m, i_l vs. Line speed v_{ls}



$D_p=0.0508 \text{ m}, d=3.000 \text{ mm}, R_{sd}=0.210, C_v=0.187, \mu_{sf}=0.416$



Conclusions

- The slip velocity or holdup function has to be divided into 3 regions: The bed region, the LDV region and the heterogeneous & (pseudo) homogeneous region.
- The slip velocity or holdup function depends strongly on the LDV and the concentration.
- The delivered concentration can be determined based on the spatial concentration with the method developed.
- The method developed matches very well with experimental data.
- A good estimate of pressure losses can only be determined based on spatial concentration, the method developed is used to determine pressure losses based on delivered concentration.





Concentration Distribution

Chapter 7.10 & 8.13



Research Question

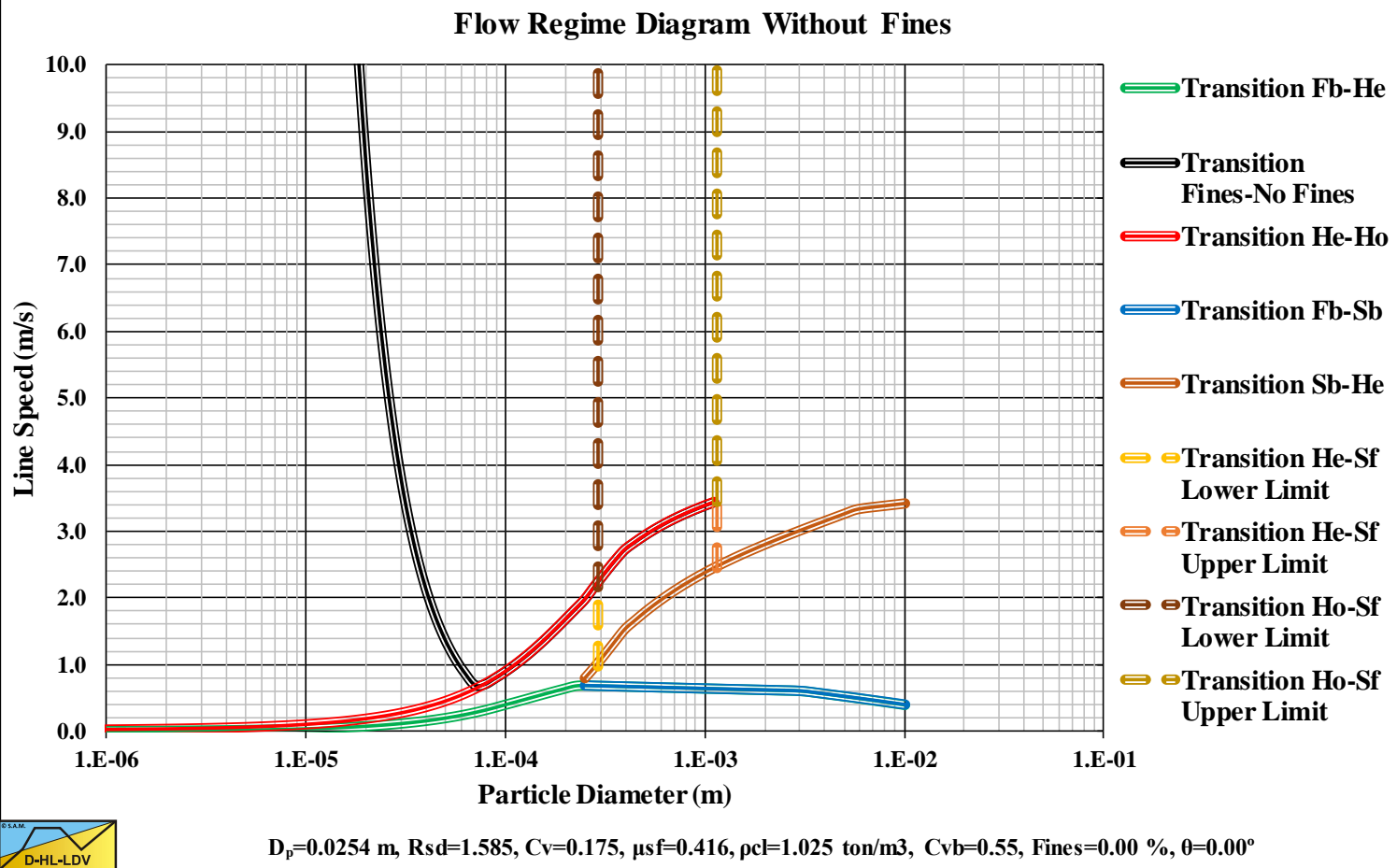
Problem definition:

Existing methods for determining the concentration distribution in slurry transport are based on an average hindered settling velocity according to Richardson & Zaki for 1D open channel flow.

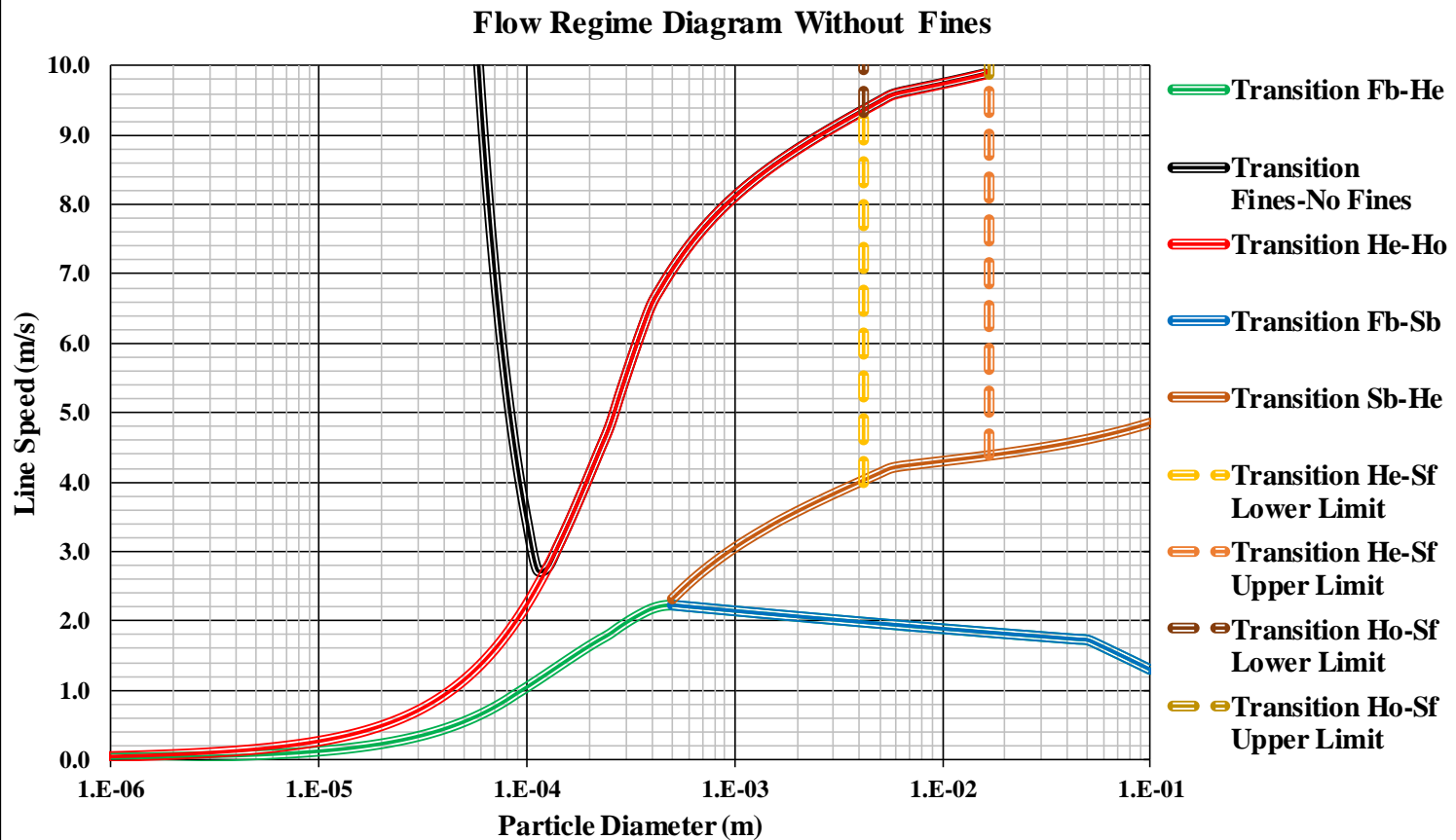
- In pipe flow the flow is 2D.
- The flow is turbulent, not still water.
- The hindered settling depends on the local concentration and thus on the position in the pipe.
- The Richardson & Zaki equation is valid for low concentrations.
- The advection diffusion equation is valid for small particles.
- Maximum bed concentration at line speed $< LDV$.



Flow Regimes, Small Pipes



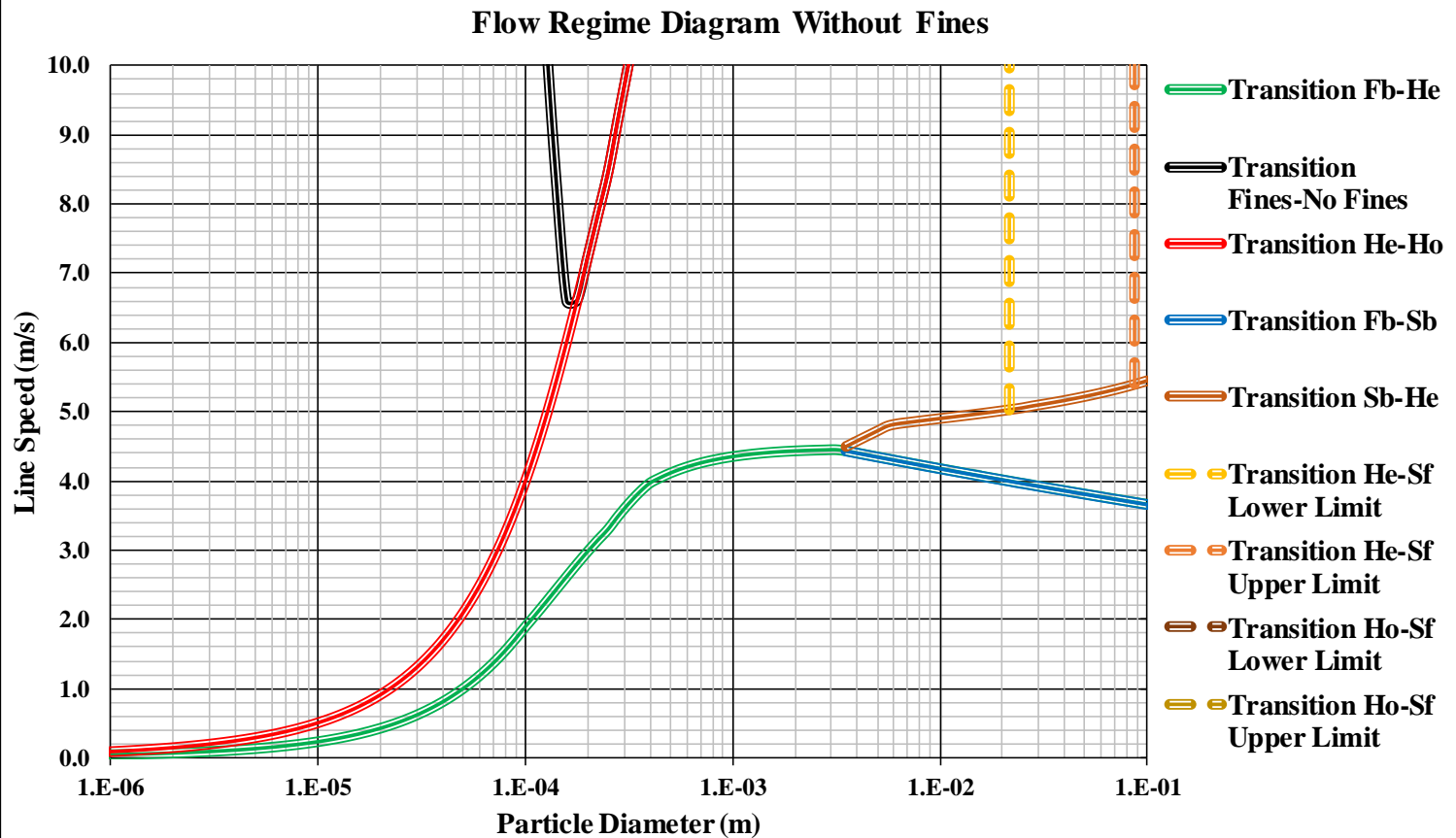
Flow Regimes, Medium Pipes



$D_p=0.2540$ m, $R_{sd}=1.585$, $C_v=0.175$, $\mu_{sf}=0.416$, $\rho_{cl}=1.025$ ton/m³, $C_{vb}=0.55$, Fines=0.00 %, $\theta=0.00^\circ$



Flow Regimes, Large Pipes



$D_p=1.2192$ m, $R_{sd}=1.585$, $C_v=0.175$, $\mu_{sf}=0.416$, $\rho_{cl}=1.025$ ton/m³, $C_{vb}=0.55$, Fines=0.00 %, $\theta=0.00^\circ$



Advection-Diffusion Equation

$$C_{vs}(r) \cdot v_{th} + \varepsilon_s \cdot \frac{dC_{vs}(r)}{dr} = C_{vs}(r) \cdot v_{th} + \beta_{sm} \cdot \varepsilon_m \cdot \frac{dC_{vs}(r)}{dr} = 0$$

$$\frac{dC_{vs}(r)}{C_{vs}(r)} = -\frac{v_{th}}{\beta_{sm} \cdot \varepsilon_m} \cdot dr \quad \Rightarrow \quad \ln(C_{vs}(r)) = -\frac{v_{th}}{\beta_{sm} \cdot \varepsilon_m} \cdot r + C$$

$$C_{vs}(r) = C_{vB} \cdot e^{-\frac{v_{th}}{\beta_{sm} \cdot \varepsilon_m} \cdot r} = C_{vB} \cdot e^{-12 \cdot \frac{v_{th}}{\beta_{sm} \cdot \kappa \cdot u_*} \cdot \frac{r}{D_p}}$$

- Used in the Wasp model.
- Derived for 2D open channel flow.
- It is assumed particles follow the turbulent eddies.
- It is assumed the (hindered) terminal settling velocity is constant over the cross section of the pipe.
- There is no influence of the pipe wall.



Advection-Diffusion Equation, Modified

$$C_{vs}(r) \cdot v_{th}(r) + \varepsilon_s \cdot \frac{dC_{vs}(r)}{dr} = C_{vs}(r) \cdot v_{th}(r) + \beta_{sm} \cdot \varepsilon_m \cdot \frac{dC_{vs}(r)}{dr} = 0$$

$$\frac{dC_{vs}(r)}{C_{vs}(r)} = -\frac{v_{th}(r)}{\beta_{sm} \cdot \varepsilon_m} \cdot dr \quad \Rightarrow \quad \ln(C_{vs}(r)) = -\frac{v_{th}(r)}{\beta_{sm} \cdot \varepsilon_m} \cdot r + C$$

$$C_{vs}(r) = C_{vB} \cdot e^{-\frac{v_{th}}{\beta_{sm} \cdot \varepsilon_m} \cdot r} = C_{vB} \cdot e^{-12 \cdot \frac{v_{th}}{\beta_{sm} \cdot \varepsilon_m} \cdot r}$$

- Derived for 2D open channel flow.
- It is assumed the (hindered) terminal settling velocity is constant over the cross section of the pipe.
- The hindered settling equation of Richardson & Zaki gives a velocity above $C_{vs}=0.5-0.6$ or $C_{vr}=1$





Diffusivity based on the LDV



Diffusivity Based on LDV

$$C_{vB} = C_{vs} \cdot \frac{\left(\frac{12 \cdot v_{th}}{\beta_{sm} \cdot \kappa \cdot u_*} \right)}{\left(1 - e^{-12 \cdot \frac{v_{th}}{\beta_{sm} \cdot \kappa \cdot u_*}} \right)} \Rightarrow C_{vb} = C_{vs} \cdot \frac{\left(\frac{12 \cdot v_{th,ldv}}{\beta_{sm,ldv} \cdot \kappa \cdot u_{*,ldv}} \right)}{\left(1 - e^{-12 \cdot \frac{v_{th,ldv}}{\beta_{sm} \cdot \kappa \cdot u_{*,ldv}}} \right)}$$

$$\beta_{sm,ldv} = 12 \cdot \frac{C_{vs}}{C_{vb}} \cdot \frac{v_{th,ldv}}{\alpha_{sm} \cdot \kappa \cdot u_{*,ldv}} = 12 \cdot C_{vr} \cdot \frac{v_{th,ldv}}{\alpha_{sm} \cdot \kappa \cdot u_{*,ldv}}$$

$$C_{vs}(r) = C_{vB} \cdot e^{-12 \cdot \frac{v_{th}}{\left(12 \cdot C_{vr} \cdot \frac{v_{th,ldv}}{\alpha_{sm} \cdot \kappa \cdot u_{*,ldv}} \right) \cdot \kappa \cdot u_*} \cdot \frac{r}{D_p}} = C_{vB} \cdot e^{-\frac{\alpha_{sm} \cdot u_{*,ldv}}{C_{vr} \cdot u_*} \cdot \frac{v_{th}}{v_{th,ldv}} \cdot \frac{r}{D_p}}$$



The Bottom Concentration

$$C_{vB} = C_{vs} \cdot \frac{\left(\frac{\alpha_{sm}}{C_{vr}} \cdot \frac{u_{*,ldv}}{u_*} \cdot \frac{v_{th}}{v_{tv,ldv}} \right)}{\left(1 - e^{-\frac{\alpha_{sm}}{C_{vr}} \cdot \frac{u_{*,ldv}}{u_*} \cdot \frac{v_{th}}{v_{tv,ldv}}} \right)} = C_{vb} \cdot \frac{\left(\alpha_{sm} \cdot \frac{u_{*,ldv}}{u_*} \cdot \frac{v_{th}}{v_{th,ldv}} \right)}{\left(1 - e^{-\frac{\alpha_{sm}}{C_{vr}} \cdot \frac{u_{*,ldv}}{u_*} \cdot \frac{v_{th}}{v_{th,ldv}}} \right)}$$

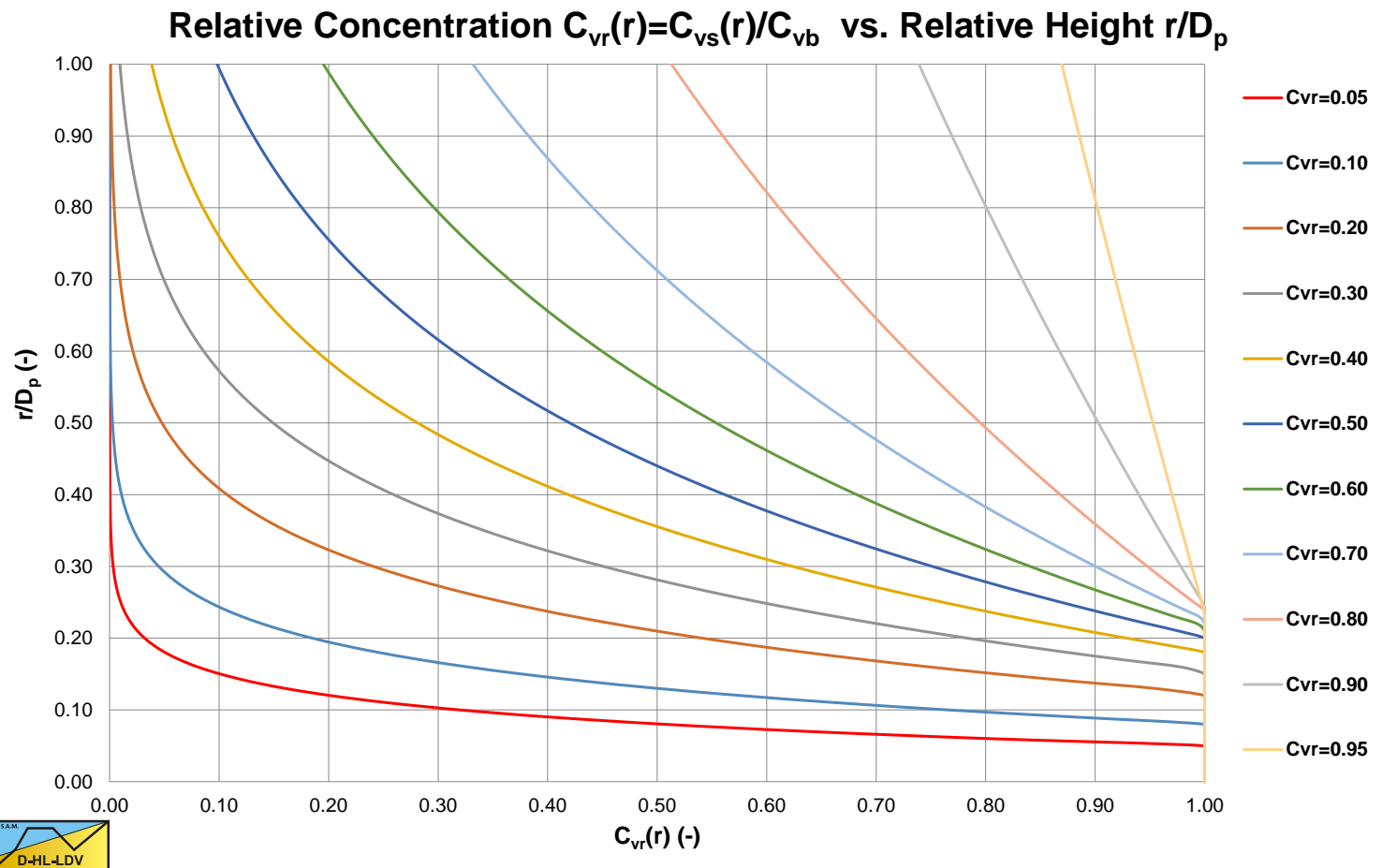
$$= C_{vb} \cdot \frac{u_{*,ldv}}{u_*} \cdot \frac{v_{th}}{v_{th,ldv}}$$

$$\alpha_{sm} = \left(1 - e^{-\frac{\alpha_{sm}}{C_{vr}}} \right)$$

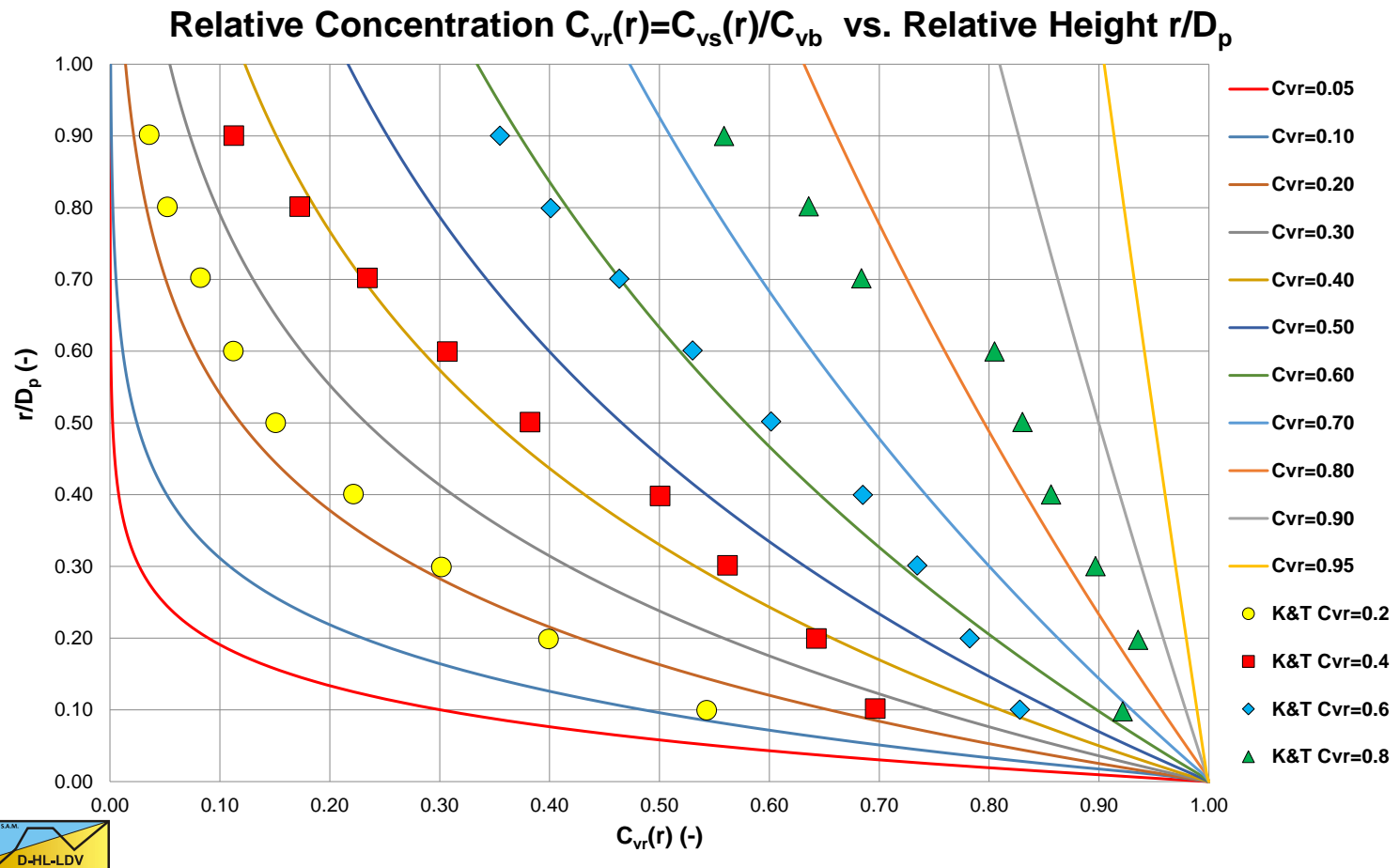
$$\alpha_{sm} = 0.9847 + 0.304 \cdot C_{vr} - 1.196 \cdot C_{vr}^2 - 0.5564 \cdot C_{vr}^3 + 0.47 \cdot C_{vr}^4$$



Concentration Distribution at 0.5·LDV



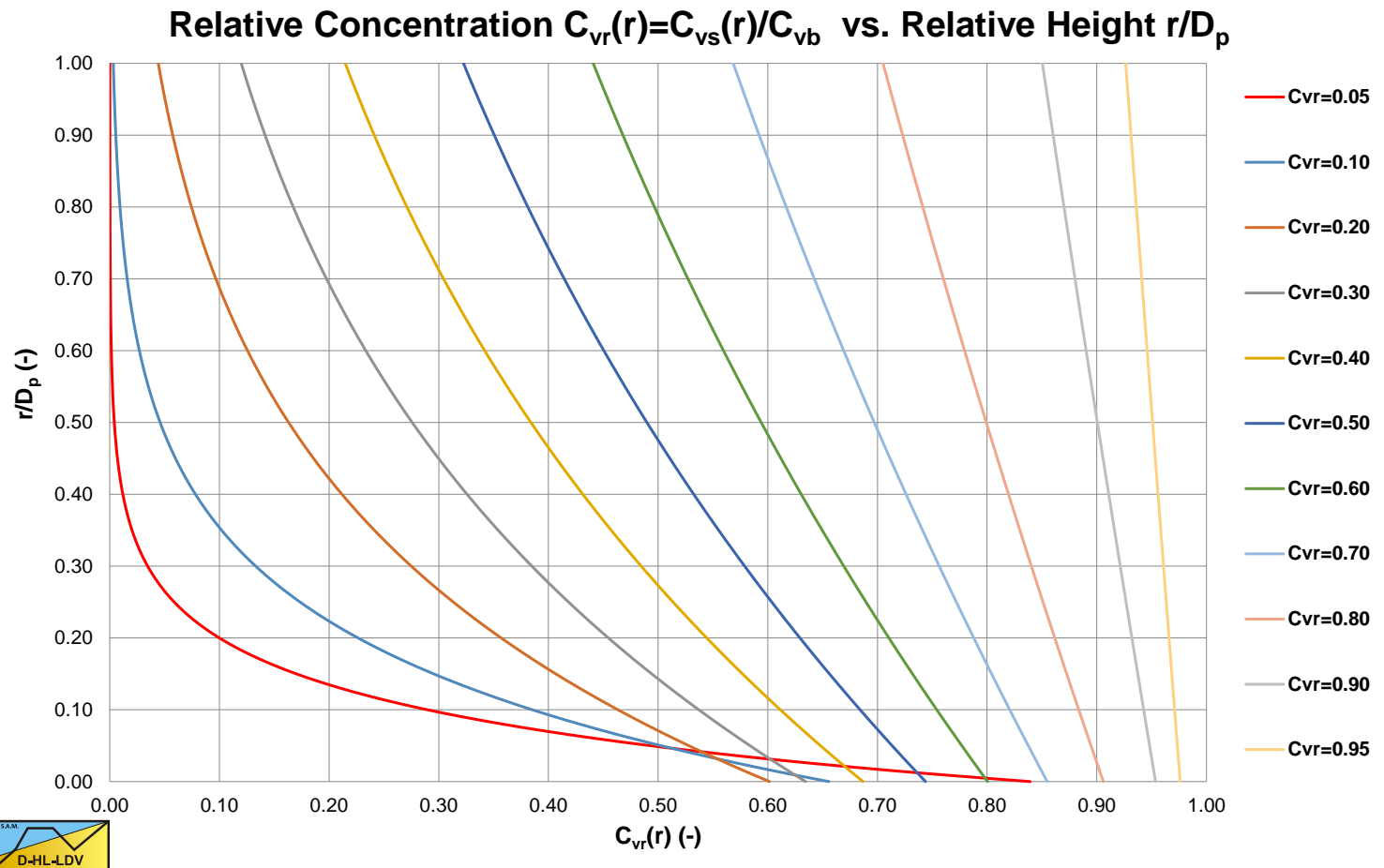
Concentration Distribution at LDV



Kaushal et al. (2005)



Concentration Distribution at 2·LDV





Additional Velocity Ratio



Additional Velocity Ratio 1

$$C_{vB} = C_{vb} \cdot \frac{\left(\alpha_{sm} \cdot \left(r_{LDV} \cdot \frac{v_{ls,ldv}}{v_{ls}} \right)^{1.15} \right)}{\left(1 - e^{-\frac{\alpha_{sm}}{C_{vr}} \cdot \left(r_{LDV} \cdot \frac{v_{ls,ldv}}{v_{ls}} \right)^{1.15}} \right)} \quad \text{and} \quad C_{vs}(f) = C_{vB} \cdot e^{-\frac{\alpha_{sm}}{C_{vr}} \cdot \left(r_{LDV} \cdot \frac{v_{ls,ldv}}{v_{ls}} \right)^{1.15}} \cdot f$$

At the LDV the concentration at the bottom will have a value of about 50%. The maximum bed concentration however is about 60%. So this will occur at a lower line speed.

An additional velocity ratio is required between the LDV and the velocity where the maximum bed concentration will occur.



Additional Velocity Ratio 2

SF = Shape Factor SF=0.77 for sand SF=1.0 for spheres

$$C_{vrMax} = \frac{0.175}{C_{vb}}$$

$$\alpha_\beta = 1.8 - 56 \cdot v_t \quad \text{with: } \alpha_\beta \geq 1.1$$

If $C_{vr} < C_{vrMax}$ then

$$r_{LDV} = 0.6 \cdot \frac{e^{(\beta/2.34)^{\alpha_\beta}}}{e} \cdot \left(\frac{0.0005}{d}\right)^{SF^6} \cdot \left(\frac{C_{vrMax}}{C_{vr}}\right)^{1/3} \quad \text{with: } r_{LDV} \geq 1.2 \cdot \left(\frac{C_{vrMax}}{C_{vr}}\right)^{1/3}$$

If $C_{vr} \geq C_{vrMax}$ then

$$r_{LDV} = 0.6 \cdot \frac{e^{(\beta/2.34)^{\alpha_\beta}}}{e} \cdot \left(\frac{0.0005}{d}\right)^{SF^6} \cdot \left(\frac{C_{vr}}{C_{vrMax}}\right)^{1/6} \quad \text{with: } r_{LDV} \geq 1.2 \cdot \left(\frac{C_{vr}}{C_{vrMax}}\right)^{1/6}$$

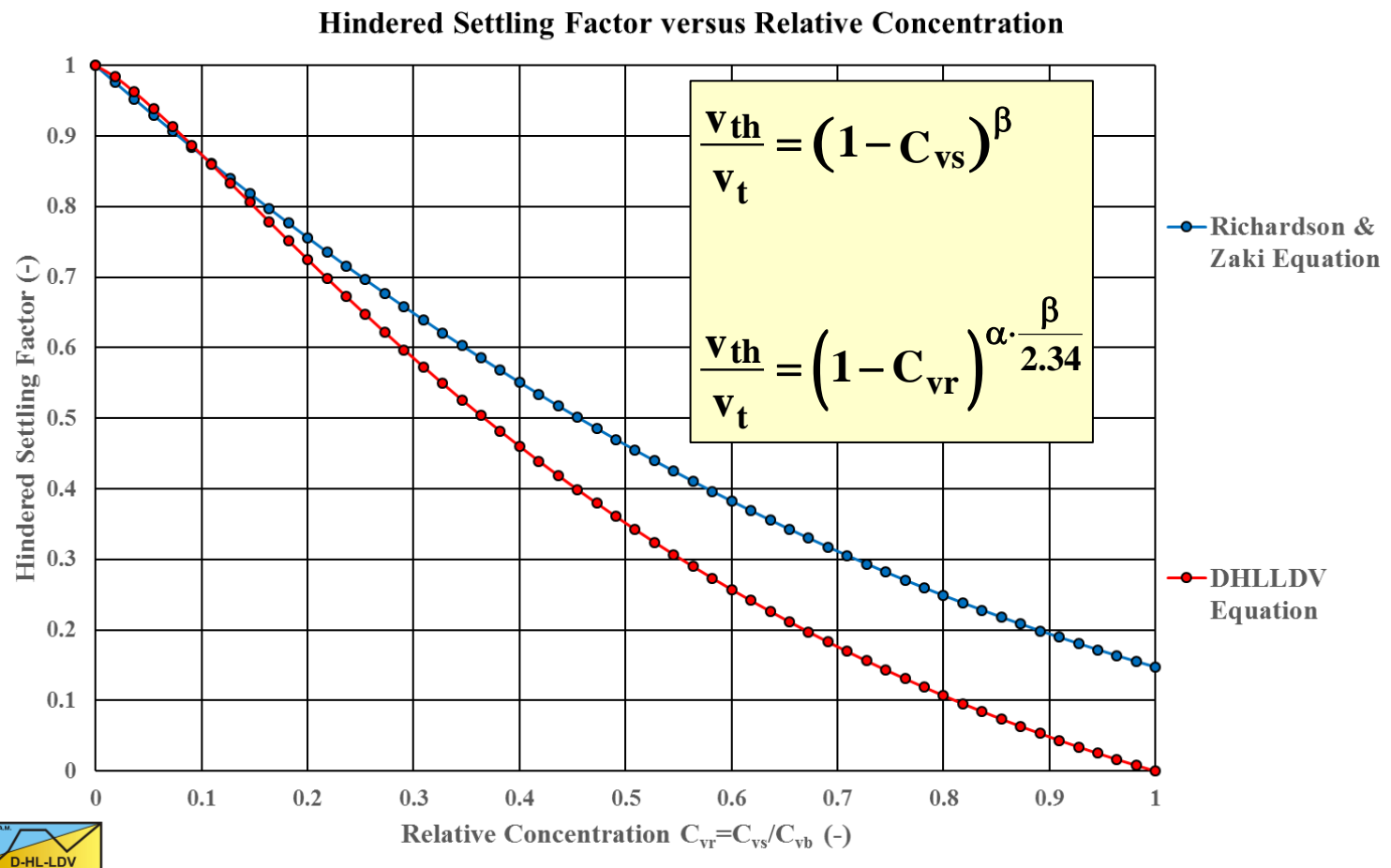




Modified Hindered Settling Velocity



Modified Hindered Settling Velocity

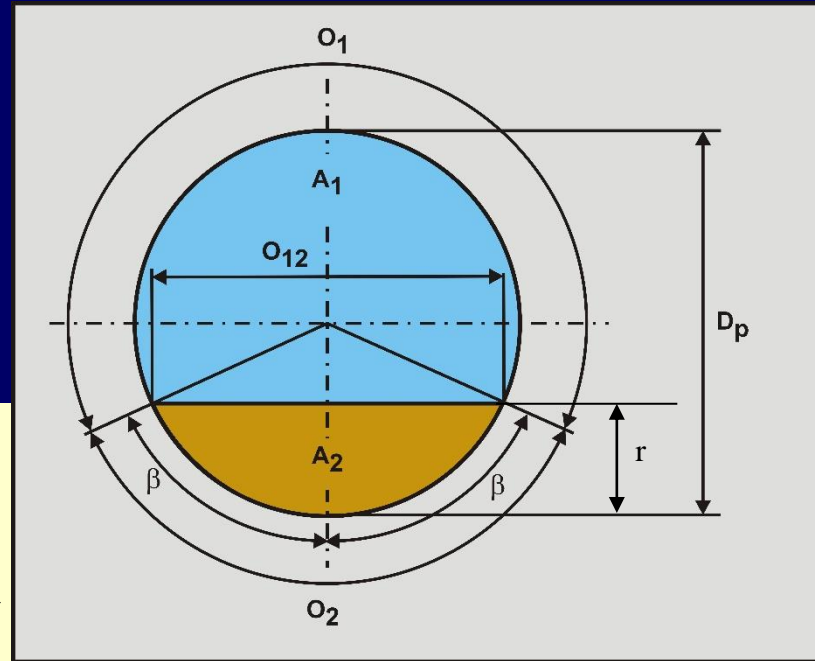




1D Open Channel Flow versus 2D Pipe Flow



Fraction versus Height, 1D vs. 2D



Original Relative Height

$$C_{vs}(r) = C_{vB} \cdot e^{-\frac{\alpha_{sm}}{C_{vr}} \cdot \frac{u_{*,ldv}}{u_*} \cdot \frac{v_{th}}{v_{th,ldv}} \cdot \frac{r}{D_p}}$$

Modified Relative Fraction

$$C_{vs}(r) = C_{vB} \cdot e^{-\frac{\alpha_{sm}}{C_{vr}} \cdot \frac{u_{*,ldv}}{u_*} \cdot \frac{v_{th}}{v_{th,ldv}} \cdot f} \quad \text{with:} \quad f = \frac{A_2}{A_p} = \frac{A_2}{A_1 + A_2}$$





Local Hindered Settling Velocity



Local Hindered Settling, Step 0

Prepare Iteration

$$\frac{dC_{vs,0}(f)}{df} = -\frac{v_{th}}{\beta_{sm} \cdot \epsilon_m} \cdot C_{vs,0}(f) \quad \Rightarrow \quad \text{Analytical Solution}$$

$$\frac{dC_{vs,0}(f)}{C_{vb} \cdot df} = -\frac{v_{th}}{\beta_{sm} \cdot \epsilon_m} \cdot \frac{C_{vs,0}(f)}{C_{vb}}$$

$$\Rightarrow \quad \frac{dC_{vr,0}(f)}{df} = -\frac{v_{th}}{\beta_{sm} \cdot \epsilon_m} \cdot C_{vr,0}(f)$$

$$\Rightarrow \quad \frac{dC_{vr,0}(f)}{df} = -\frac{v_t \cdot (1 - C_{vr})^{\alpha \cdot \frac{\beta}{2.34}}}{\beta_{sm} \cdot \epsilon_m} \cdot C_{vr,0}(f)$$



Local Hindered Settling, Step 1

First Iteration Step

$$\frac{dC_{vs,1}(f)}{df} = -\frac{v_{th,0}(f)}{\beta_{sm} \cdot \varepsilon_m} \cdot C_{vs,0}(f)$$

$$= -\frac{v_t \cdot \left(1 - C_{vr,0}(f)\right)^{\alpha \cdot \frac{\beta}{2.34}}}{\beta_{sm} \cdot \varepsilon_m} \cdot C_{vs,0}(f)$$

$$\left(\frac{dC_{vs,1}(f)}{df}\right) = \left(\frac{\left(1 - C_{vr,0}(f)\right)^{\alpha \cdot \frac{\beta}{2.34}}}{\left(1 - C_{vr}\right)}\right)$$



Local Hindered Settling, Step 2+

Next Iteration Steps

$$\frac{dC_{vr,i}(f)}{df} = -\frac{v_{th,i-1}(f)}{\beta_{sm} \cdot \varepsilon_m} \cdot C_{vr,i-1}(f)$$

$$= -\frac{v_t \cdot e^{-\beta \cdot C_{vr,i-1}(f)^{1.25}} \cdot (1 - C_{vr,i-1}(f))^{2 \cdot \beta}}{\beta_{sm} \cdot \varepsilon_m} \cdot C_{vr,i-1}(f)$$

$$\left(\frac{dC_{vr,i}(f)}{df} \right) = \left(\frac{C_{vr,i-1}(f)}{C_{vr,i-2}(f)} \right) \cdot \left(\frac{(1 - C_{vr,i-1}(f))}{(1 - C_{vr,i-2}(f))} \right)^{\alpha \cdot \frac{\beta}{2.34}}$$

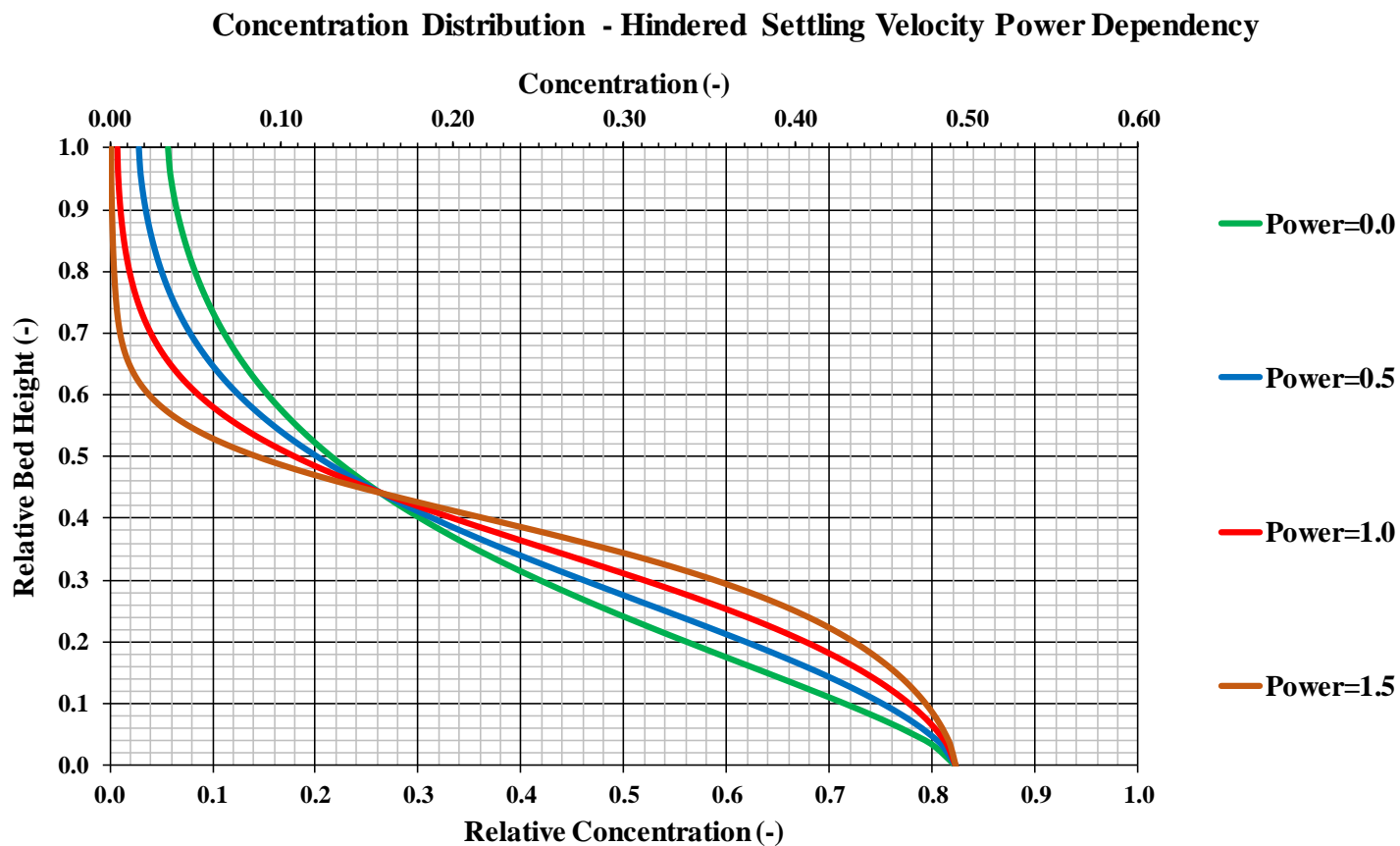




The Power Alpha



Local Hindered Settling Power Alpha



$D_p=0.152$ m, $C_{vb}=0.60$, $C_{vs}=0.175$, $V_s=3.20$ m/s, $d=1.000$ mm, $\beta=2.738$



The Power Alpha

SF = Shape Factor SF=0.77 for sand SF=1.0 for spheres

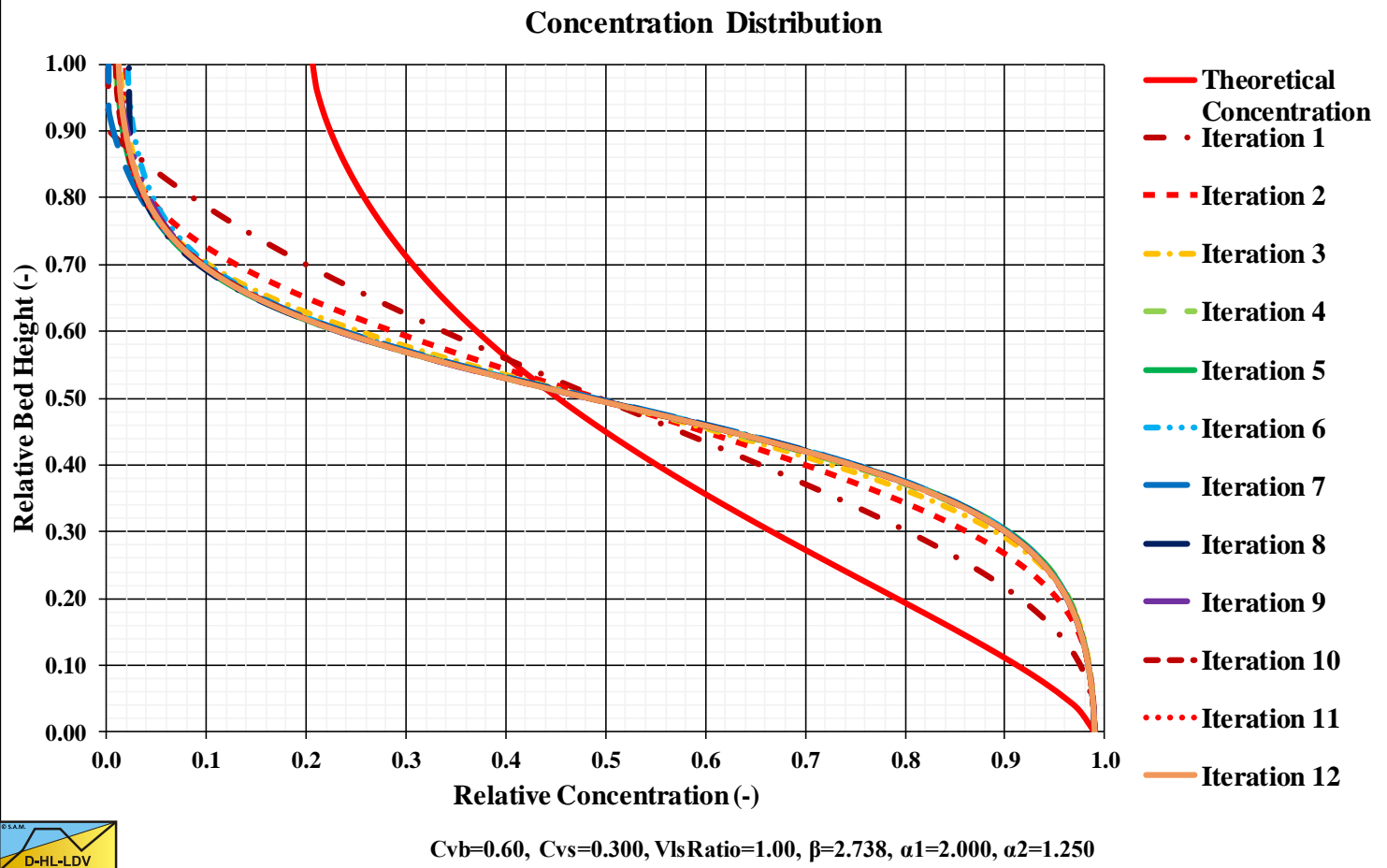
$$C_{vrMax} = \frac{0.175}{C_{vb}}$$

$$\alpha = 0.275 \cdot \left(\frac{SF}{0.77} \right)^{1.5} \cdot \left(\frac{C_{vr}}{C_{vrMax}} \right)^3 \cdot \left(\frac{v_{ls,LDV}}{v_{ls}} \right)^{0.15} \quad \text{for } C_{vr} < C_{vrMax}$$

$$\alpha = 0.275 \cdot \left(\frac{SF}{0.77} \right)^{1.5} \cdot \left(\frac{C_{vr}}{C_{vrMax}} \right)^{2/3} \cdot \left(\frac{v_{ls,LDV}}{v_{ls}} \right)^{0.15} \quad \text{for } C_{vr} \geq C_{vrMax}$$



Iterations at LDV, $C_{vr}=0.5$

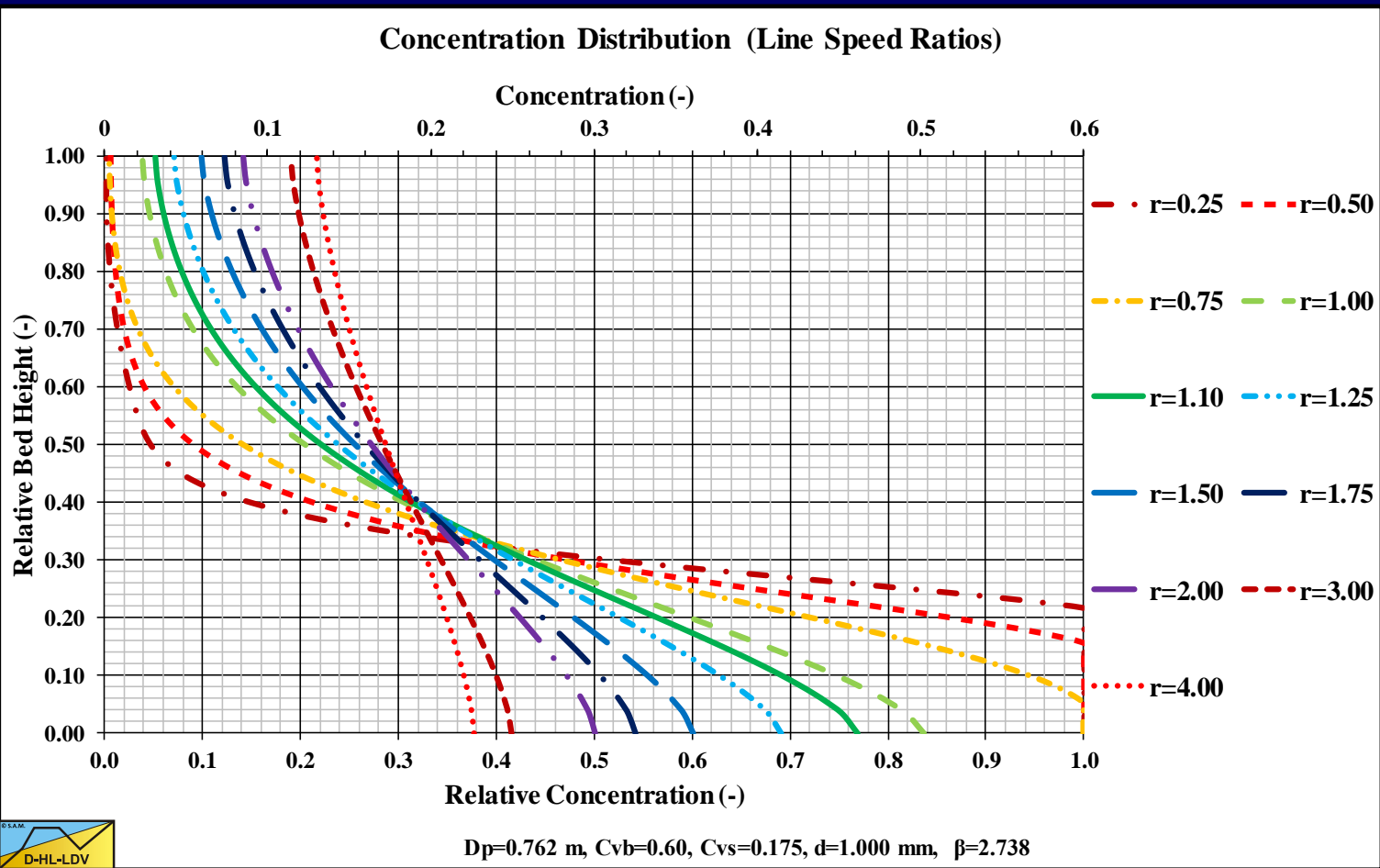




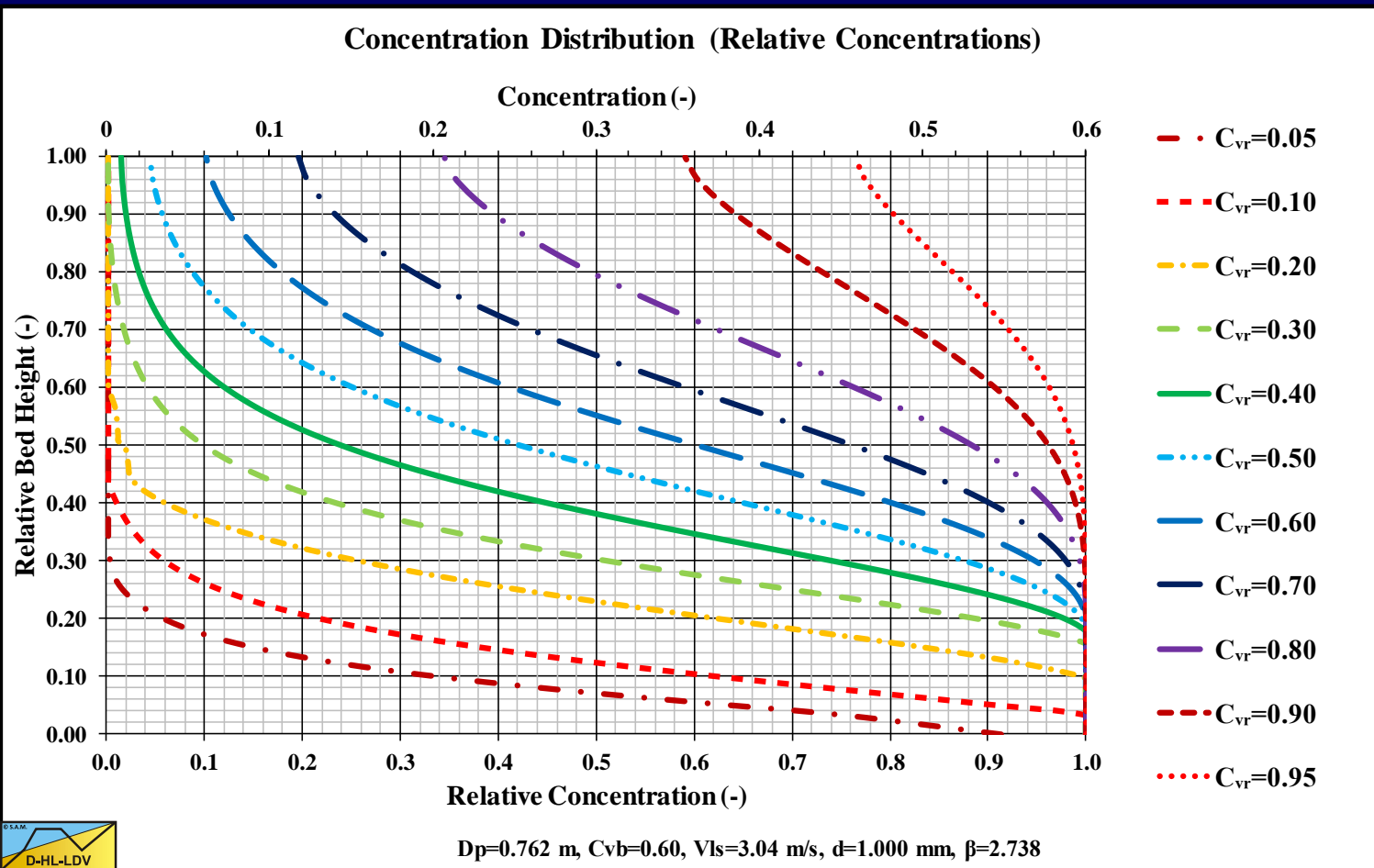
Resulting Concentration Curves



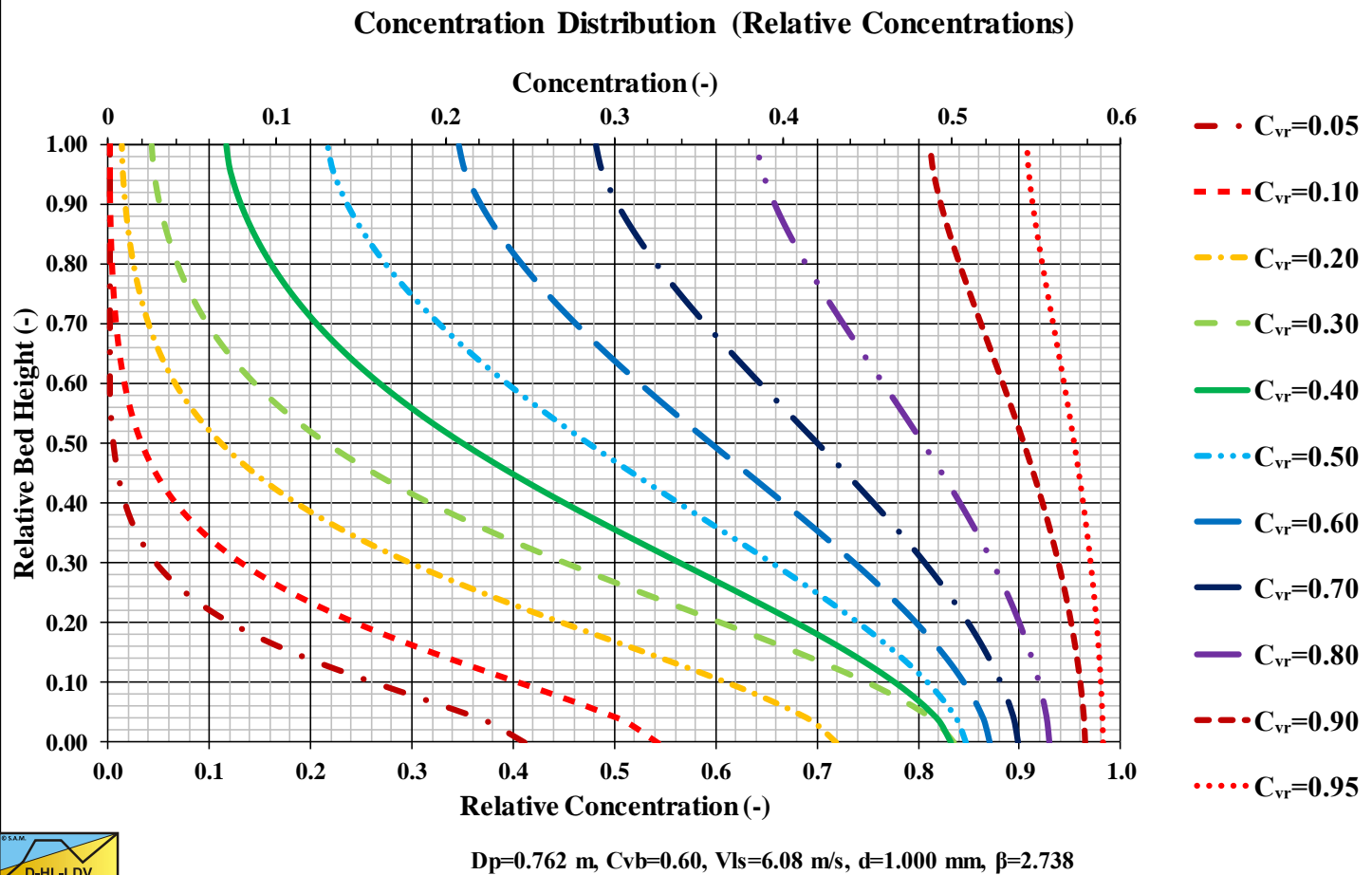
Different Line Speeds, $C_{vr}=0.175$



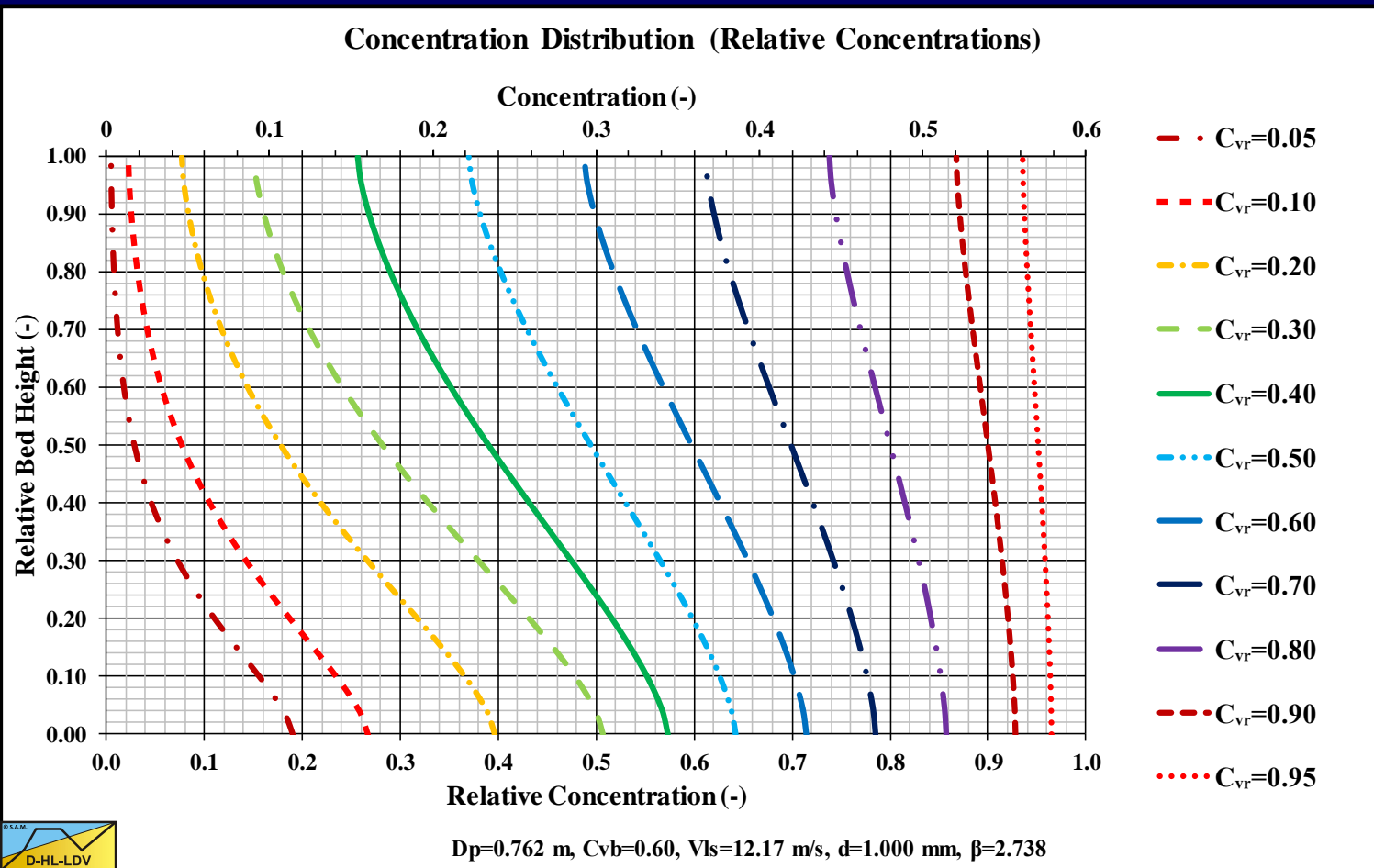
Different Concentrations at the 0.5*LDV



Different Concentrations at the LDV



Different Concentrations at the 2*LDV

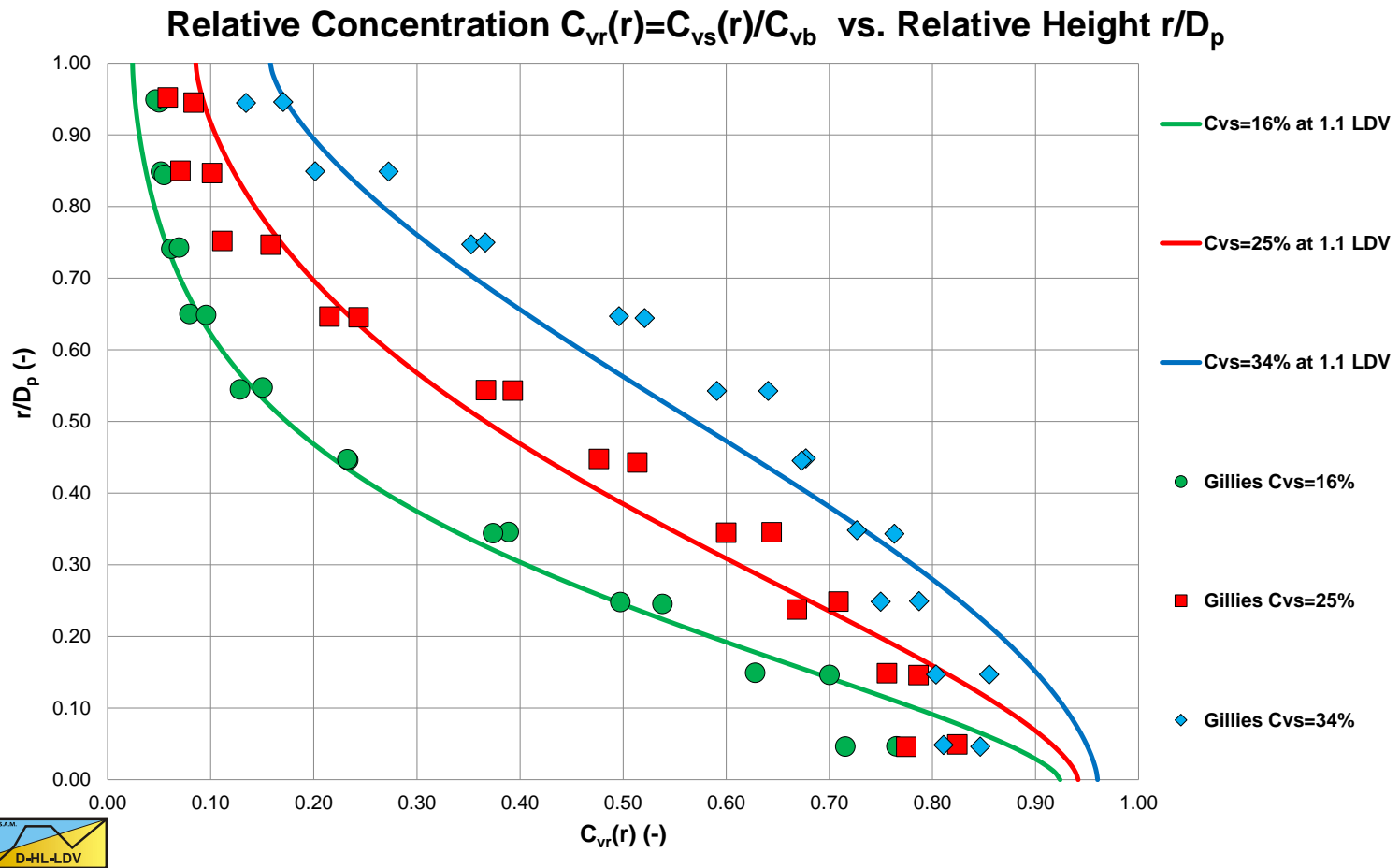




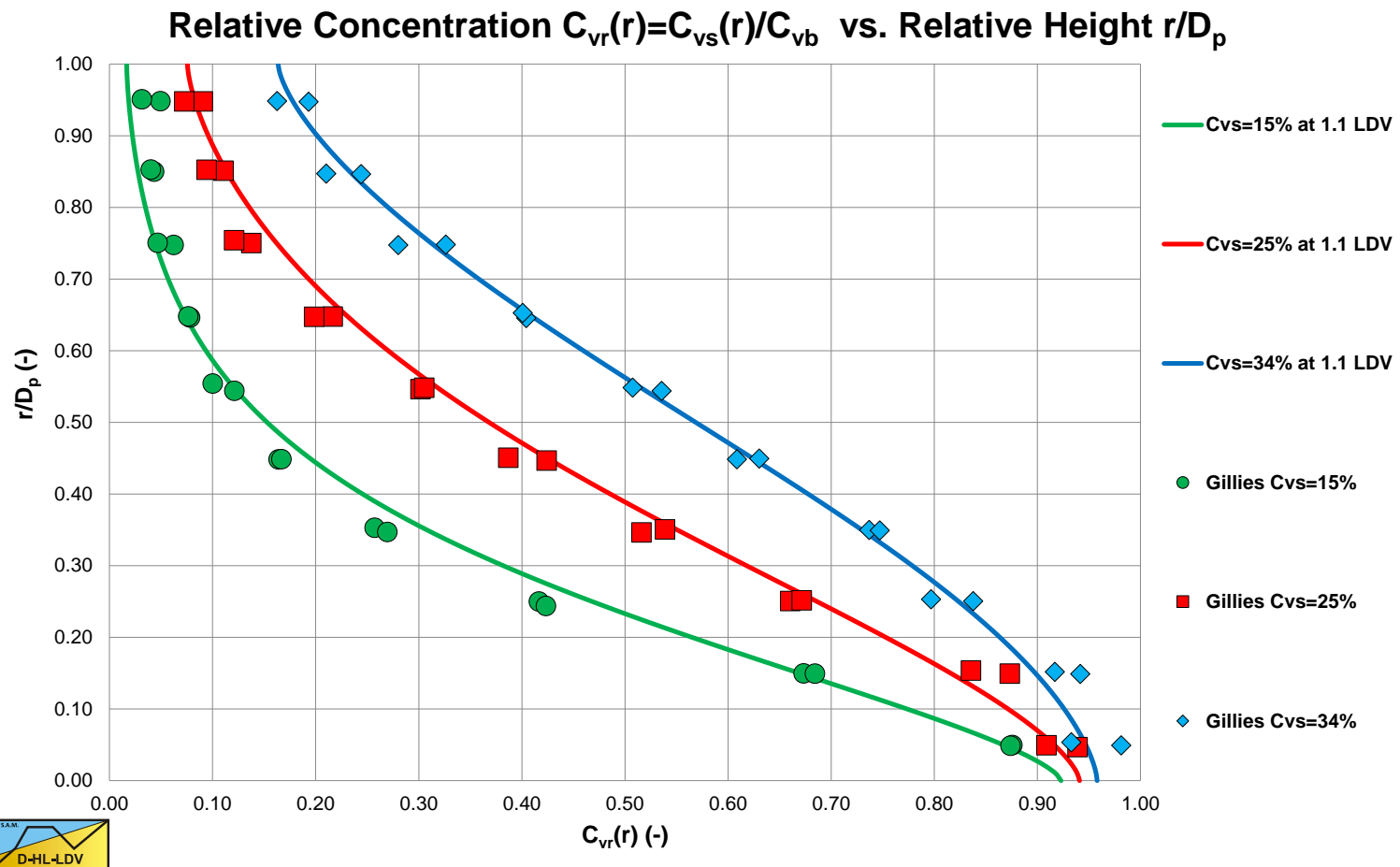
Experiments/Validation



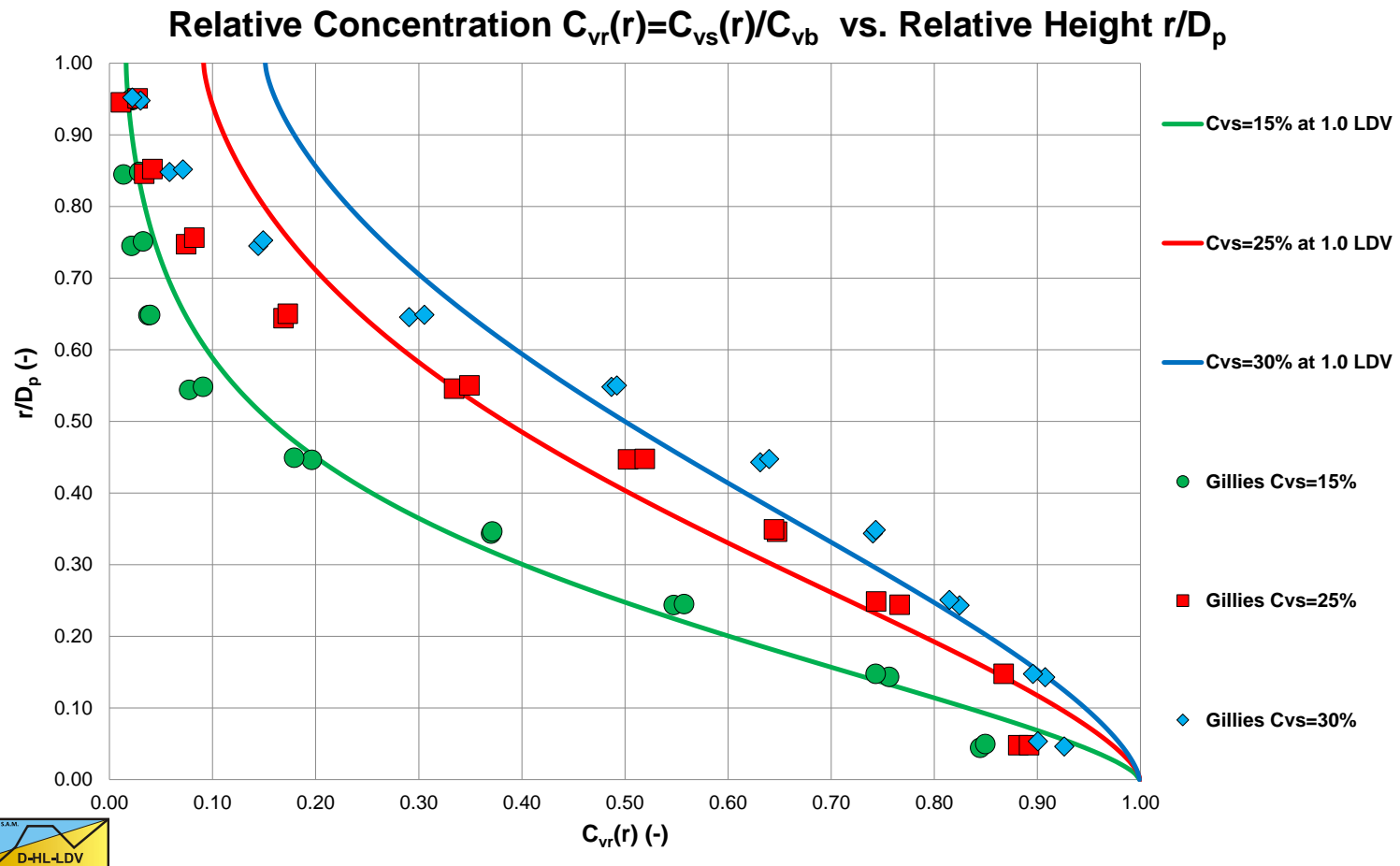
Experiments Gillies (1993), $d=0.29$ mm



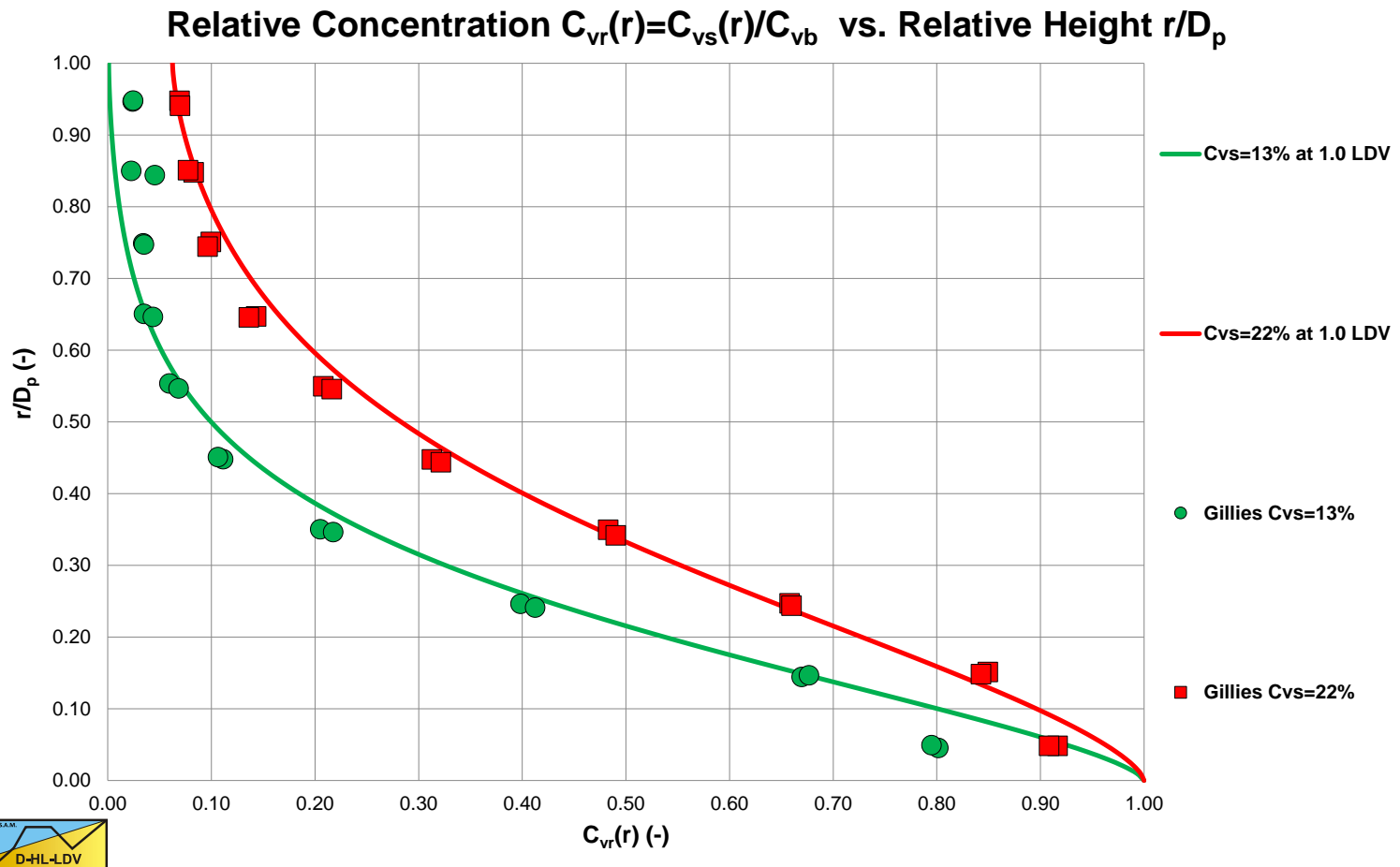
Experiments Gillies (1993), $d=0.38$ mm



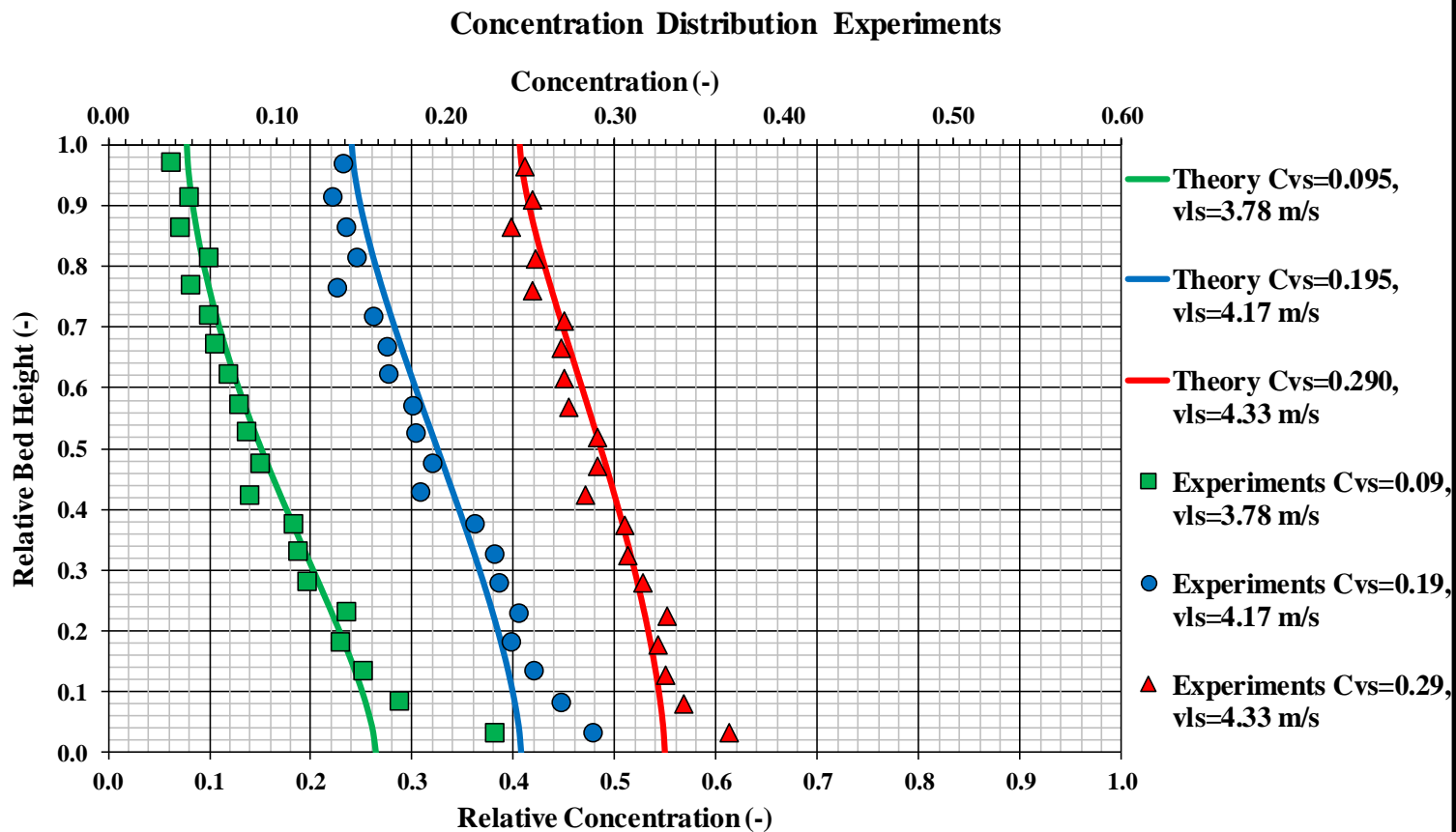
Experiments Gillies (1993), $d=0.55$ mm



Experiments Gillies (1993), $d=2.40$ mm



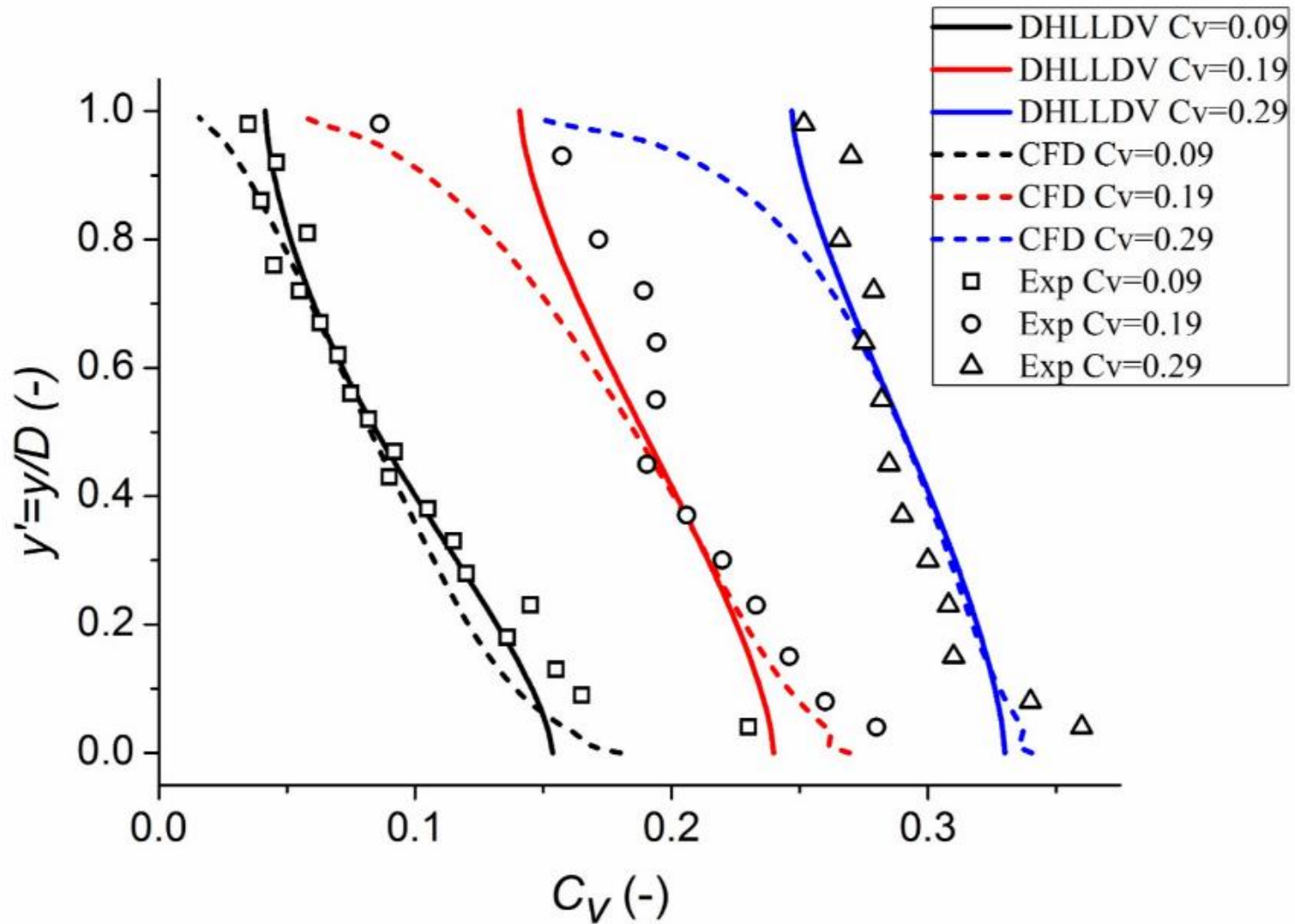
Experiments Roco & Shook (1983)



Roco & Shook (1983), $C_{vb}=0.60$, $D_p=0.0515$ m, $d=0.165$ mm, $v_{ls}=3.78-4.33$ m/s, Sand



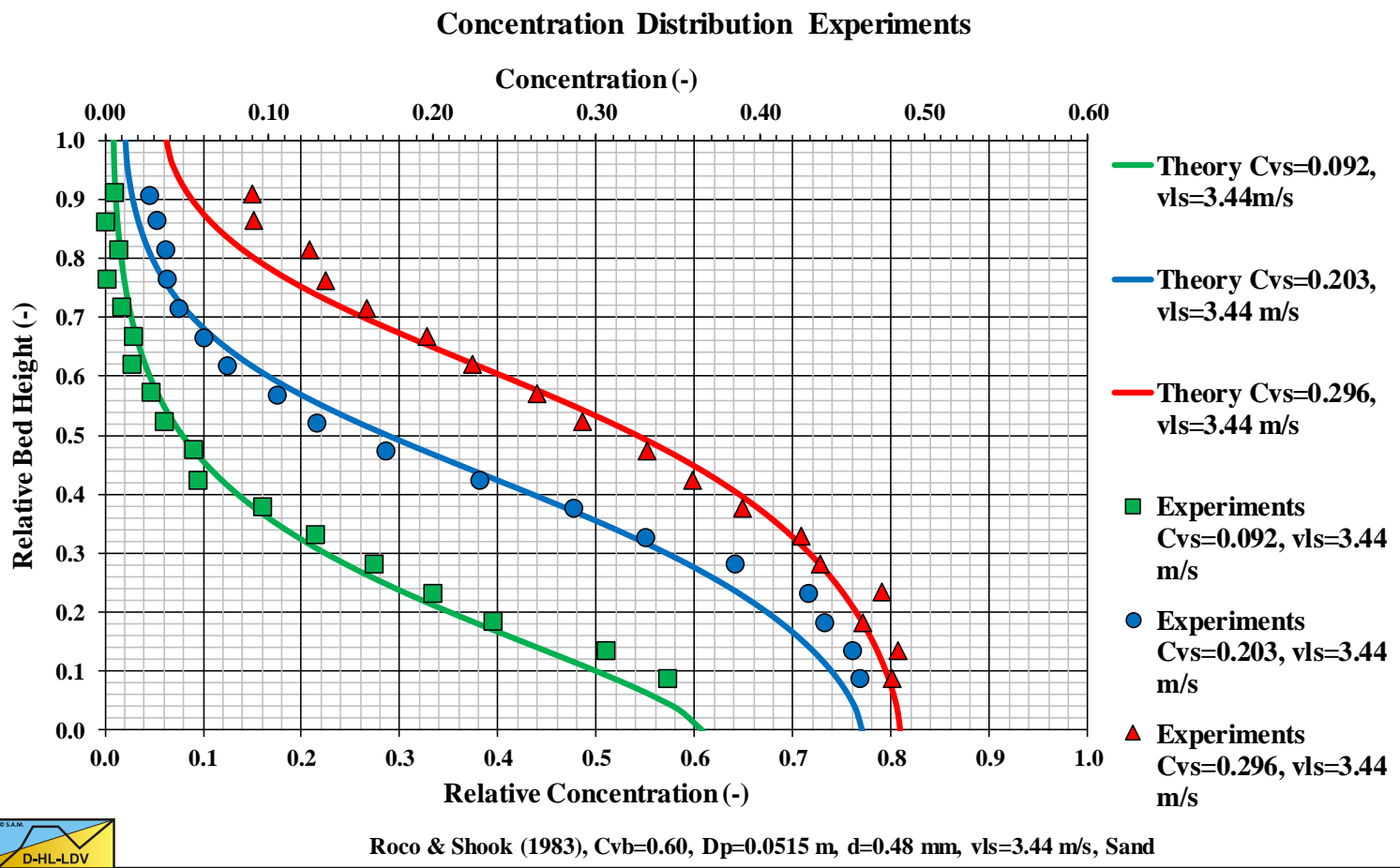
Experiments Roco & Shook (1983)



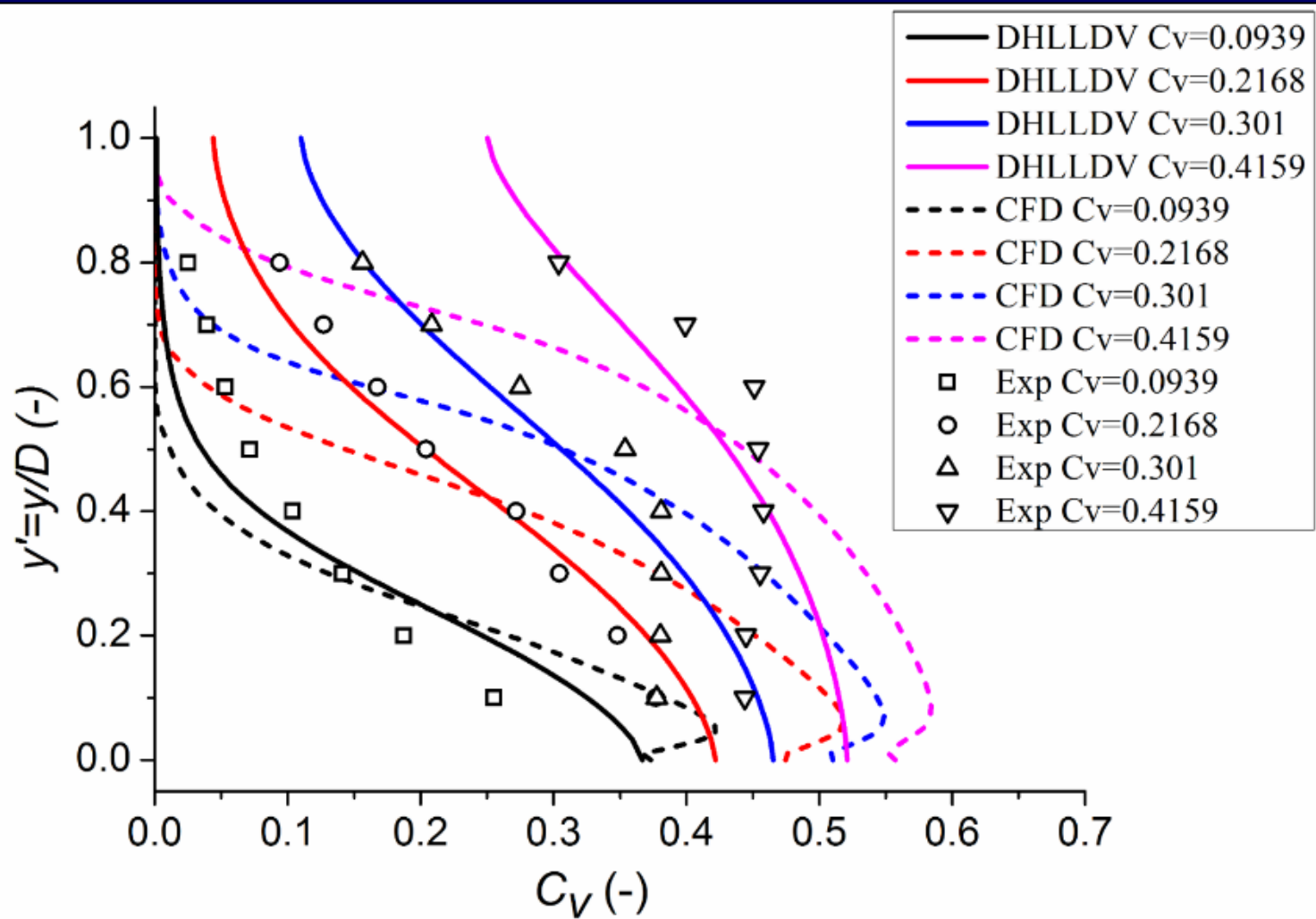
Roco & Shook (1983) $d=165\mu\text{m}$, $D=51.5\text{mm}$, $V=3.78\text{-}4.33\text{m/s}$.
 Delft University of Technology – Offshore & Dredging Engineering



Experiments Roco & Shook (1983)



Experiments Kaushal & Tomita (2002)



Kaushal & Tomita (2002B) $d=440\mu\text{m}$, $D=54.9\text{mm}$, $V=3\text{m/s}$.

Delft University of Technology – Offshore & Dredging Engineering



Conclusions

- The concentration distribution using a diffusivity based on the Limit Deposit Velocity gives good results.
- However, the hindered settling equation has to be modified in order to have zero settling velocity at the bed concentration.
- Local hindered settling has to be applied.
- The vertical coordinate has to be replaced by the bed fraction in order to find the correct cross sectional averaged volumetric concentration.
- An additional velocity ratio has to be added.



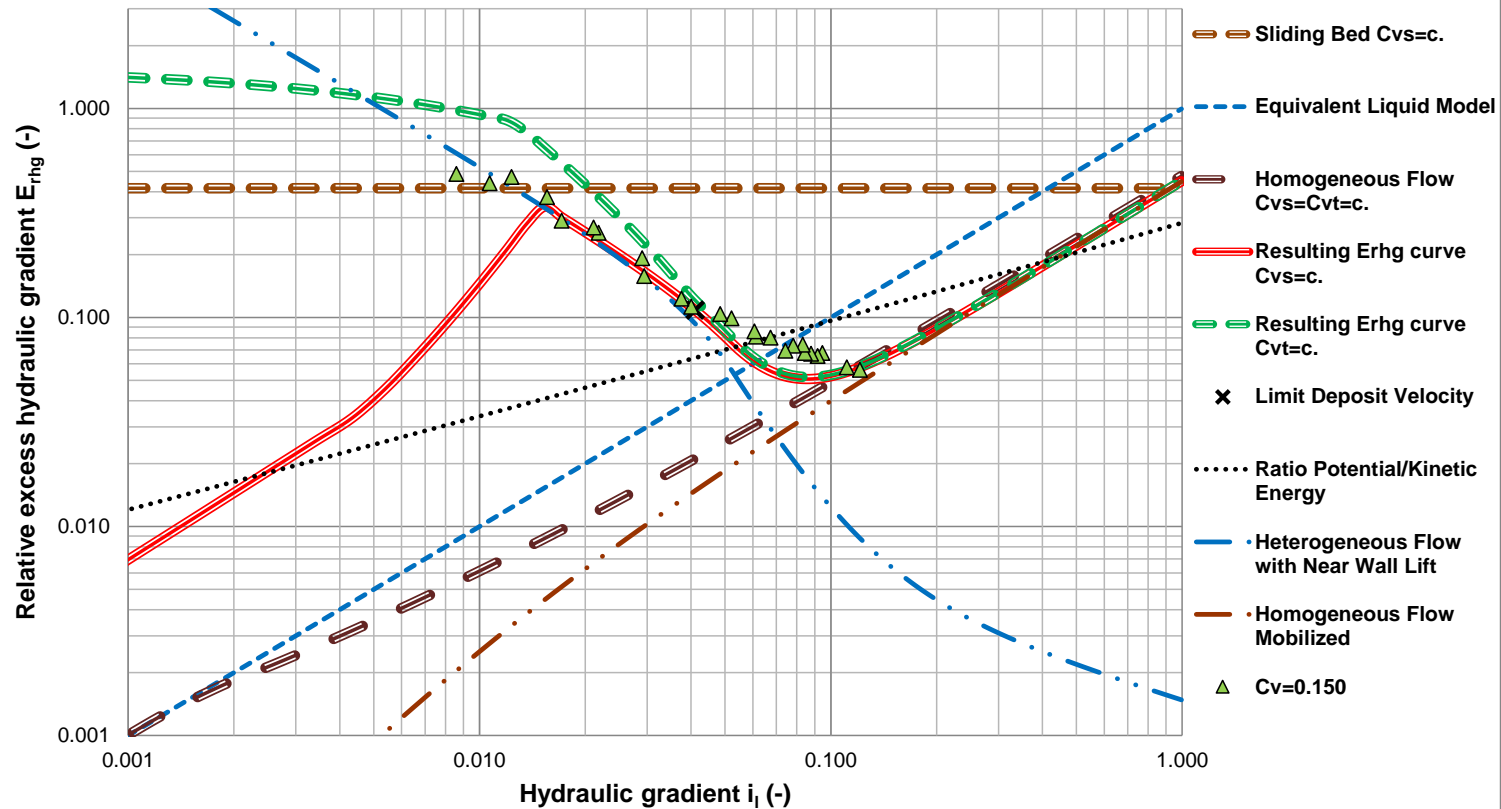


Transition Heterogeneous-Homogeneous Chapter 7.11 & 8.7



Small Diameter Pipe

Relative excess hydraulic gradient E_{rhg} vs. Hydraulic gradient i_1



$D_p=0.2032$ m, $d=0.420$ mm, $R_{sd}=1.585$, $C_v=0.150$, $\mu_{sf}=0.416$

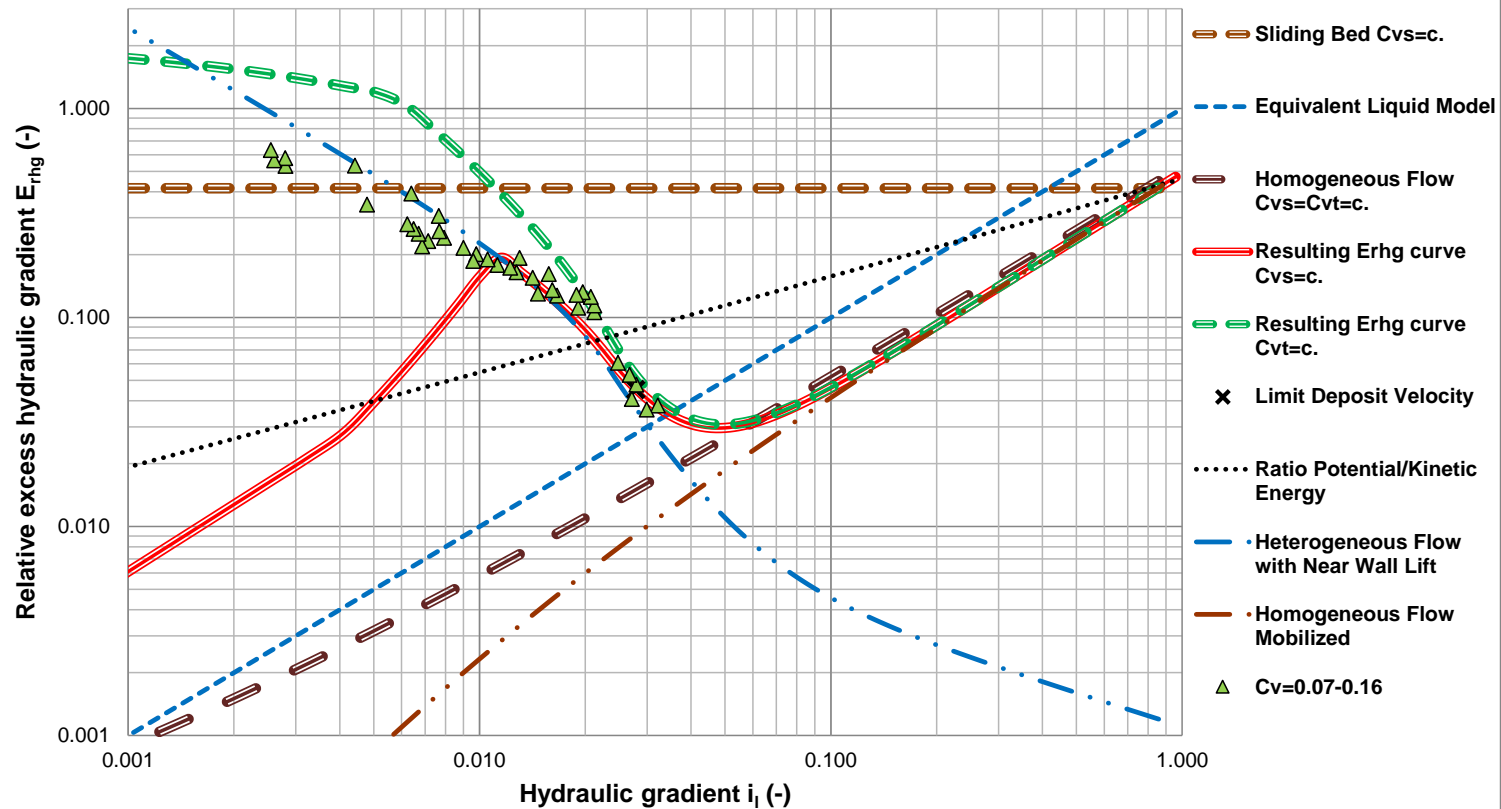
Clift et al. (1982) in a 0.2082 m diameter pipe
and a 0.42 mm particle

Delft University of Technology – Offshore & Dredging Engineering



Large Diameter Pipe

Relative excess hydraulic gradient E_{rhg} vs. Hydraulic gradient i_i



$D_p=0.4400$ m, $d=0.420$ mm, $Rsd=1.585$, $Cv=0.110$, $\mu_{sf}=0.416$

Clift et al. (1982) in a 0.44 m diameter pipe
and a 0.42 mm particle

Delft University of Technology – Offshore & Dredging Engineering



The Lift Ratio

$$F_L = C_L \cdot \frac{1}{2} \cdot \rho_l \cdot u_*^2 \cdot \frac{\pi}{4} \cdot d^2$$

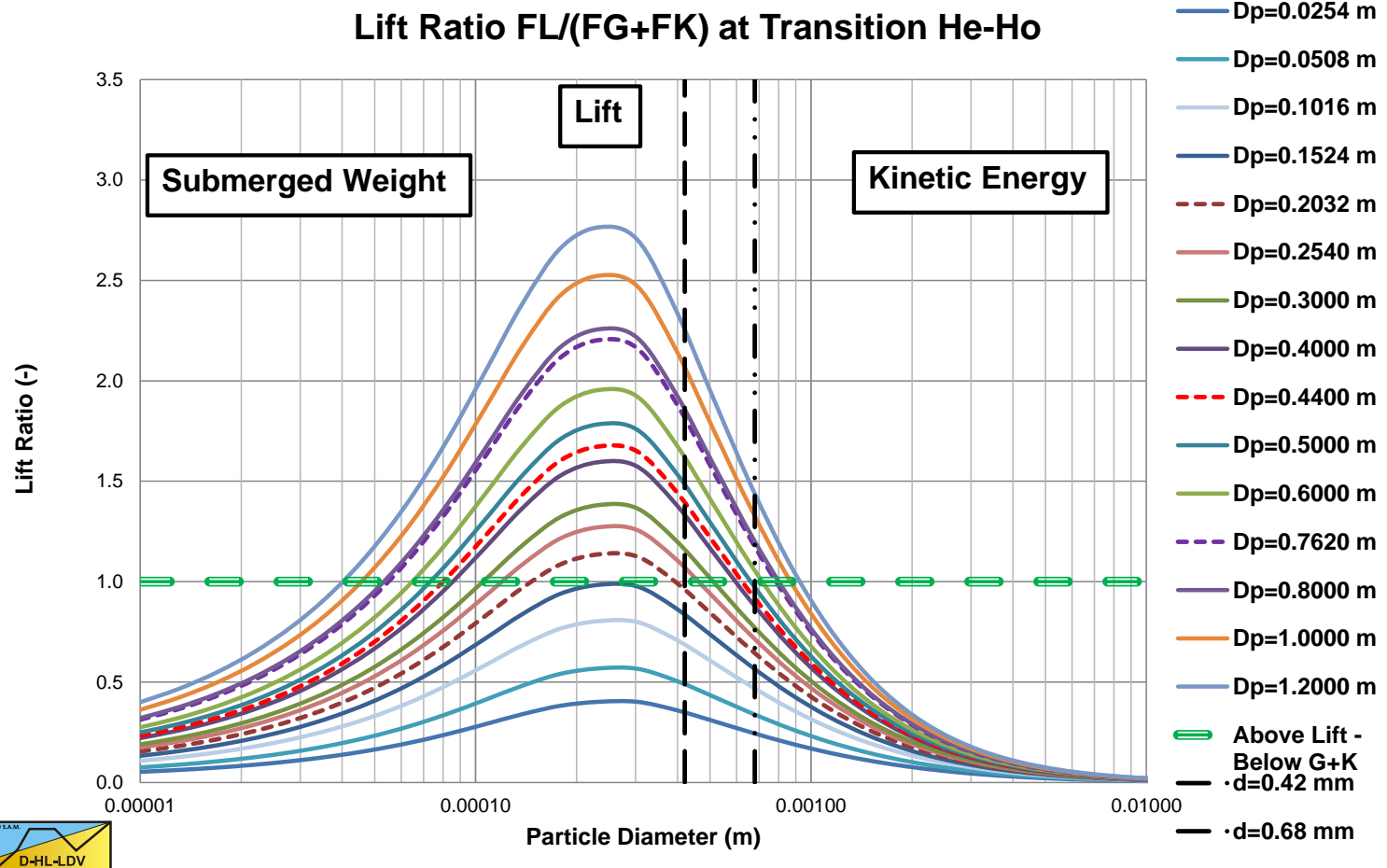
$$F_G = (\rho_s - \rho_l) \cdot g \cdot \frac{\pi}{6} \cdot d^3 \cdot \psi$$

$$F_K = \frac{1}{2} \cdot m_p \cdot \frac{v_{th}^2}{x} = \frac{1}{2} \cdot \rho_s \cdot \frac{\pi}{6} \cdot d^3 \cdot \psi \cdot \frac{v_{th}^2}{x} = \frac{E_K}{x}$$

$$L_R \frac{F_L}{F_G + F_K} = \frac{C_L \cdot u_*^2}{d \cdot \left(R_{sd} \cdot g + \frac{1}{2} \cdot \frac{\rho_s}{\rho_l} \cdot \frac{v_{th}^2 \cdot u_*}{\alpha \cdot 11.6 \cdot v_l} \right)} \cdot \left(1 - \frac{C_{vs}}{C_{vb}} \right)$$



Lift Ratio at He=Ho



The Collapse of Heterogeneous Flow

$$L_R < 0.5$$

$$E_{rhg} = \frac{v_t \cdot \left(1 - \frac{C_{vs}}{0.175 \cdot (1 + \beta)}\right)^\beta}{v_{ls}} + 8.5^2 \cdot \left(\frac{1}{\lambda_1}\right) \cdot \left(\frac{v_t}{\sqrt{g \cdot d}}\right)^{10/3} \cdot \left(\frac{(v_1 \cdot g)^{1/3}}{v_{ls}}\right)^2 \cdot (1 - L_R^2)$$

$$L_R \geq 0.5$$

$$E_{rhg} = \frac{v_t \cdot \left(1 - \frac{C_{vs}}{0.175 \cdot (1 + \beta)}\right)^\beta}{v_{ls}} + 8.5^2 \cdot \left(\frac{1}{\lambda_1}\right) \cdot \left(\frac{v_t}{\sqrt{g \cdot d}}\right)^{10/3} \cdot \left(\frac{(v_1 \cdot g)^{1/3}}{v_{ls}}\right)^2 \cdot (1 - \zeta) \cdot \frac{\zeta}{L_R^2}$$



Mobilization of Homogeneous Flow

$$C_{vs}(r) = C_{vB} \cdot e^{-\frac{\alpha_{sm} \cdot u_{*,ldv} \cdot v_{th}}{C_{vr} \cdot u_* \cdot v_{th,ldv}} \cdot \frac{r}{D_p}} \quad \text{with:} \quad \alpha_{sm} = 1.0046 + 0.1727 \cdot C_{vr} - 1.1905 \cdot C_{vr}^2$$

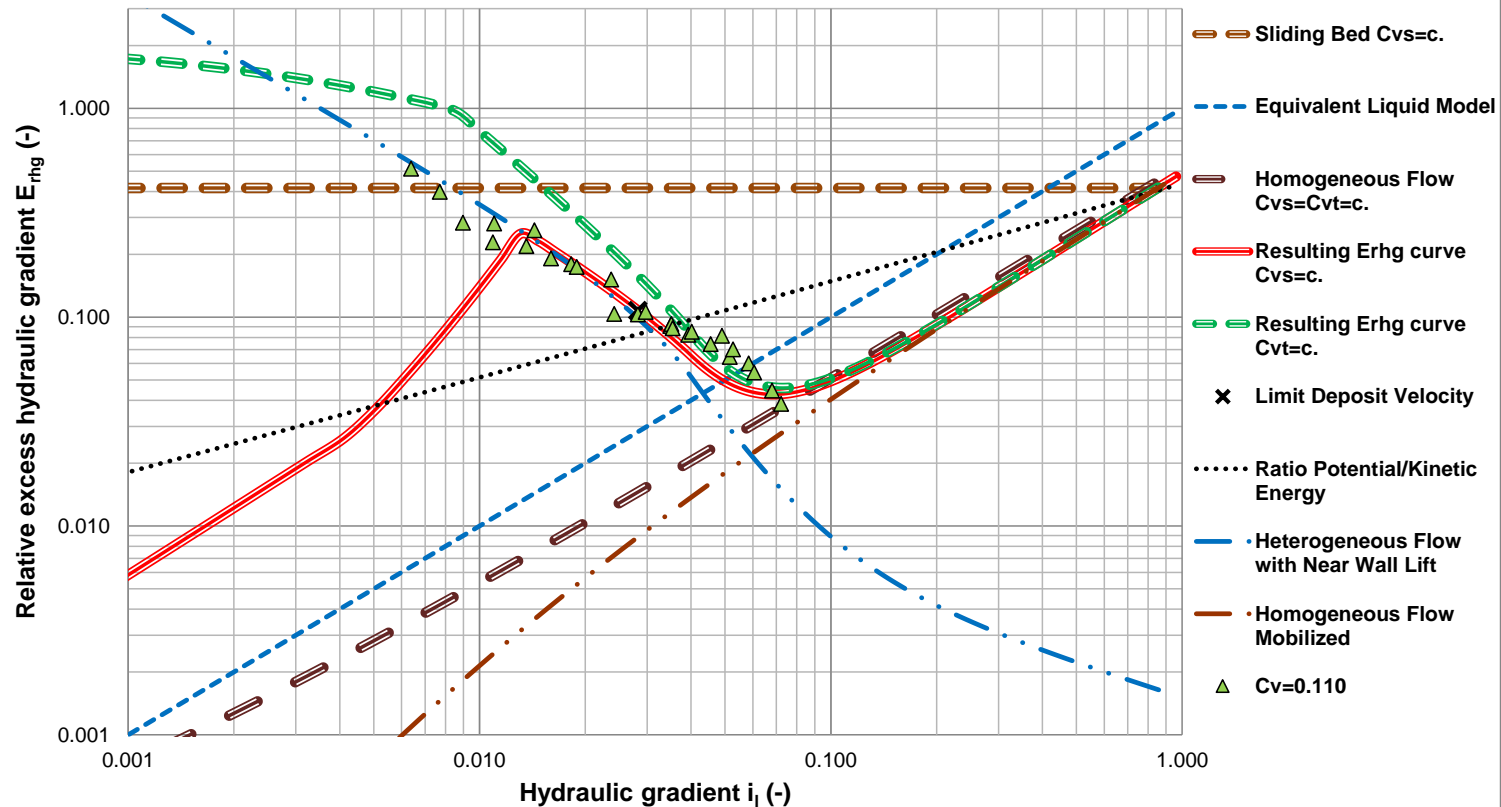
$$m = \frac{C_{vs}(r_2)}{C_{vs}(r_1)} = \frac{e^{-\frac{\alpha_{sm} \cdot u_{*,ldv} \cdot v_{th}}{C_{vr} \cdot u_* \cdot v_{th,ldv}} \cdot 0.55}}{e^{-\frac{\alpha_{sm} \cdot u_{*,ldv} \cdot v_{th}}{C_{vr} \cdot u_* \cdot v_{th,ldv}} \cdot 0.45}} = e^{-0.1 \cdot \frac{\alpha_{sm} \cdot u_{*,ldv} \cdot v_{th}}{C_{vr} \cdot u_* \cdot v_{th,ldv}}}$$

$$E_{rhg} = \frac{i_m - i_l}{R_{sd} \cdot C_{vs}} = m \cdot i_l \cdot \left(1 - \frac{1 + R_{sd} \cdot C_{vs} - \left(\frac{A_{C_v}}{\kappa} \cdot \ln \left(\frac{\rho_m}{\rho_l} \right) \cdot \sqrt{\frac{\lambda_l}{8} + 1} \right)^2}{R_{sd} \cdot C_{vs} \cdot \left(\frac{A_{C_v}}{\kappa} \cdot \ln \left(\frac{\rho_m}{\rho_l} \right) \cdot \sqrt{\frac{\lambda_l}{8} + 1} \right)^2} \right) \left(1 - \left(\frac{\delta_v}{d} \right) \right)$$



Validation

Relative excess hydraulic gradient E_{rhg} vs. Hydraulic gradient i_1



$D_p=0.4900$ m, $d=0.600$ mm, $Rsd=1.780$, $Cv=0.110$, $\mu_{sf}=0.416$

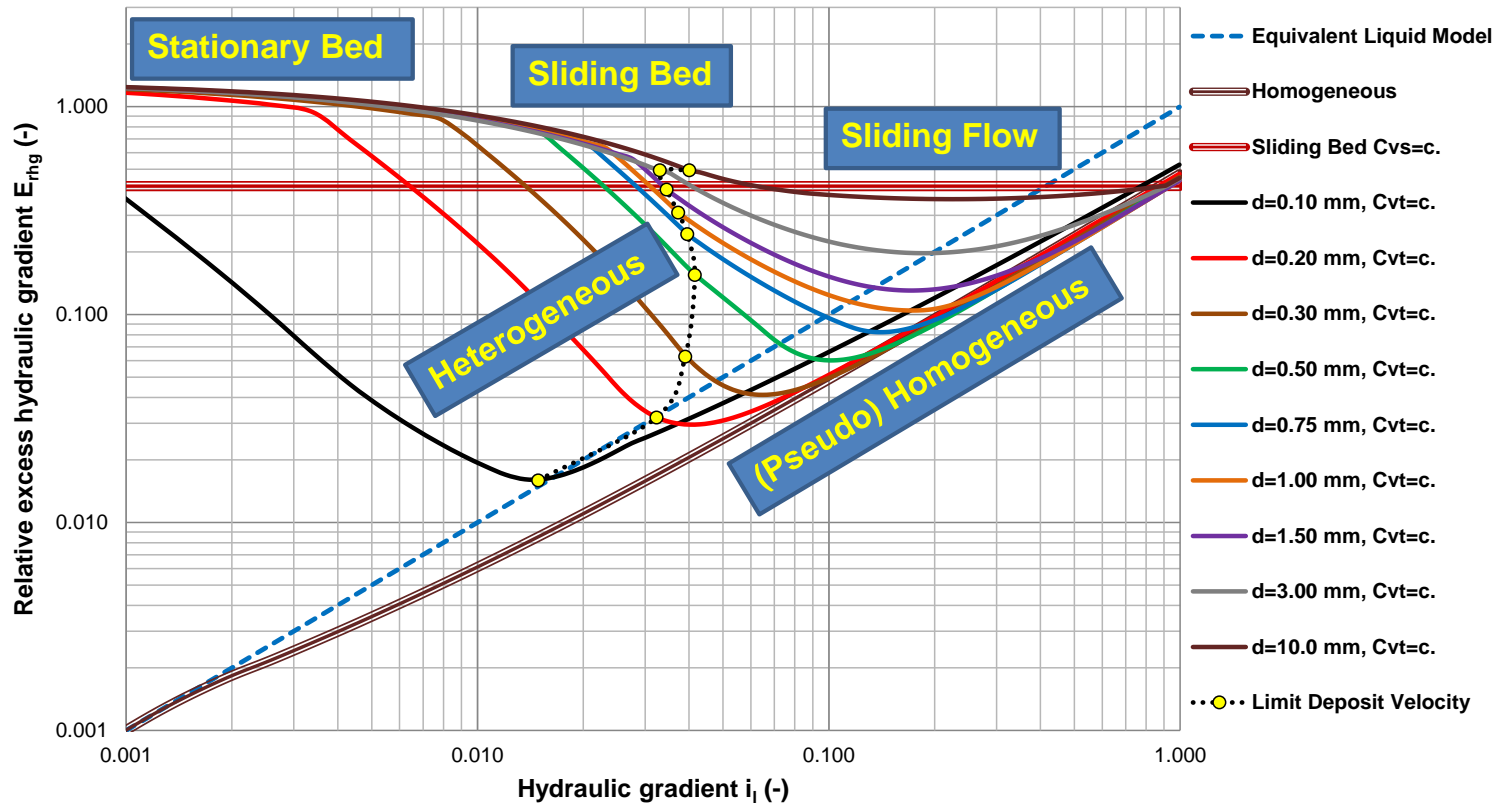
Clift et al. (1982) in a 0.49 m diameter pipe
and a 0.60 mm particle

Delft University of Technology – Offshore & Dredging Engineering



Small Diameter Pipe ($D_p=0.20$ m)

Relative excess hydraulic gradient E_{rhg} vs. Hydraulic gradient i_1

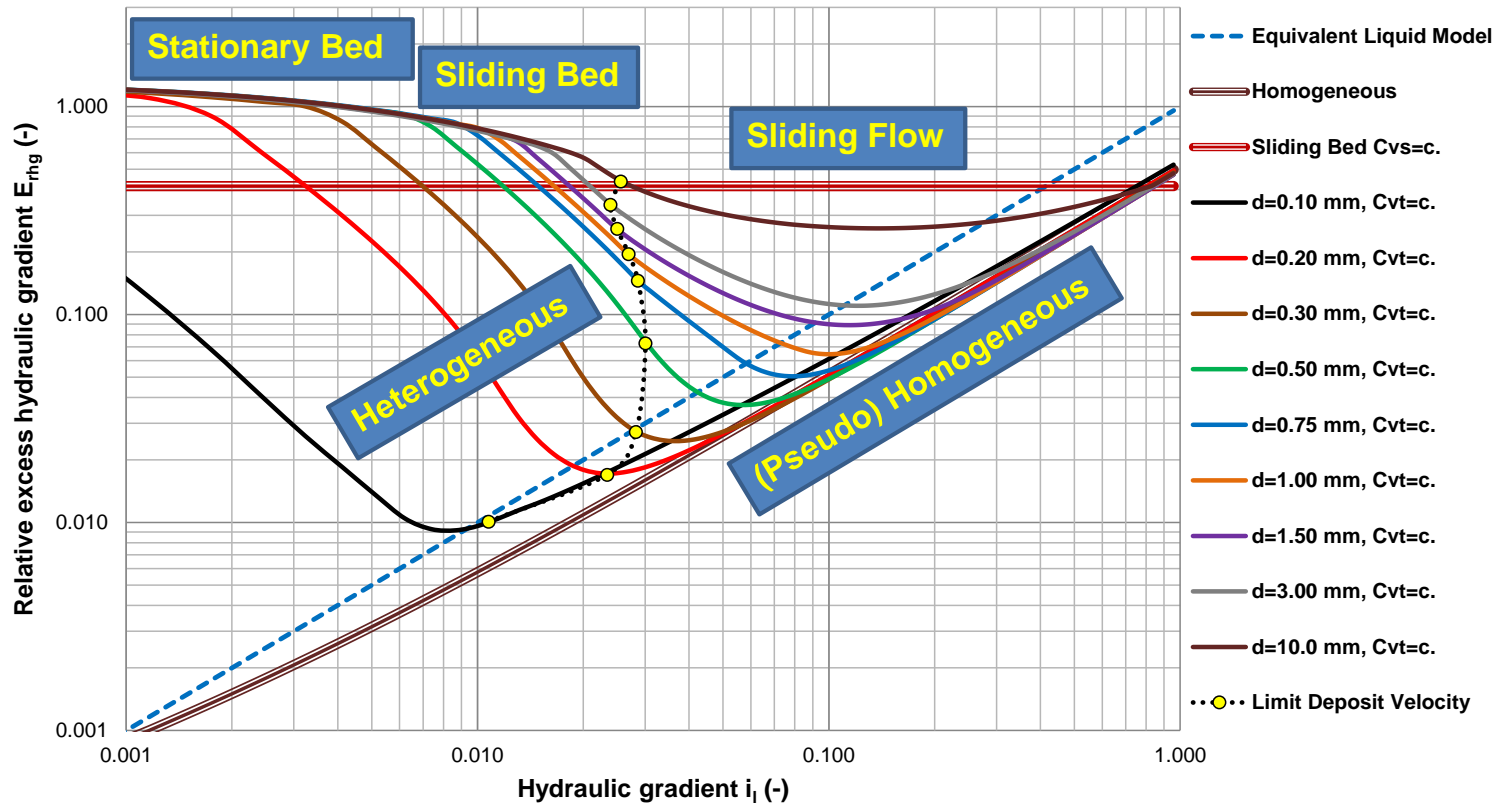


$D_p=0.2032$ m, $Rsd=1.585$, $Cvt=0.175$, $\mu_{sf}=0.416$



Large Diameter Pipe ($D_p=0.44$ m)

Relative excess hydraulic gradient E_{rhg} vs. Hydraulic gradient i_1



$D_p=0.4400$ m, $Rsd=1.585$, $Cvt=0.175$, $\mu sf=0.416$





Comparison Transition Line Speed Heterogeneous – Homogeneous

Chapter 9

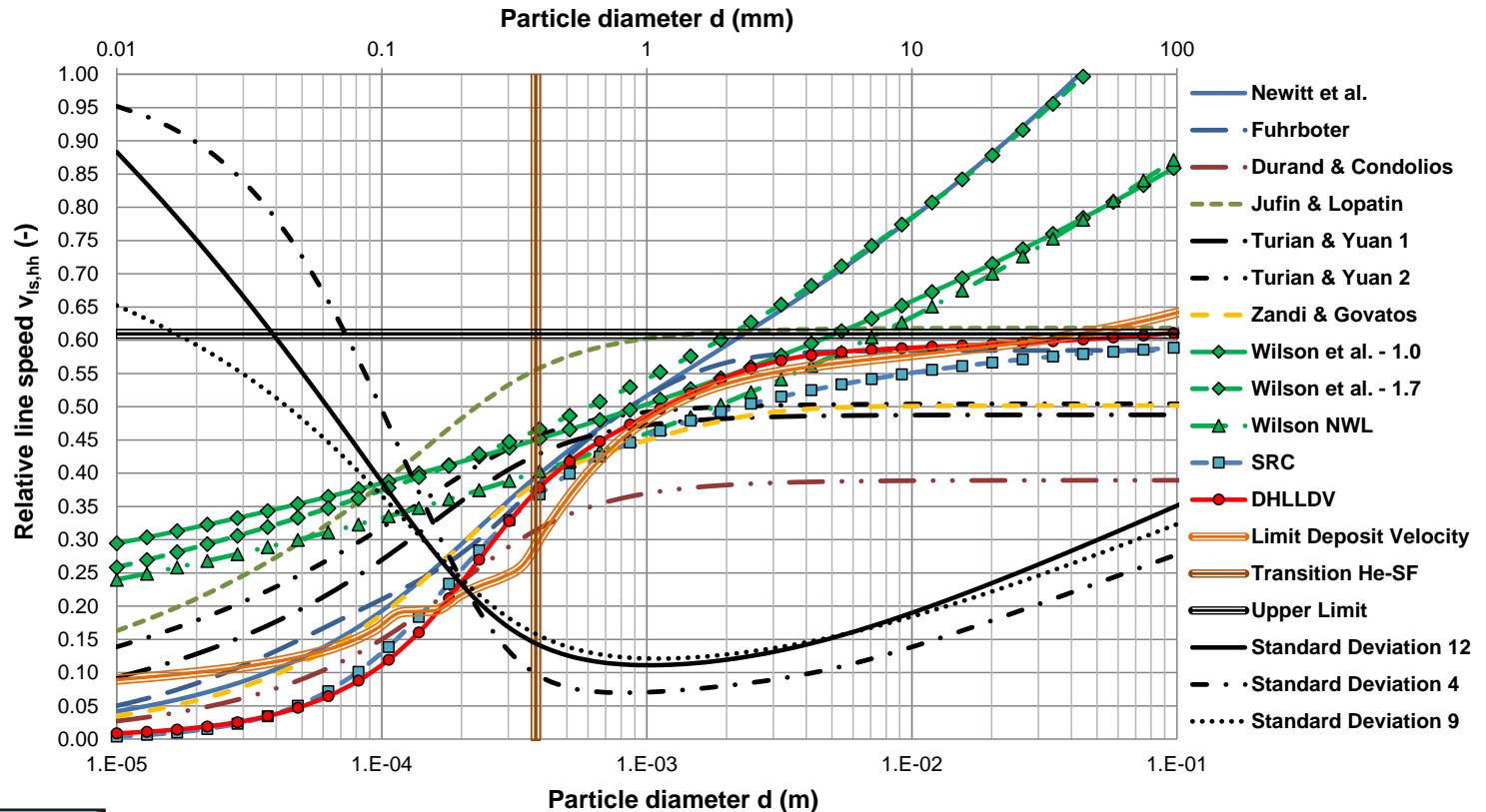


Relative transition line speed $v_{ls,hh}$

$D_p=0.0254$ m



Transition Heterogeneous - Homogeneous



$D_p=0.0254$ m, $Rsd=1.59$, $Cvs=0.300$, $\mu sf=0.416$

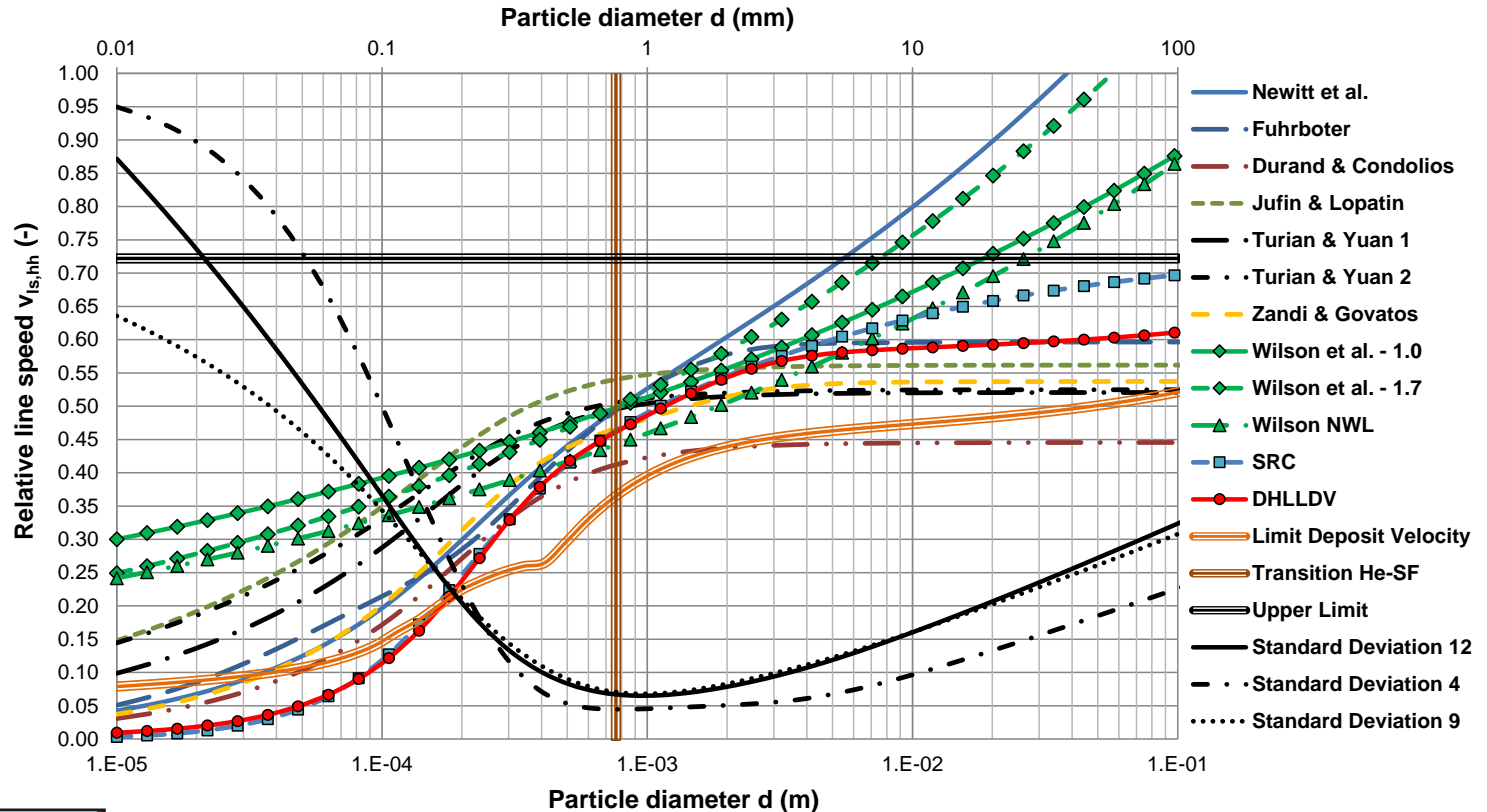
$v_{ls,hh,max}=5.3$ m/sec



Relative transition line speed $v_{ls,hh}$ $D_p = 0.0508 \text{ m}$



Transition Heterogeneous - Homogeneous



$D_p = 0.0508 \text{ m}$, $R_{sd} = 1.59$, $C_{vs} = 0.300$, $\mu_{sf} = 0.416$

$v_{ls,hh,max} = 7.0 \text{ m/sec}$

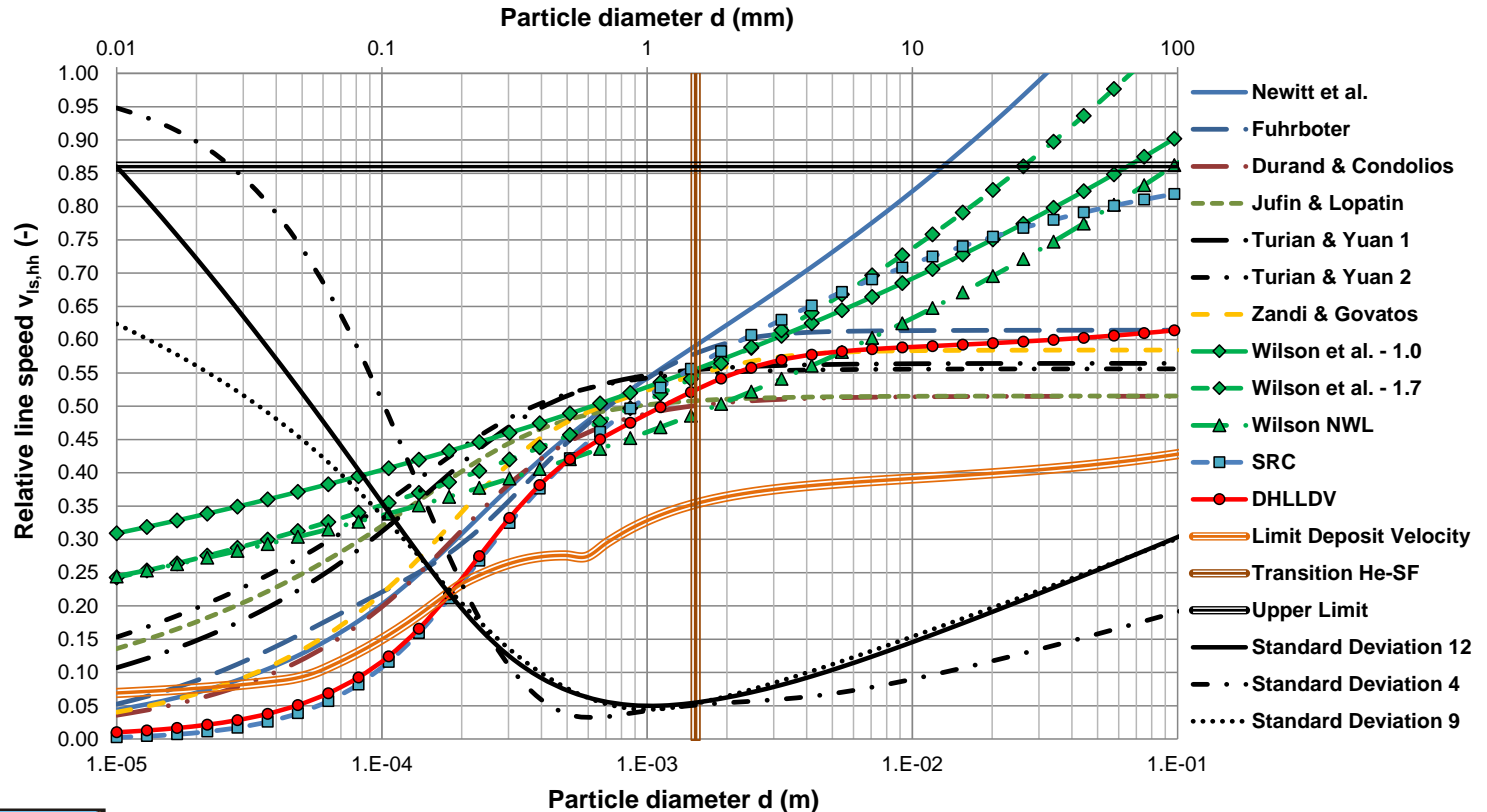


Relative transition line speed $v_{ls,hh}$

$D_p=0.1016$ m



Transition Heterogeneous - Homogeneous



$D_p=0.1016$ m, $Rsd=1.59$, $Cvs=0.300$, $\mu sf=0.416$

$v_{ls,hh,max}=9.1$ m/sec

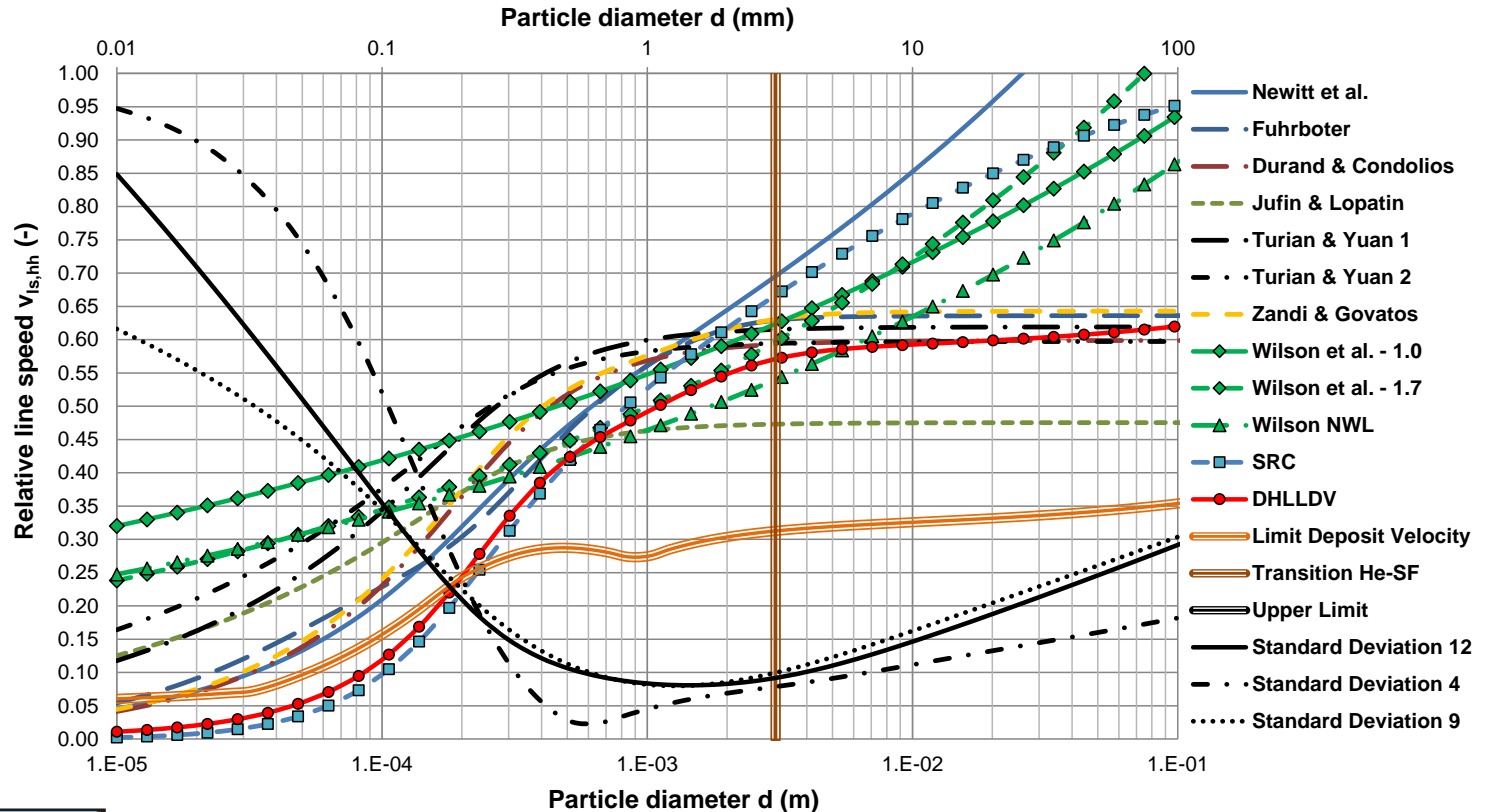


Relative transition line speed $v_{ls,hh}$

$D_p=0.2032$ m



Transition Heterogeneous - Homogeneous



$D_p=0.2032$ m, $Rsd=1.59$, $Cvs=0.300$, $\mu_{sf}=0.416$

$v_{ls,hh,max}=11.7$ m/sec

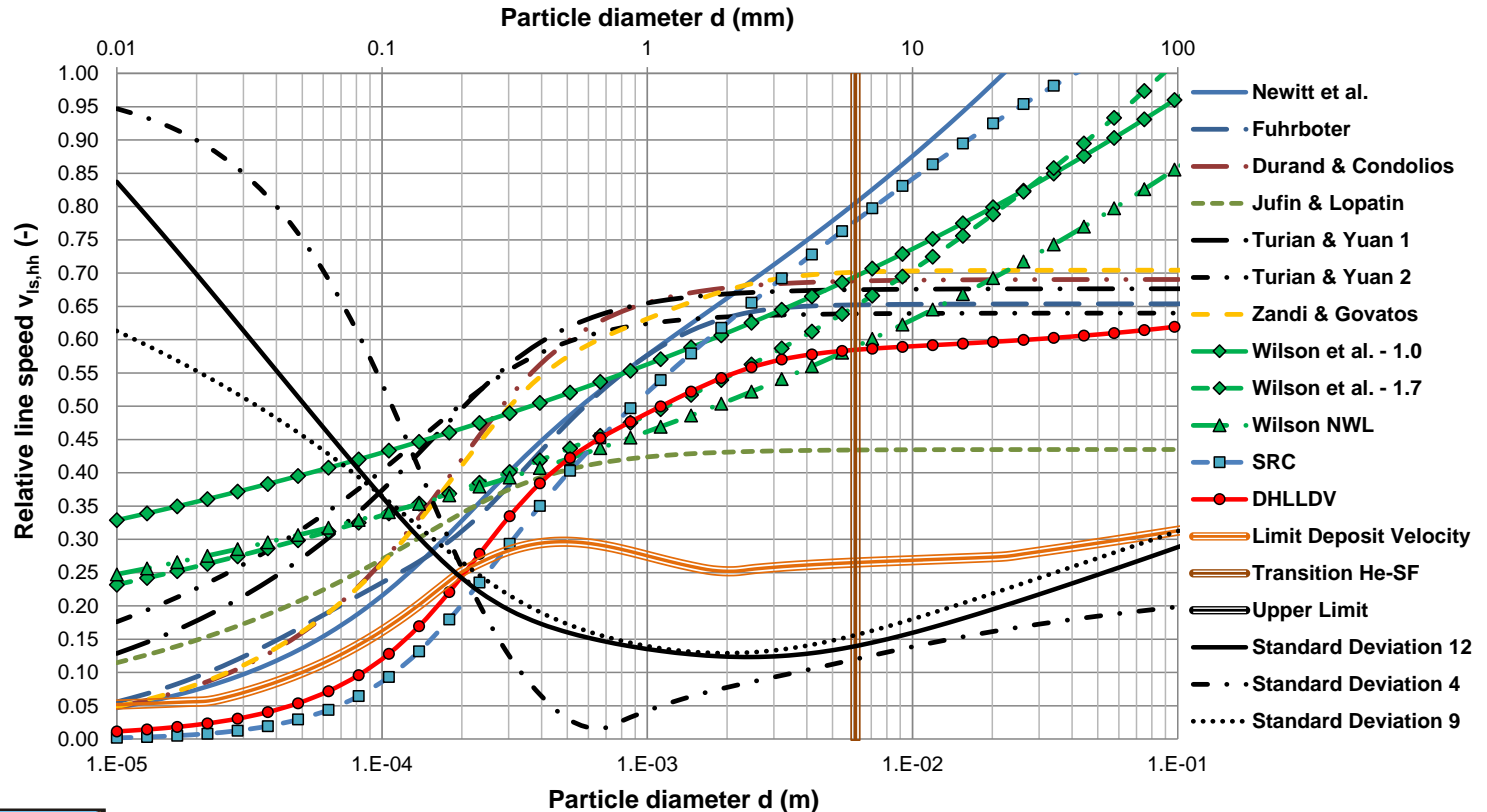


Relative transition line speed $v_{ls,hh}$

$D_p=0.4064$ m



Transition Heterogeneous - Homogeneous



$D_p=0.4064$ m, $Rsd=1.59$, $Cvs=0.300$, $\mu sf=0.416$

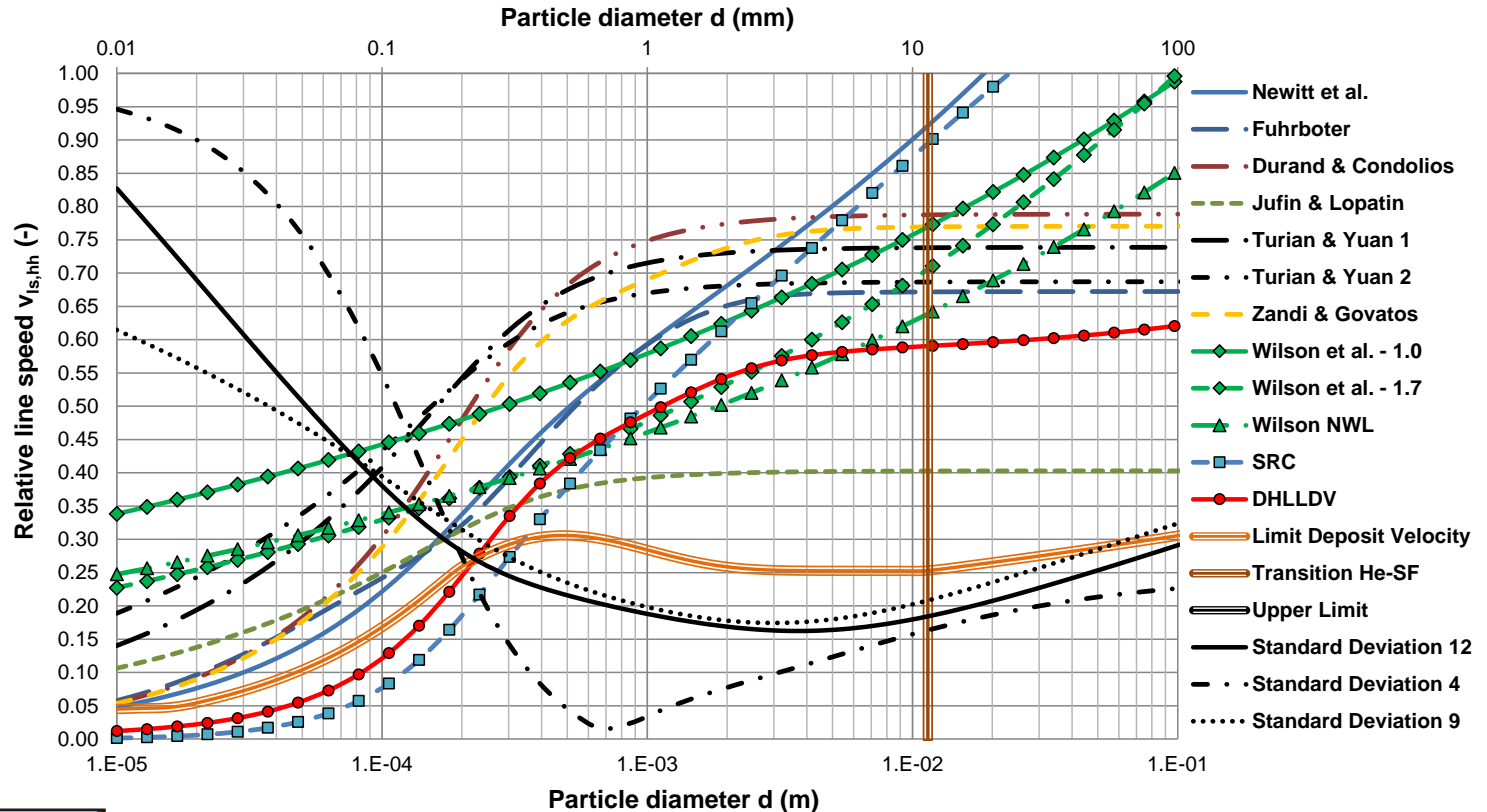
$v_{ls,hh,max}=15.1$ m/sec



Relative transition line speed $v_{ls,hh}$ $D_p=0.7620$ m



Transition Heterogeneous - Homogeneous



$D_p=0.7620$ m, $Rsd=1.59$, $Cvs=0.300$, $\mu sf=0.416$

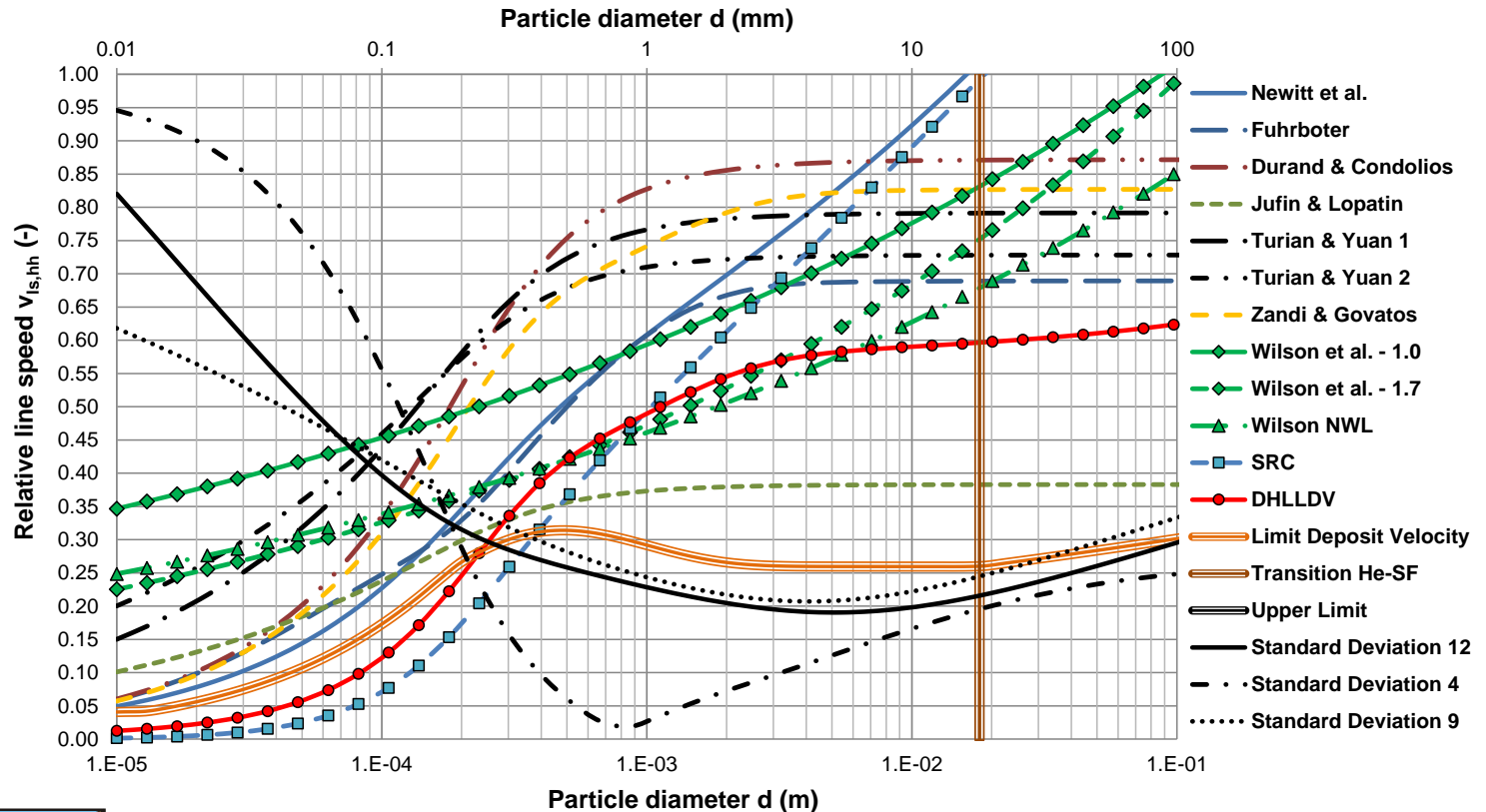
$v_{ls,hh,max}=18.9$ m/sec



Relative transition line speed $v_{ls,hh}$ $D_p=1.2000$ m



Transition Heterogeneous - Homogeneous



$D_p=1.2000$ m, $Rsd=1.59$, $Cvs=0.300$, $\mu sf=0.416$

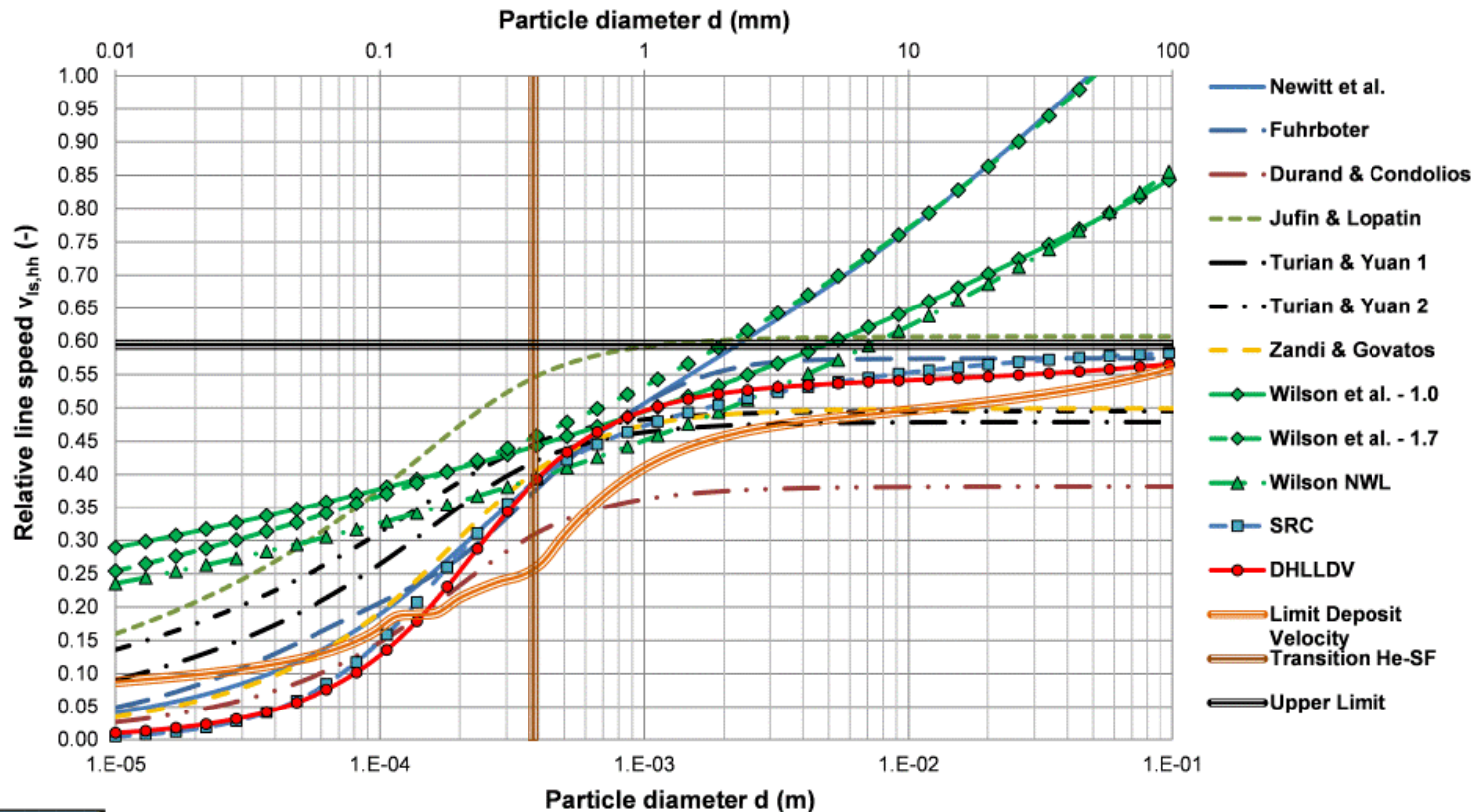
$v_{ls,hh,max}=22.1$ m/sec



Relative transition line speed, Animation



Transition Heterogeneous - Homogeneous

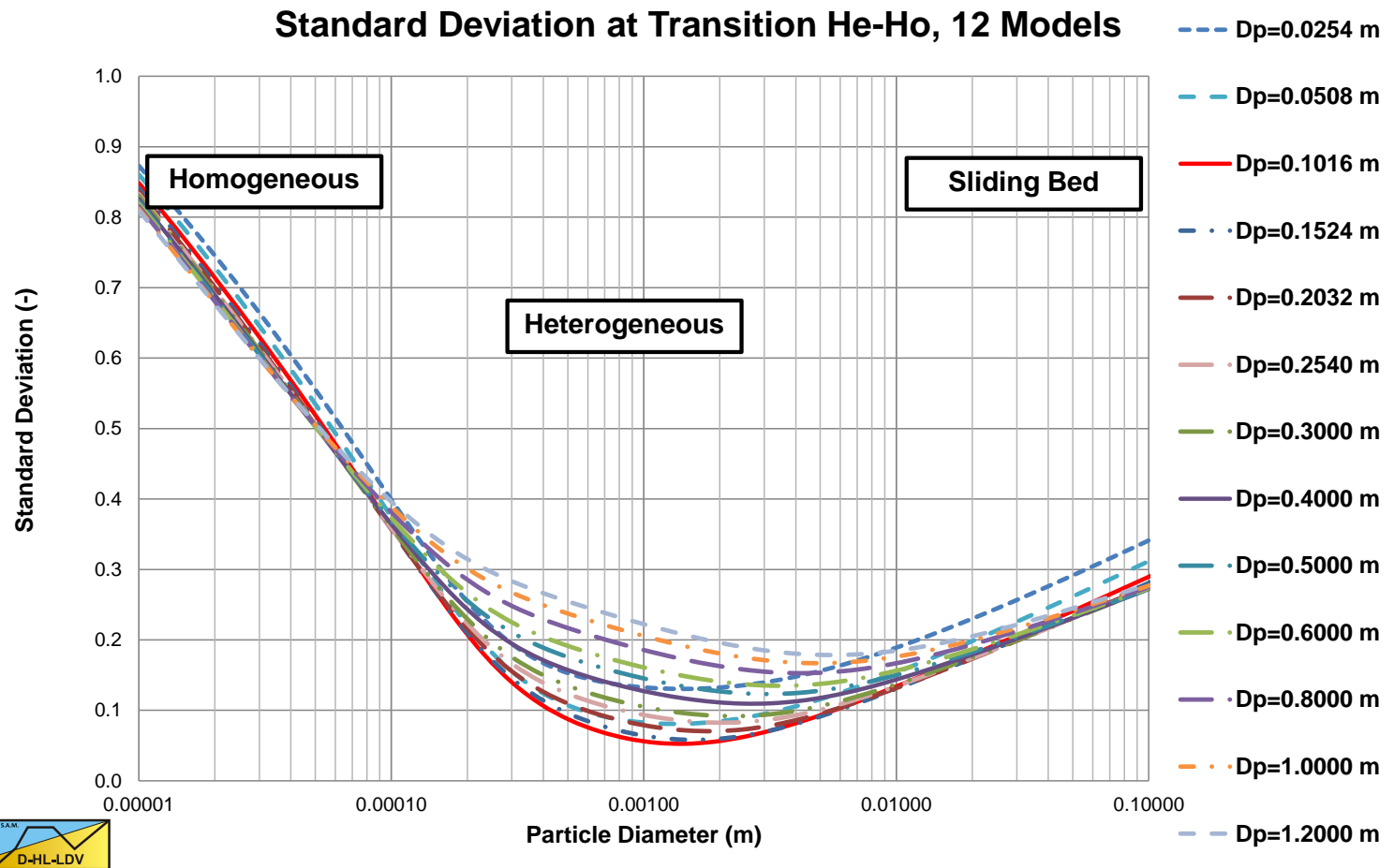


$D_p=0.0254$ m, $R_{sd}=1.59$, $C_{vs}=0.300$, $\mu_{sf}=0.416$

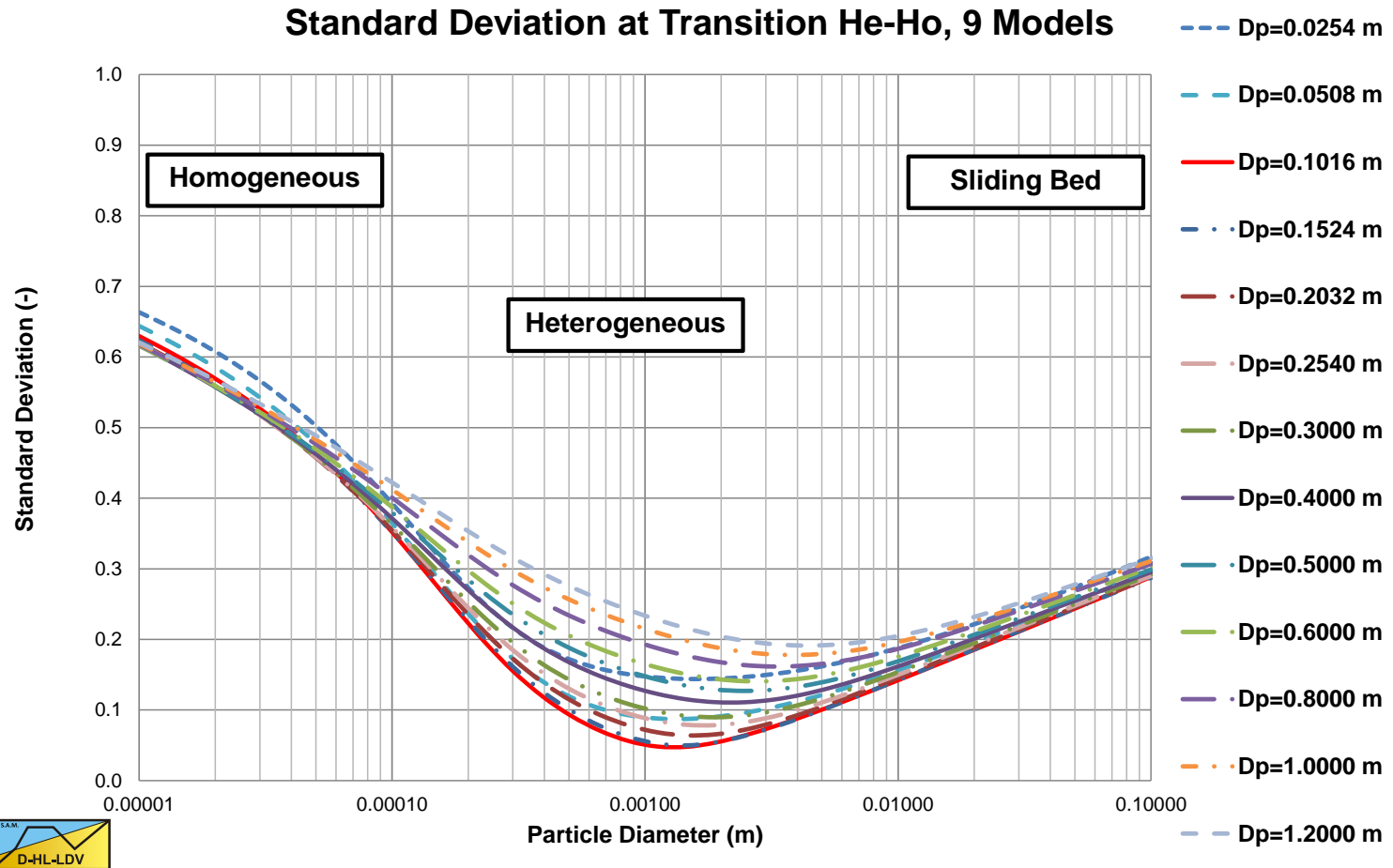
$v_{ls,hh,max}=5.4$ m/sec



Standard Deviation 12 Models



Standard Deviation 9 Models

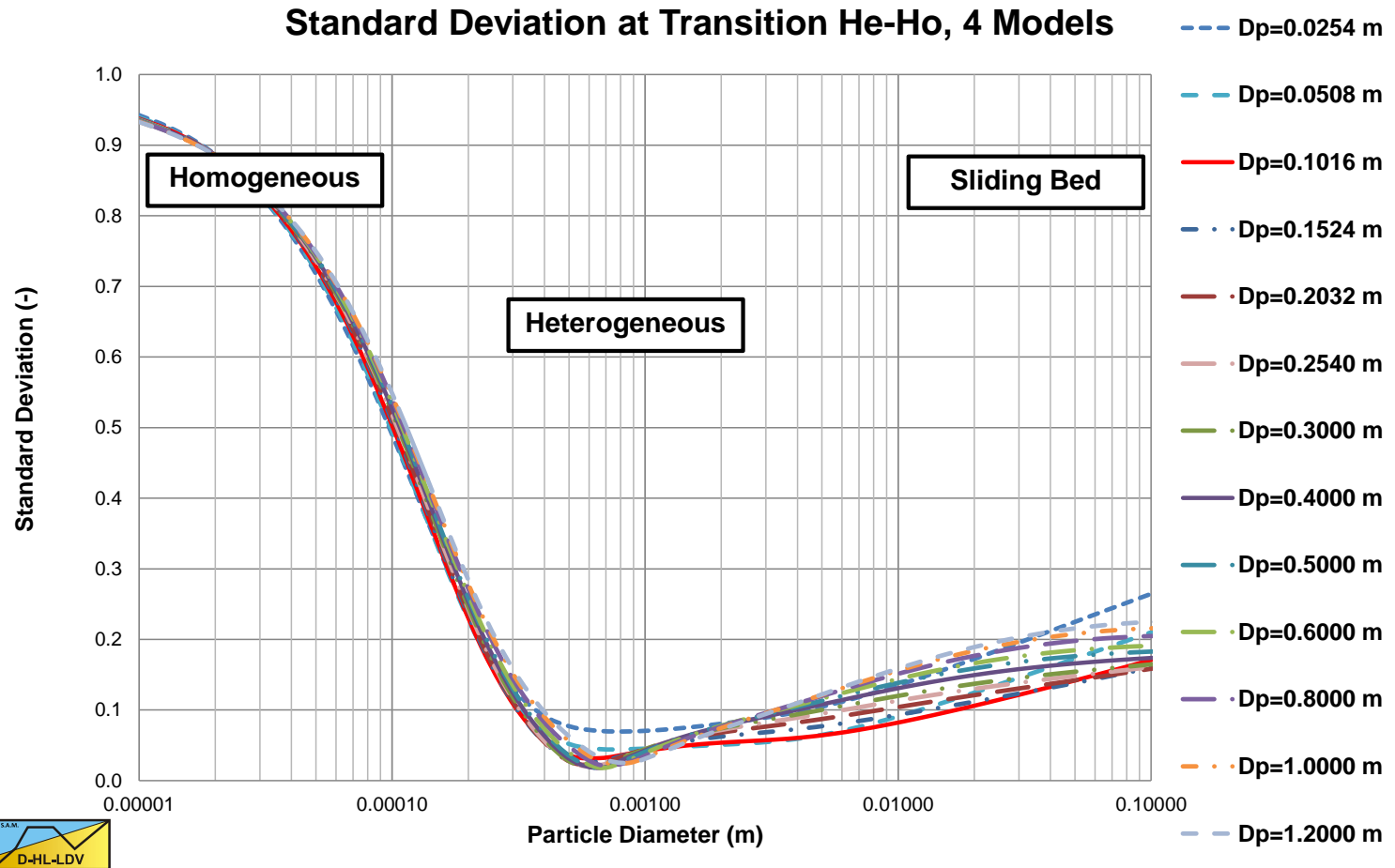


Wilson mixes homogeneous and heterogeneous for very small particles. So without Wilson we get:

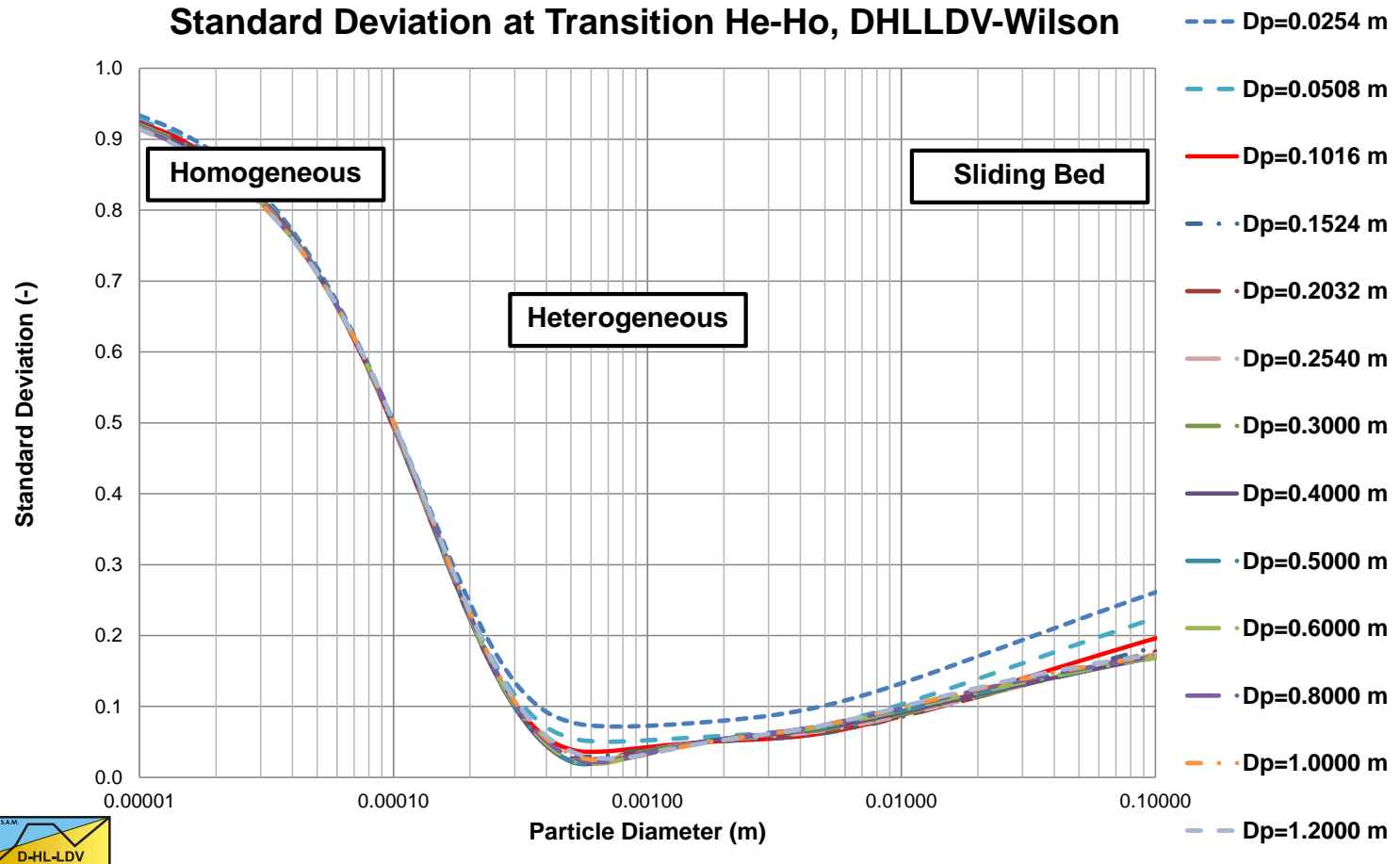
Delft University of Technology – Offshore & Dredging Engineering



Standard Deviation 4 Models



Standard Deviation DHLLDV-Wilson



Conclusions

- The transition line speed of the heterogeneous flow regime with the homogeneous flow regime is a good indicator for comparing different head loss models.
- For pipe diameters near 4-6 inch most models perform the same. For smaller and larger pipe diameters the different models deviate.
- Very small particles behave according to the homogeneous flow regime, while very large particles behave according to the sliding bed or sliding flow regime, where this method is not valid.
- Based on numerous experimental data, the Wilson et al., the SRC and the DHLLDV models are the most reliable over a wide range of pipe and particle diameters.





Bed Height

Chapter 7.12 & 8.12



Starting Points

- 0% bed at the LDV.
- 100% bed at zero line speed.
- The slip velocity or holdup function.
- The slip in the suspended phase above the bed is equal to the slip at the **LDV**.



Derivation Slip Ratio

$$\xi = \frac{v_{sl}}{v_{ls}}$$

$$C_{vt} = \left(1 - \frac{v_{sl}}{v_{ls}}\right) \cdot C_{vs} = (1 - \xi) \cdot C_{vs}$$

$$C_{vs} = \left(\frac{v_{ls}}{v_{ls} - v_{sl}}\right) \cdot C_{vt} = \left(\frac{1}{1 - \xi}\right) \cdot C_{vt}$$

$$\kappa = \left(\frac{1}{1 - \xi}\right)$$



The Bed Fraction Equation

$$C_{vs,s} = \kappa_{ldv} \cdot C_{vt} \quad \text{with: } \kappa_{ldv} = \left(\frac{v_{ls,ldv}}{v_{ls,ldv} - v_{sl,ldv}} \right) = \left(\frac{1}{1 - \xi_{ldv}} \right)$$

$$\zeta = \frac{A_b}{A_p} = \frac{(1 - \kappa_{ldv} \cdot (1 - \xi)) \cdot C_{vt}}{(C_{vb} - \kappa_{ldv} \cdot C_{vt}) \cdot (1 - \xi)}$$

At the LDV :

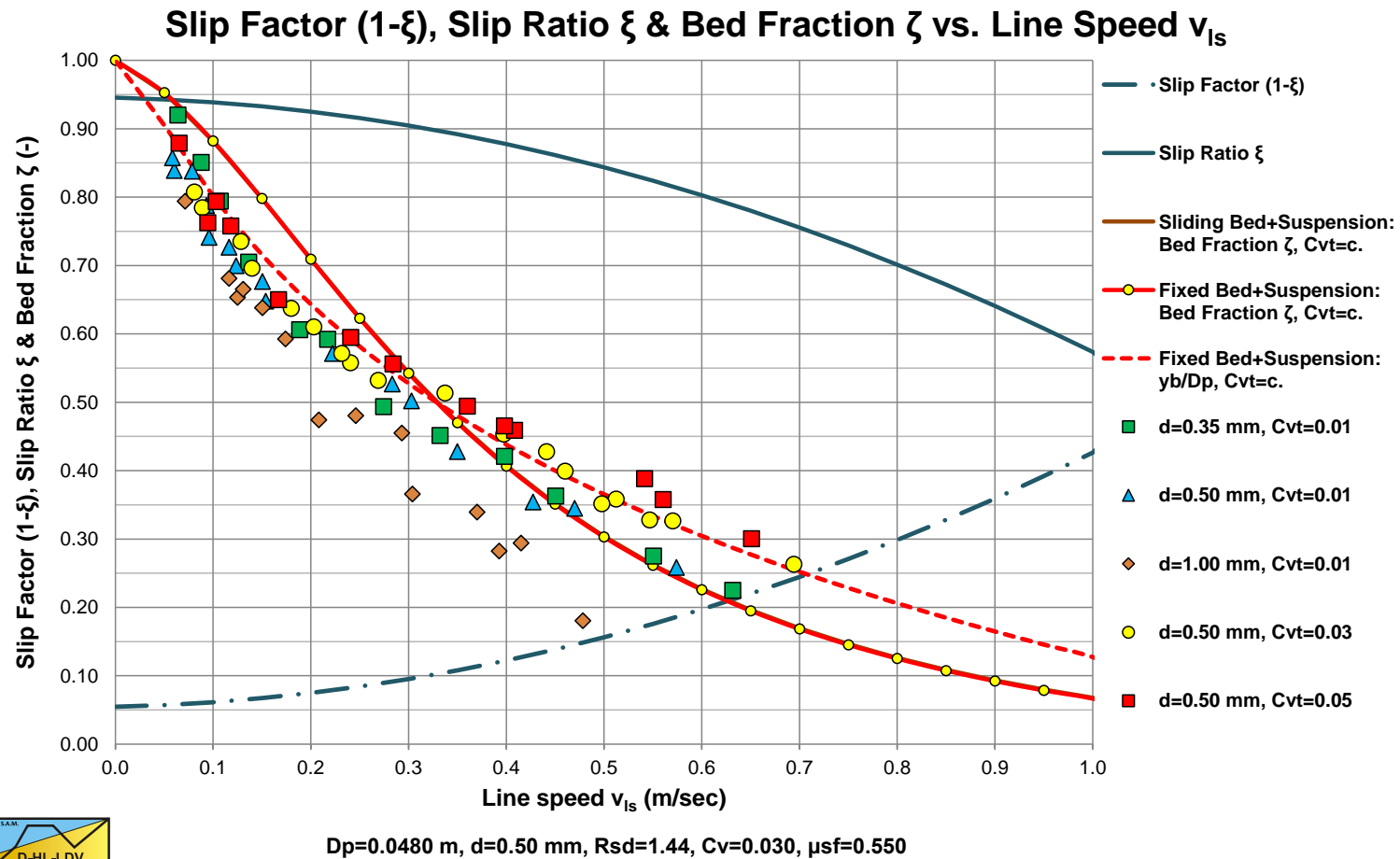
$$\zeta_{ldv} = \frac{A_b}{A_p} = \frac{(1 - \kappa_{ldv} \cdot (1 - \xi_{ldv})) \cdot C_{vt}}{(C_{vb} - \kappa_{ldv} \cdot C_{vt}) \cdot (1 - \xi_{ldv})} = \frac{0}{(C_{vb} - \kappa_{ldv} \cdot C_{vt}) \cdot (1 - \xi_{ldv})} = 0$$

At line speed zero : $\xi_0 = \frac{v_{sl}}{v_{ls}} = 1 - \frac{C_{vt}}{C_{vb}}$

$$\zeta_0 = \frac{A_b}{A_p} = \frac{(1 - \kappa_{ldv} \cdot (1 - \xi_0)) \cdot C_{vt}}{(C_{vb} - \kappa_{ldv} \cdot C_{vt}) \cdot (1 - \xi_0)} = \frac{\left(1 - \kappa_{ldv} \cdot \frac{C_{vt}}{C_{vb}}\right) \cdot C_{vt}}{\left(1 - \kappa_{ldv} \cdot \frac{C_{vt}}{C_{vb}}\right) \cdot C_{vt}} = 1$$



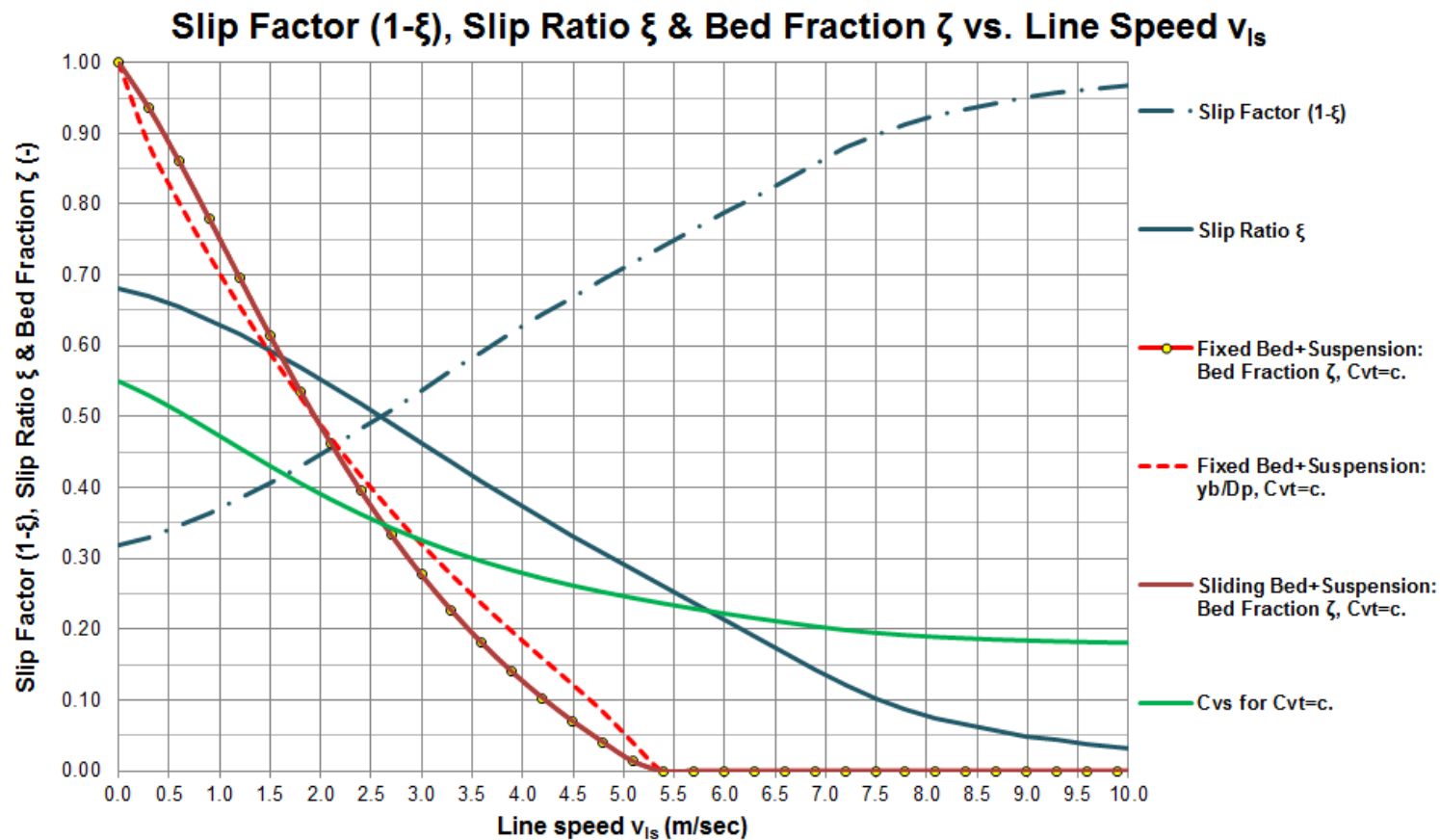
Validation



Harada et al. (1989)



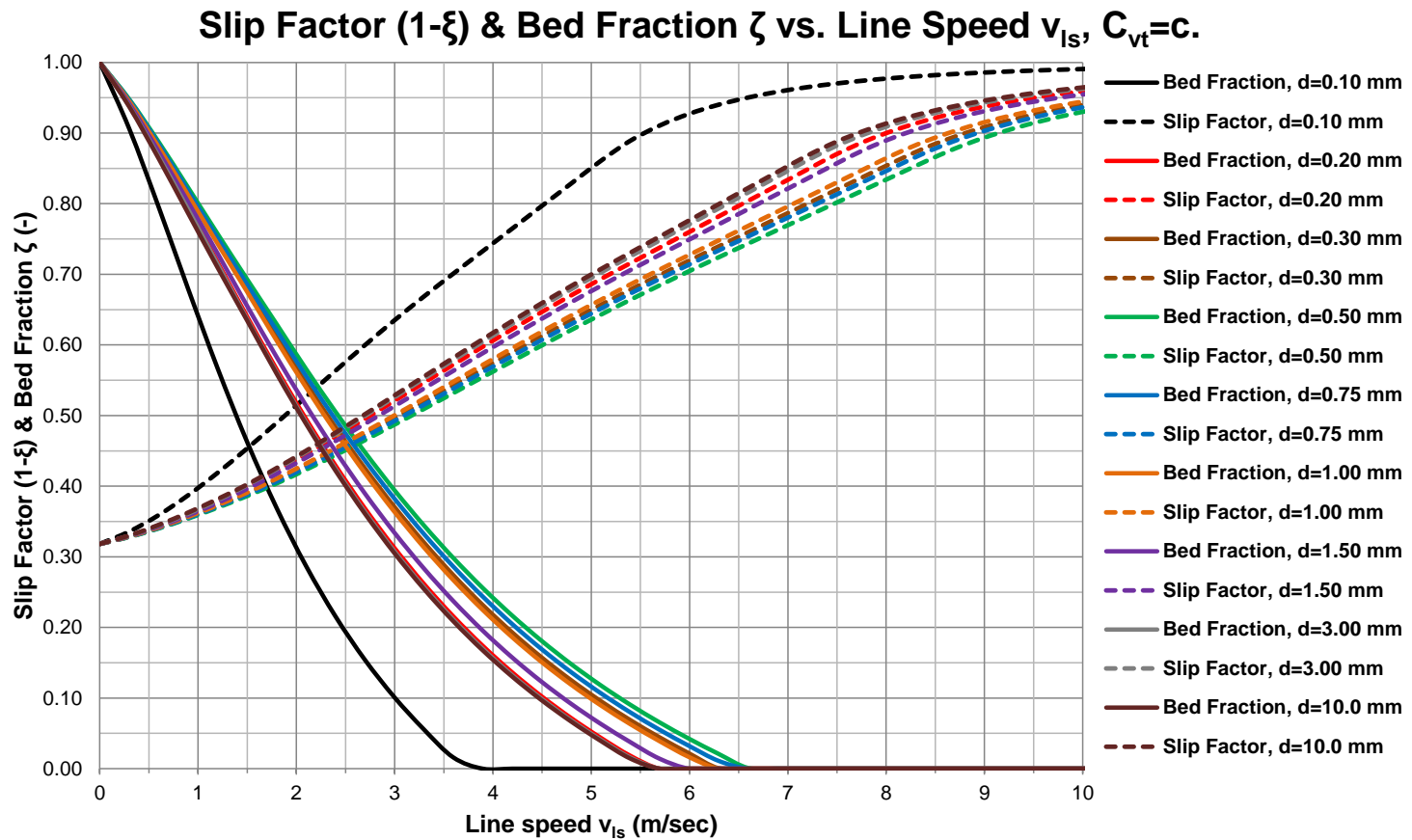
Some Results, 1 Particle Diameter



$D_p=0.7620$ m, $d=0.200$ mm, $R_{sd}=1.585$, $C_v=0.175$, $\mu_{sf}=0.416$



Some Results, 9 Particle Diameters



$D_p=0.7620$ m, $R_{sd}=1.585$, $C_{vs}=0.175$, $\mu_{sf}=0.416$





Graded Sands & Gravels

Chapter 7.13 & 8.14



Adjusting the Liquid Properties

$$d_{\text{lim}} = \sqrt{\frac{\text{Stk} \cdot 9 \cdot \rho_l \cdot v_l \cdot D_p}{\rho_s \cdot v_{\text{ls,ldv}}}} \approx \sqrt{\frac{\text{Stk} \cdot 9 \cdot \rho_l \cdot v_l \cdot D_p}{\rho_s \cdot 7.5 \cdot D_p^{0.4}}}$$

$$\rho_x = \rho_l + \rho_l \cdot \frac{X \cdot C_{\text{vs}} \cdot R_{\text{sd}}}{(1 - C_{\text{vs}} + C_{\text{vs}} \cdot X)}$$

$$C_{\text{vs,x}} = \frac{X \cdot C_{\text{vs}}}{(1 - C_{\text{vs}} + C_{\text{vs}} \cdot X)} \quad \text{and} \quad C_{\text{vs,r}} = (1 - X) \cdot C_{\text{vs}}$$

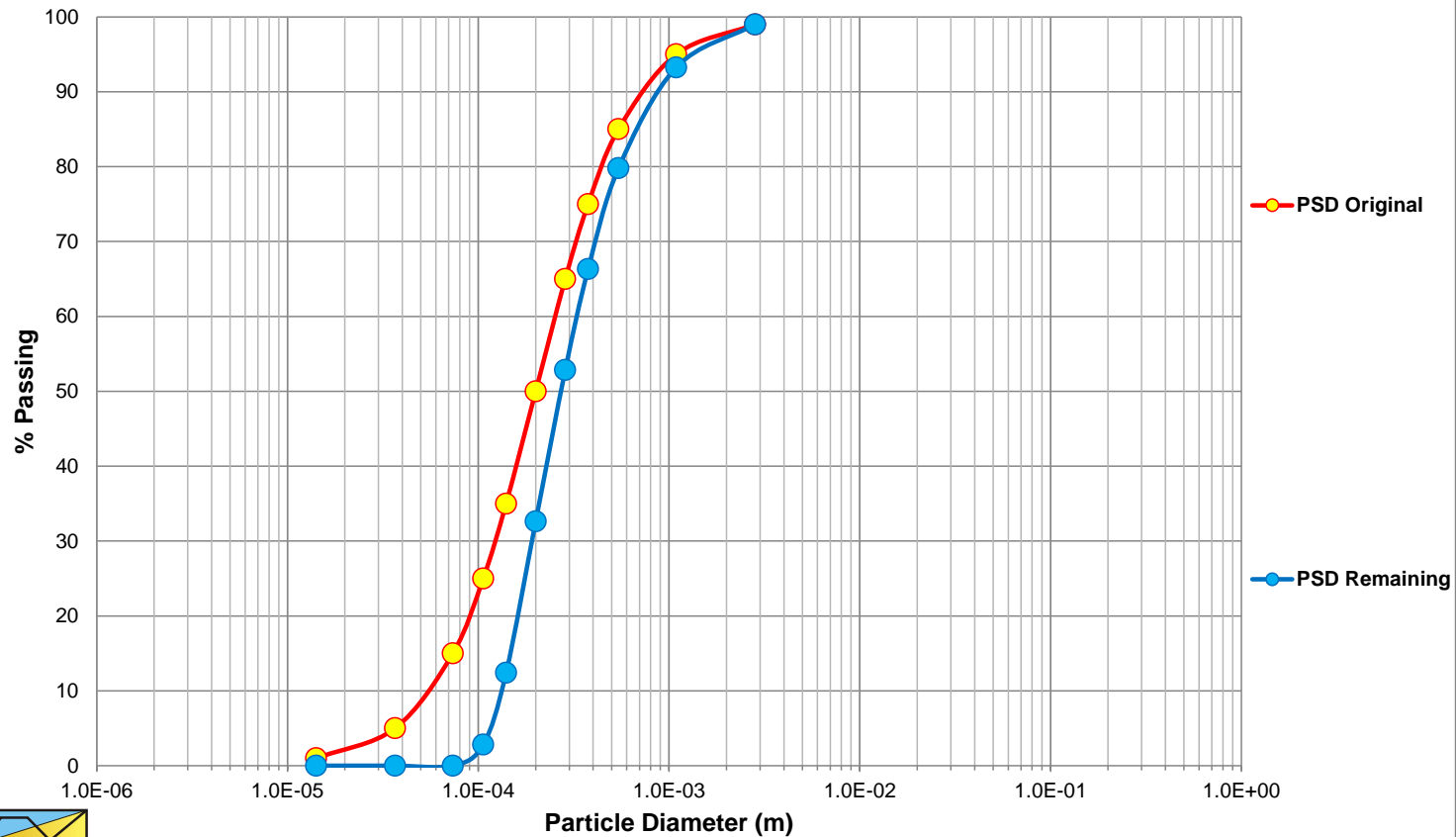
$$\mu_x = \mu_l \cdot \left(1 + 2.5 \cdot C_{\text{vs,x}} + 10.05 \cdot C_{\text{vs,x}}^2 + 0.00273 \cdot e^{16.6 \cdot C_{\text{vs,x}}} \right)$$

$$v_x = \frac{\mu_x}{\rho_x} \quad \text{and} \quad R_{\text{sd,x}} = \frac{\rho_s - \rho_x}{\rho_x}$$



Adjusting the PSD, $d_{50}=0.2$ mm

Cumulative Grain Size Distribution



Procedure/Equations

Step 1:

$$i_{m,x} = \sum_{i=1}^n f_i \cdot i_{m,x,i} \cdot w_i \quad \text{with:} \quad \sum_{i=1}^n f_i = 1 \quad \text{and} \quad \frac{1}{n} \cdot \sum_{i=1}^n w_i = 1$$

$$E_{rhg,x} = \frac{i_{m,x} - i_{l,x}}{R_{sd,x} \cdot C_{vs}} \quad \text{or} \quad E_{rhg,x} = \frac{i_{m,x} - i_{l,x}}{R_{sd,x} \cdot C_{vt}}$$

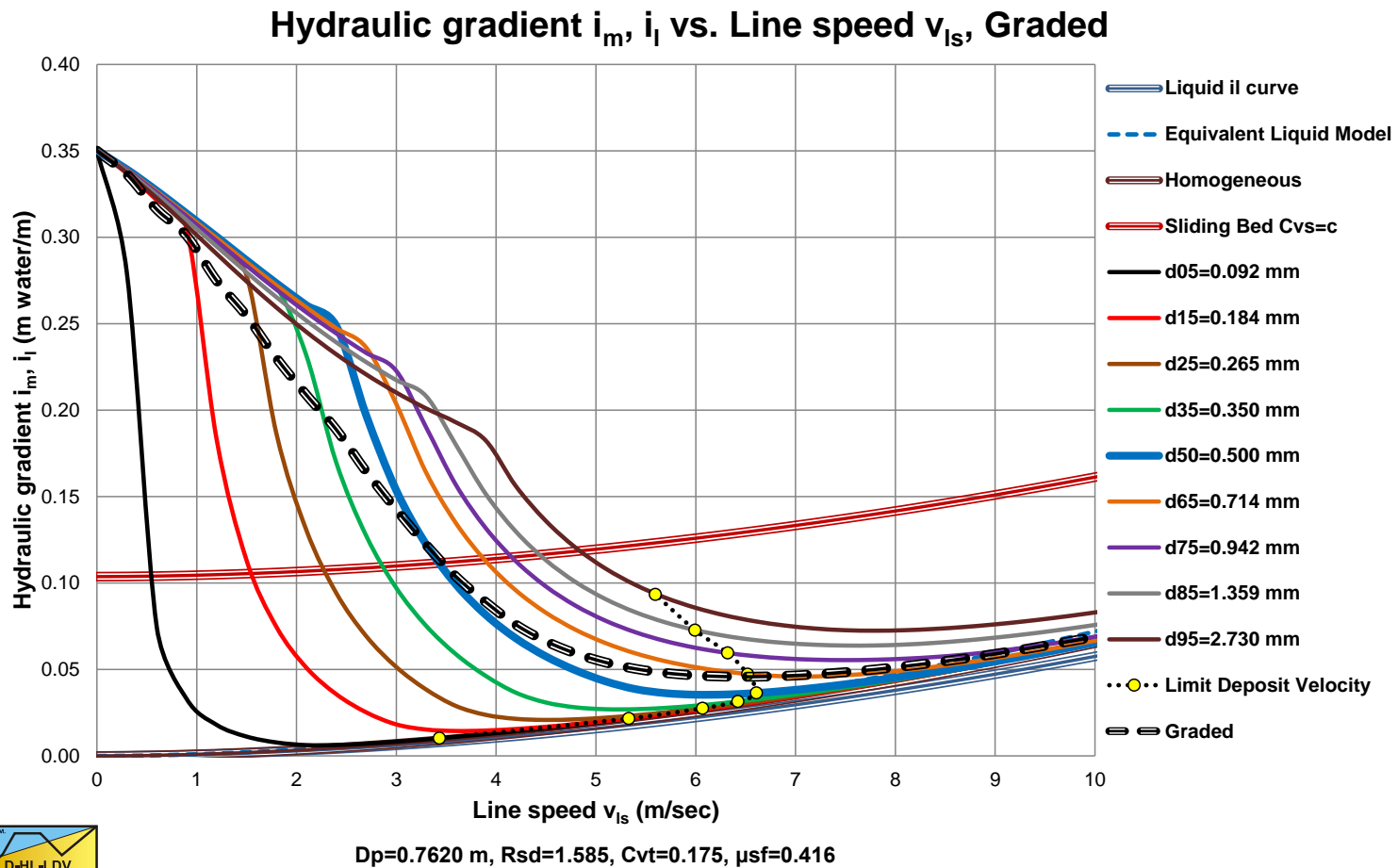
Step 2:

$$i_m = \frac{\rho_x}{\rho_l} \cdot i_{m,x} = \frac{\rho_x}{\rho_l} \cdot \sum_{i=1}^n f_i \cdot i_{m,x,i} \cdot w_i \quad \text{with:} \quad \sum_{i=1}^n f_i = 1 \quad \text{and} \quad \frac{1}{n} \cdot \sum_{i=1}^n w_i = 1$$

$$E_{rhg} = \frac{i_m - i_l}{R_{sd} \cdot C_{vs}} \quad \text{or} \quad E_{rhg} = \frac{i_m - i_l}{R_{sd} \cdot C_{vt}}$$



Resulting Hydraulic Gradient

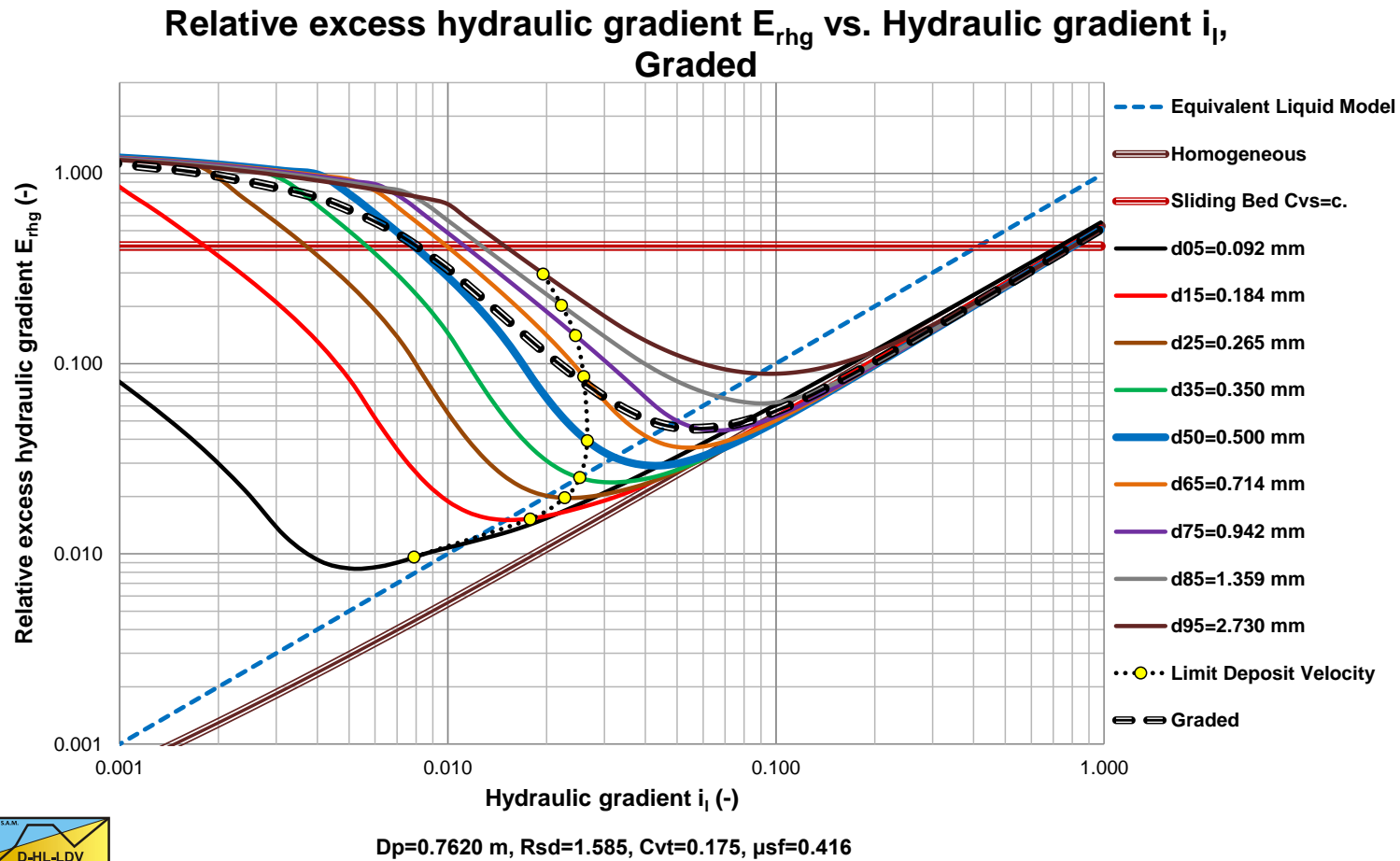


The thick blue curve shows the uniform HG.
The dashed black curve the HG of the graded sand.

Delft University of Technology – Offshore & Dredging Engineering



Resulting Relative Excess Hydraulic Gradient

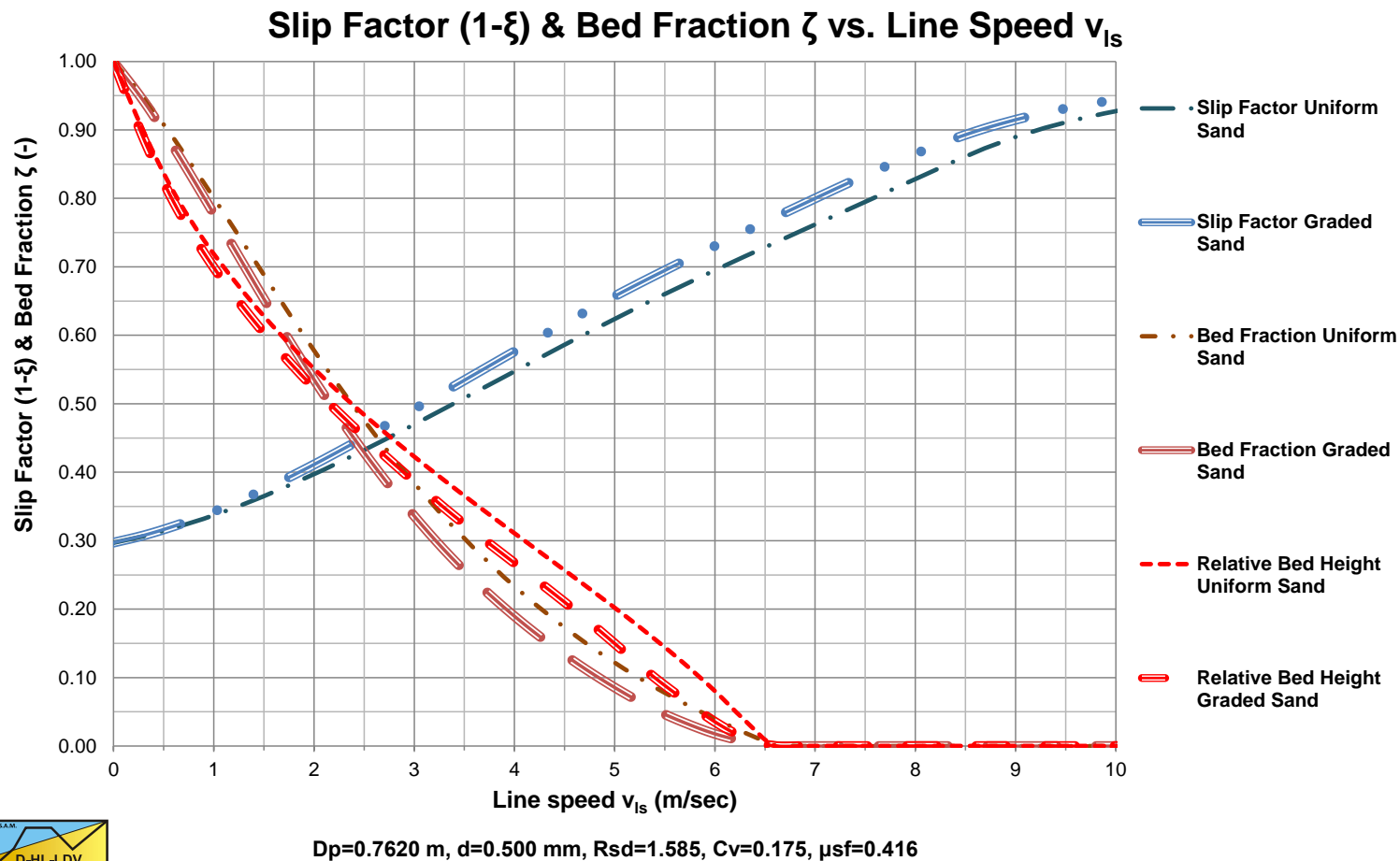


The resulting graded E_{rhg} curve is less steep than the curve for a uniform sand, matching Wilson.

Delft University of Technology – Offshore & Dredging Engineering

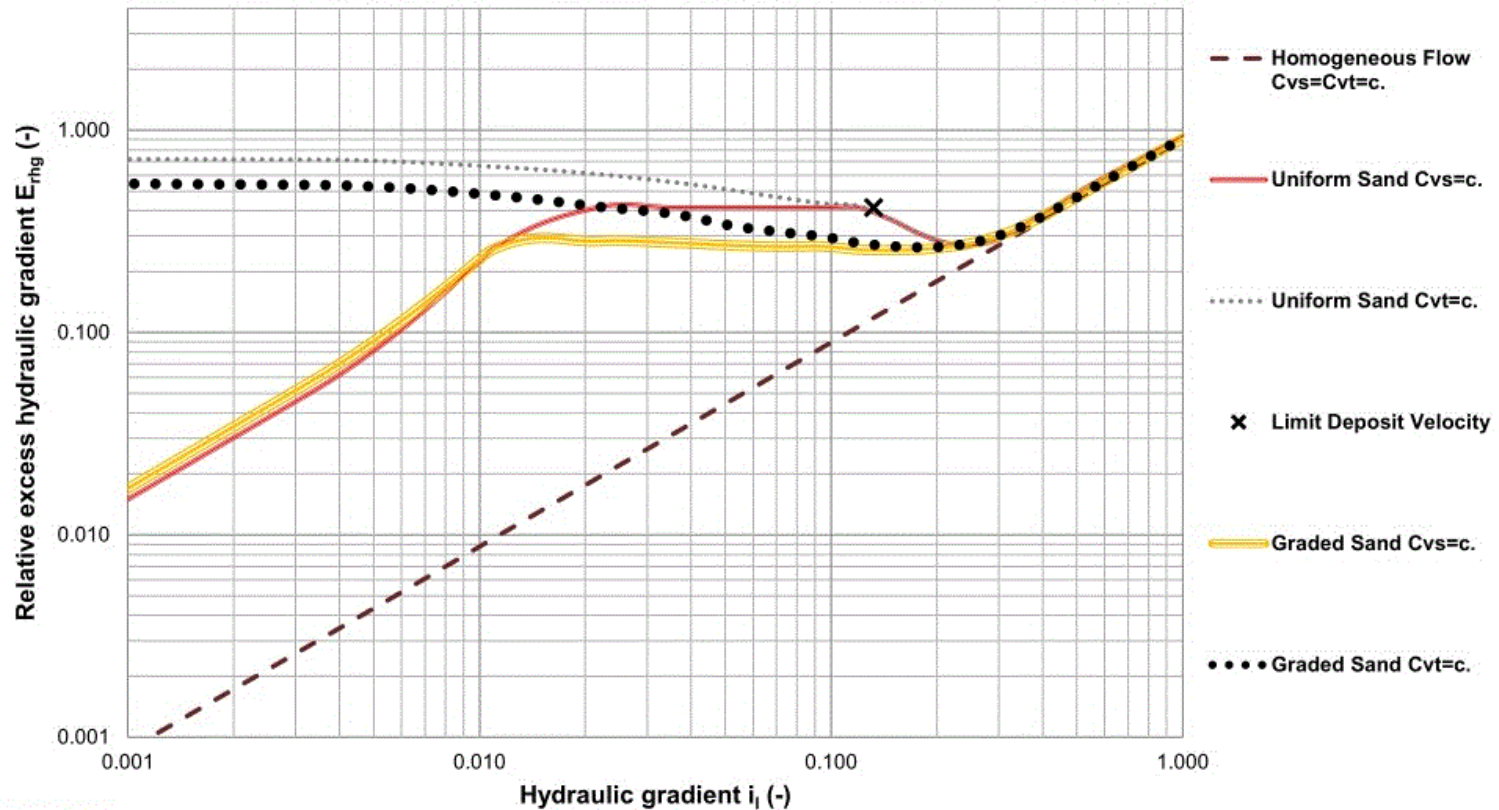


Bed Fraction & Slip Factor



Graded Sands, Animation

Relative excess hydraulic gradient E_{rhg} vs. Hydraulic gradient i_l



$D_p=0.0254$ m, $d=0.50$ mm, $R_{sd}=1.59$, $C_v=0.300$, $\mu=0.415$



Conclusions

- The resulting graded E_{rhg} curve is less steep than the curve for a uniform sand, matching Wilson.
- The resulting steepness however depends strongly on the particle diameter d_{50} , the pipe diameter D_p and the volumetric concentration C_{vs}/C_{vt} .
- The resulting steepness strongly depends on the presence of a homogeneous fraction on one hand and a sliding bed (fully stratified) fraction on the other hand.
- The resulting steepness strongly depends on the grading of the sand or gravel. A higher grading might result in a less steep curve.



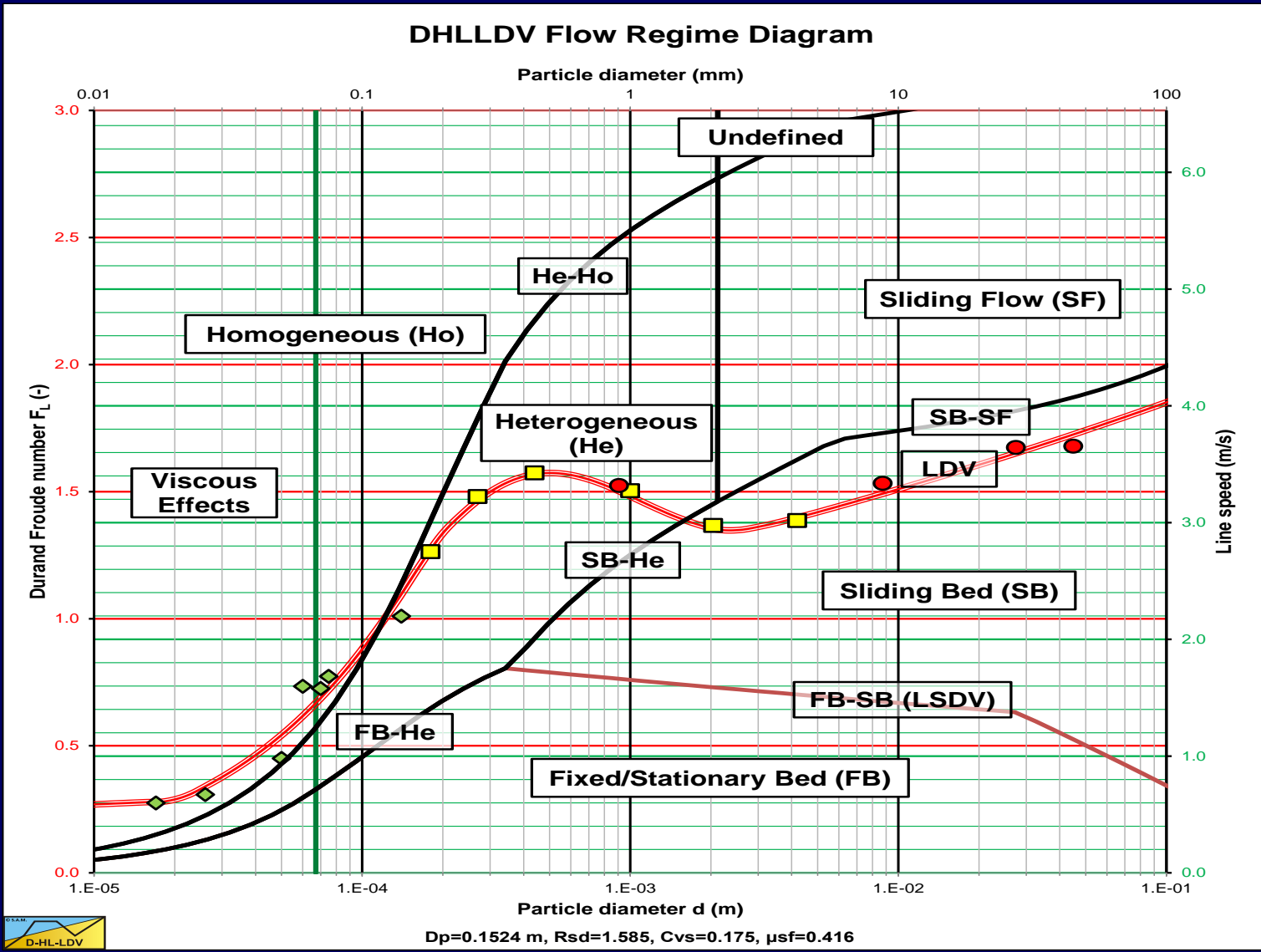


Flow Regime Diagrams

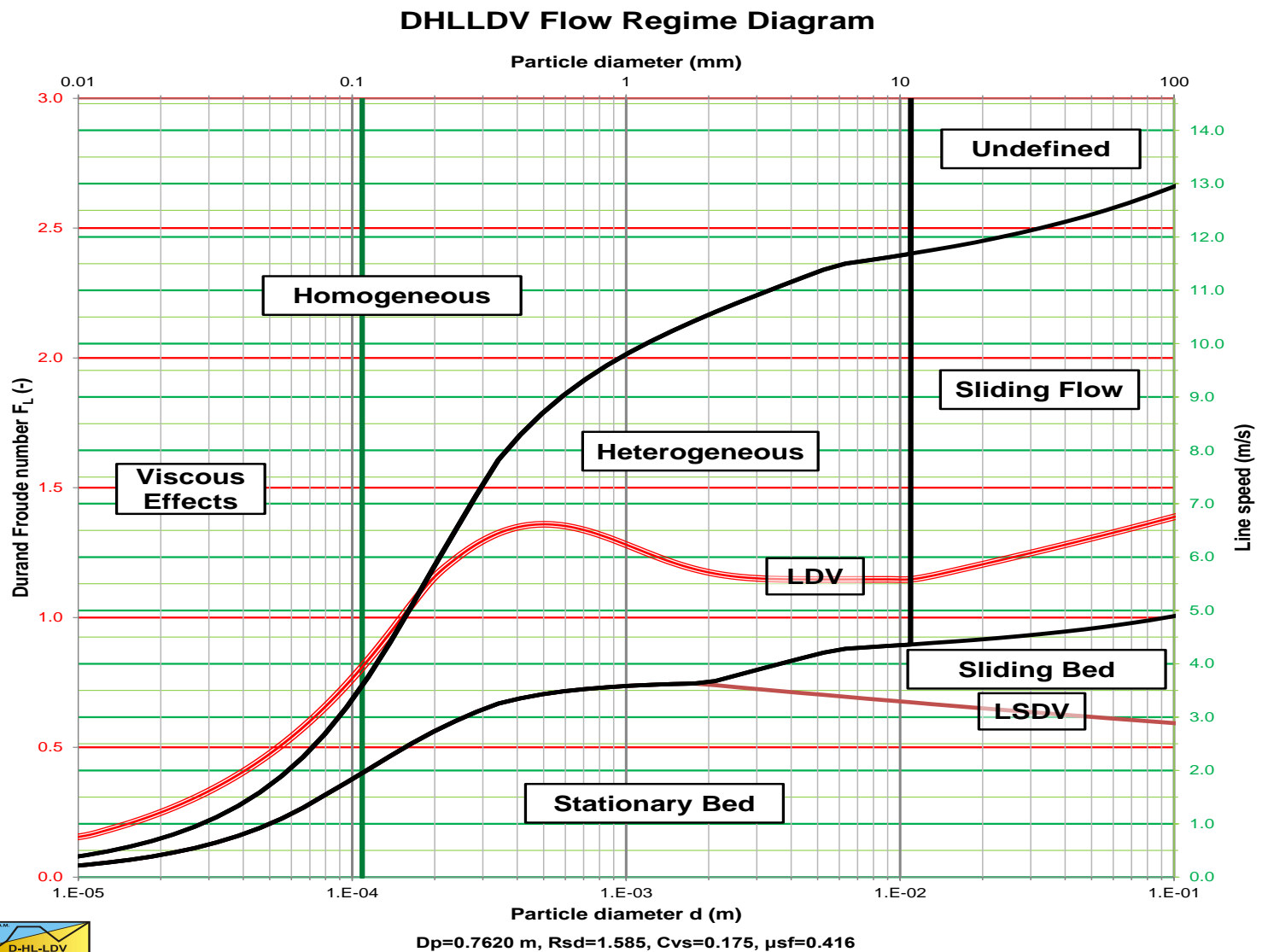
Chapter 7.8 & Appendix D



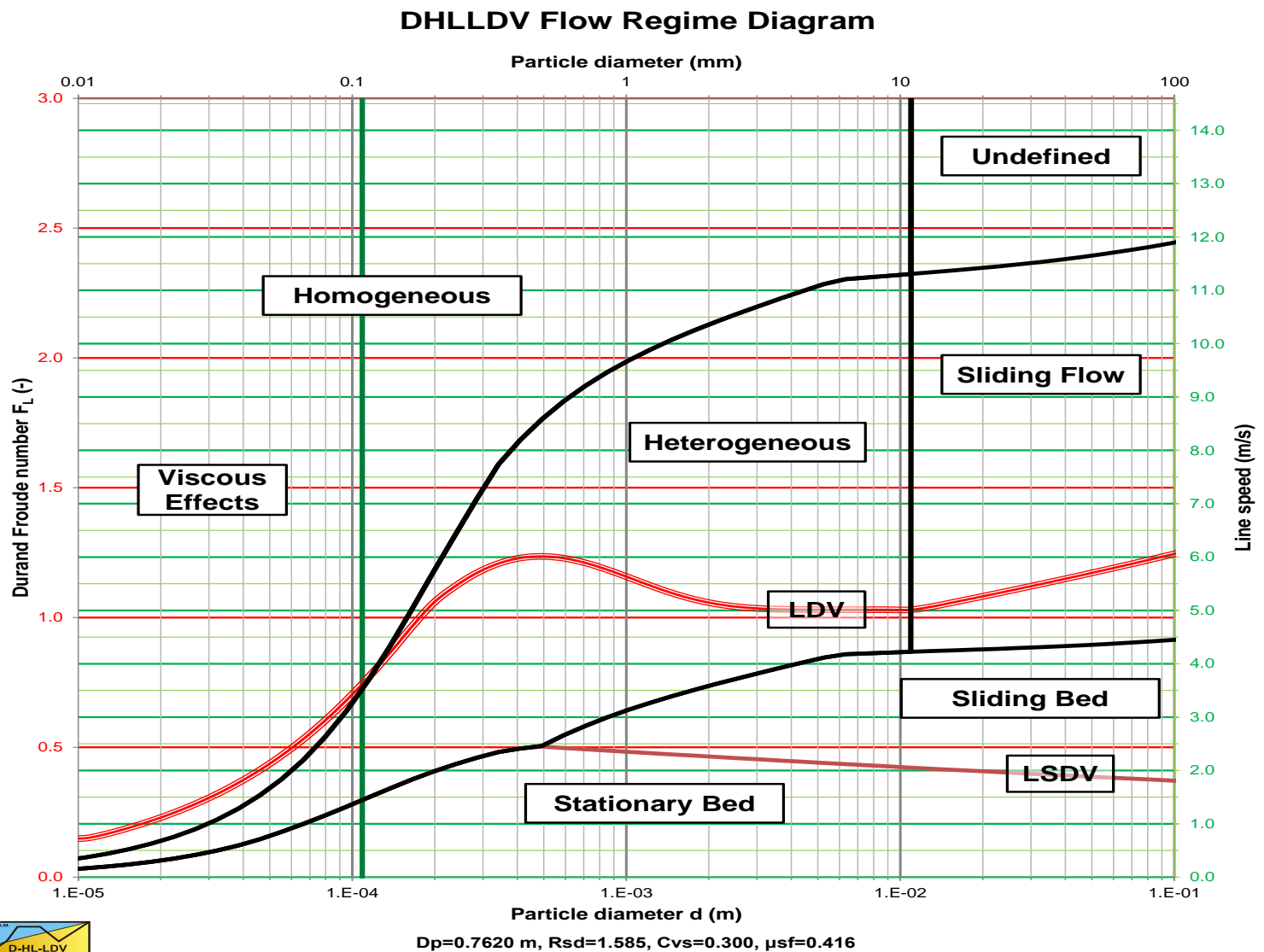
Small Pipe Diameter, $C_{vs}=0.175$



A Large Diameter Pipe, $C_{vs}=0.175$



A Large Diameter Pipe, $C_{vs}=0.3$



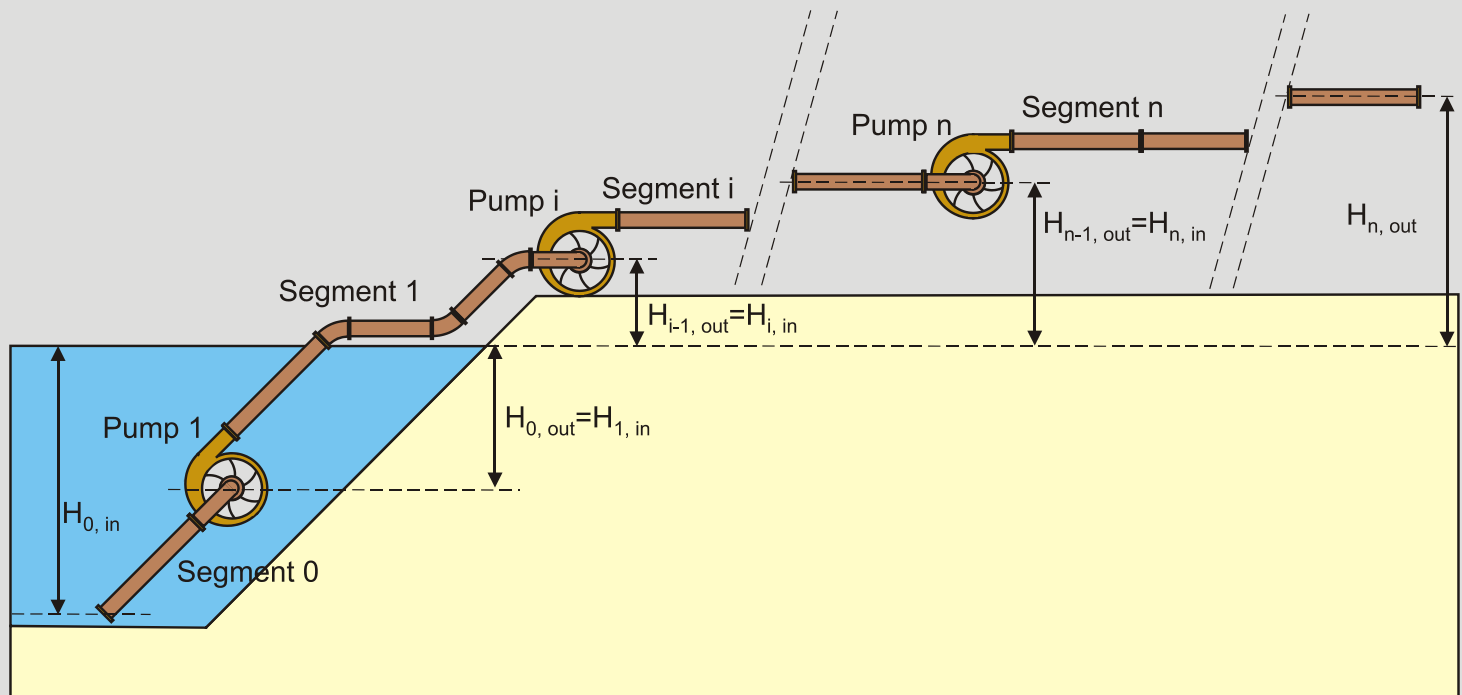


Inclined Pipes

Chapter 7.14 & 8.15



Pump/Pipeline System



- Total pressure/power required
- Cavitation limit of each pump
- Deposition/plugging the pipeline
- Limit Deposit Velocity



Research Question

Problem definition:

Existing methods for determining the hydraulic gradient (pressure losses) in inclined pipes simply multiply the hydraulic gradient of a horizontal pipe with the cosine of the inclination angle (to a certain power) and add the potential energy term. These methods do not consider the flow regimes.

- Flow regimes may respond differently to the inclination angle.
- The transition line speed between flow regimes may shift.
- Some flow regimes may not occur at all.
- The influence of the inclination angle has to be determined for each flow regime individually.





Inclined Pipes History



Durand, Condolios & Gibert (1952)

$$i_{m,\theta} = i_1 + \sin(\theta) \cdot (1 + R_{sd} \cdot C_{vt}) + i_1 \cdot 81 \cdot \left(\frac{v_{ls}^2 \cdot \sqrt{C_x}}{g \cdot D_p \cdot R_{sd}} \right)^{-3/2} \cdot C_{vt} \cdot \cos(\theta)^{3/2}$$



Worster & Denny (1955)

$$i_{m,\theta} = i_1 + \sin(\theta) \cdot (1 + R_{sd} \cdot C_{vt}) + i_1 \cdot 81 \cdot \left(\frac{v_{ls}^2 \cdot \sqrt{C_x}}{g \cdot D_p \cdot R_{sd}} \right)^{-3/2} \cdot C_{vt} \cdot \cos(\theta)$$



Wilson (1992)

$$i_{m,\theta} = i_1 + \sin(\theta) \cdot (1 + R_{sd} \cdot C_{vt}) + \frac{\mu_{sf}}{2} \cdot \left(\frac{v_{50}}{v_{ls}} \right)^M \cdot R_{sd} \cdot C_{vt} \cdot \cos(\theta)^M$$



Expected Equation

$$\begin{aligned}
 i_{m,\theta} = & i_1 \cdot \left(1 + \alpha \cdot R_{sd} \cdot C_{vs} \cdot \sin(\theta)^{\beta_1} \right) \\
 & + \sin(\theta) \cdot \left(1 + R_{sd} \cdot C_{vs} \right) \\
 & + E_{rhg} \cdot R_{sd} \cdot C_{vs} \cdot \cos(\theta)^{\beta_2}
 \end{aligned}$$

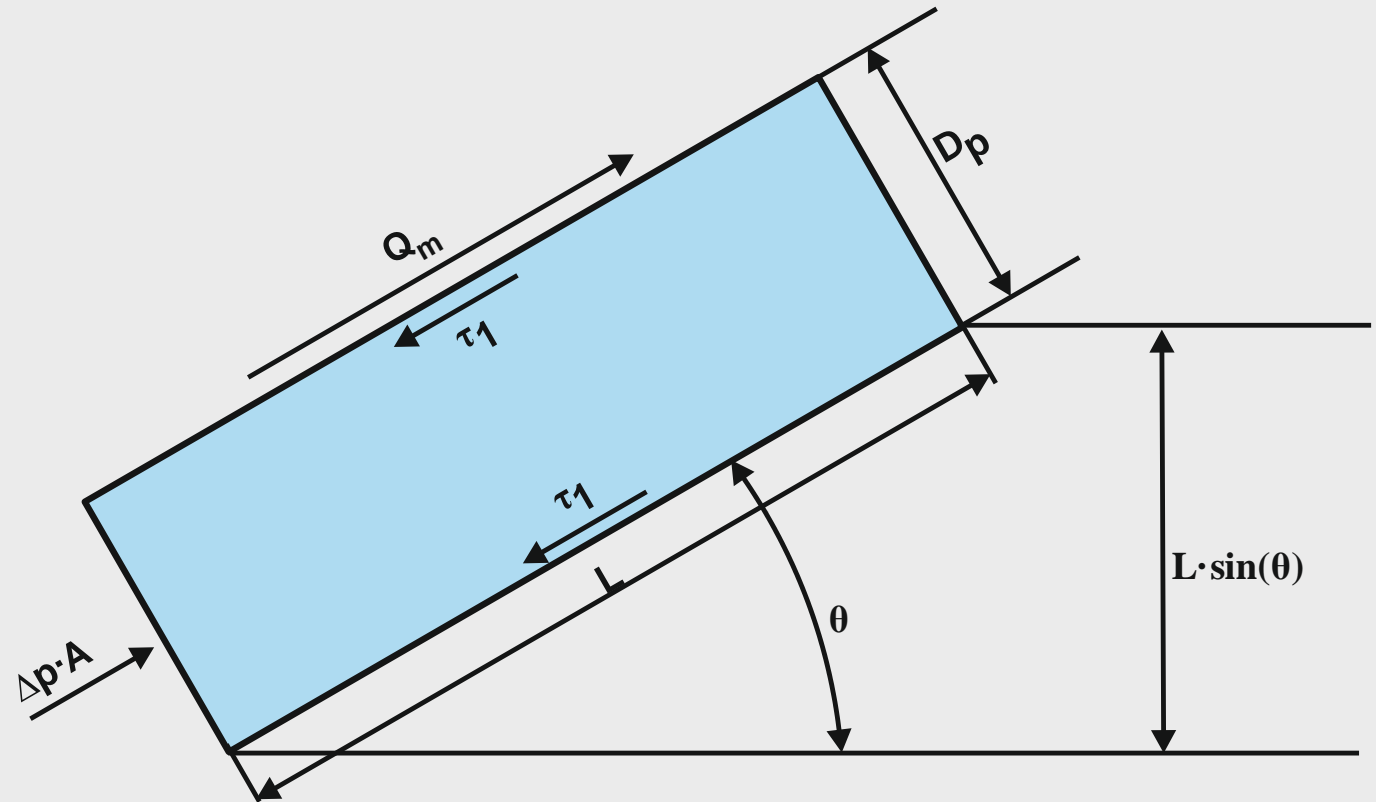




Inclined Pipes Physics



Pure Carrier Liquid



Pure Carrier Liquid

$$-\frac{dp}{dx} \cdot A \cdot L = \tau_1 \cdot O \cdot L + \rho_1 \cdot A \cdot L \cdot g \cdot \sin(\theta)$$

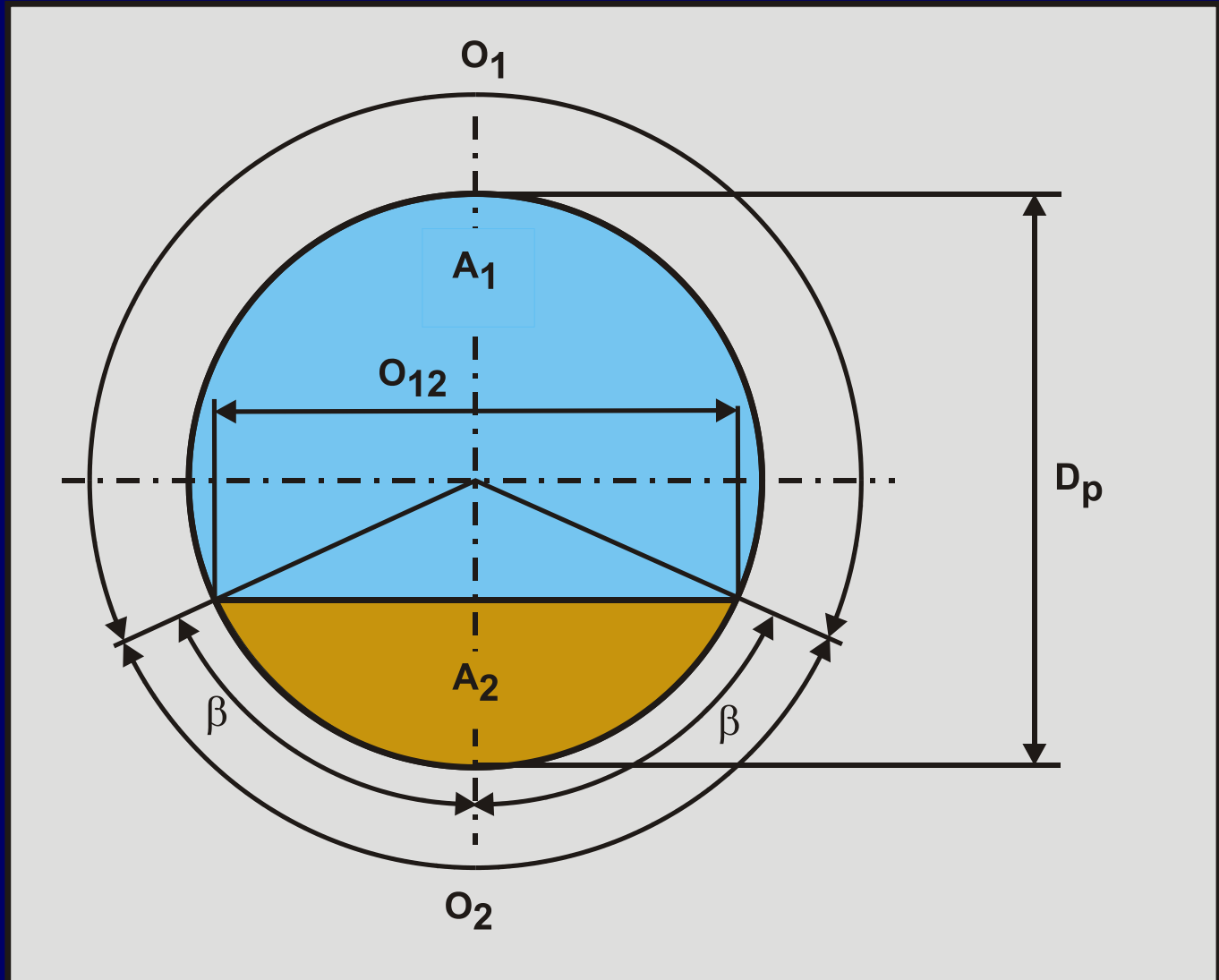
$$i_{1,\theta} = -\frac{dp}{dx} \cdot \frac{A \cdot L}{\rho_1 \cdot A \cdot L \cdot g}$$

$$= \frac{\tau_1 \cdot O \cdot L}{\rho_1 \cdot A \cdot L \cdot g} + \frac{\rho_1 \cdot A \cdot L \cdot g \cdot \sin(\theta)}{\rho_1 \cdot A \cdot L \cdot g}$$

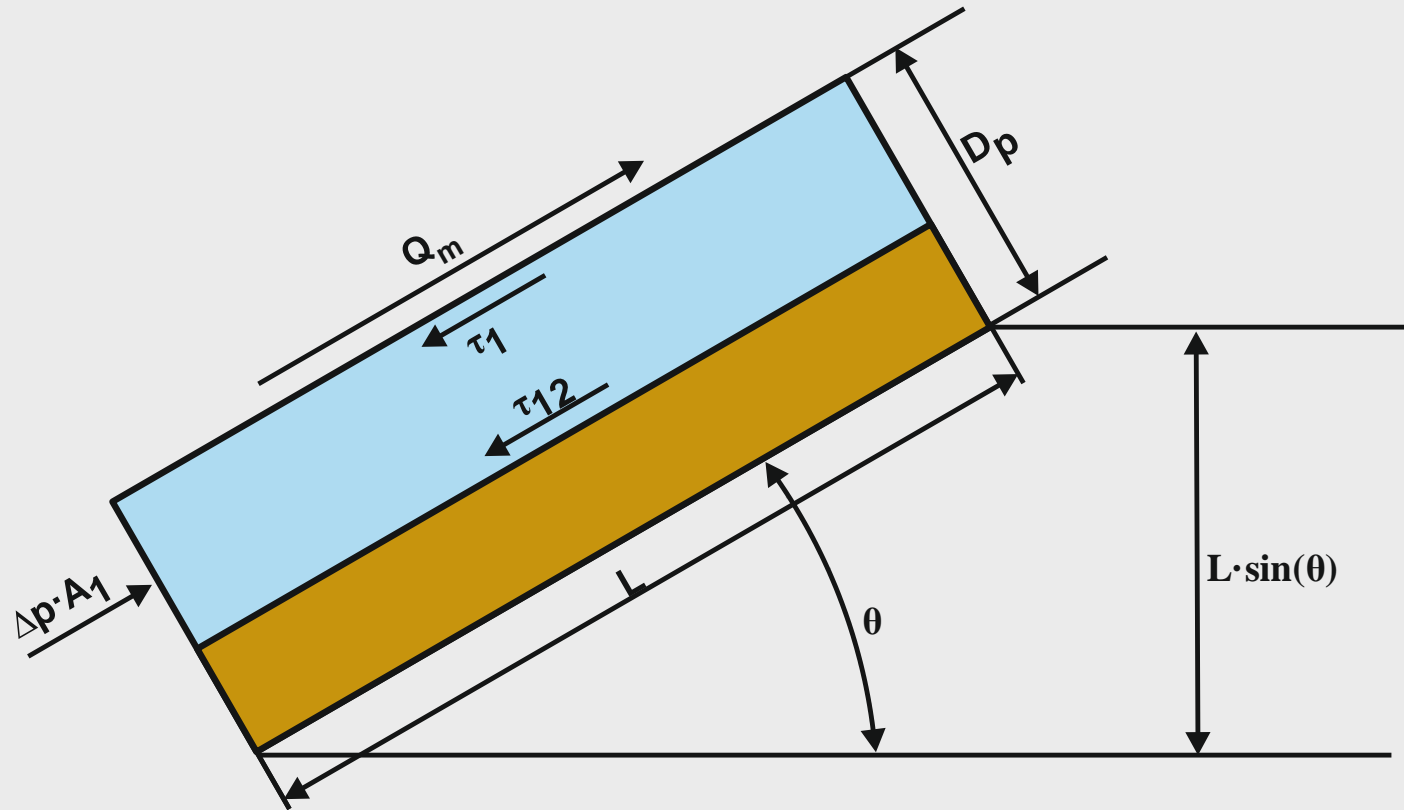
$$= i_1 + \sin(\theta)$$



Fixed/Sliding Bed Regime



Fixed/Sliding Bed Regime



Fixed Bed Regime

$$-\frac{dp}{dx} \cdot A_1 \cdot L = \tau_1 \cdot O_1 \cdot L + \tau_{12} \cdot O_{12} \cdot L + \rho_1 \cdot A_1 \cdot L \cdot g \cdot \sin(\theta)$$

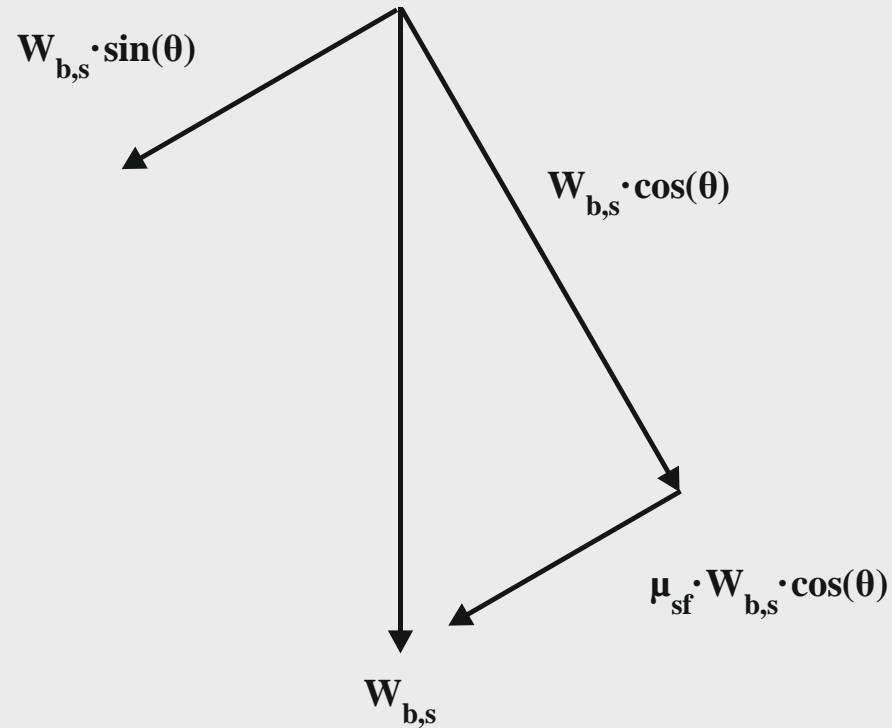
$$i_{m,\theta} = -\frac{dp}{dx} \cdot \frac{A_1 \cdot L}{\rho_1 \cdot A_1 \cdot L \cdot g}$$

$$= \frac{\tau_1 \cdot O_1 \cdot L}{\rho_1 \cdot A_1 \cdot L \cdot g} + \frac{\tau_{12} \cdot O_{12} \cdot L}{\rho_1 \cdot A_1 \cdot L \cdot g} + \frac{\rho_1 \cdot A_1 \cdot L \cdot g \cdot \sin(\theta)}{\rho_1 \cdot A_1 \cdot L \cdot g}$$

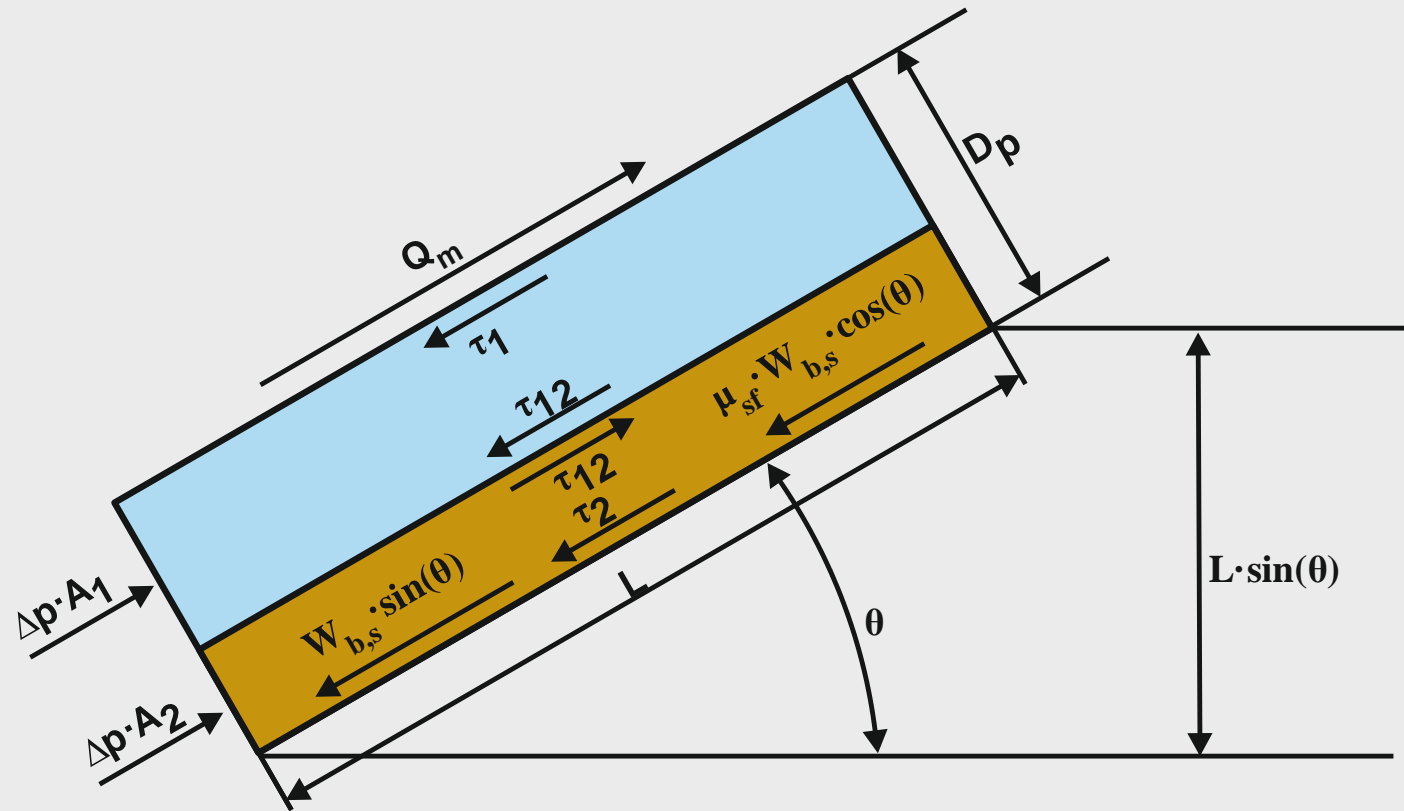
$$= i_m + \sin(\theta)$$



Sliding Bed Regime, Gravity



Sliding Bed Regime, Forces



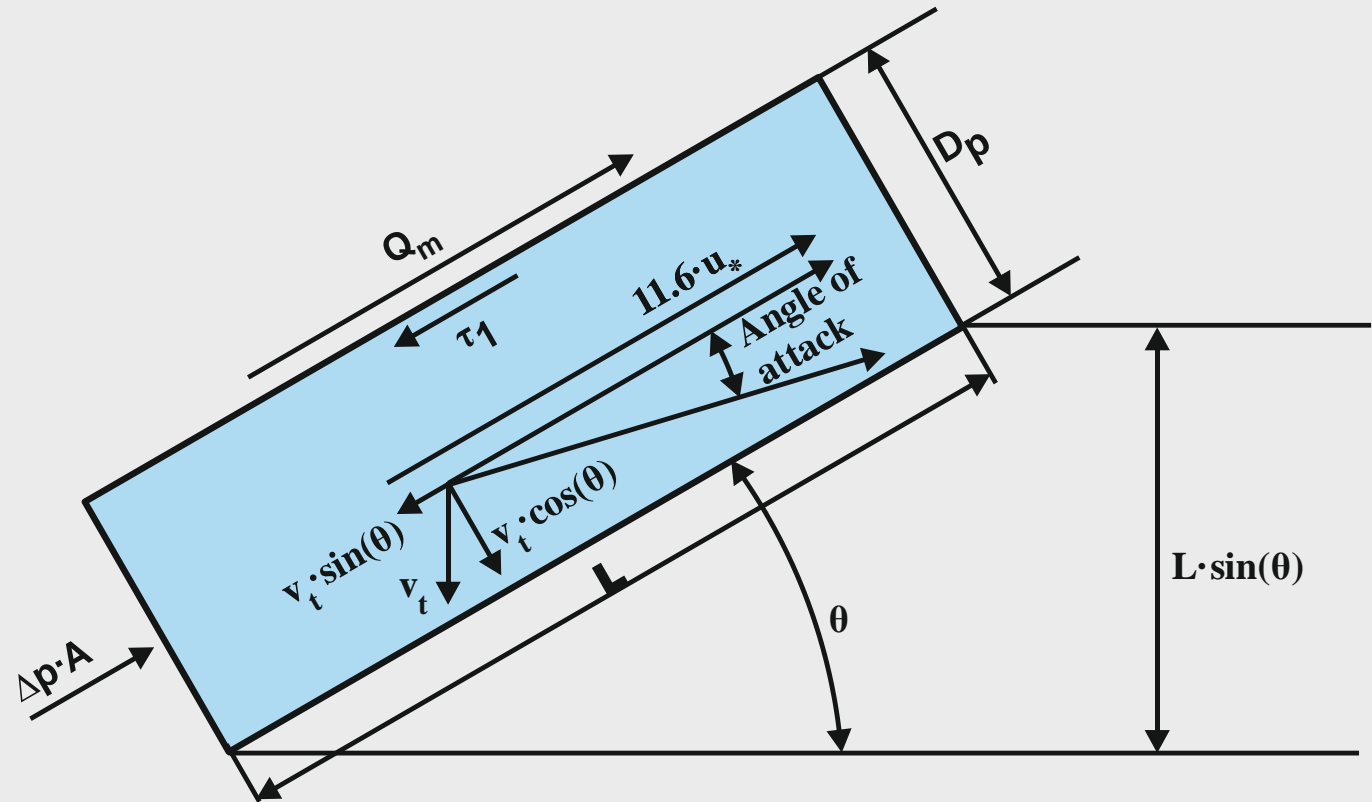
Sliding Bed Regime

$$i_{m,\theta} = i_{l,\theta} + R_{sd} \cdot C_{vs} \cdot (\mu_{sf} \cdot \cos(\theta) + \sin(\theta))$$

$$E_{rhg,\theta} = \frac{i_{m,\theta} - i_{l,\theta}}{R_{sd} \cdot C_{vs}} = \mu_{sf} \cdot \cos(\theta) + \sin(\theta)$$



Heterogeneous Flow Regime



Heterogeneous Flow Regime

$$S_{hr,\theta} = S_{hr} \cdot \cos(\theta) = \frac{v_t \cdot \cos(\theta) \cdot \left(1 - \frac{C_{vs}}{\kappa_C}\right)^\beta}{v_{ls}}$$

$$S_{rs,\theta} = c \cdot \left(\frac{\delta_v}{d}\right)^{2/3} \cdot \left(\frac{v_t \cdot \cos(\theta)}{11.6 \cdot u_* - v_t \cdot \sin(\theta)}\right)^{4/3} \cdot \left(\frac{v_t}{\sqrt{g \cdot d}}\right)^2$$

$$E_{rhg,\theta} = S_{hr,\theta} + S_{rs,\theta} + \sin(\theta)$$

$$i_{m,\theta} = i_{l,\theta} + \left(S_{hr,\theta} + S_{rs,\theta} + \sin(\theta)\right) \cdot R_{sd} \cdot C_{vs}$$



Homogeneous Flow Regime 1

$$i_{lm,\theta} = \frac{\lambda_1 \cdot (v_{ls} + v_{th} \cdot \sin(\theta) \cdot C_{vs})^2}{2 \cdot g \cdot D_p} + \sin(\theta)$$

$$\begin{aligned} i_{lm,\theta} &\approx i_1 + \sin(\theta) + i_1 \cdot \frac{2 \cdot v_{th} \cdot \sin(\theta) \cdot C_{vs}}{v_{ls}} \\ &= i_{1,\theta} + i_1 \cdot \frac{2 \cdot v_{th} \cdot \sin(\theta) \cdot C_{vs}}{v_{ls}} \end{aligned}$$

Homogeneous Regimes

$$i_{m,\theta} = i_1 \cdot (1 + \alpha_E \cdot R_{sd} \cdot C_{vs}) + (1 + R_{sd} \cdot C_{vs}) \cdot \sin(\theta)$$

Sliding Flow Regime

$$i_{m,\theta} = i_1 \cdot \left(1 + \frac{2 \cdot v_{th} \cdot \sin(\theta) \cdot C_{vs}}{v_{ls}} \right) + (1 + R_{sd} \cdot C_{vs}) \cdot \sin(\theta)$$



Homogeneous Flow Regime 2

Homogeneous Regimes

$$i_{m,\theta} = i_{l,\theta} + R_{sd} \cdot C_{vs} \cdot (\alpha_E \cdot i_1 + \sin(\theta))$$

Sliding Bed Regime

$$i_{m,\theta} = i_{l,\theta} + R_{sd} \cdot C_{vs} \cdot \sin(\theta) + i_1 \cdot \frac{2 \cdot v_{th} \cdot \sin(\theta) \cdot C_{vs}}{v_{ls}}$$

Homogeneous Regimes

$$E_{rhg,\theta} = \frac{i_{m,\theta} - i_{l,\theta}}{R_{sd} \cdot C_{vs}} = \alpha_E \cdot i_1 + \sin(\theta)$$

Sliding Bed Regime

$$E_{rhg,\theta} = \frac{i_{m,\theta} - i_{l,\theta}}{R_{sd} \cdot C_{vs}} = i_1 \cdot \frac{2 \cdot v_{th} \cdot \sin(\theta)}{v_{ls} \cdot R_{sd}} + \sin(\theta)$$



Limit Deposit Velocity

$$V_{ls,ldv,\theta} = V_{ls,ldv} \cdot \cos(\theta)^{1/3}$$

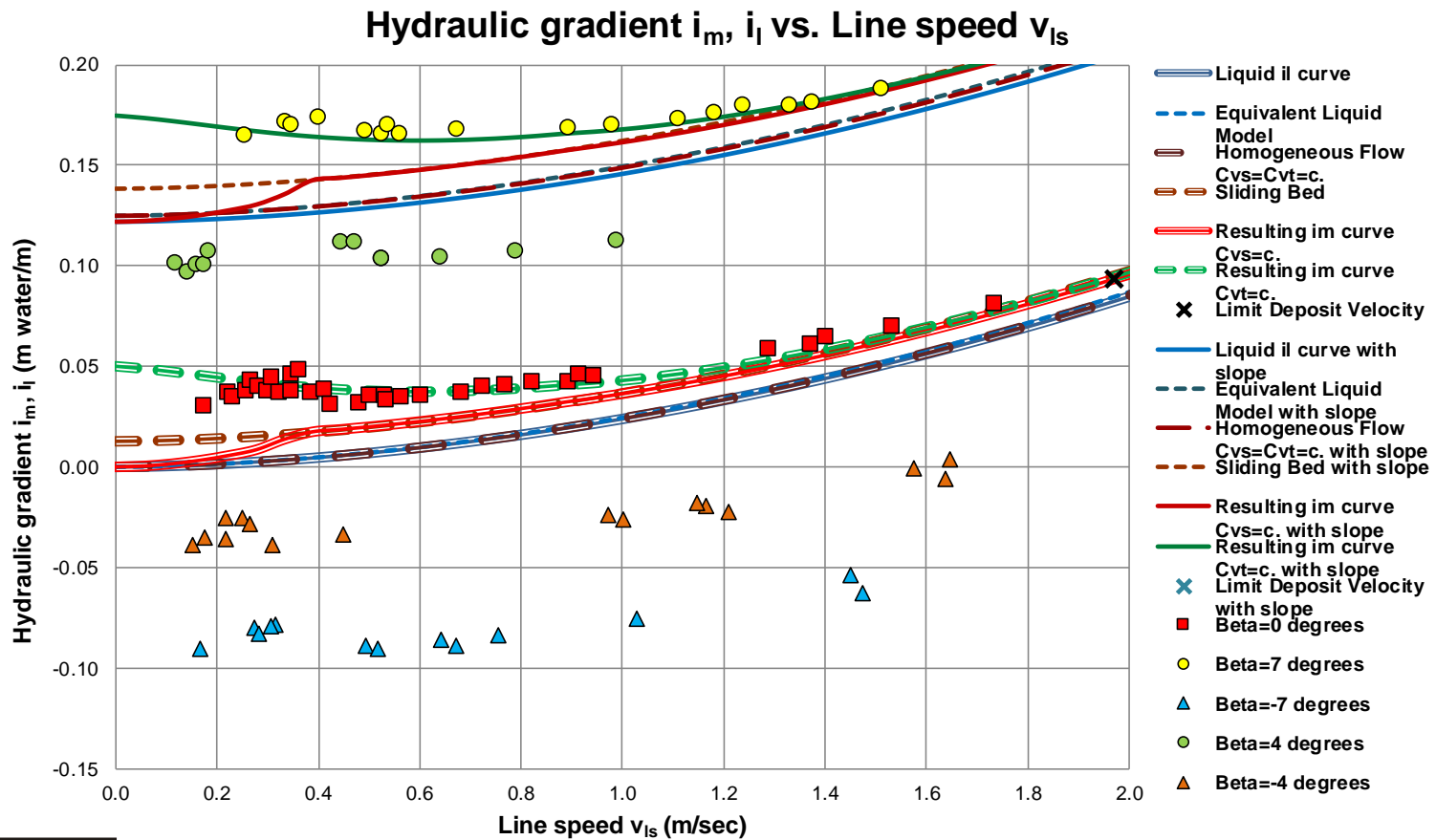




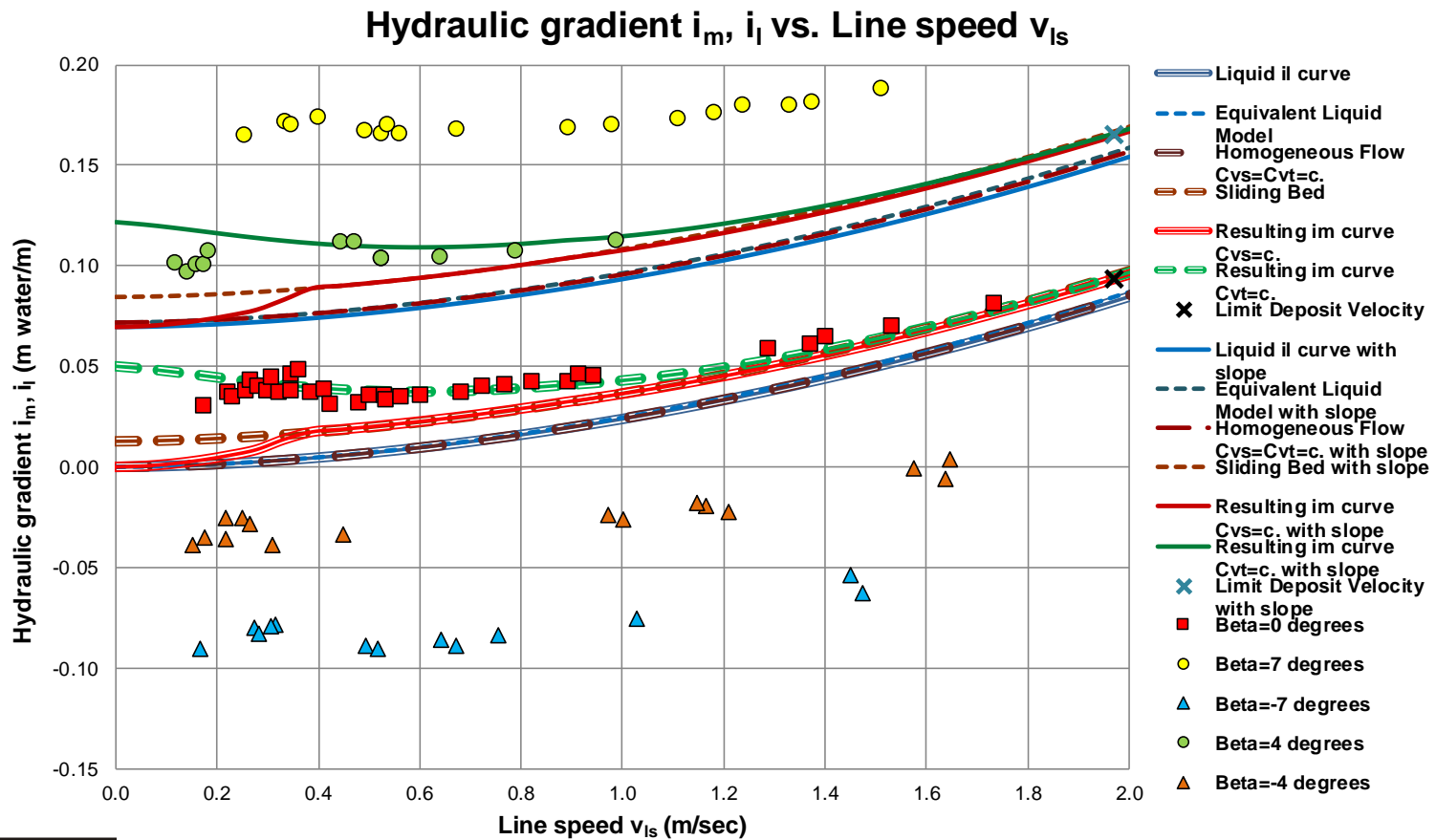
Experiments Doron & Barnea



Inclined Pipe, Doron & Barnea (1997)



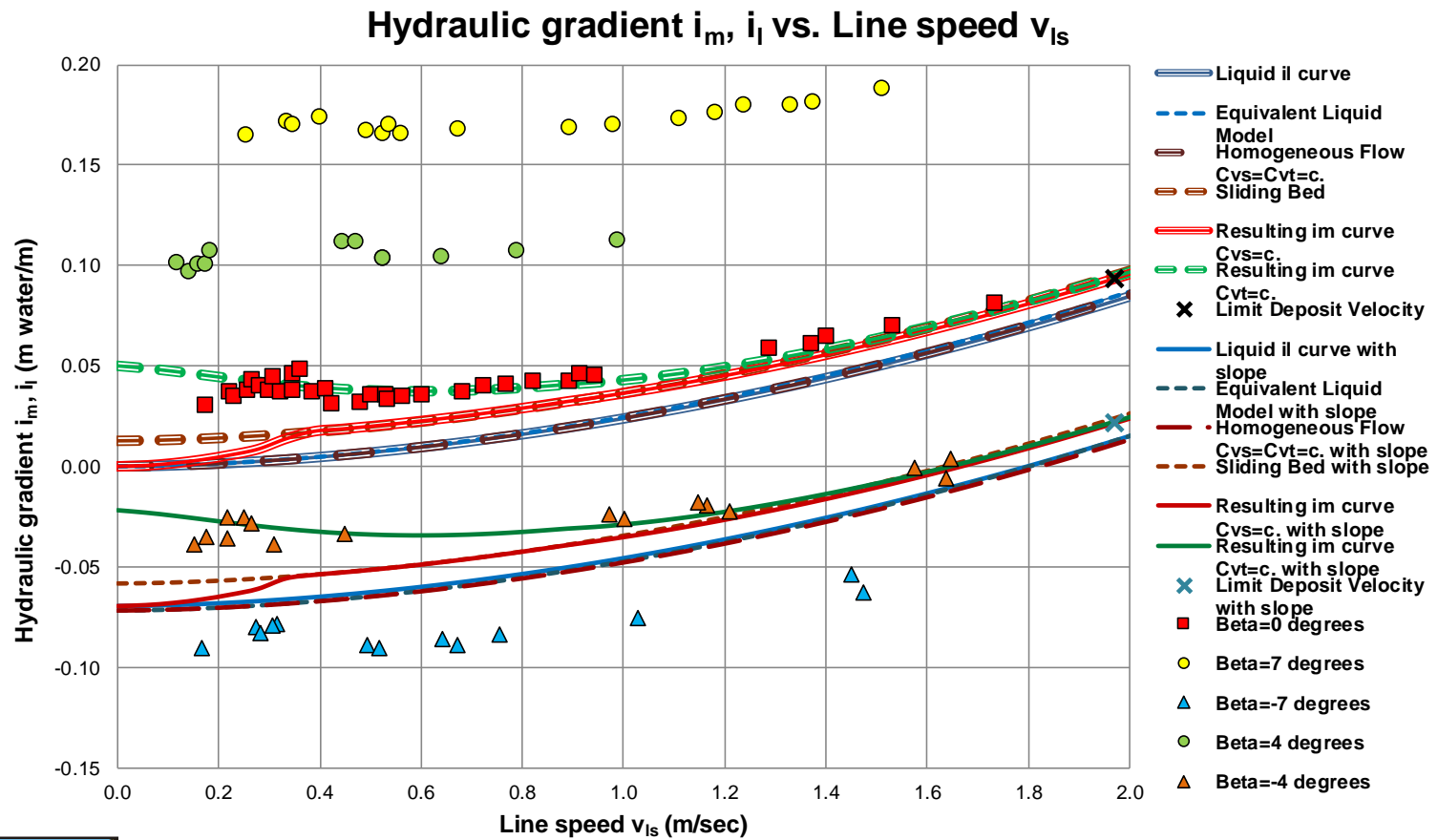
Inclined Pipe, Doron & Barnea (1997)



$D_p=0.0500$ m, $d=3.000$ mm, $R_{sd}=0.210$, $C_v=0.130$, $\mu_{sf}=0.480$, Slope= 4.0°



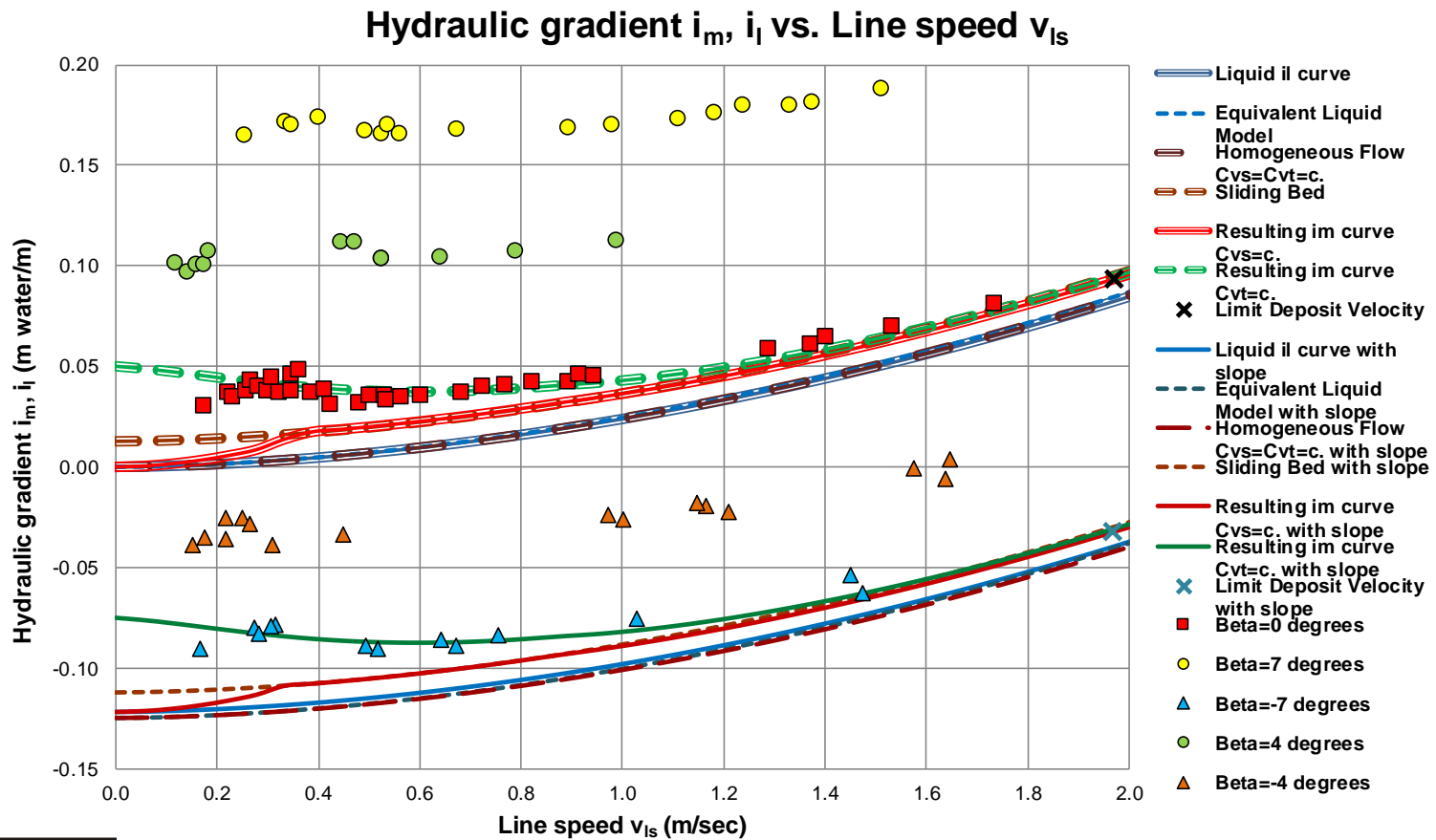
Inclined Pipe, Doron & Barnea (1997)



$D_p=0.0500$ m, $d=3.000$ mm, $R_{sd}=0.210$, $C_v=0.130$, $\mu_{sf}=0.480$, Slope= -4.0°



Inclined Pipe, Doron & Barnea (1997)



$D_p=0.0500$ m, $d=3.000$ mm, $R_{sd}=0.210$, $C_v=0.130$, $\mu_{sf}=0.480$, Slope= -7.0°

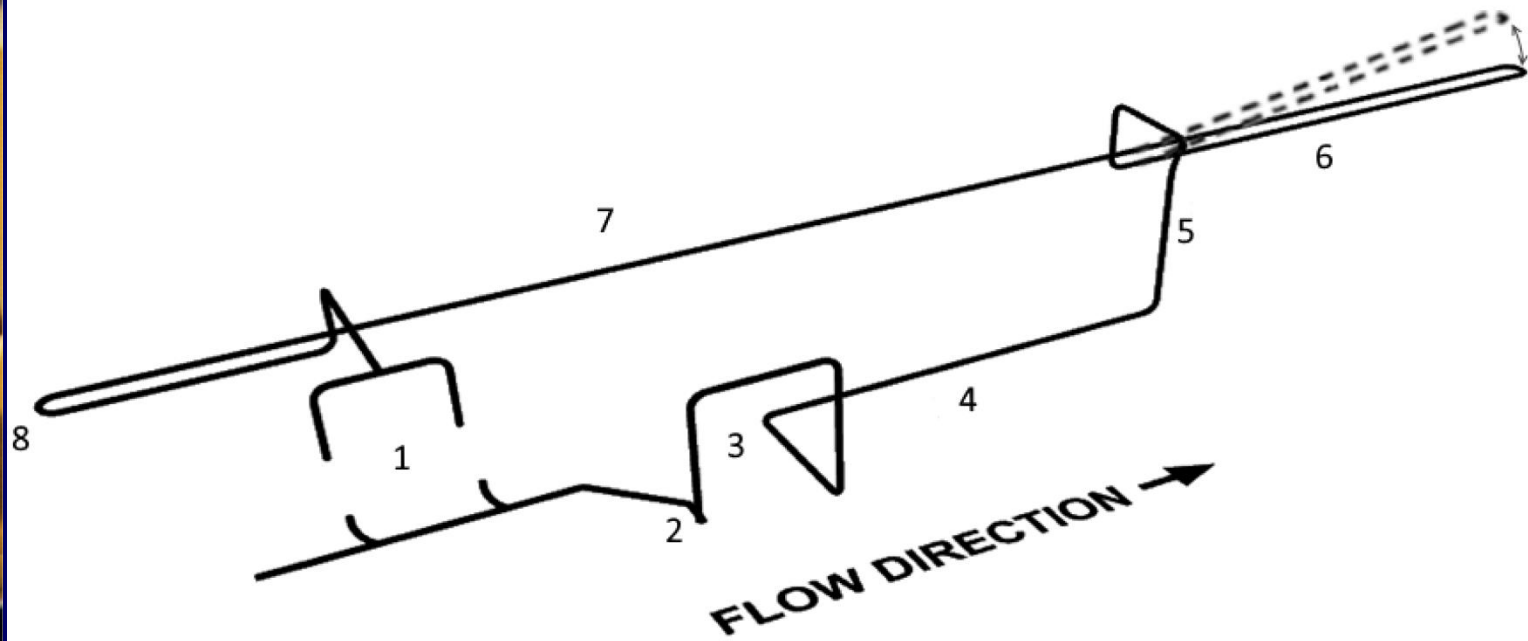




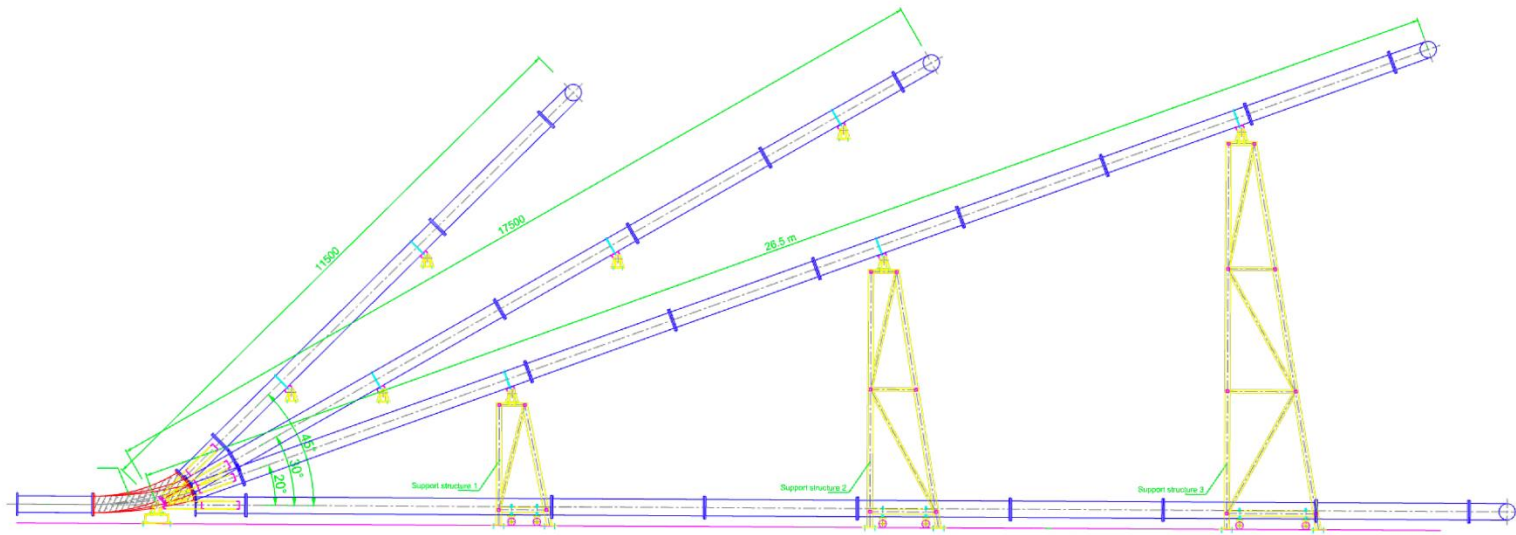
Experiments NERCDC Shanghai



Inclined Pipe, Configuration



Inclined Pipe, Configuration



Inclined Pipe, Configuration



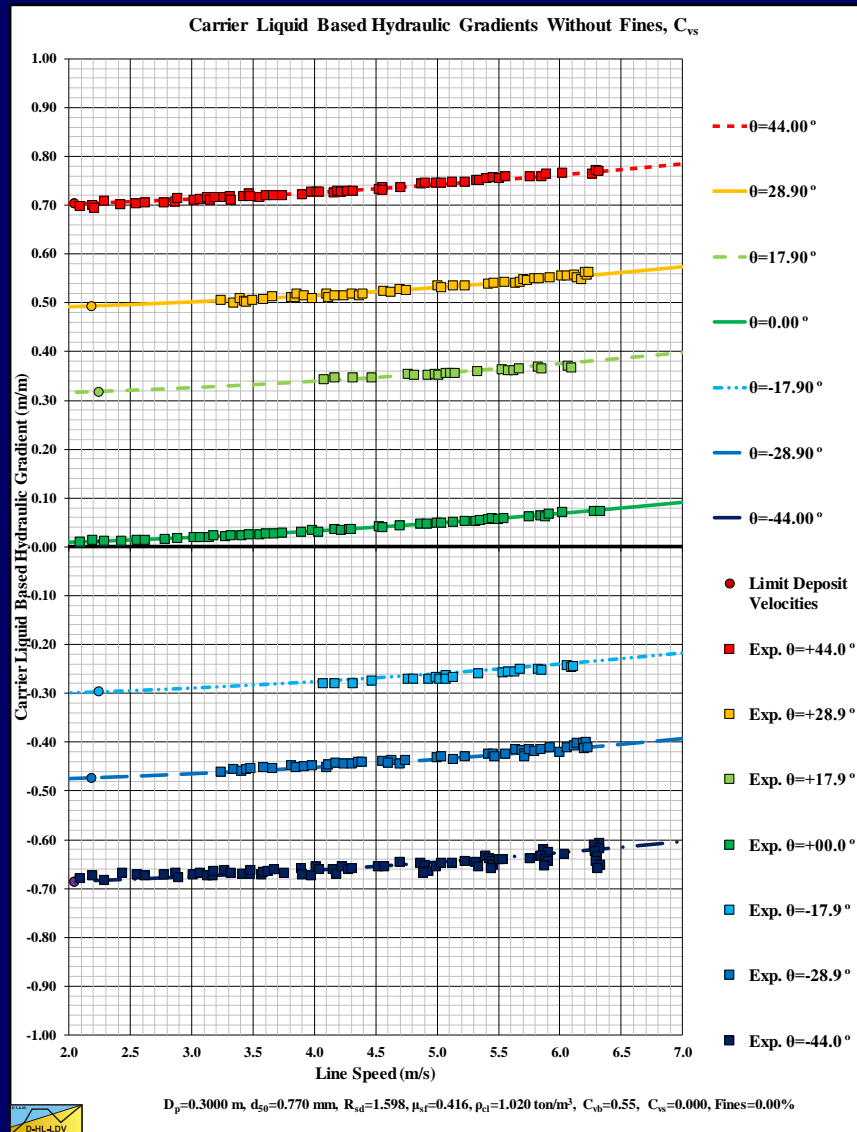
Inclined Pipe, Configuration



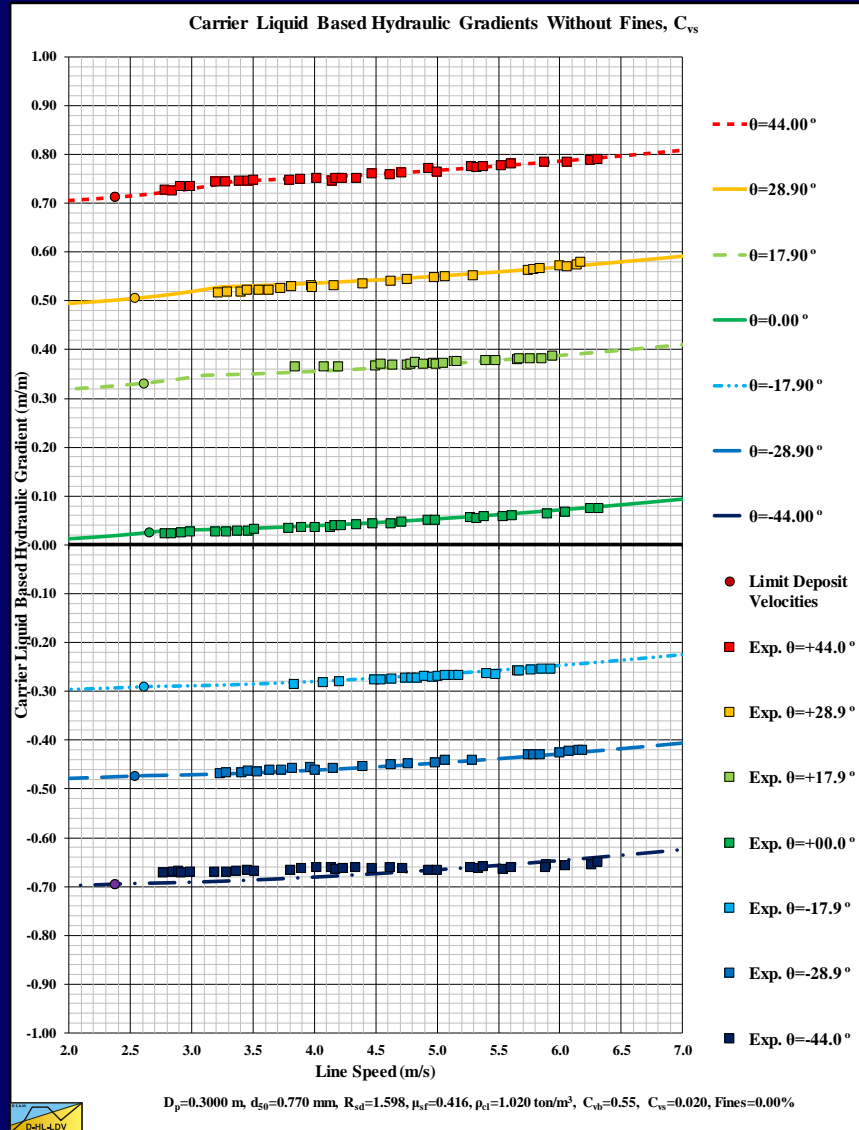
Inclined Pipe, Configuration



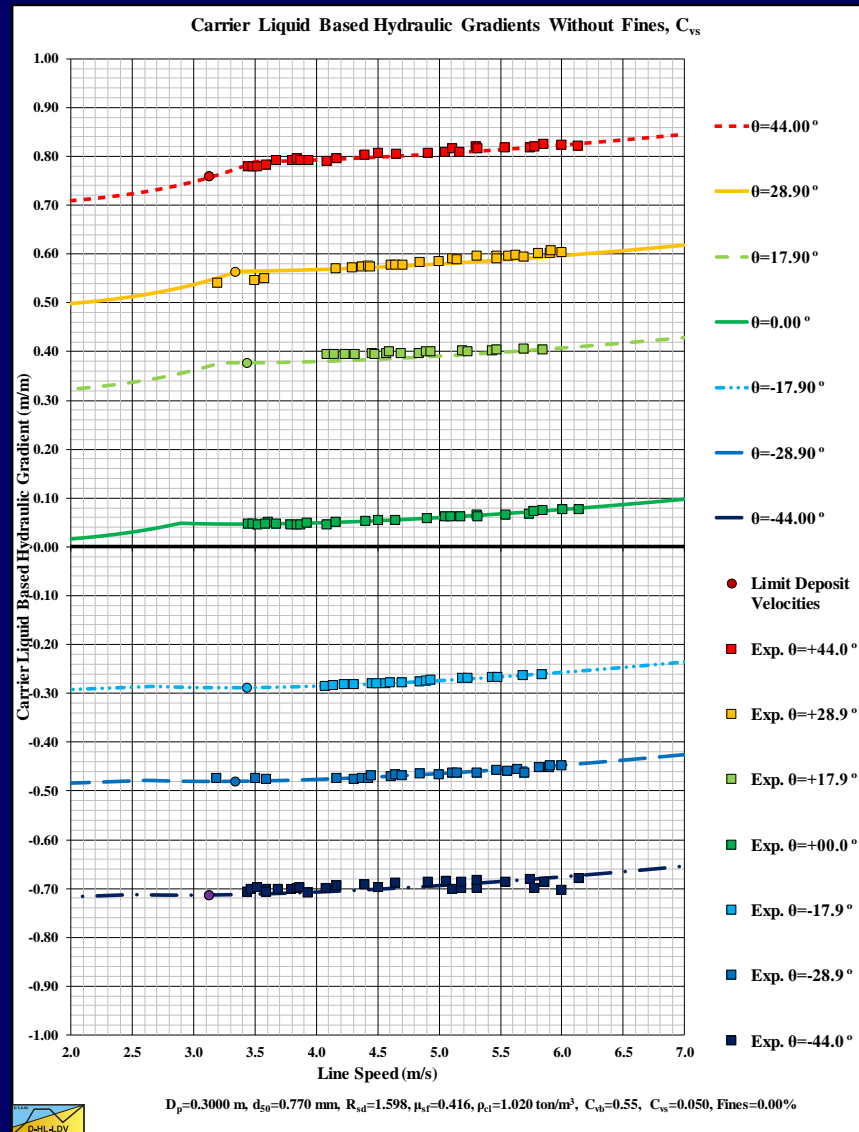
Inclined Pipe, de Vreede (2018), $C_v=0.00$



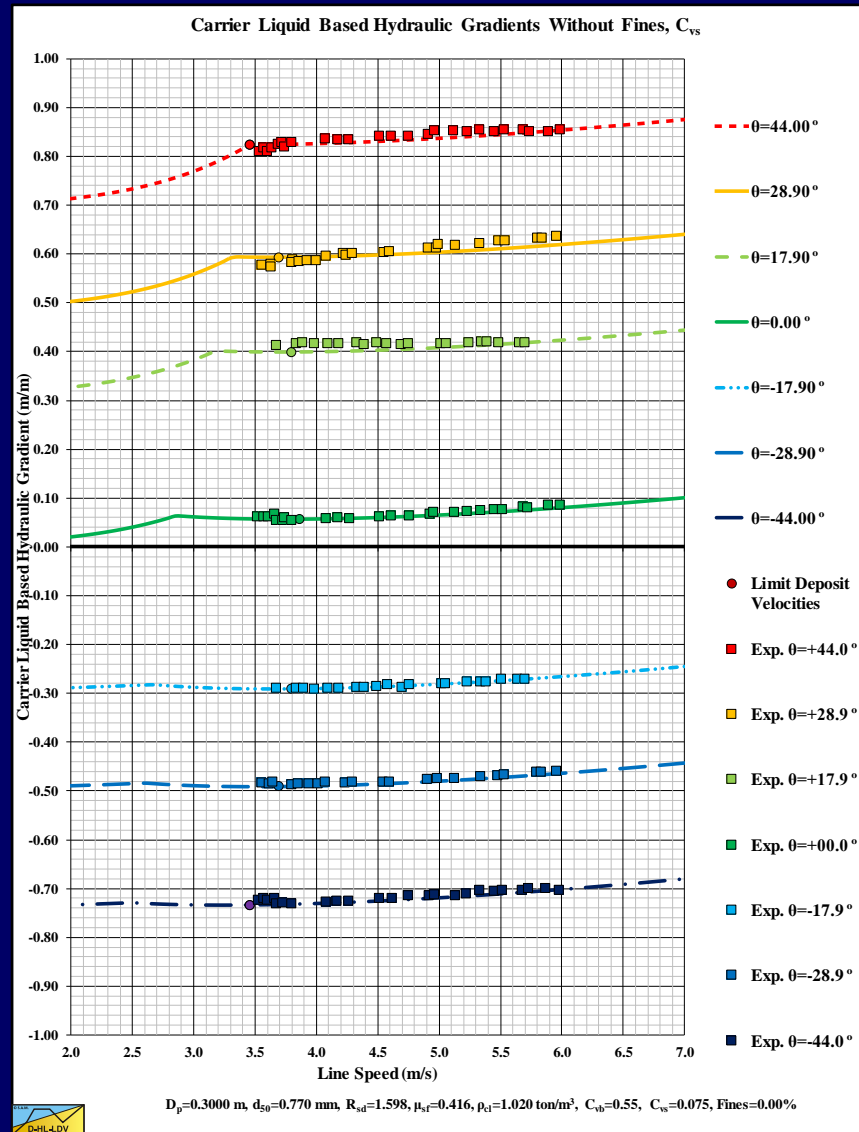
Inclined Pipe, de Vreede (2018), $C_v=0.02$



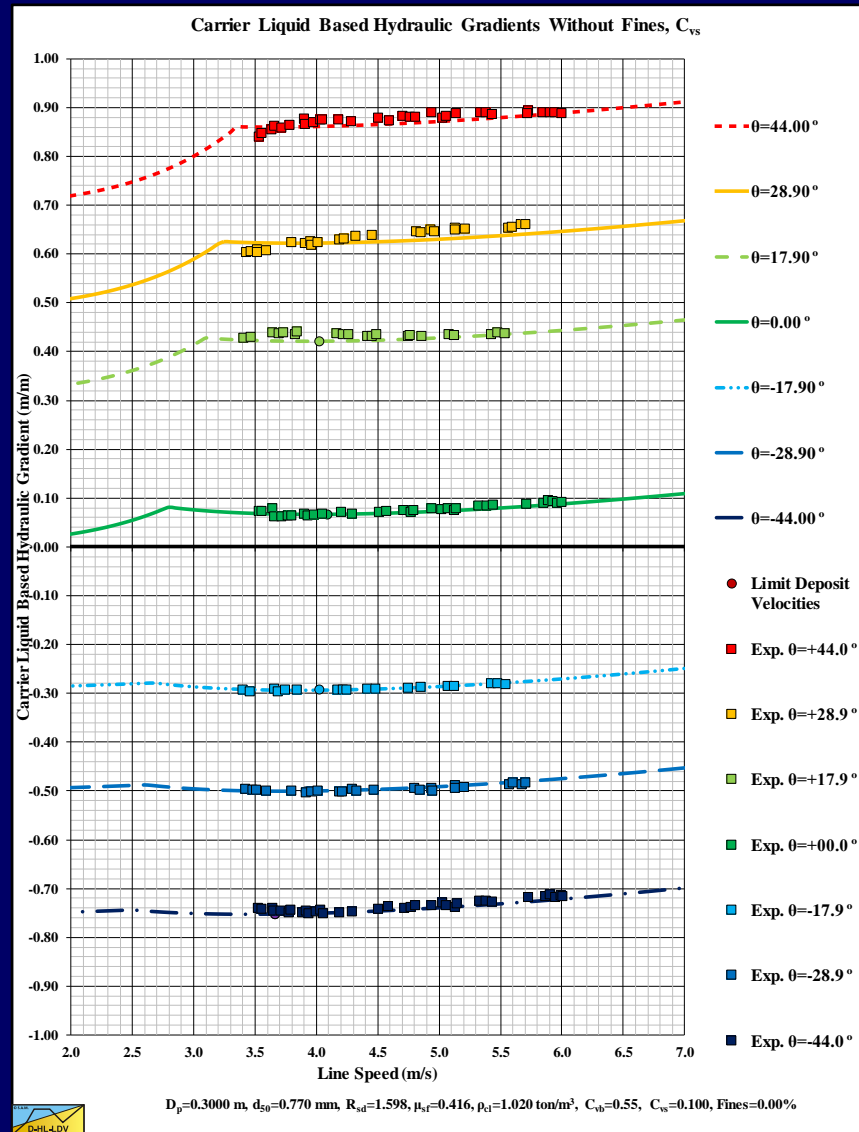
Inclined Pipe, de Vreede (2018), $C_v=0.05$



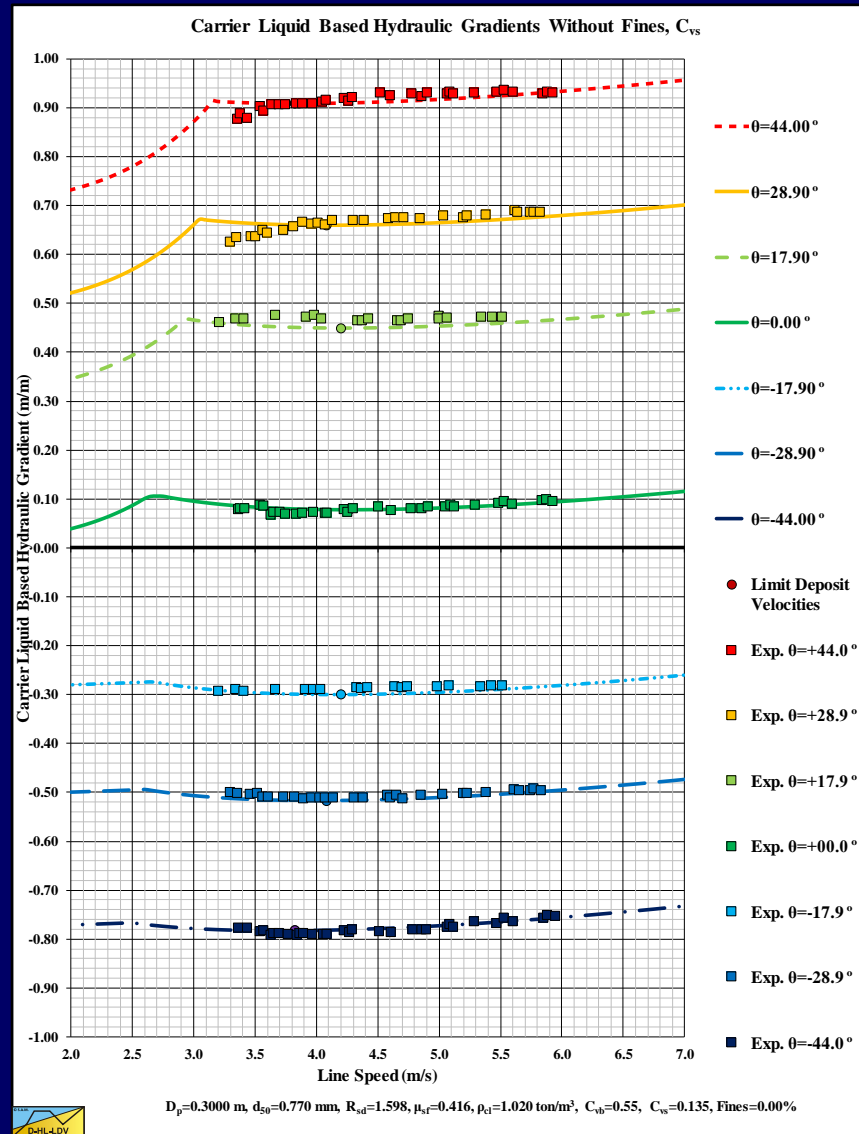
Inclined Pipe, de Vreede (2018), $C_v=0.075$



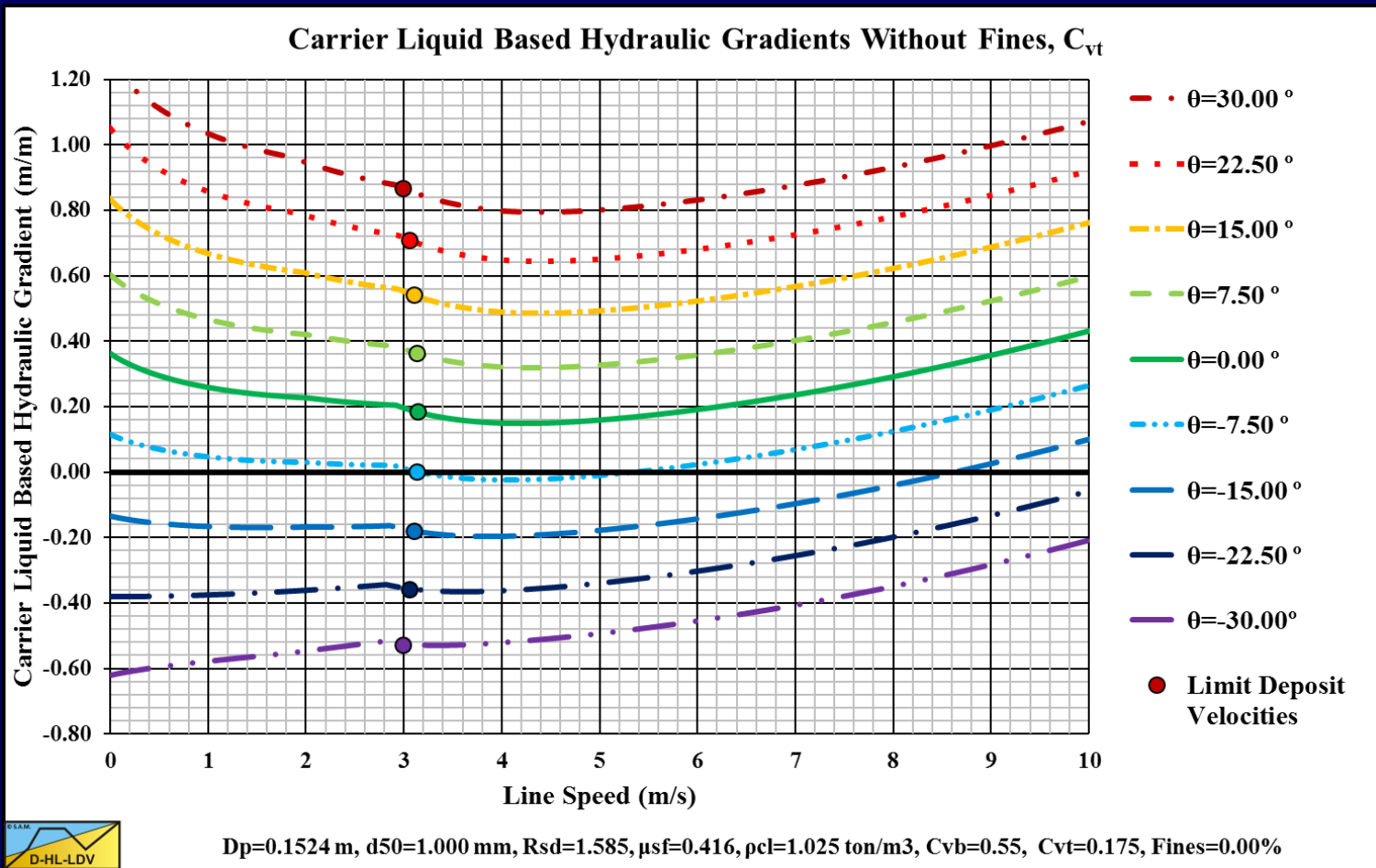
Inclined Pipe, de Vreede (2018), $C_v=0.10$



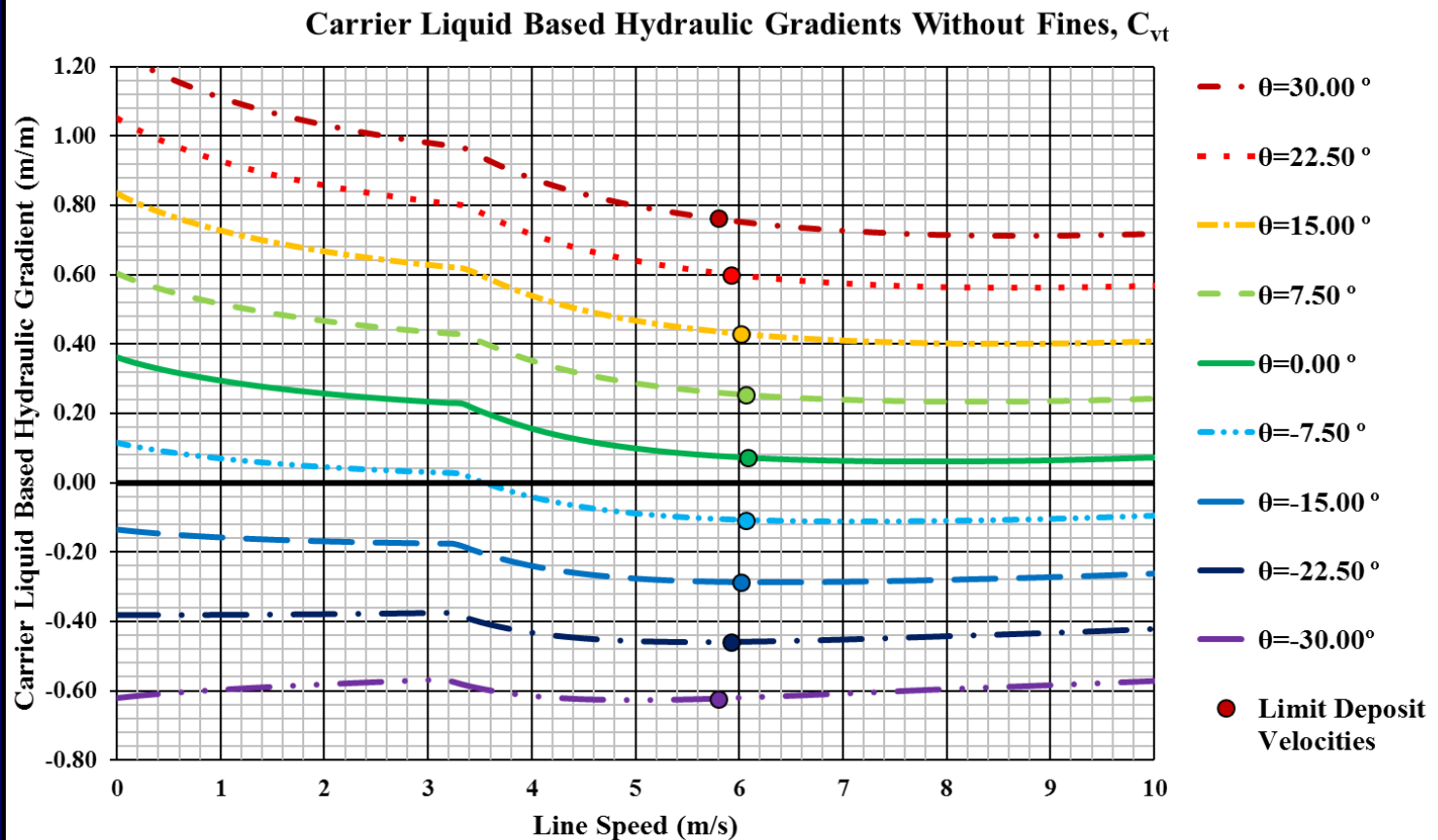
Inclined Pipe, de Vreede (2018), $C_v=0.135$



Inclined Pipe, $D_p=0.1524$ m, C_{vt}



Inclined Pipe, $D_p=0.762$ m, C_{vt}



$D_p=0.7620$ m, $d_{50}=1.000$ mm, $R_{sd}=1.585$, $\mu_{sf}=0.416$, $\rho_{cl}=1.025$ ton/m³, $C_{vb}=0.55$, $C_{vt}=0.175$, Fines=0.00%



Conclusions

- To construct the hydraulic gradient curve or relative solids effect curve for inclined pipes, first the curves for the different flow regimes have to be constructed.
- Secondly from the individual curves, a resulting curve can be constructed.
- The different flow regimes may behave differently with inclined pipes.
- The method described matches well with experimental data of Doron & Barnea, de Vreede, etc.



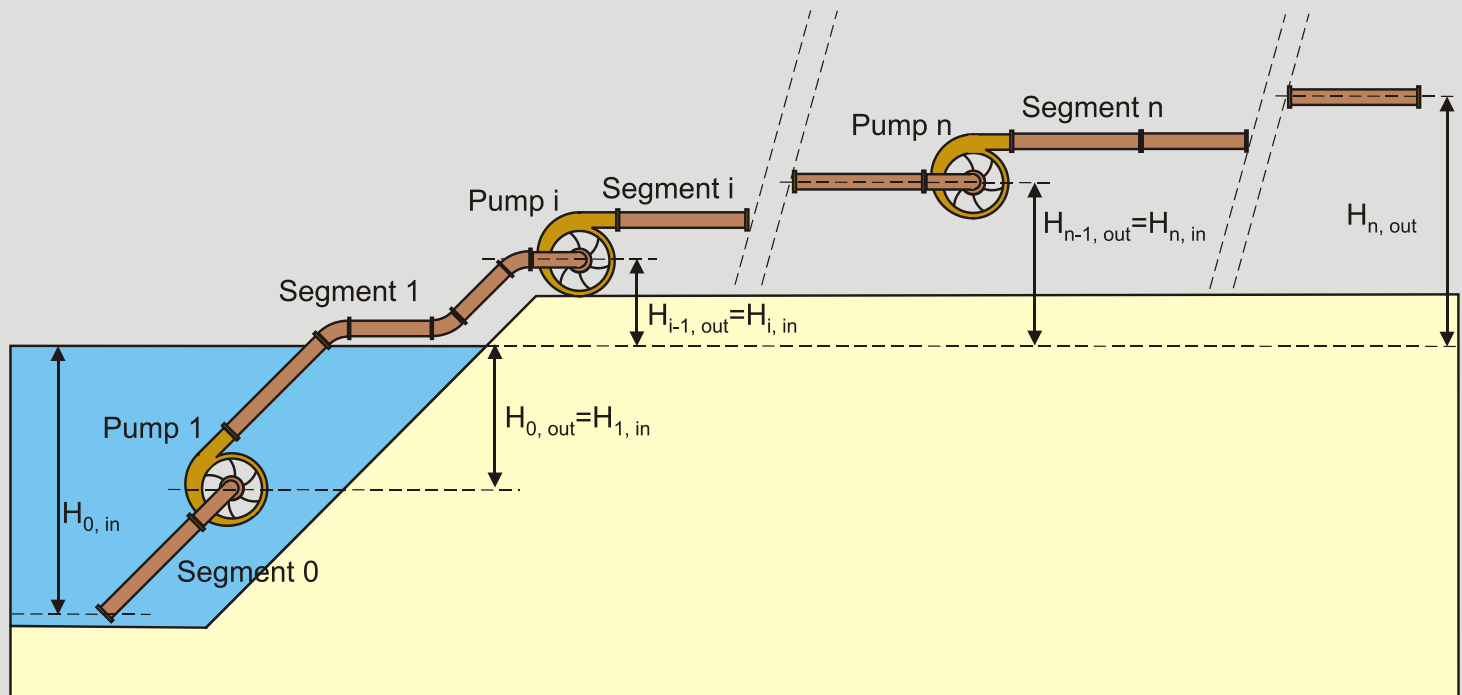


Using The DHLLDV Framework

Chapter 10



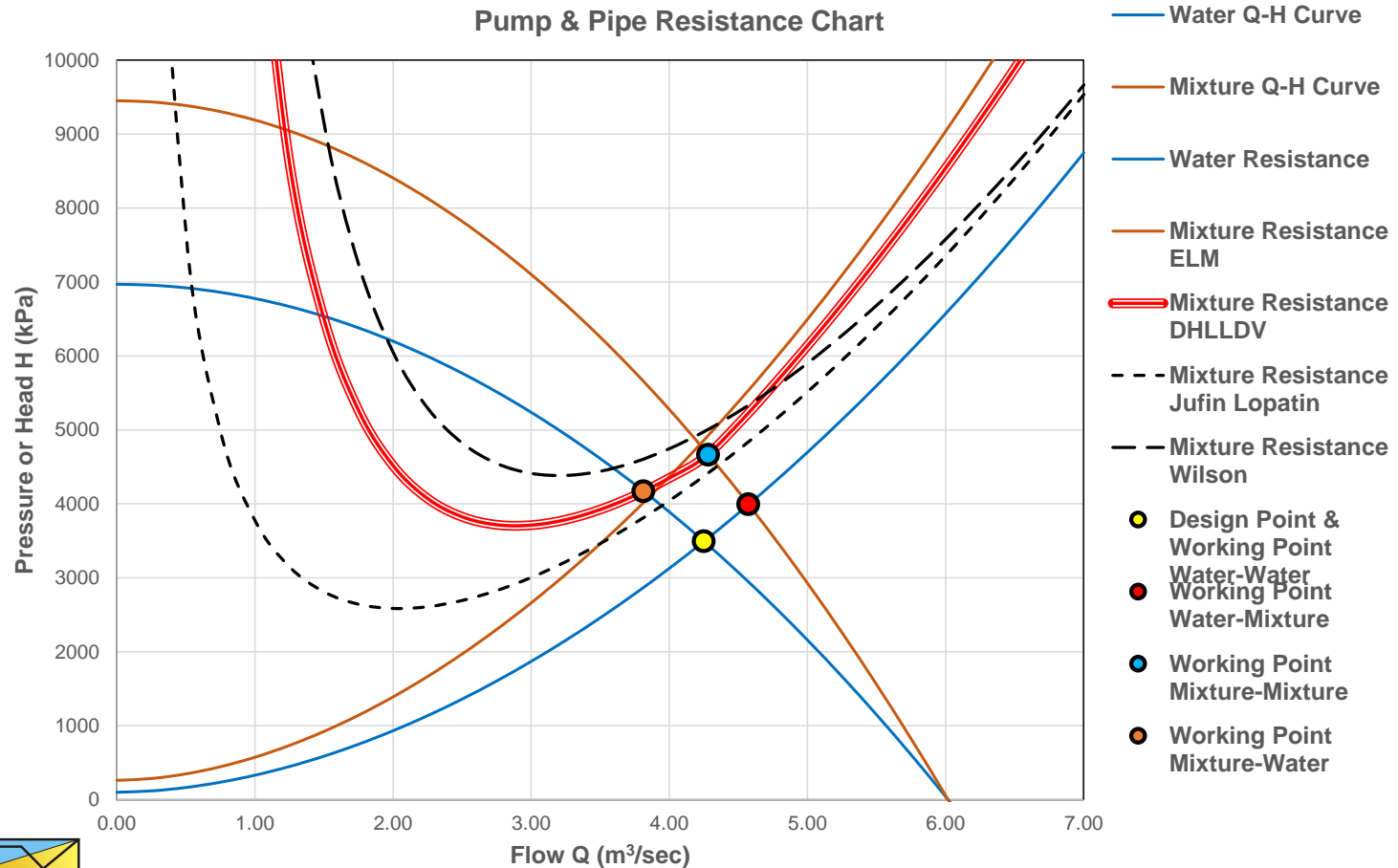
Pump/Pipeline System



- Total pressure/power required
- Cavitation limit of each pump
- Deposition/plugging the pipeline
- Limit Deposit Velocity



Pressure/Flow Graph



- Working points/working area



The Pipeline Resistance Equation

$$\Delta p_m = \frac{1}{2} \cdot \rho_m \cdot v_{ls}^2$$

$$+ \lambda_1 \cdot \frac{L_{tot}}{D_p} \cdot \frac{1}{2} \cdot \rho_l \cdot v_{ls}^2$$

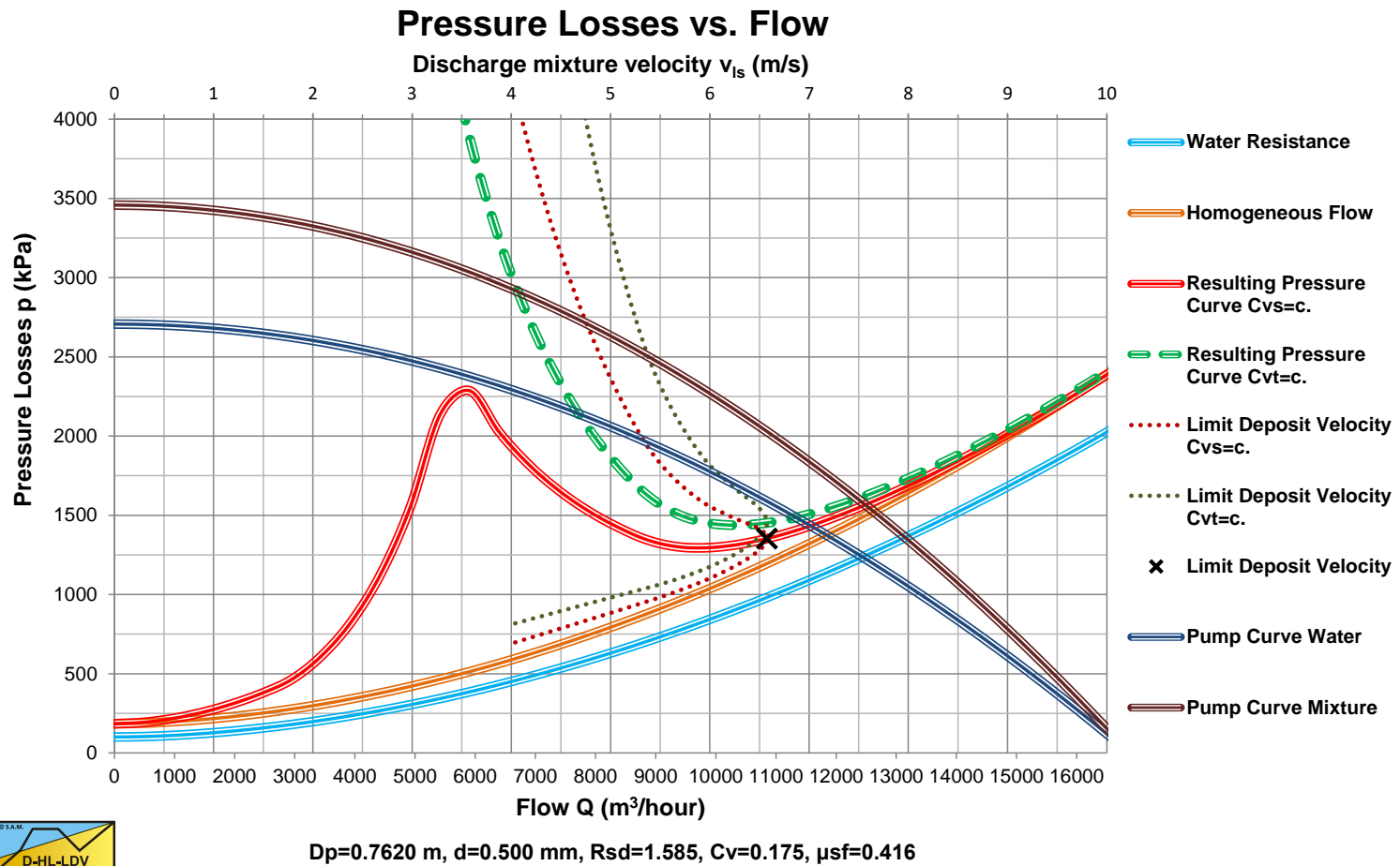
$$+ \rho_l \cdot g \cdot L_{tot} \cdot R_{sd} \cdot C_{vt} \cdot E_{rhg}$$

$$+ \frac{1}{2} \cdot \rho_m \cdot v_{ls}^2 \cdot \sum_{i=1}^n \left(\sum_{l=1}^{m_i} (\xi_{l,i}) \right)$$

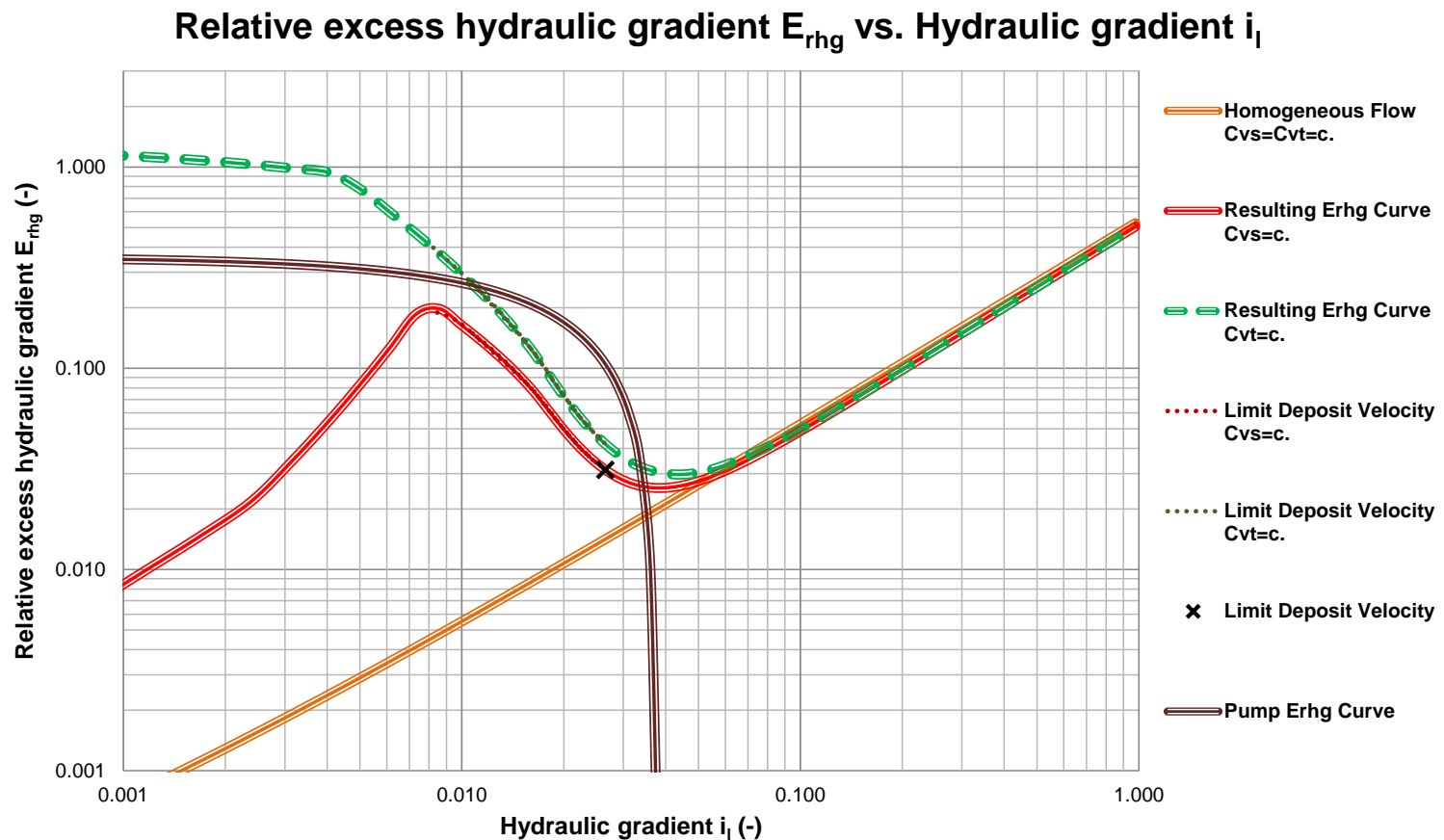
$$+ \rho_m \cdot g \cdot (H_{n,out} - H_{0,in})$$



The Resulting Pressure Losses



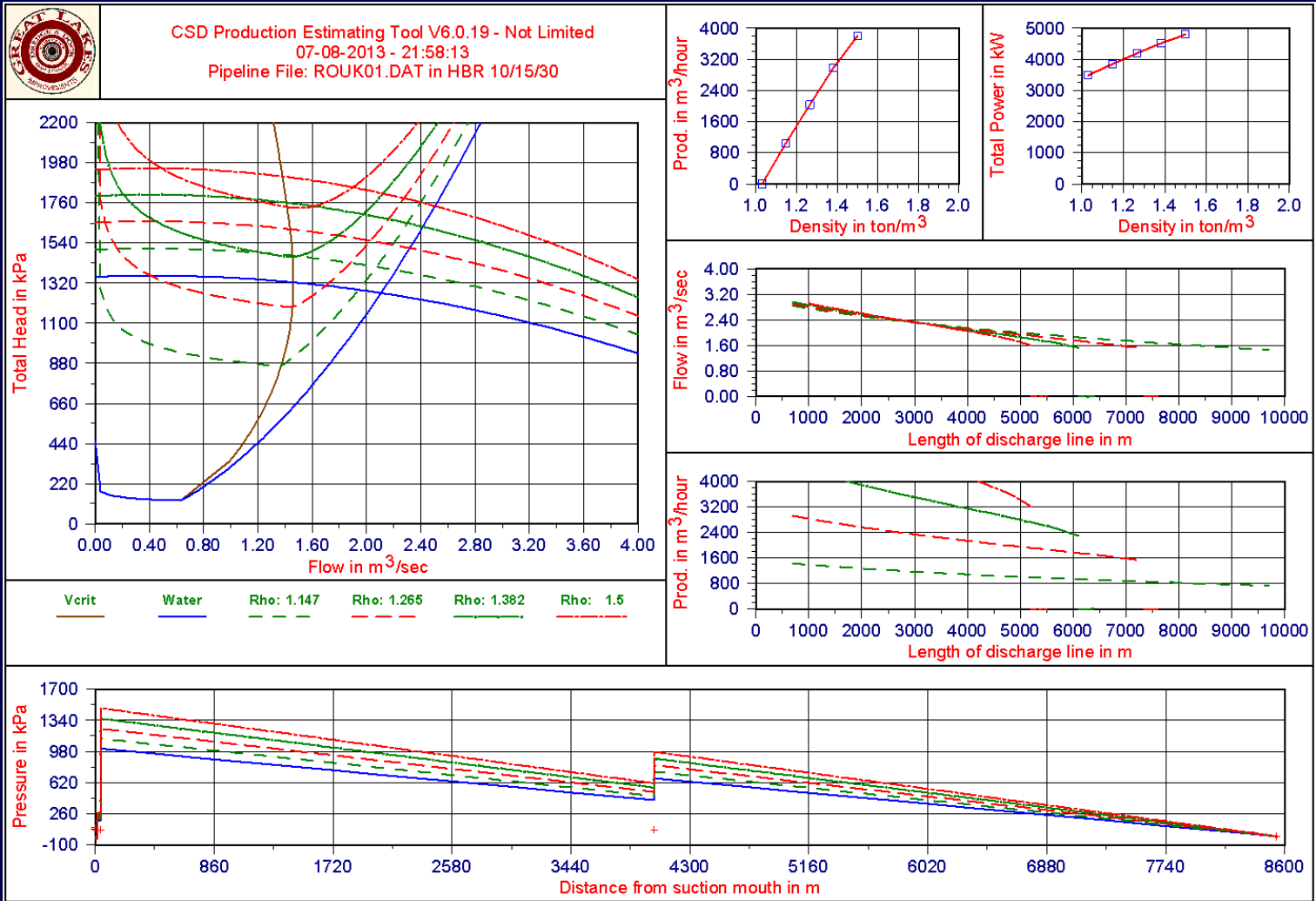
The Relative Excess Hydraulic Gradient



$D_p=0.7620$ m, $d=0.500$ mm, $Rsd=1.585$, $Cv=0.175$, $\mu sf=0.416$



System Curves



Inertial Effects

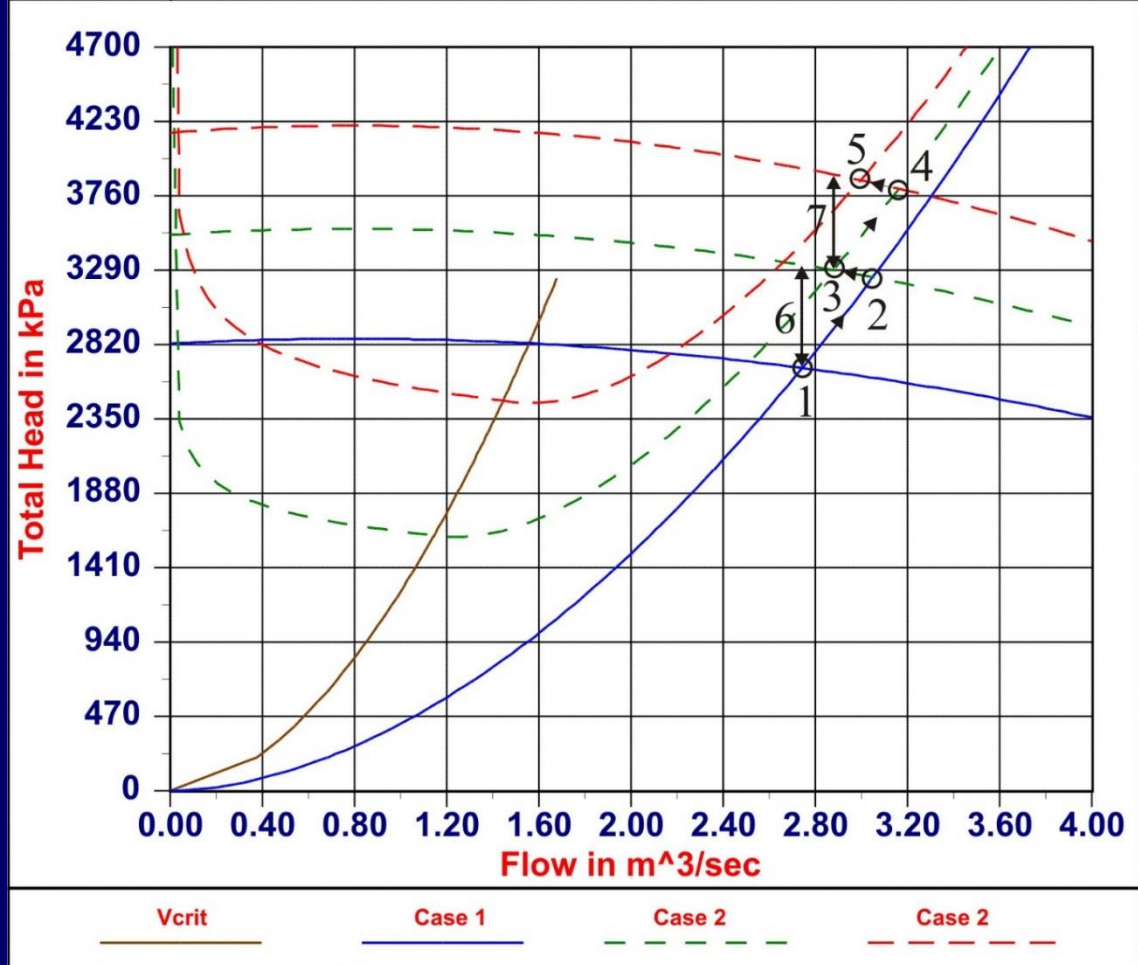
1. Very fast (within a second), the change in discharge pressure of a centrifugal pump due to a sudden change of the mixture density in the pump.
2. Fast (seconds), the change in revolutions of the pump drive and the change in line speed (acceleration and deceleration).
3. Slow (minutes), filling up the pipeline with mixture or a change in mixture content. In large diameter pipelines this may take 2-2.5 minutes per kilometer of pipeline length.



Increasing Mixture Density



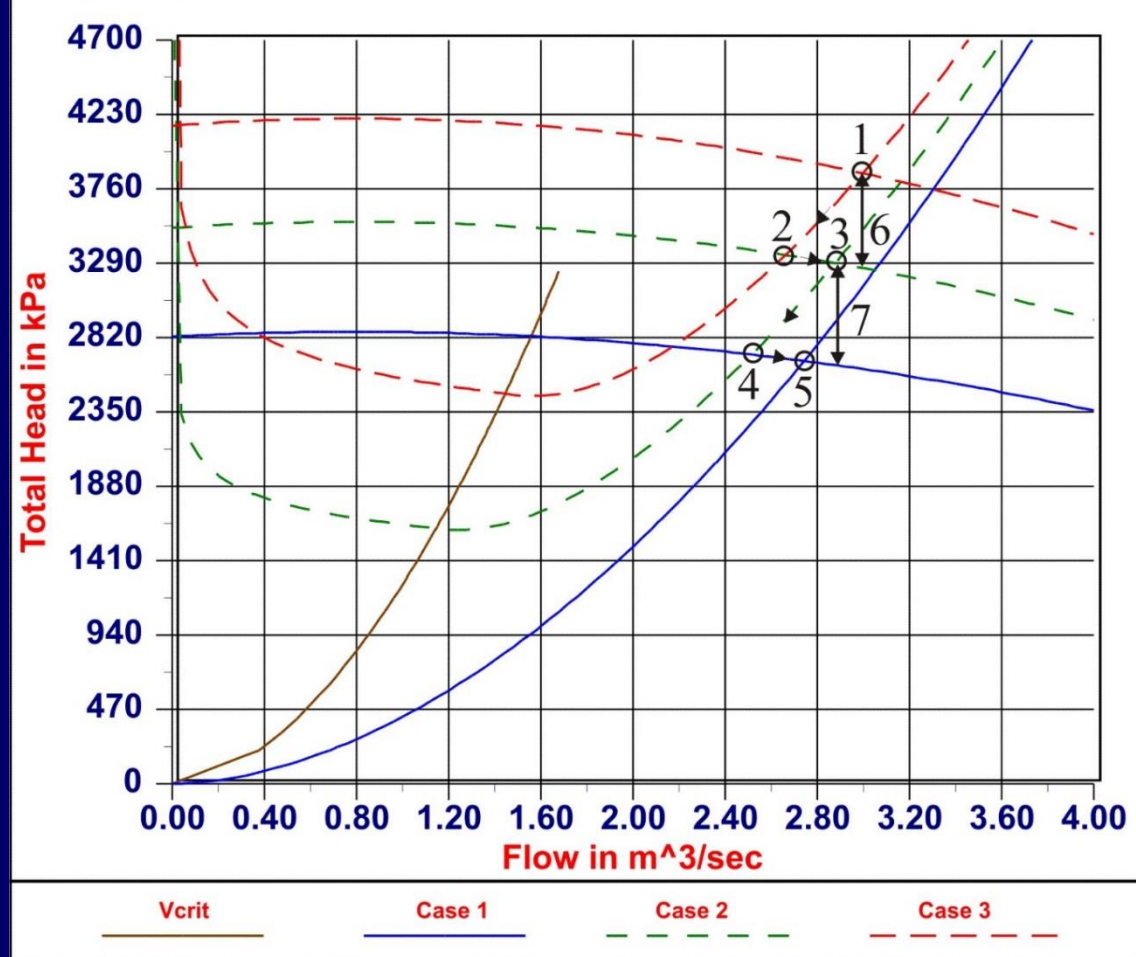
Stationary Pump Behaviour Windows V4.01 - Not Limited
 05-07-2001 - 08:23:50
 c:\samcons\spbw\pipeline\pipeline.inp in Default Sand



Decreasing Mixture Density



Stationary Pump Behaviour Windows V4.01 - Not Limited
05-07-2001 - 08:23:50
c:\samcons\spbw\pipeline\pipeline.inp in Default Sand





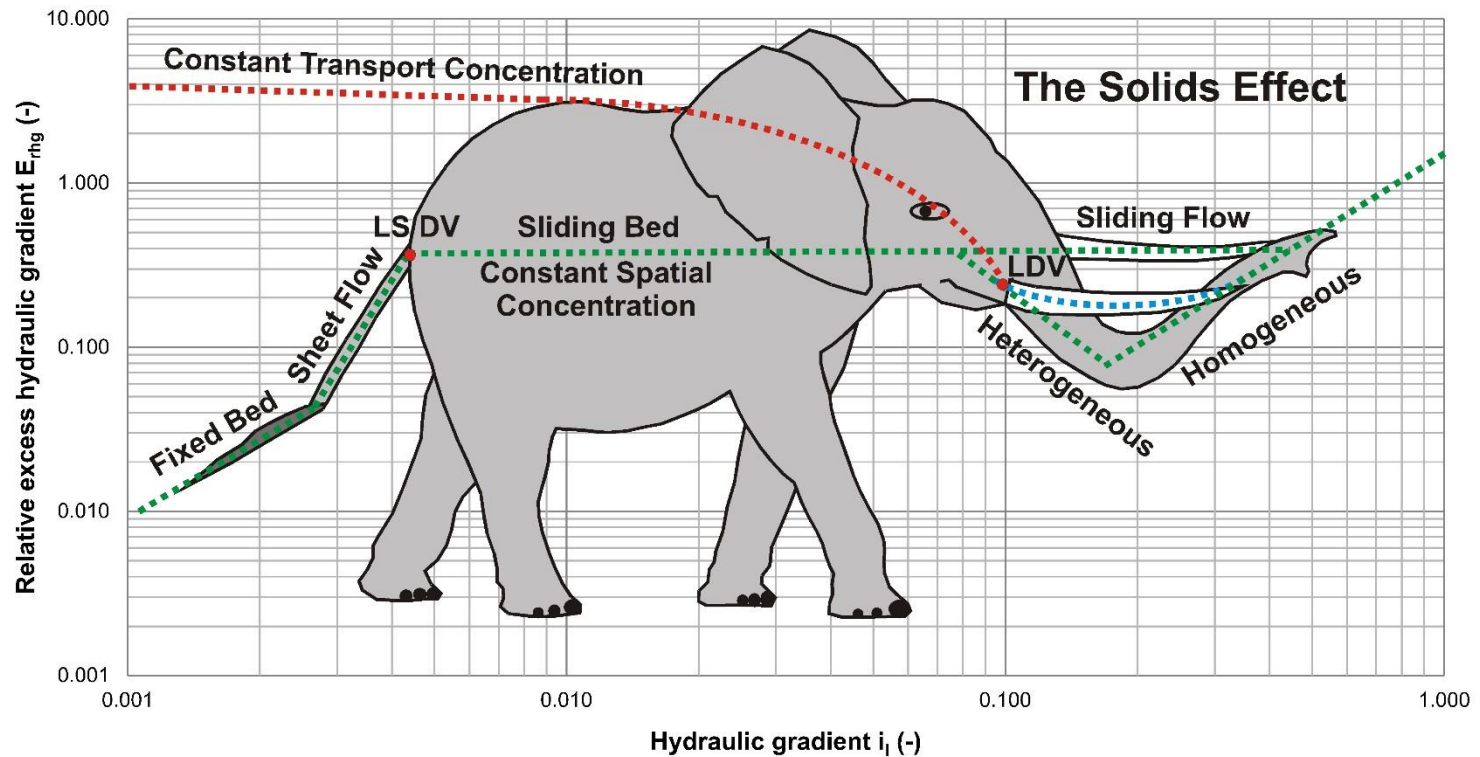
Main Conclusion



The Name of the Elephant is Leeghwater



The DHLLDV Framework The Double Logarithmic Elephant: Leeghwater



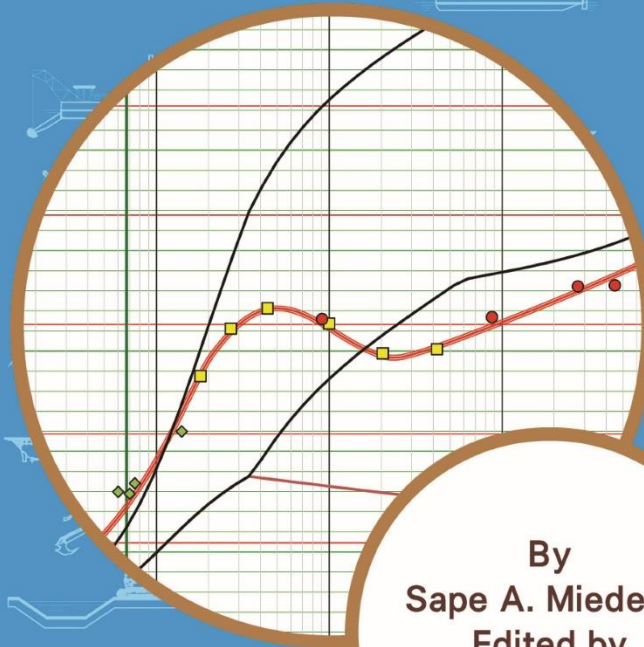
So the Wilson elephant really exists!!





SLURRY TRANSPORT

Fundamentals, A Historical Overview
& The Delft Head Loss & Limit
Deposit Velocity Framework



By
Sape A. Miedema
Edited by
Robert C. Ramsdell



The Elephant of Wilson is our best Friend

